



الجمهورية الجزائرية الديمقراطية الشعبية
وزارة التعليم العالي و البحث العلمي
جامعة قاصدي مرباح ورقلة
كلية الرياضيات و علوم المادة
قسم الكيمياء
رسالة مقدمة لنيل درجة دكتوراه (الطور الثالث)

تخصص: تحاليل الكيميوفيزيائية وفعالية العينات الجزيئية

الدراسة كيميائية-نباتية و بعض الفعاليات لنباتات من جنس
Pulicaria (الفصيلة المركبة)

من تقديم:

كميليا بيرش

في: 2023/09/16

أما أعضاء اللجنة المناقشة المكونة من:

السيد مختار سعدي	جامعة قاصدي مرباح ورقلة	أستاذ التعليم العالي	رئيسا
السيد حسين دندوقي	جامعة قاصدي مرباح ورقلة	أستاذ التعليم العالي	مشرفا
السيد محمد حجاج	جامعة قاصدي مرباح ورقلة	أستاذ التعليم العالي	مساعد مشرف
السيدة ونيسة سمارة	جامعة قاصدي مرباح ورقلة	أستاذة التعليم العالي	ممتحنة
السيد صالح عكال	جامعة منتوري قستطينة	أستاذ التعليم العالي	ممتحنا
السيد عاطف شويخ	جامعة حمة لخضر الوادي	أستاذ التعليم العالي	ممتحنا

السنة الجامعية 2023-2022



PEOPLE'S DEMOCRATIC REPUBLIC OF ALGERIA
MINISTRY OF HIGHER EDUCATION AND SCIENTIFIC
RESEARCH

UNIVERSITY OF KASDI MERBAH - OUARGLA
MATHEMATICS AND MATTER SCIENCE FACULTY
CHEMISTRY DEPARTMENT

Thesis for obtaining a doctoral degree (The third cycle)

Specialty: Physic-Chemical Analyzes And Reactivity Of Molecular
Species

Titled

**Phytochemical study and some activities of plants
from the genera *Pulicaria* (Asteraceae family)**

Presented publicly by:

Kamilia Bireche

On: 16/09/2023

In front of the jury composed by

Mr.Mokhtar Saidi	Professor	U.K.M Ouargla	President
Mr. Hocine Dendougui	Professor	U.K.M Ouargla	Reporter
Mr. Mohamed Hadjaj	Professor	U.K.M Ouargla	Asst.Reporter
Mme. Ouanissa Smara	Professor	U.K.M Ouargla	Examinator
Mr.Salah Akkal	Professor	U.M Constantine	Examinator
Mr. Atef Chouikh	Professor	U.E.H.KH El-Ouadi	Examinator

The academic year 2022-2023



Acknowledgements

All gratitude to Allah the Almighty
Who granted me the power to accomplish this thesis

I would like to thank **Pr. Mohamed Hadjaj**, Laboratory Director of Valorization and Promotion of Saharan Resources (VPRS), as well as for his help as an assistant supervisor in my thesis.

Also, I thank **Pr. Beraat Özcelik** for all the facilities at the technical university, Turkey.

I want to thank **Dr. Mine Gültekin-Özgüven**, for her incredible patience and direction during the training period and for always being available at Istanbul Technical University, Turkey.

I sincerely thank **Pr. Ramzan Erenler** for his welcome to his Natural Products Chemistry Laboratory at Tokat University, Turkey.

Special thanks to my supervisor, **Mr. Hocine Dendougui**, for his patience, support, and guidance.

I want to thank **Pr. Mokhtar Saidi** for agreeing to the presidency of the jury.

I am also thankful to the jury members who read and evaluated my work:

Pr. Salah Akkal, Pr. Atef Chouikh and Pr. Ouanissa Smara

Special thanks to you **Dr. Ilyase Yildiz, Dr. Souad Seghir and Dr. Sara Hasni**

My thanks and gratitude to **Pr. Segni Ladjal, Pr. Hadj Mohammed Mahfoud, Pr. Haba Hamada, Dr. Halis Youcef and Mr. Hadj Soudani** for their support in my academic path.

Finally, I want to thank all the members of (VPRS) laboratory and all my friends.



Dedication

This work is a fruit of countless and arduous sacrifices. through the researcher's effort, this work is

heartily and proudly dedicated to the people who serve as an inspiration. from parents and guardians, to friends whom extended their help in the midst of problems while making this work

I dedicate this thesis to my dear mother Salima and my dear father Ahmed, who encouraged and helped me all the time with pleasure since my birth until now, there are no words to express my gratitude to you and my grandmother Saadia, my brothers: Samir, M. Chouiki, Abdel Nour and their families, my sister Linda, my husband Riadh and my daughter Sidra, my uncle Mohamed nour eddine, my friends and every single person gave me a hand to accomplish my studies.

kamilia

Abstract:

The plants of the Asteraceae family (Compositae) have always aroused researchers' interest in the differentiation of their secondary metabolites, as they are considered the largest bank of lactone sesquiterpenes and polyacetylenes, along with flavonoids and other terpenes, or in terms of their various biological effects.

In our research, we relied on selecting the *Pulicaria laciniata* plant, which belongs to this family, because it is known for its use in traditional medicine, and there are minimal studies on this plant.

Different extracts of *P. laciniata* were obtained after maceration and then liquid-liquid extraction using increasingly polar solvents. The obtained phases were tested for their contents of phenolic compounds, flavonoids and tannins using colourimetric methods. Six methods evaluated the antioxidant activity of the extracts: DPPH, ABTS and FRAP. And Fe²⁺ chelating, superoxide anion and phosphomolybdate, and some biological activities such as Alzheimer's, obesity and diabetes were also evaluated by using some enzymes such as acetylcholine esterase lipase, alpha-amylase and alpha-glucosidase.

The results indicate that this plant contains moderate amounts of total flavonoids in the n-butanol and ethyl acetate extracts with the following values (2.416 ± 497.92 and 437.66 ± 1.82) mg QE/g, respectively, and total phenols (231.67 ± 20.051 and $(221.59) \pm 12.918$ mg GAE/g, respectively). On the other hand, the results showed significant antioxidant activity where the n-butanol extract was the best in antioxidant activity against DPPH and ABTS radicals with IC₅₀ equal to ($500.8 \pm 8,16$ and 469.93 ± 2.14) micrograms, respectively. As well as the results of the evaluation of biological activities showed that the n-butanol extract showed the best activity against the enzyme alpha-amylase with IC₅₀ equal to (414 ± 0.34) micrograms. In contrast, the chloroform extract was the best against three enzymes cholinesterase, lipase and alpha-amylase with different values of IC₅₀.

On the other hand, we concluded in this research to separate about 14 compounds using different chromatographic techniques. Now we have reached to identify the

structures of six compounds, including five flavonoid compounds separated for the first time from the specie *P. laciniata* and a new sesquiterpene lactone compound for the genera *Pulicaria*. Also, nine compounds were identified from the chloroform extract by gas chromatography coupled with mass spectrometry.

Also, the antioxidant activity of these pure compounds was evaluated using DPPH and ABTS radicals and their effectiveness in inhibiting the enzymes acetylcholine-esterase and amylase. The results showed significant activity, especially the sesquiterpene lactone compound, which showed the best inhibition against acetylcholine-esterase with IC_{50} equal to $19,68. \pm 0.89 \mu\text{g}$.

All these results strongly demonstrate that *P. laciniata* aerial part extract and the isolated pure compounds, a very effective therapeutic property, could be a new and promising candidate for treating many diseases with natural sources.

Keywords: *Asteraceae*; *Pulicaria*; antioxidant: phenols; biological activities; phytochemical; one- and two-dimensional magnetic resonance.

المخلص:

لطالما أثارت نباتات الفصيلة النجمية (المركبة) اهتمام الباحثين من حيث تمايز منتوجات أبيضها الثانوي إذ تعد البنك الأكبر : لسيكوتريينات الاكتونية و عديدات الاسيتيلينات إلى جانب الفلافونيدات و التريينات الأخرى، أو من حيث تأثيراتها البيولوجية المتنوعة.

اعتمدنا في بحثنا على اختيار نبات *Pulicaria laciniata* المنتمي لهذه الفصيلة لما لها من استخدام واسع في الطب التقليدي. إلى جانب كون الاعمال المنجزة حوله قليلة وهو الدافع الذي جعلنا نوليها عناية خاصة في بحثنا الكيميائي على مستخلص أسيتات الايثل والكلوروفورم لنبته *P. laciniata* لالتحصار الدراسات النباتية حولها.

نجحنا في الحصول على مستخلصات مختلفة من *P. laciniata* بعد النقع ثم استخلاص سائل-سائل باستخدام مذيبات متزايدة القطبية حيث قمنا باختبار محتوياتها من المركبات الفينولية ، الفلافونويدية والتانينات باستخدام طرق قياس الألوان، بالإضافة الى قيامنا بتقييم الفعالية المضاد للأكسدة باستخدام ستة طرق: DPPH و ABTS و FRAP و Fe²⁺ chelating و superoxide anion و phosphomolybdate ، هذا وقد وفقنا في تقييم بعض الفعاليات البيولوجية كالزهايمر والسمنة ومرض السكري باستخدام بعض الانزيمات مثل أستيل كولين استيرازو والليباز وألفا أميلاز وألفا جلوكوزيداز.

تشير النتائج التي انتهينا إلى الحصول عليها أيضا إلى أن هذا النبات يحتوي على كميات معتدلة من إجمالي الفلافونيدات في المستخلص البيتانولي واسيتات الإيثيل بالقيم التالية:

(497.92±2.416 و 437.6437.6 ±1.82) mg QE/g على التوالي .

والفينيزات: (231.67 ± 20.051 و 221.59 ± 12.918) mg GAE/g على التوالي.

من ناحية أخرى، فقد أظهرت النتائج أيضا نشاطا مهما مضادا للأكسدة حيث كان المستخلص البيتانول الأفضل في النشاط مضاد للأكسدة ضد جذور DPPH و ABTS مع IC₅₀ يساوي:

(500.8±8،16 و 469.93 ±2،14) ميكروغرام على التوالي.

وكذلك أظهرت نتائج تقييم الفعاليات البيولوجية أن مستخلص البوتانولي أفضل فعالية ضد إنزيم ألفا أميلاز مع IC₅₀ يساوي (0.34 ± 414) ميكروغرام، هذا دون أن نغفل فاعلية مستخلص الكلوروفورم إذ أظهرت النتائج أنه كان الأفضل ضد ثلاثة إنزيمات كولين استيرازو والليباز وألفا أميلاز بقيم مختلفة لـ IC₅₀.

من جهة اخرى خلصنا في بحثنا هذا إلى فصل ما يقارب 14 مركب باستخدام التقنيات الكروماتوجرافية المختلفة، في حين توصلنا لحد الساعة لتعيين بنى ستة مركبات منها خمس مركبات فلافونيدية تفصل لأول مرة من هذا النوع *P. laciniata* و مركب سيسكوتريبيني لاكتوني جديدا بالنسبة لجنس *Pulicaria*، كما وفقنا أيضا إلى التعرف على تسع مركبات في مستخلص الكلوروفوم من خلال تقنية الكروماتوغرافيا الغازية المقرنة بمطيافية الكتلة.

كذلك تم تقييم الفعالية المضادة للأكسدة لهذه المركبات النقية بالاستعمال جذر DPPH و ABTS و فعاليتها في تثبيط انزيم الالاسيتيل كولين استيراز و أميلاز، بحيث اظهرت النتائج نشاطا معتبرا، خاصة مع المركب التريبيني الذي أعطى أفضل تثبيط ضد أستيل-إستراز مع IC₅₀ يساوي $0.89 \pm 19,68$ ميكروغرام.

كل هذه النتائج تثبت بقوة أن مستخلص الجزء الهوائي من *P. laciniata* والمركبات النقية المعزولة نو خاصية علاجية فعالة للغاية ، يمكن أن تكون مرشحا جديدا وواعدا لعلاج العديد من الأمراض بمصادر طبيعية.

كلمات مفتاحية: *Asterasea*؛ *Pulicaria*، مضادات الأكسدة، الفينولات، الفعالية البيولوجية؛ كيمياء النبات، الرنين المغناطيسي احادي وثنائي البعد.

Résumé

Les plantes de la famille des Astéracées (Composées) ont toujours suscité l'intérêt des chercheurs pour la différenciation de leurs métabolites secondaires, puisqu'elles sont considérées comme la plus importante banque de lactones sesquiterpènes et polyacétylènes, avec les flavonoïdes et autres terpènes, ou pour leurs diverses propriétés biologiques effets.

Dans nos recherches, nous nous sommes appuyés sur la sélection de la plante *Pulicarialaciniata*, qui appartient à cette famille, car elle est connue pour son utilisation en médecine traditionnelle et il existe peu d'études sur cette plante.

Différents extraits de *P. laciniata* ont été obtenus après macération puis extraction liquide-liquide à l'aide de solvants de plus en plus polaires. Les phases obtenues ont été testées pour leur teneur en composés phénoliques, flavonoïdes et tanins par des méthodes colorimétriques. Six méthodes ont évalué l'activité antioxydante des extraits : DPPH, ABTS, FRAP, Fe²⁺ chélatant, anion superoxyde et phosphomolybdate et certaines activités biologiques telles que la maladie d'Alzheimer, l'obésité et le diabète ont également été évalués en utilisant certaines enzymes telles que l'acétylcholine estérase lipase, alpha-amylase et alpha-glucosidase.

Les résultats indiquent que cette plante contient des quantités modérées de flavonoïdes totaux dans les extraits de n-butanol et d'acétate d'éthyle avec les valeurs suivantes (497,92 ± 2,416 et 437,66 ± 1,82) mg QE/g, respectivement. Et les phénols totaux (231,67 ± 20,051 et 221,59 ± 12,918) mg GAE/g, respectivement. D'autre part, les résultats ont montré une activité antioxydante significative où l'extrait de n-butanol était le meilleur en activité antioxydante contre les radicaux DPPH et ABTS avec IC₅₀ égaux à (500,8 ± 8,16 et 469,93 ± 2,14) microgrammes, respectivement. Ainsi que les résultats de l'évaluation des activités biologiques ont montré que l'extrait de n-butanol a montré la meilleure activité contre l'enzyme alpha-amylase avec IC₅₀ égal à (414 ± 0,34)

microgrammes En revanche, l'extrait au chloroforme était le meilleur contre trois enzymes cholinestérase, lipase et alpha-amylase avec différentes valeurs d'IC₅₀.

D'autre part, nous avons conclu dans cette recherche à séparer environ 14 composés en utilisant différentes techniques chromatographiques. Nous sommes maintenant parvenus à identifier les structures de six composés, dont cinq composés flavonoïdes séparés pour la première fois de l'espèce *P. laciniata* et un nouveau composé lactone sesquiterpène pour le genre *Pulicaria*. Aussi, neuf composés ont été identifiés à partir de l'extrait chloroforme par chromatographie en phase gazeuse couplée à la spectrométrie de masse.

De plus, l'activité antioxydante de ces composés purs a été évaluée à l'aide des radicaux DPPH et ABTS et leur efficacité à inhiber les enzymes acétylcholine-estérase et amylase. Les résultats ont montré une activité significative, en particulier le composé sesquiterpène lactone, qui a montré la meilleure inhibition contre l'acétylcholine-estérase avec une CI 50 égale à 19,68. ± 0,89 µg.

Tous ces résultats démontrent fortement que l'extrait de partie aérienne de *P. laciniata* et les composés purs isolés, une propriété thérapeutique très efficace, pourraient être un nouveau candidat prometteur pour traiter de nombreuses maladies avec des sources naturelles.

Mots clés : *Asterasea* ; *Pulicaria* ; antioxydant : phénols ; activités biologiques ; phytochimique; résonance magnetic mono et bidimensionnelle.

LIST OF FIGURES

Figure N°	Title of figure	Page
1	Geographic distribution map <i>P.laciniata</i> .	7
2	Chemical structure of phenol and its derivatives compound separated from different <i>Pulicaria</i> species.	9
3	Chemical Structure of flavonoids and their derivatives compound separated from different <i>Pulicaria</i> species.	12
4	Chemical Structure of flavonoids and its derivatives compound separated from different <i>Pulicaria</i> species.	13
5	Monoterpene and Germacrans compound separated from different <i>Pulicariaspecies</i> .	15
6	Xanthanolids and Guaianolids compounds that separated from different species of <i>Pulicaria</i> genus	18
7	Pseudoguaianolides and Eudesmanes compounds separated from different <i>Pulicaria</i> genera species.	20
8	Caryophyllans compounds separated from different <i>Pulicariaspecies</i>	23
9	Bisabolens and Diterpenes compounds separated from different <i>Pulicaria</i> species	26
10	Triterpenoids, steroids, and other terpenoid compounds separated from different <i>Pulicaria</i> species	30
11	Biogenesis of simple phenols and phenolic acids	46
12	Flavonoids biosynthesis..	51
13	Present examples of terpenoids compounds	53
14	Biosynthesis of the terpenoids	54
15	<i>Pulicaria laciniata</i> (Cross. and kral.) 2016	59
16	<i>Protocal extraction</i>	60
17	Phytochemical fingerprint Chromatograms. The chromatograms were developed in the different solvents.	64
18	TLC of the first column fractions after collection of similar ones after the revelation	69
19	TLC of the second collection of the LH-20 column after the revelation with an acidic solution	69
20	TLC of the fraction A separation using C-18 after revelation.	70
21	TLC of fraction during purification of compound K1	71
22	TLC of the fraction C+D separation using C-18 after revelation with an acid solution	72
23	Phytochemical study of the Ethyl acetate and Chloroform extracts.	78
24	Spectrum :RMN ¹³ C (125MHz,CDCL ₃) of compound K1	81
25	Spectrum RMN DEPT -135 (500 MHz,CDCL ₃) of compound K1	81
26	Spreadspectrum of RMN 1H(125 MHz,CDCL ₃) of compound K1	82
27	SpreadSpectrum RMN 1H(500 MHz,CDCL ₃) of compound K1	82

28	Spreadspectrum RMN ¹ H(500 MHz,CDCL ₃) of compound K1	83
29	Spectrum of HSQC (500 MHz,CDCL ₃)of compound K1	83
30	Spectrum of HMBC (500 MHz, CDCL ₃) of compound K1	85
31	Spectrum of COSY (500 MHz,CDCL ₃) of compound K1	86
32	semi-structure	87
33	Chemical structure of K1Humulene-glucoside	89
34	Specter RMN ¹ H(500 MHz,CD ₃ OD) of compound K2	90
35	Specter RMN ¹³ C (125 MHz,CD ₃ OD) of compound K2	90
36	Specter Cosy (500 MHz,CD ₃ OD) of compound K2.	91
37	Specter of HSQC (500 MHz,CD ₃ OD)of compound K2	92
38	Specter of HMBC (500 MHz,CD ₃ OD)of compound K2	92
39	Chemical structure of compound K2.Quercetin -3-methylether	
40	Spectrum RMN ¹ H(500 MHz,CD ₃ OD) of compound K3	95
41	Specter RMN ¹³ C (125MHz,CD ₃ OD) of compound K3	96
42	Specter of HSQC (500 MHz,CD ₃ OD)of compound K3	97
43	Specter of Cosy (500 MHz,CD ₃ OD)of compound K3	97
44	Specter of HMBC (500 MHz,CD ₃ OD)of compound K3	98
45	Chemical structure of compound K3Quercetagetin 3,7-dimethyl ether.	
46	Specter RMN ¹ H(500 MHz,CD ₃ OD) of compound K4	101
47	Specter RMN ¹³ C (125MHz,CD ₃ OD) of compound K4.	101
48	Specter of HSQC (400 MHz,CD ₃ OD)of compound K4	102
49	Specter of Cosy (400 MHz,CD ₃ OD)of compound K4.	103
50	Specter of HMBC (400 MHz,CD ₃ OD)of compound K4.	103
51	Chemical structure of compound K4 Kaempferol -6-hydroxy-3,7-dimethyl ether	105
52	Specter RMN ¹ H(500 MHz,CD ₃ OD) of compound K5.	106
53	Specter RMN ¹³ C (125MHz,CD ₃ OD) of compound K5.	108
54	Specter of Cosy (500 MHz,CD ₃ OD) of compound K5.	108
55	Specter of HSQC (500 MHz,CD ₃ OD) of compound K5	109
56	Specter of HMBC (500 MHz,CD ₃ OD) of compound K5.	109
57	Chemical structure of K5 Quercetin-3-O-β-glucoside.	111
58	Specter RMN ¹ H(400 MHz,CD ₃ OD) of compound K6.	112
59	Specter RMN ¹³ C (100 MHz,CD ₃ OD) of compound K6.	112
60	Specter of Cosy (400 MHz,CD ₃ OD) of compound K6.	113
61	Specter of HSQC(400 MHz,CD ₃ OD) of compound K6.	114
62	Specter of HMBC (400 MHz,CD ₃ OD) of compound K6.	114
63	Chemical structure of compound K6 Quercetin -3-O-β-glucuronide.	116
64	Gc-Ms chromatogram of the CHCl ₃ extract	117

65	The identified compounds structure from the CHCl ₃ extract using Gc-Ms	118
66	Formation of stable ABTS radical from ABTS with potassiumper sulfate	122
67	Reaction between DPPH• and antioxidant to form DPPH	123
68	Formation of (TPTZ -Fe ²⁺) complex from (TPTZ- Fe ³⁺) –complex by antioxidants	124
69	Metal chelating reaction mechanism.	125
70	Inhibition rate of different extract of <i>Pulicaria laciniata</i> in ABTS assay	129
71	Inhibition rate of purified compounds in ABTS assay.	130
72	Inhibition rate of different extract of <i>P. laciniata</i> in DPPH assay.	131
73	Inhibition rate of purified compounds in DPPH assay.	132
74	Absorbance of different extract of <i>P. laciniata</i> in FRAP assay.	133
75	Chelating effect on ferrous ions of <i>P.laciniata</i> different extracts.	134
76	The global antioxidant activity of <i>P.laciniata</i> different extracts.	135
77	Pyrogallol auto-oxidation of of <i>P.laciniata</i> different extracts.	136
78	α -amylase inhibition rate of <i>P.laciniata</i> different extracts.	137
79	α -amylase inhibition rate of the purified compound.	138
80	α -glucosidase inhibition rate of <i>P.laciniata</i> different extracts.	139
81	lipase inhibition rate of <i>P.laciniata</i> different extracts.	140
82	Acetylcholine-esterase inhibition rate of <i>P.laciniata</i> different extracts.	141
83	Acetylcholine-esterase inhibition rate of the purified compounds.	141

LIST OF TABLES

Table N°	Titel of table	Page
1	Phenol and its derivatives compound separated from different <i>Pulicaria</i> species.	7
2	Flavonoids and their derivatives compounds separated from different <i>Pulicaria</i> species	9
3	Monoterpene and Germacrans compounds separated from different <i>Pulicaria</i> species.	13
4	Xanthanolides and guaianolids compounds separated from different <i>Pulicaria</i> species	15
5	Pseudoguaianolides and Eudesmanes compounds separated from different <i>Pulicariagera</i> species.	18
6	Caryophyllans compounds separated from different <i>Pulicaria</i> species.	20
7	Bisabolens compounds separated from different <i>Pulicaria</i> species.	23
8	Diterpene compounds separated from different <i>Pulicaria</i> species.	23
9	Triterpenoid compounds that separated from different species of <i>Pulicariagenus</i> .	27
10	Steroid compounds that separated from different species of <i>Pulicariagenus</i> .	27
11	Other Terpenoid compounds separated from different <i>Pulicaria</i> species.	27
12	Present the main classes of phenolic compounds.	40
13	Present the main classes of terpenoids compounds	51
14	Phytochemicals screening of <i>P.laciniata</i> extracts.	65
15	Different extracts' total phenolic, flavonoid, and tannin content.	65
16	The obtained results of Separation chromatography on the Sephadex LH-20 column of the EtOAc extract.	68
17	The obtained results of Separation chromatography on C18 column of fraction A	70
18	The obtained results of Separation chromatography on Silica gel column of F-7 and F-8 sub-fraction	71
19	The obtained results of Separation chromatography on C18 column of fractions C and D.	73
20	The obtained results of Separation chromatography on Silica gel and Sephadex LH-20 column of sub-fraction 11	74
21	The obtained results of Separation chromatography on Silica gel and Sephadex LH-20 column of sub-fraction 14	75
22	The obtained results of Separation chromatography on Silica gel and Sephadex LH-20 column of sub-fraction 7	76
23	The obtained results of Separation chromatography on Silica gel and Sephadex LH-20 column of sub-fraction 4.	77

24	Chemical shift values of 1D and 2D NMR of compound K1.	84
25	Chemical shift values of 1D and 2D NMR of compound K2	93
26	Chemical shift values of 1D and 2D NMR of compound K3	99
27	Chemical shift values of 1D and 2D NMR of compound K4.	104
28	Chemical shift values of 1D and 2D NMR of compound K5.	110
29	Chemical shift values of 1D and 2D NMR of compound K6.	115
30	Represent the most abundant identified compounds from the GC-MS.	117
31	Summarized results of anti-oxidant activities of <i>P.laciniata</i> different extracts.	142
32	Summarized results of enzymatic activities of <i>P.laciniata</i> different extracts.	142
33	Summarized results of anti-oxidants and enzymatic activities of the purified compounds extracts.	143

ABREVIATIONS LIST

δ	: Chemical displacement
ABTS	: 2,2'-azinobis-(3-ethylbenzothiazoline-6-sulfonate)
DPPH	: 2, 2-diphenyl-1-picrylhydrazyl
Ach	: Acetylcholine
AChE	: Acetylcholinesterase
AD	: Alzheimer's Disease
ANOVA	: Analysis of Variance
COSY	: Correlation spectroscopy
d	: Doublet
dd	: Doublet doublet
DNS	: 3,5-dinitro salicylic acid
DNTB	: 5,5'-dithiobis-(2-nitrobenzoic acid)
Gal	: Galactose
GC-MS	: Gas chromatographic couplet with mass spectroscopy
Glc	: Glucose
Gal	: Galactose
Glu	: Glucuronide
Rut	: Rutinoside
Rhglc	: Rhamnoglucoside
Rhgal	: Rhamnosgalactoside
FRAP	: Ferric Reducing Antioxidant Power
HMBC	: <i>Heteronuclear Multiple Bond Coherence</i>
HSQC	: Heteronuclear Single Quantum Coherence
Hz	: Hertz
IC₅₀	: Inhibitory concentration at 50%
J	: Constante couplage
pNPG	: p-nitrophenyl- α -d-glucoopyranoside
PNP	: P-nitrophenyl
SPSS	: Statistical Package for the Social Sciences
EDTA	: Ethylene diamine tetra-acetic acid

TABLE OF CONTENTS

Content	Page
Acknowledgment	I
Dedication	II
Abstract	III
المخلص	V
Résumé	VII
List of figures	IX
List of tables	XII
Abbreviations list	XIV
Introduction	1
CHAPTER I: BIBLIOGRAPHIC RESEARCH	
I.1 Asteraceae family	5
I.1.1. Generality	5
I.1.2. Chemistry of Asteraceae	5
I.1.3. Botanical description	5
I.1.4. <i>Pulicaria</i>	6
I.1.4.1. <i>Pulicaria laciniata</i>	6
I.1.4.2 Botanical description	6
I.1.4.3 Botanical classification	7
I.2. <i>Pulicaria</i> Secondary metabolism investigation	7
I.2.1. <i>Pulicaria</i> Phytochemical Screening	7
I.2.1.1 Phenol and its derivatives	7
I.2.1.2. Flavonoids and their derivatives	9
I.2.1.3. Terpenoids and their derivatives	13
I.2.1.4. Essential oil	31
I.3. <i>Pulicaria</i> Biological Screening	31
I.3.1. Anti-microbial activities:	31
I.3.2. Antioxidant activity	32
I.3.3. Cytotoxic Activities	33
I.3.4. Other Activities	33
References	34
CHAPTER II: SECONDARY METABOLITES	
II.1 Phenolic compounds generality	40
II.1.2. Simple phenols	41
II.1.3. Phenolic acids	41
II.1.4. Phenolic acids Classification:	41
II.1.5. Phenolic acid derived from benzoic acid	42
II.1.6. Phenolic acids derived from cinnamic acid	42
II.1.7. Biogenesis of simple phenols and phenolic acids	43

II.2. Flavonoids	46
II.2.1. Flavonoids Classification	46
II.2.2. Flavonoids biosynthesis	49
II.3. Terpenoids	51
II.3.1. Biosynthesis of the terpenoids, the voice of the mevalonate	52
References	56
CHAPTER III: PHYTOCHEMICAL SCREENING	
III.1. Materials	59
III.1.1. Plant material	59
III.1.2. Sample preparation	59
III.2. Methods	61
III.2.1. Phytochemical fingerprint	61
III.2.2. Screening of Phytochemicals	61
III.2.3. Quantification of phenolic classes	61
III.2.3.1.1 Total phenol quantification	61
III.2.3.2 Flavonoid quantification	62
III.2.3.3 Tannin quantification	62
III.3 Result	62
III.3.1 Extraction yield	62
III.3.2. Phytochemical fingerprint	63
III.3.3. Phytochemicals screening	65
III.3.4. Quantification of phenolic classes	65
Reference	66
CHAPTER IV: SEPARATION AND PURIFICATION	
IV.1 Fractionation of Ethyl acetate extract	68
IV.2. Fractionation of fraction A	68
IV.3. Fractionation of fraction F	72
IV.4. Fractionation of fraction C and D	72
IV.4.1. Fractionation of sub-fraction F-11 from the separation of fractions C and D	74
IV.4.2. Fractionation of sub-fraction F-14 from the separation of fractions C and D	75
IV.4.3. Fractionation of sub-fraction F-7 from the separation of fractions C and D	75
IV.4.4. Fractionation of sub-fraction F-4 from the separation of fractions C and D	76
IV.5. Gc-MS analyses of the Chloroform extract	77
CHAPTER V: STRUCTURE ELUCIDATION	
V.1. Structure elucidations	80
V.1.1. Structure elucidation of compound K1	80
V.1.2. Structure elucidation of compound K 2	89
V.1.3. Structure elucidation of K3	94
V.1.4. Structure elucidation of K4	100
V.1.5. Structure elucidation of K5	105
V.1.6. Structure elucidation of K6	111

V.2.GC-MS analysis of the Chloroform extract	116
References	119
CHAPTER VI: BIOLOGICAL ACTIVITIES EVALUATION	
VI.2.4 Anti-oxidant activities	121
VI.2.4.1 2,2-azino-bis-3-ethyl benzthiazoline-6-sulfonic acid assay (ABTS • ⁺)	121
VI.2.4.2 1,1-diphenyl-2-picrylhydrazyl (DPPH•) assay	122
VI.2.4.3 2,4,6-tri(2-pyridyl)-1,3,5-triazine FRAP assay	123
VI.2.4.4 Chelating effect on ferrous ions	124
VI.2.4.5 Anti-oxidant capacity	125
VI.2.4.6 Pyrogallol	126
VI.2.5 Enzymatic activities	126
VI.2.5.1 Inhibition of α -amylase	126
VI.2.5.2 Inhibition of α -glucosidase	127
VI.2.5.3 Inhibition of lipase	127
VI.2.5.4 Anti-acetylcholine esterase	128
VI.2.6 Statistical analysis	129
VI.3. Result	129
VI.3.1 Anti-oxidants activity	129
VI.3.1.1 ABTS assay	130
VI.3.1.2 DPPH assay	131
VI.3.1.3 FRAP assay	133
VI.3.1.4 Chelating effect on ferrous ions	134
VI.3.1.5 Anti-oxidant capacity	135
VI.3.1.6 Pyrogallol	136
VI.3.6 Enzymatic activities	137
VI.3.6.1 Inhibition of α -amylase	137
VI.3.6.2 Inhibition of α -glucosidase	139
VI.3.6.3 Inhibition of lipase	139
VI.3.6.4 Inhibition of acetylcholine esterase (Anti-acetylcholine-esterase)	140
VI.4 Discussion	143
VI.4.1 Anti-oxidant activities	143
VI.4.2 Anti-diabetic	146
VI.4.2 Anti-obesity	148
VI.4.3 Anti-acetylcholine –esterase	148
References	150
Conclusion	156

INTRODUCTION

Introduction

Introduction:

Medicinal plants have been used as a medical resource in almost all cultures for millennia: from the Mesopotamian civilization to the present day, including Chinese, Indian, Greek, and Arab civilizations, to treat or prevent illnesses[1]. Pharmacology benefits from this return to nature, finding medicinal plants a new inspiration in the study of medicinal plants, an inexhaustible reservoir of raw materials and models of previously unsuspected and pharmacologically active molecular structures.

Ensuring the safety, quality, and efficacy of medicinal plants and herbal medicines has recently become a key objective in industrialized and developing countries. By standardizing and evaluating the effectiveness of active plant compounds, herbal medicines can contribute to the emergence of a new era of the health system to treat human diseases in the future. Valuing traditional knowledge of medicinal plants can play an important role in exploiting and discovering natural plant resources [2].

One of the most prominent families in the plant kingdom is the Asteraceae family, representing more than 10% of the total number of flowering plants. It contains 21000 species, distributed in most parts of the world, and is found in almost all environments except the South Pole. This species is considered the most important in Algeria because it includes 408 species distributed among 109 genera [3].

The chemistry of the Asteraceae species is characterized by its richness in secondary metabolites distributed among the various tribes. Notably, all species of this family contain flavonoid compounds, most of which contain volatile oils and terpenes, especially lactones and polyacetylenes.

Various studies confirmed the presence of bioactive compounds such as phenolic, flavonoids, alkaloids, terpenoids, tannins, sterols, cardenolides, steroid derivatives, and essential oils in the *Pulicaria* species [4].

Due to these secondary metabolites, *Pulicaria* species exhibited many biological activities such as anti-inflammatory, anti-fungal, anti-diarrheal, hypoglycemic, and anti-oxidant activities to treat chills, diabetes, cardiac disorders, skin diseases, intestinal disorder, and heart disease[5]. Therefore, studies on *Pulicaria* species have become increasingly important in the last few years for the pharmacological industry searching for

Introduction

active, novel, and safe therapeutic agents to treat oxidative reaction diseases and metabolic disorders

Oxidation reactions induced the development of free radicals during cell metabolism and intracellular energy production. Naturally, free radical amounts are controlled due to the scavenging activity of both enzymatic and non-enzymatic antioxidants. Still, the balance is disturbed between the generation and the reduction of free radicals under pathological conditions. The terrified disturbed by the free radicals cause many neurological disorders by adding macromolecules such as lipids, protein, and DNA. Its results in cell damage are related to several diseases, such as diabetes mellitus [6], Alzheimer's disease[7], cancer[8], cardiovascular disorders, arthritis, and inflammatory diseases[9].

In this context, we chose *the P.laciniata* plant as a medicinal plant for our study by highlighting the composition of the *P.laciniata* plant and exploring new secondary metabolites as well as establishing a relationship between the biological activities (antioxidant, anti-diabetic, and anti-Alzheimer's activities) of *P.laciniata* plant and the compounds responsible for these activities.

This thesis has five chapters:

- Chapter one: The botanical and bibliographic study of previous works of *Pulicaria genera*.
- Chapter two: Secondary metabolism study, highlighting their classes and biosynthesis.
- Chapter three: Phytochemical investigation.
- Chapterfour: Separation and purification.
- Chapter Five: Structure elucidation.
- Chapter Six: Clarifying the material and methods used for the phytobiological investigations of the different extracts of *P. laciniata* and the purified compounds.

References

References

1. Hamburger M, Hostettmann K. Bioactivity in plants: the link between phytochemistry and medicine. *Phytochemistry*. 1991;30(12):3864-74.
2. Jamshidi-Kia F, Lorigooini Z, Amini-Khoei H. Medicinal plants: Past history and future perspective. *Journal of herbmed pharmacology*. 2018;7(1):1-7.
3. Quezel, P. and Santa S. Nouvelle flore de l'Algérie et des régions desertiques méridionales. 1963.
4. Dendougui H, Benayache S, Benayache F, Connoly JD. Sesquiterpene lactones from *Pulicaria crispa*. *Fitoterapia*. 2000;71:373-8.
5. Znini M, Cristofari G, Majidi L, Paolini J, Desjobert J, Costa J. Essential oil composition and antifungal activity of *Pulicaria mauritanica* Coss., against postharvest phytopathogenic fungi in apples. *LWT-Food Science and Technology*. 2013;54:564-9.
6. Lappas M, Hiden U, Desoye G, Froehlich J, Mouzon SH-d, Jawerbaum A. The role of oxidative stress in the pathophysiology of gestational diabetes mellitus. *Antioxidants & redox signaling*. 2011;15:3061-100.
7. Dumont M, Beal MF. Neuroprotective strategies involving ROS in Alzheimer disease. *Free Radical Biol Med*. 2011;51:1014-26.
8. Lau AT, Wang Y, Chiu JF. Reactive oxygen species: current knowledge and applications in cancer research and therapeutic. *J Cell Biochem*. 2008;104:657-67.
9. Gelderman KA, Hultqvist M, Olsson LM, Bauer K, Pizzolla A, Olofsson P, et al. Rheumatoid arthritis: the role of reactive oxygen species in disease development and therapeutic strategies. *Antioxidants & Redox Signaling*. 2007;9:1541-68.

CHAPTER I
BIBLIOGRAPHIC
RESEARCH

I.1 Asteraceae family:

I.1.1. Generality:

The word Asteraceae (Compositae) is one of the most influential families of angiosperms. It designates a family of compounds belonging to dicotyledons comprising more than 1300 genera and more than 21000 species, including 750 endemics[1]. In Algeria, this family has about 109 genera and more than 408 species, sixteen species in Algeria, (*P. odora* (L), *P. dysenterica* (L), *P. filaginoids* Pomel , *P. mauritanica* Coss, *P. arabica* (L) *P. sicula* (L), *P. vulgaris* Gaerth, *P. lothei* M , *P. volskonskyana* M, *P. Geraeca* (Sch.Bip) , *P. radiata* (DC), *P. polmelia* (F et M),) including 4 of them in the desert. *P. undulata* (L), *P. inuloides* DC, *P. crispera*-Shults, *P. laciniata* (Cross.Kral), *Pulicaria laciniata*, the chosen one for our study[2].

I.1.2. Chemistry of Asteraceae:

The chemistry of the Compositae species is characterized by its richness in secondary metabolites distributed to the various tribes. Almost all species of this family contain flavonoid compounds and volatile oils. The presence of unique structural models for two types of natural compounds, namely terpenes and polyacetylenes, also this family is characterized by the absence of non-protein amino acids and the absence of the main sections of the alkaloids. More than 90 of the known sesquiterpene compounds belong to this family. It is the same for polyacetylenes; more than 90 known polyacetylenes exist in the Compositae family. Some of these compounds have properties that stop bacteria and inhibit the growth of fungi. They also participate in the pharmaceutical activities of some drugs [3].

I.1.3. Botanical description:

This family has various morphological characteristics: annual or perennial herbs, rare shrubs, trees or climbing plants, and sometimes fleshy plants[4]. Although usually, they are herbaceous plants with isolated leaves[5]. The aspect of the vegetative system is too variable to characterize Asteraceae on this criterion alone. On the other hand, this family is homogeneous in its inflorescences characteristics in the capitulum.

Asteraceae flowers are always grouped in an inflorescence (group of flowers on the same stem) called a head or capitulum that functions as a single flower. Half of the species, the small central flowers, are tubular, shaped like tiny disks so that those of the periphery

have corollas in the form of tongues flared towards the outside, like so many petals attract pollinating insects. The base of bracts surrounds the corollas. The calyx (or Pappus) of each flower is formed of scales or long hairs, favouring the dispersion of the seeds. The Pappus consists of fine egrets in dandelions that allow the fruit to float in the breeze [6-8].

The petals of the flower heads are welded at the base into a tubular corolla. The anthers join to form a tube that crosses the style (middle part of the pistil between the ovary and the stigma). The anthers discharge the pollen into the tube, and the style lengthens to push the pollen out of the pollen tube and make it accessible to pollinating insects or facilitate its dispersion by the wind.

The stigma (upper part of the pistil receiving the pollen) retracts after the lengthening of the style to avoid self-pollination, which sometimes happens when the stigma curls into the pollen tube. After fertilization, the pistil carrying the flower's ovary and other floral elements develops to form a hard-shell, single-seeded fruit [6,8]. The fruit is an achene generally surmounted by a Pappus from the calyx.

I.1.4. *Pulicaria*:

I.1.4.1. *Pulicaria laciniata*:

The species of *Pulicaria* are either perennial herbs or small sub-shrubs with leaves alternate, sessile, more or less lanceolate, and margin entire, toothed, or shredded. They have flower heads consisting of yellow flowers, the central hermaphroditic tubules, and anthers are swollen at the base, often branched, the other ligulated female peripherals, whose ligules are either well marked and spread out or erect and barely exceeding the involucre. The involucre is formed of narrow bracts on a few rows, the outer short and foliaceous, sometimes scarious interior.

I.1.4.2 Botanical description:

Pulicaria laciniata named also *francoeuria laciniata* (Cross. and kral.) Leaves , glabrescent or hairy, short, Capitulum bigger (Capitules plus gros), , Ligules clearly radiant (Ligules nettement radiantes). Woolly, whitish stems (Tiges laineuses, blanchâtres), High terminal capitula (Capitules en corymbe terminal). Akenas with feathery hairs all along their length (Akenes à poils de l'aigrette plumeux sur toute leur longueur), annual or

perennial plant. Temporarily flooded places endemic in Algeria: Biskra – Laghouat et Ghardaia and South-Tunisia [2].



Figure1: Geographic distribution map *P. laciniata* [2].

I.1.4.3. Botanical classification:

Kingdom: Planta

Branch: Spermatophytæ

Under Branch: Angiospermae

Class: Dicotyledones

Order: Campanula

Family: Compositae

Under family: Tubuliflorae

Tribe: Inuleae

Genera: *Pulicaria*

Specie: *Pulicaria laciniata* (Cross. and kral.)

I.2. *Pulicaria* Secondary metabolites investigation:

I.2.1 *Pulicaria* Phytochemical Screening:

I.2.1.1. Phenol and its derivatives:

Table 1: Phenol and its derivatives compound separated from different *Pulicaria* species.

N°	Phenolic names	References
1	Benzoic acid	<i>P.angustifolia</i> [9]
2	p-Hydroxybenzoic acid	<i>P. paludosa</i> [10]
3	Veratric acid	<i>P. paludosa</i> [11]
4	Anisic acid	<i>P. paludosa</i> [11]
5	p-Methoxyacetophenone	<i>P. paludosa</i> [11]
6	1-Acetyl-2-hydroxy-4,6-dimethoxybenzene	<i>P.incisa</i> [12] <i>P.arabica</i> [13]
7	Caffeic acid	<i>P.dysenterica</i> [14]
8	Eugenol	<i>P. paludosa</i> [10]
9	Cinnamic acid	<i>P. paludosa</i> [10]
10	1,3,5-trimethoxybenzene	<i>P.laciniata</i> [15]
11	5-Hydroxy-2-methyl-2,3-dihydro-4H-chromen-4-one	<i>P.Wightiana</i> [16]
12	2-hydroxy-4,6-dimethoxyacetophenone	<i>P.incisa</i> [17]

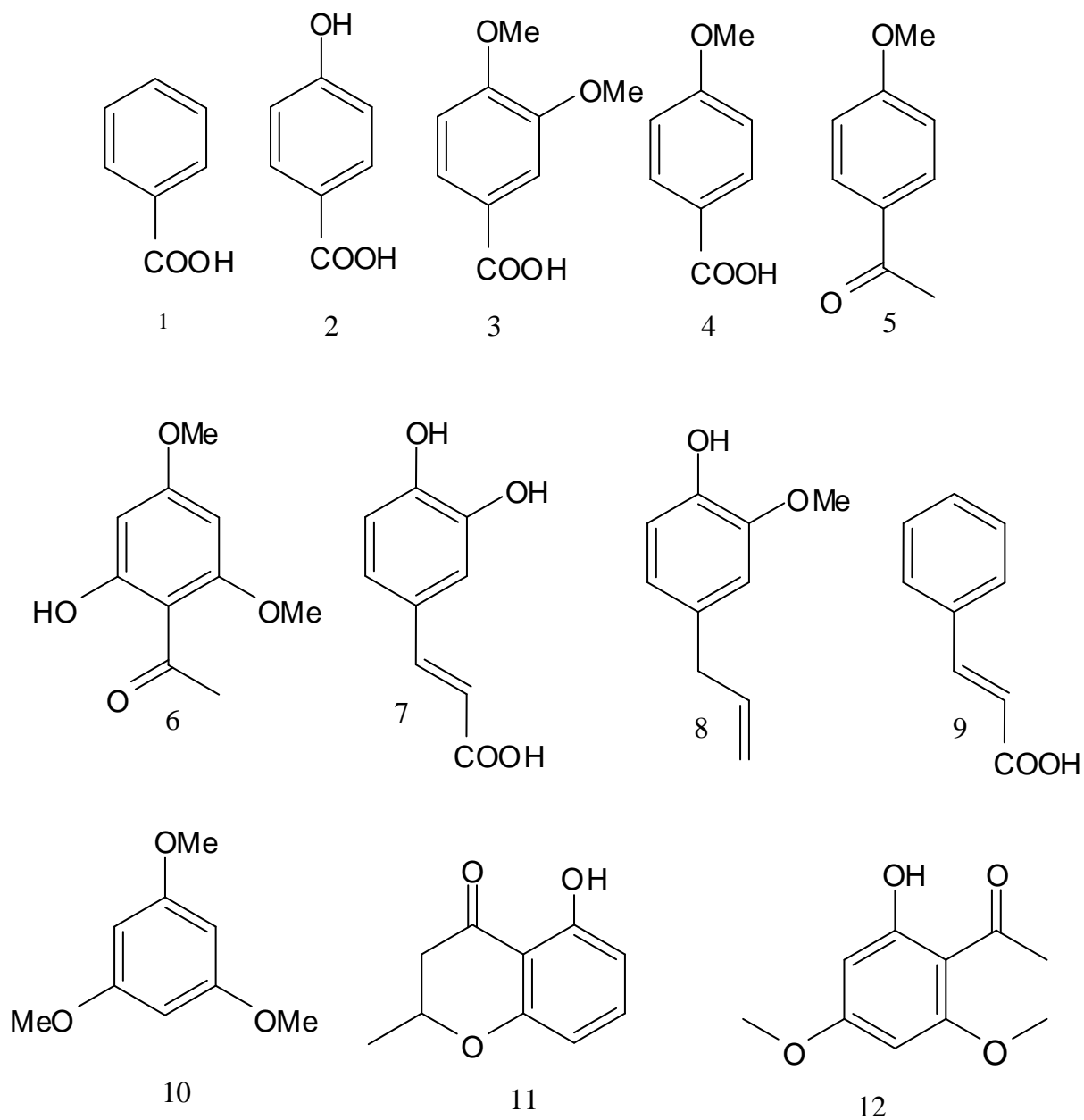


Figure 2: chemical structure of phenol and its derivatives compound separated from different *Pulicaria* species.

I.2.1.2. Flavonoids and their derivatives:

Table 2: Flavonoids and their derivatives compounds separated from different *Pulicaria* species

N°	Flavonoid Name	References
13	Quercetin	<i>P. crisp</i> [18] <i>P. orientalis</i> [19] <i>P. incisa</i> [20] <i>P. arabica</i> [21]
14	Quercetin -3-methylether	<i>P. crisp</i> [18] <i>P. orientalis</i> [19] <i>P. incisa</i> [12, 20] <i>P. arabica</i> [21]
15	Quercetin -3'-methylether	<i>P. arabica</i> [22]
16	Quercetin -7-methylether (Rhamnetin)	<i>P. undulata</i> [22]
17	Quercetin -3,7-dimethylether	<i>P. undulata</i> [22, 23] <i>P. insica</i> [20] <i>P. arabica</i> [13]
18	Quercetin -3,3'-dimethylether	<i>P. incisa</i> [12, 20]
19	Quercetin -3-glucoside	<i>P. crisp</i> [18] <i>P. orientalis</i> [19] <i>P. incisa</i> [20] <i>P. arabica</i> [21]
20	Quercetin -3-galactoside	<i>P. insica</i> [20]
21	Quercetin -3-glucuronide	<i>P. arabica</i> [21] <i>P. dysenterica</i> [24]
22	Quercetin -7-glucoside	<i>P. crisp</i> [18]. <i>undulata</i> [22]
23	Rhamnetin -3-galactoside	<i>P. crisp</i> [25]
24	Quercetin -7-glucuronide	<i>P. sicula</i> [26]
25	Quercetin -3-rutinoside	<i>P. paludosa</i> [26]
26	Quercetin -3-rhamnoglucoside	<i>P. paludosa</i> [26] <i>P. salviifolia</i> [27]
27	Isorhamnetin -3-glucoside	<i>P. paludosa</i> [26]
28	Isorhamnetin -3-galactoside	<i>P. paludosa</i> [26]
29	Isorhamnetin -3-rhamnoglucoside	<i>P. paludosa</i> [26]
30	Isorhamnetin -3-rhamnogalactoside	<i>P. paludosa</i> [26]
31	Dihydrokaempferol	<i>P. orientalis</i> [19] <i>P. arabica</i> [13] <i>P. undulata</i> [23]
32	Dihydrokaempferol -7-methylether	<i>P. undulata</i> [28]
33	7-methy ether taxifoline	<i>P. undulata</i> [23, 28] <i>P. incisa</i> [20]
34	Dihydroquercetin	<i>P. arabica</i> [13] <i>P. undulata</i> [23]
35	Dihydroquercetine -7-methyether	<i>P. undulata</i> [23] <i>P. incisa</i> [20]
36	Dihydroquercetine -7,3'-dimethyether	<i>P. canariensis</i> [29] <i>P. undulata</i> [23]
37	Dihydrokaempferole -7,4'-dimethylether	<i>P. canariensis</i> [29]
38	Aromadendrine	<i>P. incisa</i> [17]
39	7-O-Methyaromadendrine	<i>P. undulata</i> [23, 28] <i>P. incisa</i> [12]
40	Undulatoside	<i>P. undulata</i> [23]
41	Eriodictyol -7-methylether	<i>P. undulata</i> [28]
42	Pulichalcanoid B	<i>P. incisa</i> [30, 31]
43	Pulichalcanoid C	<i>P. incisa</i> [31]
44	Quercetagetin -3,7-dimethylether	<i>P. arabica</i> [21] <i>P. dysenterica</i> [32]

45	Quercetagetin -3,6-dimethylether(Axillarine)	<i>P.undulata</i> [33] <i>P.crisp</i> [34]
46	Quercetagetin -3',4'-dimethylether	<i>P.arabica</i> [35]
47	Quercetagetin -3,7,3'-trimethylether	<i>P.dysenterica</i> [24]
48	Quercetagetin -3,6,7-trimethylether	<i>P.somalensis</i> [36]
49	Quercetagetin-3,7,4'-trimethylether	<i>P.dysenterica</i> [14]
50	Quercetagetin -3,5,7-trimethylether	<i>P.arabica</i> [21]
51	Quercetagetin -3,5,7,3'-tetramethylether	<i>P.arabica</i> [21]
52	Quercetagetin -3,6,7,3'-tetramethylether	<i>P.somalensis</i> [36]
53	Quercetagetin -3,6,7,4'-tetramethylether	<i>P.somalensis</i> [36]
54	Quercetagetin -3,7,3',4'-tetramethylether	<i>P.arabica</i> [35]
55	Quercetagetin 3,5,6,7,3' pentamethylether	<i>P.arabica</i> [35]
56	Quercetagetin 3,5,6,7,4' pentamethylether	<i>P.dysenterica</i> [24]
57	Quercetagetin -7-glucoside -6-methylether (Patuletin7-glucoside)	<i>P.odora</i> [26]
58	Kaempferol	<i>P.crispa</i> [37] <i>P.orientalis</i> [19] <i>P.incisa</i> [12] <i>P.arabica</i> [13]
59	Kaempferol -3-methylether	<i>P.orientalis</i> [19] <i>P.incisa</i> [12, 26] <i>P.arabica</i> [13] <i>P.undulata</i> [23]
60	Kaempferol -7-methylether (Rhamnocitrin)	<i>P.undulata</i> [22]
61	Kaempferol -3-glucoside (Trifoliine)	<i>P.incisa</i> [20] <i>P.dysenterica</i> [14, 24]
62	Kaempferol -3-galactoside	<i>P.incisa</i> [20]
63	Kaempferol -3,7-methylether	<i>P.orientalis</i> [19] <i>P.arabica</i> [13]
64	Kaempferol -6-methylether	<i>P.undulata</i> [33]
65	Kaempferol -3-glucoside 6-methoxy	<i>P.undulata</i> [33]
66	Kaempferol -7-glucoronide -3-methylether -6-hydroxy	<i>P.odora</i> [26]
67	Kaempferol -6-glucoside 3-methylether	<i>P.dysenterica</i> [32]
68	Kaempferol -3,7-dimethylether -6-hydroxy	<i>P.dysenterica</i> [24, 32]
69	Kaempfero -3,6- dimethyletherl	<i>P.paludosa</i> [38]
70	Kaempferol -3,6,7-trimethylether	<i>P.dysenterica</i> [32]
71	Kaempferol -3,7,4'-trimethylether 6-hydroxy	<i>P.dysenterica</i> [24]
72	Scutellarine	<i>P.dysenterica</i> [32]
73	Scutellarine -7,4'-dimethylether	<i>P.paludosa</i> [38]
74	Ladanetine	<i>P.uliginosa</i> [39]
75	Pulicaroside	<i>P.undulata</i> [33]
76	5,6-Dihydroxy-7,4'-dimethoxyflaone	<i>P.paludosa</i> [38]
77	5,6,8-trihydroxy-7,4'-dimethoxyflaone	<i>P.paludosa</i> [38]
78	5,7-dihydroxy-3,3',4'-trimethoxyflvone	<i>P.canariensis</i> [29]
79	6,3'-dihydroxy-3,5,7,4'-tetramethoxyflvone	<i>P.salviifolia</i> [40]
80	4'-Hydroxy-3,5,6,7,3'-pentamethoxyflavone	<i>P.arabica</i> [35]
81	3,5,6,7,3',4'-Hexamethoxyflavone	<i>P.arabica</i> [35]
82	5,6,3'-trihydroxy-3,7,4'-trimethoxyflavone	<i>P.wightiana</i> [16]

	R ₁	R ₂	R ₃	R ₄	R ₅	R ₆
13	OH	OH	H	OH	OH	OH
14	OMe	OH	H	OH	OH	OH
15	OH	OH	H	OH	OMe	OH
16	OH	OH	H	OMe	OH	OH
17	OMe	OH	H	OMe	OH	OH
18	OMe	OH	H	OH	OMe	OH
19	O-Glc	OH	H	OH	OH	OH
20	O-Gal	OH	H	OH	OH	OH
21	O-Glu	OH	H	OH	OH	OH
22	OH	OH	H	O-Glc	OH	OH
23	O-Gal	OH	H	OMe	OH	OH
24	OH	OH	H	O-Glu	OH	OH
25	O-Rut	OH	H	OH	OH	OH
26	O-Rhglc	OH	H	OH	OH	OH
27	O-Glc	OH	H	OH	OMe	OH
28	O-Gal	OH	H	OH	OMe	OH
29	O-Rhglc	OH	H	OH	OMe	OH
30	O-Rhgal	OH	H	OH	OMe	OH
44	OMe	OH	OH	OMe	OH	OH
45	OMe	OH	OMe	OH	OH	OH
46	OH	OH	OH	OH	OMe	OMe
47	OMe	OH	OH	OMe	OMe	OH
48	OMe	OH	OMe	OMe	OH	OH
49	OMe	OH	OH	OMe	OH	OMe
50	OMe	OMe	OH	OMe	OH	OH
51	OMe	OMe	OH	OMe	OMe	OH
52	OMe	OH	OMe	OMe	OMe	OH
53	OMe	OH	OMe	OMe	OH	OMe
54	OMe	OH	OH	OMe	OMe	OMe
55	OMe	OMe	OMe	OMe	OMe	OH
56	OMe	OMe	OMe	OMe	OH	OMe
57	OH	OH	OMe	O-Glc	OH	OH
58	OH	OH	H	OH	H	OH
59	OMe	OH	H	OH	H	OH
60	OH	OH	OMe	H	H	OH

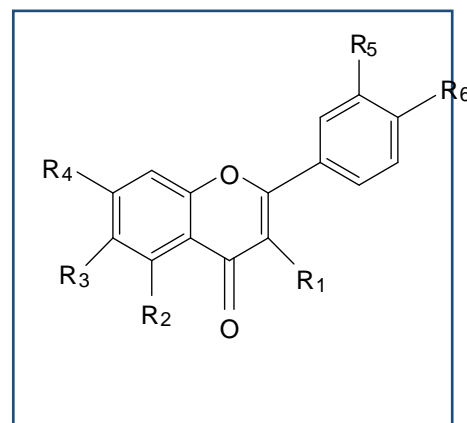
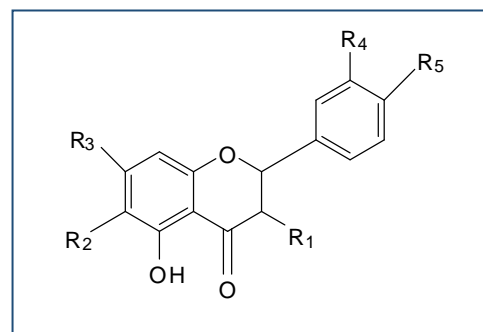


Figure 3: Chemical Structure of flavonoids and their derivatives compound separated from different *Pulicaria* species.

	R ₁	R ₂	R ₃	R ₄	R ₅
31	OH	H	OH	H	OH
32	OH	H	OMe	H	OH
33	OH	H	OMe	OH	OH
34	OH	H	OH	OH	OH
35	OH	H	OMe	OH	OH
36	OH	H	OMe	OMe	OH
37	OH	H	OMe	OH	OMe



	R ₁	R ₂	R ₃	R ₄	R ₅	R ₆
61	O-gal	OH	H	OH	H	OH
62	O-Gal	OH	H	OH	H	OH
63	OH	OMe	H	OMe	H	OH
64	OH	OMe	OH	OH	H	OH
65	O-Glc	OH	OMe	OH	H	OH
66	OH	OH	OMe	O-Glc	H	OH
67	OMe	OH	O-Glc	OH	H	OH
68	OMe	OH	OH	OMe	H	OH
69	OMe	OH	OMe	OH	H	OH
70	OMe	OH	OMe	OMe	H	OH
71	OMe	OH	OH	OMe	H	OMe
72	H	OH	OH	OH	H	OH
73	H	OH	OH	OMe	H	OMe
74	H	OH	OH	OMe	H	OMe
76	H	OH	OH	OMe	OMe	OH
78	OMe	OH	H	OH	OMe	OMe
79	OMe	OMe	OH	OMe	OH	OMe
80	OMe	OMe	OMe	OMe	OMe	OH
81	OMe	OMe	OMe	OMe	OMe	OMe
82	OMe	OH	OH	OMe	OMe	OH

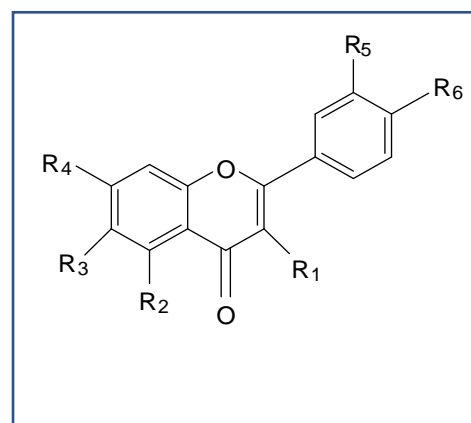


Figure 4: Chemical Structure of flavonoids and its derivatives compound separated from different *Pulicaria* species.

I.2.1.3. Terpenoids and their derivatives:

Table 3: Monoterpene and Germacrans compounds separated from different *Pulicaria* species.

N°	Monoterpene compounds	References
83	2-Isopropyl-4-methylphenol	<i>P. odora</i> [16]
84	2-Isopropyl-4-methylphenol isobutyrate	<i>P. odora</i> [16]
85	Thymol	<i>P. arabica</i> [41]
86	Thymol isobutyrate	<i>P. arabica</i> [41]
87	10-(Isobutyryloxy)-8,9-didehydrothymol isobutyrate	<i>P. sicula</i> [42]
88	10-(Isobutyryloxy)-8,9-epoxythymol isobutyrate	<i>P. sicula</i> [42] <i>P. dysenterica</i> [43,44] <i>P. arabica</i> [41]
89	4-Isopropyl-3-methoxybenzyl isobutyrate	<i>P. dysenterica</i> [43, 44]
90	4-Hydroxy-2-isopropyl-5-methylphenyl acetate	<i>P. undulata</i> [23, 28]
91	2-Methyl-5-(propan-2-yl)cyclohex -2-enone (Carvotanacetone)	<i>P. undulata</i> [23]
92	3-Methyl-6-(propan-2-yl)cyclohex-3-enone	<i>P. undulata</i> [28]
Germacrans compounds		
93	Pulicanadiene A	<i>P. canariensis</i> [29]
94	Pulicanadiene B	<i>P. canariensis</i> [29]
95	Pulicanadiene C	<i>P. canariensis</i> [29]
96	Pulicanone	<i>P. canariensis</i> [29]
97	Pulicanol	<i>P. canariensis</i> [29]
98	Pulicanaral A	<i>P. canariensis</i> [29]
99	Pulicanaral B	<i>P. canariensis</i> [29]
100	Pulicanaral C	<i>P. canariensis</i> [29]
101	Pulicanadienal A	<i>P. canariensis</i> [29]
102	Pulicanadienal B	<i>P. canariensis</i> [29]
103	Pulicanadienol	<i>P. canariensis</i> [29]
104	Puliglene	<i>P. glutinosa</i> [45]
105	Epoxyguliglene	<i>P. glutinosa</i> [45]

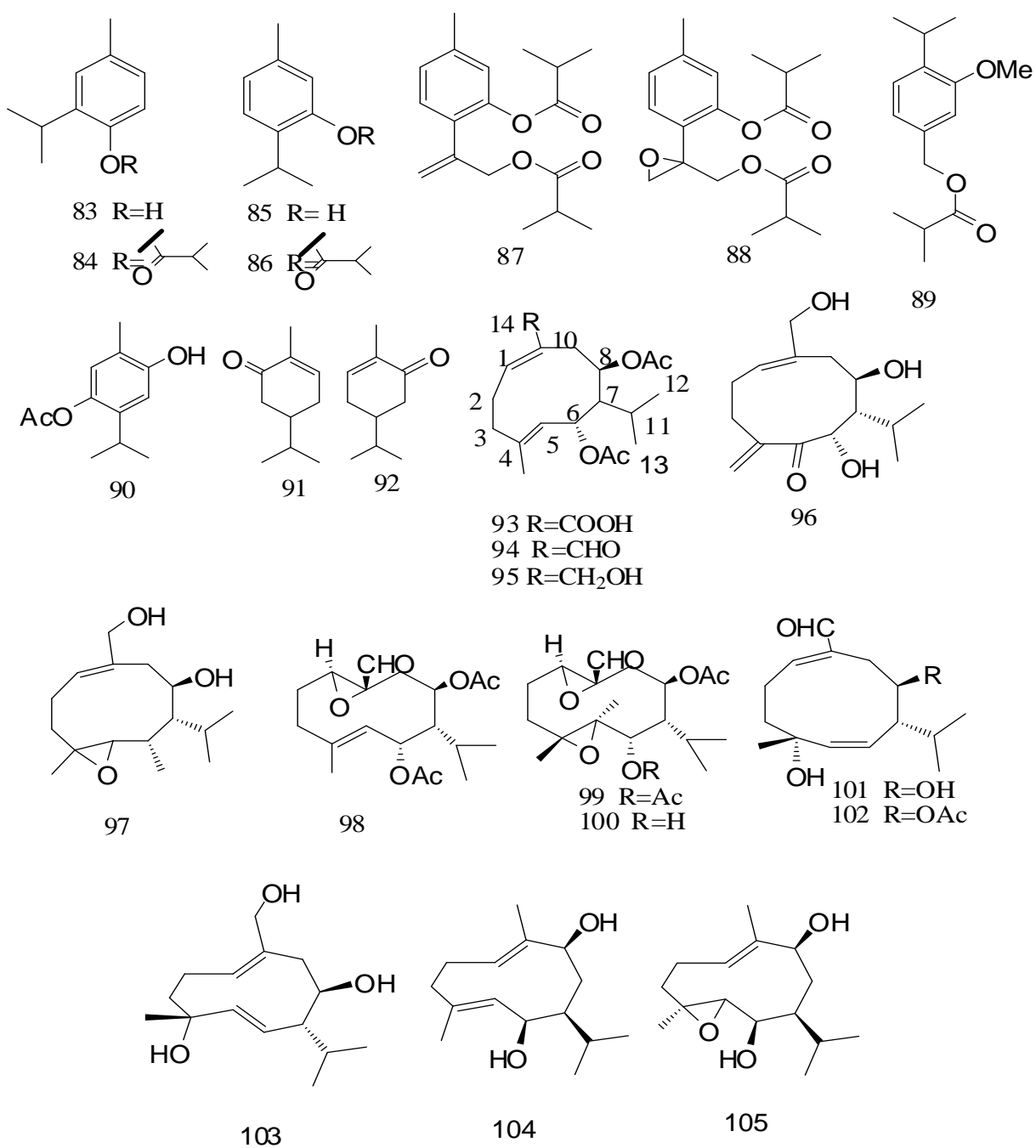


Figure 5: Monoterpene and Germacrans compound separated from different *Pulicaria* species.

Table 4: Xanthanolides and guaianolids compounds separated from different *Pulicaria* species.

N°	Xanthane and its derivatives	References
106	8-Epixanthatine	<i>P.crispa</i> [46, 47] <i>P.sicula</i> [42]
107	Xanthatine	<i>P.crispa</i> [46, 47] <i>P.undulata</i> [42]
108	Xanthinosine	<i>P.crispa</i> [46, 47], <i>P.sicula</i> [42]
109	Tomentosine	<i>P.crispa</i> [46, 47] <i>P.sicula</i> [42]
110	7 α H,8 α H,10 α H-2-Hydroxy-4-oxoxanth-11(13)-en-12,8 β -olide	<i>P.sicula</i> [42] <i>P.incisa</i> [48]
111	7 α H,8 β H,10 α H-2-Hydroxy-4-oxoxanth-11(13)-en-12,8 α -olide	<i>P.sicula</i> [42] <i>P.crispa</i> [47]
112	7 α H,8 α H,10 α H-1 β ,5 β -Epoxy-4-oxoxanth-11(13)-en-12,8 β -olide	<i>P.sicula</i> [42] <i>P.incisa</i> [48]
113	7 α H,8 α H,10 α H-2,4-Diacetoxanth-11(13)-en-12,8 β -olide(acetate Grafin)	<i>P.crispa</i> [46, 47]
114	7 α H,8 α H,10 α H-4-Hydroxy-2-acetoxanth-11(13)-en-12,8 β -olide	<i>P.crispa</i> [47]
115	7 α H, 8 α H,10 α H-2-Hydroxy-4-acetoxanth-11(13)-en-12,8 β -olide	<i>P.crispa</i> [47]
116	7 α H,8 α H,10 α H-4-Hydroxyxanth-11(13)-en-12,8 α -olide(Desacetylc xanthanole)	<i>P.crispa</i> [46, 47]
117	7 α H,8 α H,10 α H-4-Hydroxy-2-acetoxanth-11(13)-en-12,8 α -olide	<i>P.crispa</i> [46]
118	7 α H,8 α H,10 α H-2-Hydroxy-4-acetoxanth-11(13)-en-12,8 α -olide	<i>P.crispa</i> [46]
119	7 α H,8 α H,10 α H-2,4-Diacetoxanth-11(13)-en-12,8 α -olide(acetate Xanthanole)	<i>P.crispa</i> [46]
Guaianolids		
120	1,2-Dehydro-1,10 α -dihydropseudoivaline	<i>P.crispa</i> [47, 49, 50] <i>P.sicula</i> [42]
121	5 α H-4 β ,10 β -Dihydroxyguaia-1(2),11(13)-dien-12,8 α -olide	<i>P.crispa</i> [49]
122	Gaillardin	<i>P.uliginosa</i> [39]
123	5 α H-4 α -Hydroxyguaia-1(10),11(13)-dien-12,8 α -olide	<i>P.crispa</i> [49] <i>P.sicula</i> [42]
124	7 α H,8 α H,10 α H-2 α ,4 α -Dihydroxyguaia-1(5),11(13)-dien-12,8 β .olide	<i>P.crispa</i> [50]
125	5 α H-1 β ,4 β -Dihydroxyguaia-10(14),11(13)-dien-12,8 α -olide	<i>P.crispa</i> [49]

126	5 α H-1 β ,4 β -Diacetoxypuaia-10(14),11(13)-dien-12,8 α -olide	<i>P.crispa</i> [49]
127	1 α H,5 α H-4 α -Hydroxyguai-11(13)-en-12,8 α -olide	<i>P.incisa</i> [48]
128	5 α H,4 α -Hydroxy--guaia-10(14),11(13)-dien-12,8 β -olide	<i>P.crispa</i> [47] <i>P.sicula</i> [42] <i>P.incisa</i> [48]
129	5 α H-4 α -Hydroxyguaia-10(14),11(13)-dien-12,8 α -olide	<i>P.crispa</i> [47]
130	5 α H,7 α H,8 α H,10 α H-1 α ,2 α -epoxy-4 β -hydroxyguai-11(13)- en-12,8 β -olide	<i>P.crispa</i> [50]
131	5 α H,7 α H,8 α H,10 α H-1 α ,2 α -epoxy-4 α -hydroxyguai-11(13)- en-12,8 β -olide	<i>P.sicula</i> [42]
132	1 α H,10 α H-11-Hydroxy-4 α ,5 α -epoxy-13-norguai-7(11)-en-12,8 α -olide	<i>P.undulata</i> [28]
133	1 α H,10 α H-4 α ,5 α -epoxyguai-11(13)-en-12,8 α -olide	<i>P.laciniata</i> [51]
134	Liguloxid-3 β -ol	<i>P.paludosa</i> [38]
135	Liguloxid-3-one	<i>P.paludosa</i> [38]
136	Cycloepoxypuliglene	<i>P.glutinosa</i> [52]

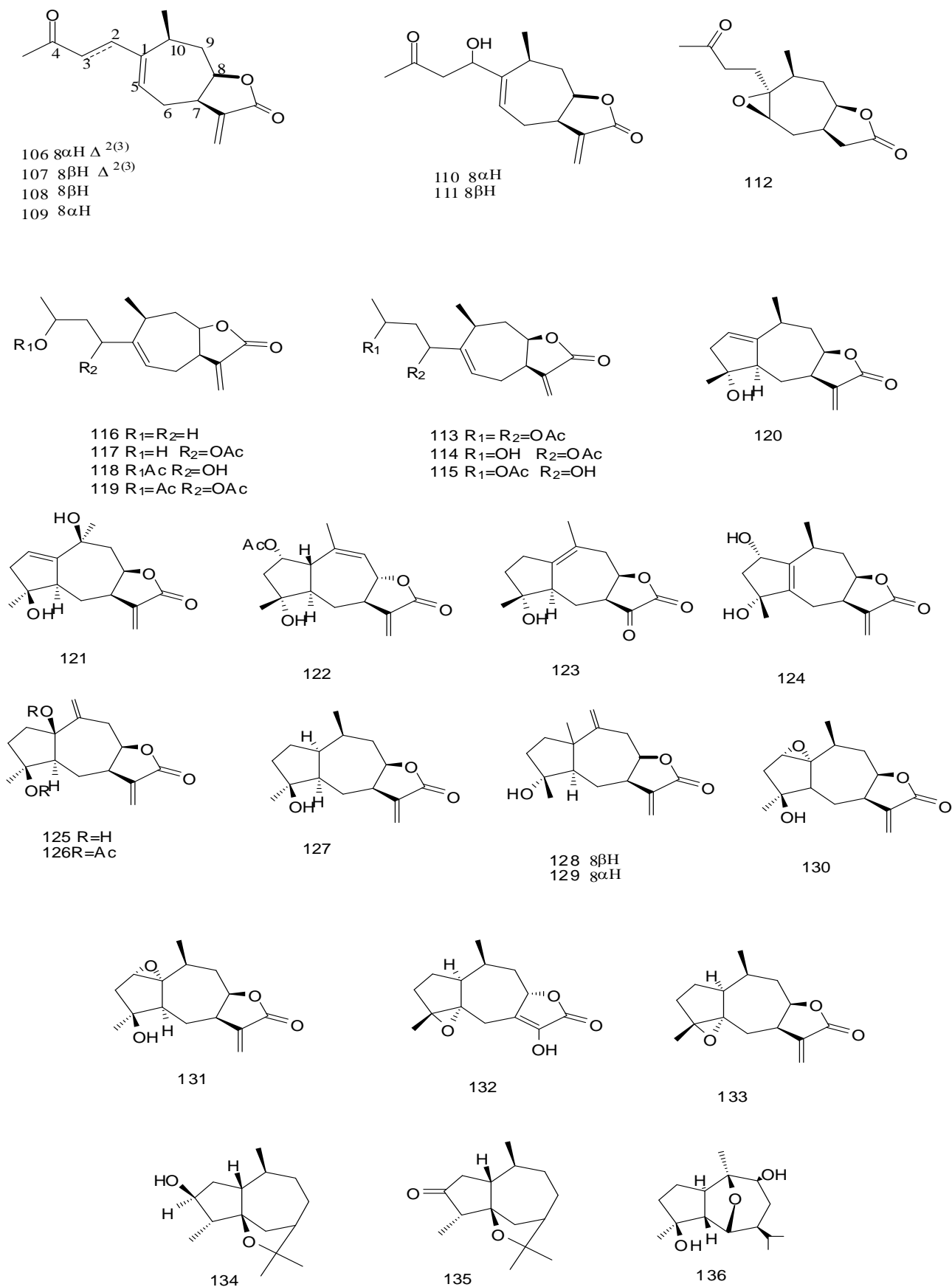


Figure 6: Xanthanolids and Guaianolids compounds that separated from different species of *Pulicaria* genera

Table 5: Pseudoguaianolides and Eudesmanes compounds separated from different *Pulicariagenera* species.

N°	Pseudoguaianes	References
137	8-Epiconfertine	<i>P.crispa</i> [47] <i>P.undulata</i> [53] <i>P.laciniata</i> [51]
138	5,10-epi-2,3-dihydroaromatin	<i>P.crispa</i> [50]
139	10 α -Hydroxy-8-epiconfertine	<i>P.crispa</i> [47]
140	Pulicariolide	<i>P.crispa</i> [46]:[47] <i>P.paludosa</i> [38]
Eudesmanes		
141	2 α -Hydroxyalantolactone	<i>P.crispa</i> [34] <i>P.undulata</i> [53]
142	2 α Hydroxyeudesma-4(5),11(13)-dien-12,8 β -olide	<i>P.undulata</i> [53]
143	Glaucolide	<i>P.undulata</i> [53]
144	2 α -Hydroxy-5 α ,6 α -epoxyalantolactone	<i>P.crispa</i> [34]
145	1 β ,4 β -Dihydroxy-6,15 α -epoxyeudesmane	<i>P.canariensis</i> [29]
146	Oplodirole	<i>P.paludosa</i> [41]
147	Isoplodirole	<i>P.paludosa</i> [43]

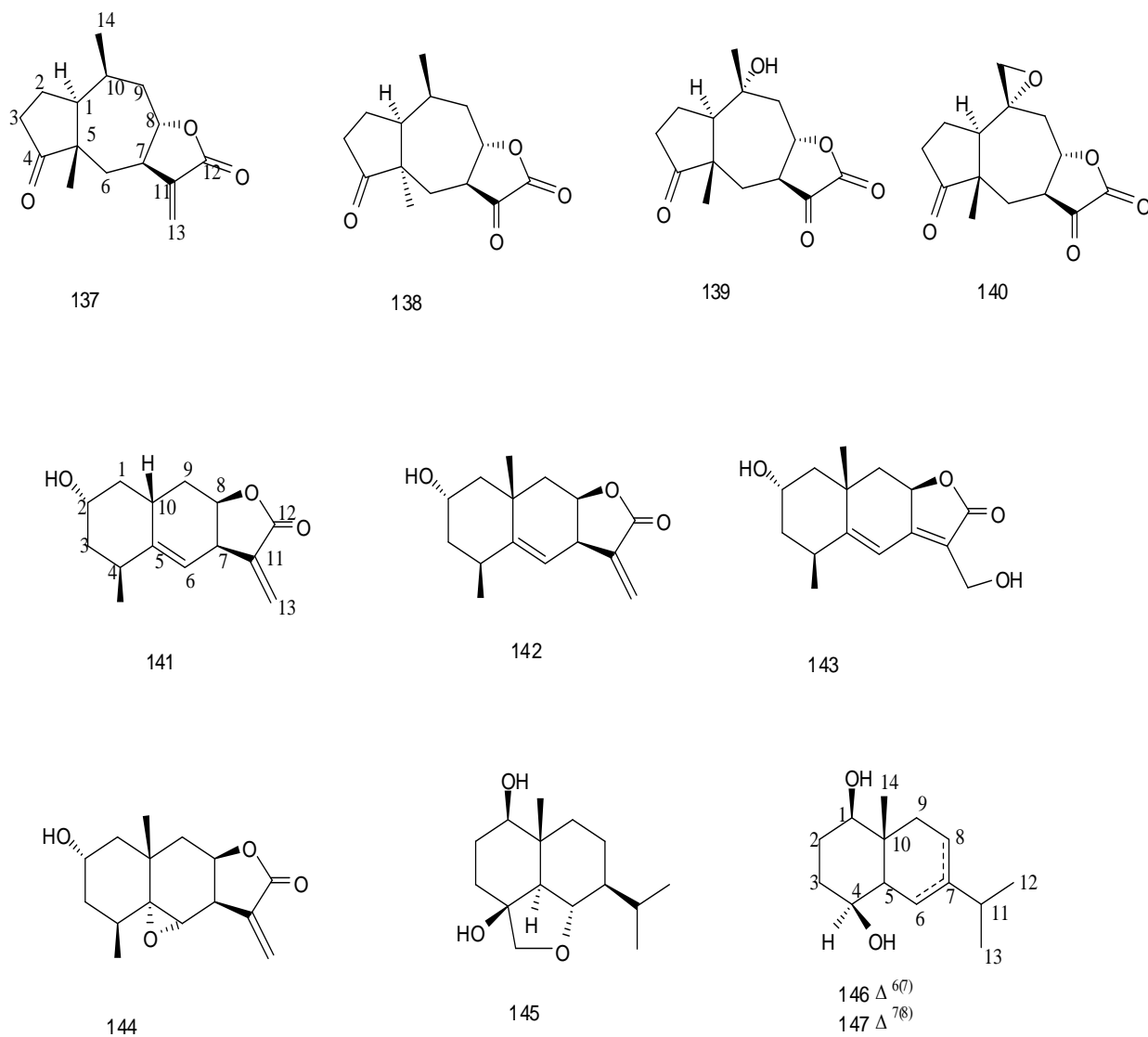


Figure 7: Pseudoguaianolides and Eudesmanes compounds separated from different *Pulicaria* genera species.

Table 6: Caryophyllans compounds separated from different *Pulicaria* species.

N°	Caryophyllanes	References
148	Buddledine C	<i>P.prostrata</i> [54]
149	Caryophyllanes	<i>P.paludosa</i> , [38] <i>P.dysenterica</i> [43]
150	Caryophyllene epoxyde	<i>P.angustifolia</i> [9]
151	(5Z)-12-Hydroxy-14-isobutanoyloxy caryophylla-2(15),5-dien-7-one	<i>P.paludosa</i> [38]
152	(5Z)-12-Hydroxy-14-(2methypropanoxy) caryophylla-2(15),5-dien-7-one	<i>P.paludosa</i> [38]
153	(1S,5Z,9R)-12,14-Diacetoxycaryophylla-2(15),5-dien-7-one	<i>P.dysenterica</i> [43] <i>P.arabica</i> [41]
154	(1S,5Z,9R,11S)-14-Methoxy-1acetoxycaryophylla-2 (15),5-dien-7-one	<i>P.dysenterica</i> [43]
155	(1S,5E,9R,11S)-14-Methoxy-12acetoxycaryophylla-2 (15),5-dien-7-one	<i>P.dysenterica</i> [43] <i>P..arabica</i> [41]
156	(1S,5Z,9R)-12-Acetoxy-14-hydroxycaryophylla-2(15),5-dien-7-one	<i>P.dysenterica</i> [43] <i>P.arabica</i> [41] <i>P.paludosa</i> [38]
157	(5Z)-14-Acetoxycaryophyllene-7-one	<i>P.arabica</i> [41] <i>P.scabra</i> [55] <i>P.paludosa</i> [38]
158	(5Z)-14-Hydroxycaryophyllene-7-one	<i>P.arabica</i> [41] <i>P.dysenterica</i> [43] <i>P.scabra</i> [55] <i>P.paludosa</i> [38]
159	(1S,5Z,9R)-12-Hydroxy-14-acetoxycaryophylla-2(15),5-dien-7-one	<i>P.arabica</i> [41] <i>P.dysenterica</i> [43]
160	(1S,5Z,9R)-14-Methoxycaryophylla-2(15),5-dien-7-one	<i>P.dysenterica</i> [43]
161	(1S,5Z,9R)-12,14-Dihydroxycaryophylla-2(15),5-dien-7-one	<i>P.dysenterica</i> [43] <i>P.paludosa</i> [38]
162	(1S,9R)-7βH-12-Acetoxycaryophylla-2(15),5E-diene-7,14-diol	<i>P.arabica</i> [41] <i>P.dysenterica</i> [43]
163	(1S,9R)-5αH-5,12-Dihydroxycaryophylla-2(15),6(14)-dien-7-one	<i>P.arabica</i> [41] <i>P.dysenterica</i> [43]
164	5αH-12-Hydroxy-5-methoxycaryophylla-2(15),6(14)-dien-7-one	<i>P.arabica</i> [41]
165	5αH-12-Acetoxy-5-methoxycaryophylla-2(15),6(14)-dien-7-one	<i>P.arabica</i> [41] <i>P.dysenterica</i> [43]
166	5βH-12-Acetoxy-5-methoxycaryophylla-2(15),6(14)-dien-7-one	<i>P.arabica</i> [41] <i>P.dysenterica</i> [43]

167	5 β H-5,12-dihydroxycaryophylla-2(15),6(14)-dien-7-one	<i>P.paludosa</i> [38] <i>P.arabica</i> [41]
168	5 β H-5-Methoxycaryophylla-2(15),6(14)-dien-7-one	<i>P.dysenterica</i> [43]
169	5 α H-5-Methoxycaryophylla-2(15),6(14)-dien-7-one	<i>P.dysenterica</i> [43]
170	(1S,5S,6S,9R,11S)-5,14-dimethoxy-12-acetoxycaryophyll-2(15)-en-7-one	<i>P.dysenterica</i> [43]
171	(1S,5S,6S,9R,11S)-5,14-dimethoxy-12-Hydroxycaryophyll-2(15)-en-7-one	<i>P.dysenterica</i> [43]
172	(1S,6R,9R)-14-Hydroxycaryophyll-2(15)-en-7-one	<i>P.dysenterica</i> [43]
173	(1S,6R,9R,11R)-13,14-Dihydroxycaryophyll-2(15)-en-7-one	<i>P. scabra</i> [55]
174	(5E)-14-Hydroxycaryophyll-5-ene-7-one	<i>P. scabra</i> [55]
175	(5E) 14-Acetoxy-5,6-trans-caryophyll-5-ene-7-one	<i>P. scabra</i> [55]
176	6,14-Didehydro-5,6-dihydro-5,13-dihydroxycaryophyllen-7-one	<i>P.dysenterica</i> [44]
177	14-Acetoxy-13-hydroxycaryophyllene-7-one	<i>P.dysenterica</i> [44]
178	13-Acetoxy-14-hydroxycaryophyllene-7-one	<i>P.dysenterica</i> [44]
179	13,14-Diacetoxycaryophyllene-7-one	<i>P.dysenterica</i> [44]
180	14-Acetoxycaryophyllene-7-one	<i>P.dysenterica</i> [44]
181	(5Z)-13,14-Dihydroxycaryophyllene-7-one	<i>P.dysenterica</i> [44]
182	(5Z)-14-Acetoxy-13-hydroxycaryophyllene-7-one	<i>P.dysenterica</i> [44]
183	(5Z)-13-Acetoxy-14-hydroxycaryophyllene-7-one	<i>P.dysenterica</i> [44]
184	Pulidysenterine	<i>P.dysenterica</i> [44]
185	Bis-[(5Z)-7-oxocaryophyllene]-14-O-ether	<i>P.arabica</i> [41]
186	Puliscabrine	<i>P. scabra</i> [55]
187	(5Z)-Puliscabrine	<i>P. scabra</i> [55]
188	(5Z)-5'-Epipuliscabrine	<i>P. scabra</i> [55]
189	2,15-Dihydropuliscabrin-4,14-dione	<i>P. scabra</i> [55]

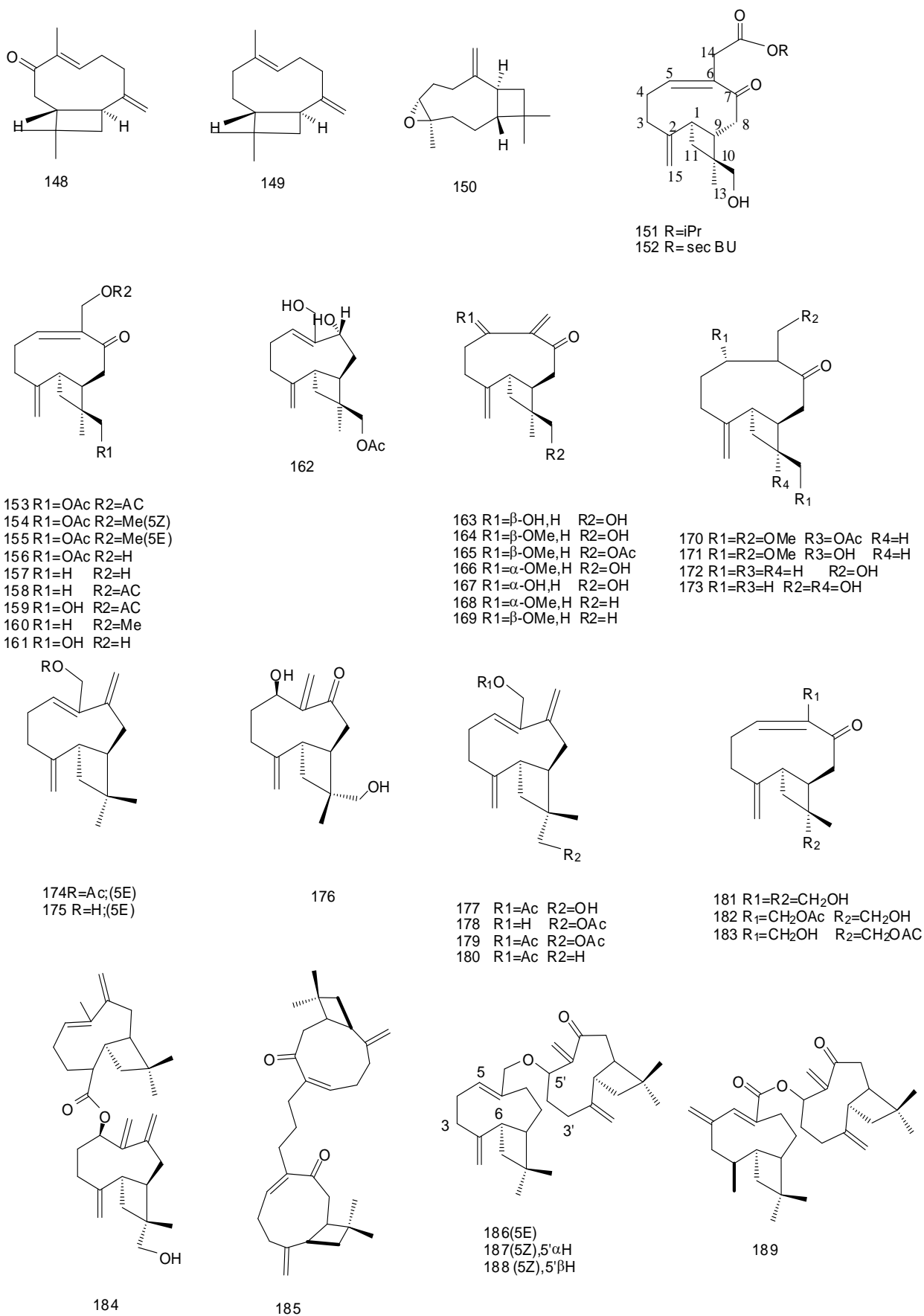


Figure 8: Caryophyllans compounds separated from different *Pulicaria* species

Table 7: Bisabolens compounds separated from different *Pulicaria* species.

N°	Bisabolenes	References
190	Puliglutoique Acid	<i>P. glutinosa</i> [52]
191	Puliglutale	<i>P. glutinosa</i> [52]
192	Puliglutole	<i>P. glutinosa</i> [52]
193	Puliglutone	<i>P. glutinosa</i> [52]

Table 8: Diterpene compounds separated from different *Pulicaria* species.

N°	Diterpenes	References
194	(1E,3Z)-6 α ,7 α -Dimethyl-10-methylidene-6-[2-(3-oxo-2,6-dioxabicyclo [3.1.0]hex-4-yl)ethyl]cyclodeca-1,3-diene-1- carboxylic acid	<i>P. angustifolia</i> [56]
195	(1E,3Z)-6 α ,7 α -Dimethyl-10-methylidene-6-[2-(5-oxo-2,5-dihydrofuran-3-yl)ethyl]cyclodeca-1,3-diene-1- acid carboxylique15- Deoxypulic acid	<i>P. angustifolia</i> [56]
196	15- Deoxypulic acid	<i>P. angustifolia</i> [56] <i>P. glutinosa</i> [57]
197	Polic acid	<i>P. glutinosa</i> [57]
198	Strictic acid	<i>P. glutinosa</i> [57]
199	(1E,3Z)-6 α ,7 β -Dimethyl-10-methylidene-6-[2-(5-oxo-2,5-dihydrofuran-3-yl)ethyl]cyclodeca-1,3-diene-1- carboxylic acid	<i>P. somalensis</i> [36]
200	Hautriwaic acid	<i>P. salviifolia</i> [58]
201	Salvicinoline	<i>P. salviifolia</i> [59]
202	Salvicinolide	<i>P. salviifolia</i> [59]
203	Hardwickiic acid	<i>P. salviifolia</i> [60]
204	Salvicine	<i>P. salviifolia</i> [27]
205	Salvicinine	<i>P. salviifolia</i> [40]
206	Methyl 5 α -hydroxyconyscabroate	<i>P. angustifolia</i> [38]
207	Salvinine	<i>P. salviifolia</i> [60]
208	7-oxo-6 α -hydroxyhardwickiic acid lactone	<i>P. gnaphalodes</i> [61]
209	Crispioside A	<i>P. crispa</i> [62] <i>P. incisa</i> [48]
210	Crispioside B	<i>P. crispa</i> [62] <i>P. incisa</i> [48]
211	2 α -Hydroxyisopimara-8(14),15-dien-7-one	<i>P. wightiana</i> [63]
212	Salvine	<i>P. salviifolia</i> [60]
213	Salvicinolide methyle ester	<i>P. wightiana</i> [64]
214	Methyl (4 α R,5R,6S,7S,8R,8 α R)-3,4,4 α ,5,6,7,8,8 α -octahydro-7,8-dihydroxy-5,6,8 α -trimethyl-5-[2-(5-oxo-2,5-dihydrofuran-3yl) ethyl] naphthalene-1-carboxylate	<i>P. wightiana</i> [64]

215	Methyl (4 α R,5S,6R,8S,8 α R)-3,4,4 α ,5,6,7,8,8 α -octahydro-8-hydroxy-5-[2-(5-hydroxy-2-oxo-2,5-dihydrofuran-3-yl) ethyl]-5,6,8 α -trimethylnaphthalene-1-carboxylate	<i>P.wightiana</i> [16]
216	Methyl (4 α R,5S,6R,8S,8 α R)-5-[2-(furan 3yl)ethyl] 3,4,4 α ,5,6,7,8,8 -octahydro-8-hydroxy-5,6,8 α -trimethylnaphthalene-1-carboxylate	<i>P.wightiana</i> [64]
217	Methyl (4 α R,5S,6R,8S,8 α R)-3,4,4 α ,5,6,7,8,8 α -octahydro-8hydroxy-5,6,8 α -trimethyl-5-[2-(2-oxo-2,5-dihydrofuran-3-yl) ethyl] naphthalene-1-carboxylate	<i>P.wightiana</i> [64]
218	Methyl (4 α R,5S,6R,8S,8 α R)-3,4,4 α ,5,6,7,8,8 α -octahydro-8hydroxy-5,6,8 α -trimethyl-5-[2-(2,5-dihydrofuran-3-yl) ethyl]-naphthalene-1-carboxylate	<i>P.wightiana</i> [64]
219	3,4,9,5,6,7,8,8 α -Octahydro-8 α -hydroxy-5 α ,6 α ,8 $\alpha\alpha$ -trimethyl-5 β -[2-(5-oxo-2,5-dihydrofuran-3-yl)]ethyl]naphthalene-18,7 β -olide	<i>P.wightiana</i> [16]
220	Pulicaroside B	<i>P. undulata</i> [33]
221	Steviobioside	<i>P.incisa</i> [12]

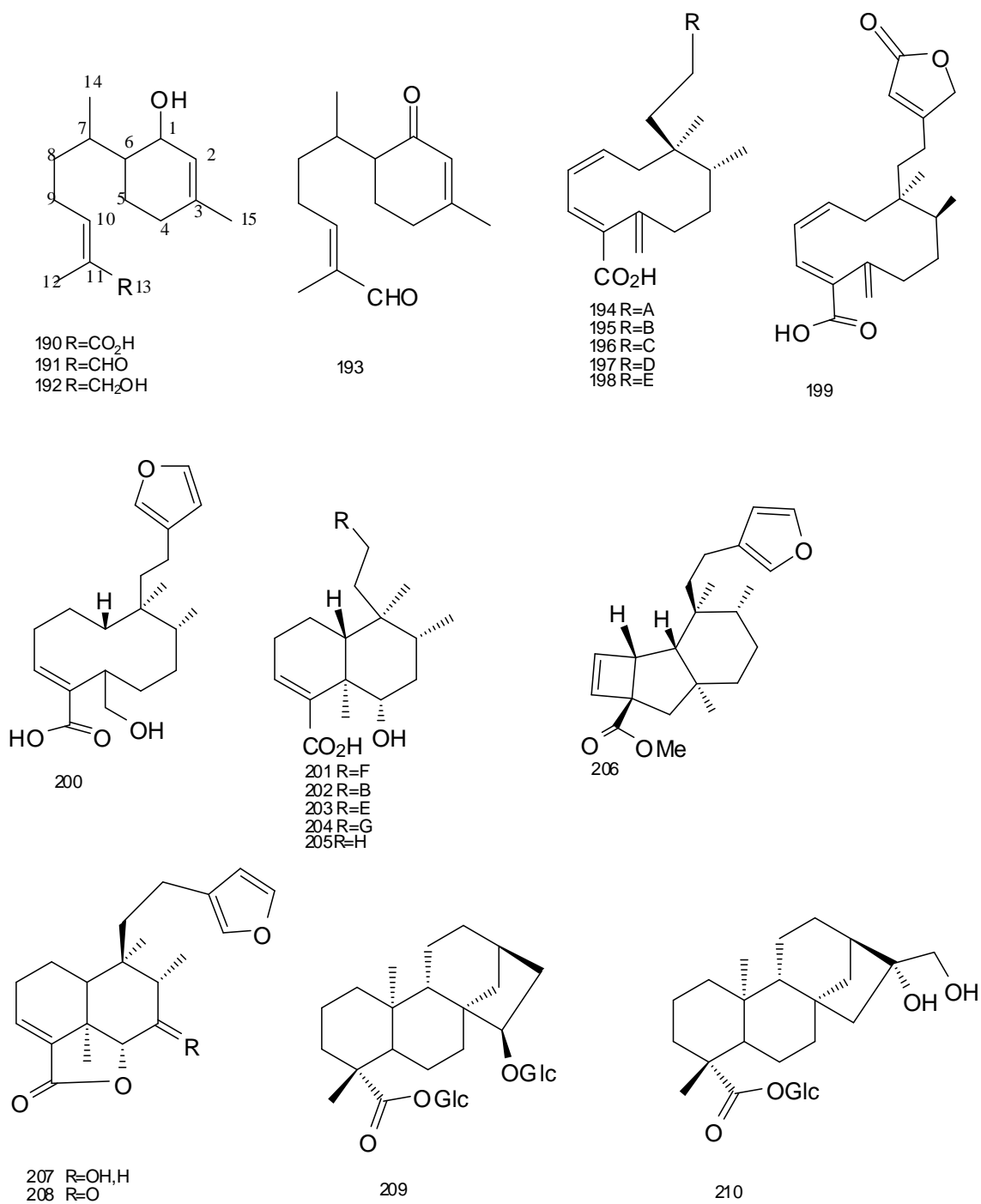


Figure 9: Bisabolens and Diterpenes compounds separated from different *Pulicaria* species

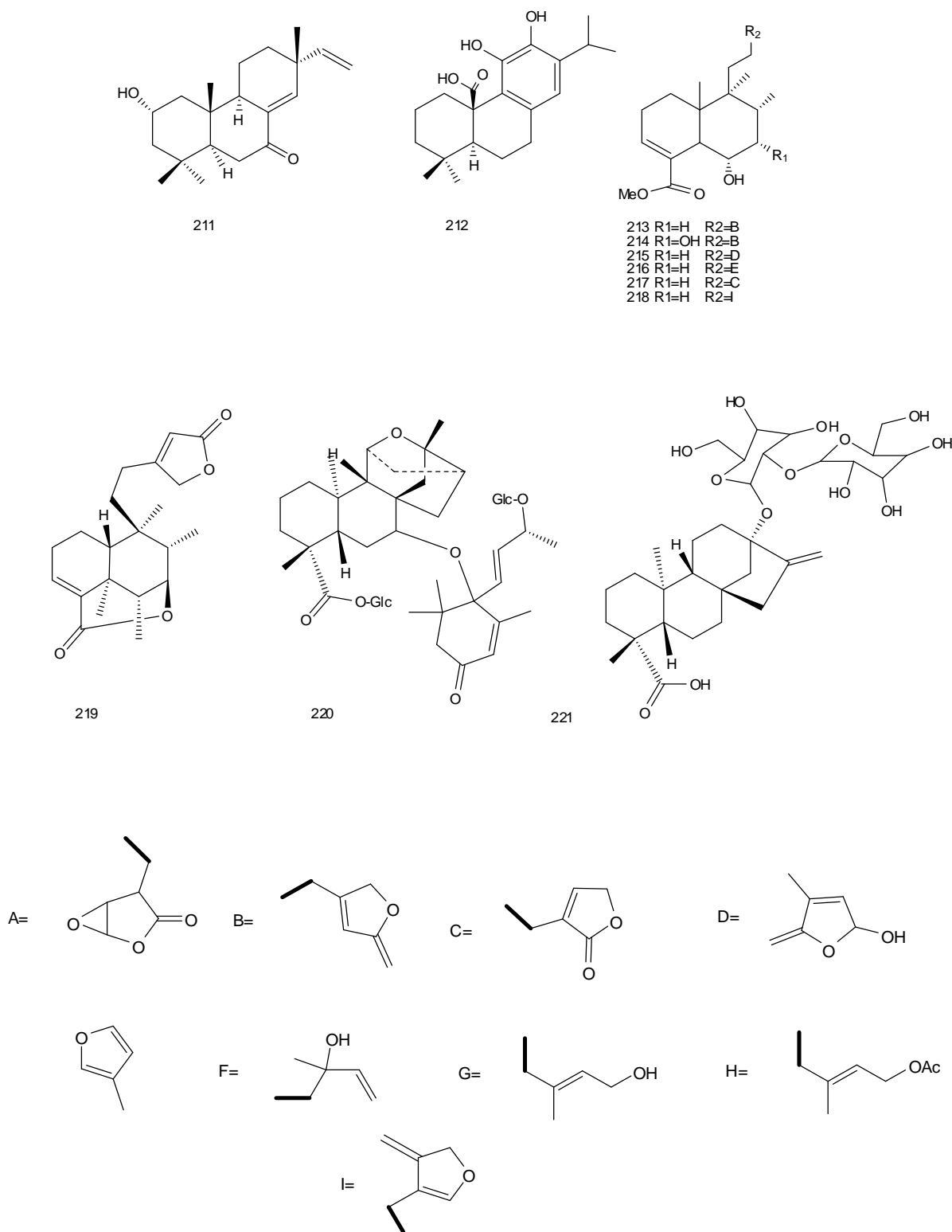


Figure 9 follows: Bisabolens and Diterpenes compounds separated from different *Pulicaria* species

Table 9: Triterpenoid compounds that separated from different species of *Pulicaria* genera.

N°	Triterpenoids	References
222	α -Amyrine	<i>P.incisa</i> [12]
223	Acetate pseudotaraxasteryl	<i>P.paludosa</i> [38]
224	Acetate traxasteryle	<i>P.angustifolia</i> [56] <i>P.paludosa</i> [38] <i>P.undulata</i> [23] <i>P.salviifolia</i> [65]
225	Amyrine B	<i>P.crispa</i> [66]
226	Acetate lupeol	<i>P.incisa</i> [12] <i>P.angustifolia</i> [56]
227	Lupeol	<i>P.angustifolia</i> [56] <i>P.undulata</i> [23]
228	Calenduladiol	<i>P.canariensis</i> [65]

Table 10: Steroid compounds that separated from different species of *Pulicaria*genera.

N°	Steroids	References
229	β -Sitosterol	<i>P.angustifolia</i> [56] <i>P.crispa</i> [66] <i>P.salviifolia</i> [65] <i>P.arabica</i> [41]
230	3-O- β -glucoside Sitosterol	<i>P.incisa</i> [48]
231	Stigmasterol	<i>P.angustifolia</i> [56] <i>P.paludosa</i> [38]
232	peroxide Ergosterol	<i>P.canariensis</i> [29]
233	Acetate Dammaradienyle	<i>P.arabica</i> [41]
234	Cholesterol	<i>P.salviifolia</i> [65]

Table 11: Other Terpenoid compounds separated from different *Pulicaria* species.

N°	Another Terpanoids	References
235	Alloaromadendrane-10 β , 14- diole	<i>P.paludosa</i> [38]
236	Viridiflorole	<i>P.paludosa</i> [38]
237	T-Cadinole	<i>P.paludosa</i> [38]
238	14-Hydroxy-T-cadinole	<i>P.paludosa</i> [38]
239	1 α -Hydroxyisocomene	<i>P.scabra</i> [10]
240	1 β -Hydroxyisocomene	<i>P.dysenterica</i> [44]
241	Presilphiperfolanole	<i>P.dysenterica</i> [44]
242	Paludolone	<i>P.paludosa</i> [38]
243	Pulioplopanone A	<i>P.canariensis</i> [29]
244	Pulioplopanone B	<i>P.canariensis</i> [29]
245	Lacitemzine	<i>P.laciniata</i> [15]

246	Secocrispiolide	<i>P. crispa</i> [46]
247	Pulicrispiolide	<i>P. crispa</i> [46]
248	Pulicarale	<i>P. paludosa</i> [67]
249	Acid pulicarique	<i>P. paludosa</i> [67]
250	9-Glucopyranosylpropanopentalene-3-carboxaldehyde	<i>P. paludosa</i> [38]
251	9-(2',3',4',6'-Tetraacetylglucopyranosyle)oxypropanopentalene-3-acid carboxylic	<i>P. paludosa</i> [67]
252	Corchoionole C	<i>P. undulata</i> [33]
253	Roseoside A	<i>P. undulata</i> [33]
254	Loliolide	<i>P. incisa</i> [48]
255	Pulicazine	<i>P. lacianta</i> [15]
256	Rel-(4 α R,5S,8 α R)-4 α ,5,6,7,8,8 α -Hexahydro-4a-hydroxy-5,8-dimethylnaphthalene-2(1H)-one	<i>P. insignis</i> [68]
257	Rel-(5R,8 α S,9 α S)-6,7,8,8 α ,9,9 α -Hexahydro-3-(Hexahydroxymethyl)-5,8adimethylnaphtho[2,3-b]furane-2(5H)-one	<i>P. insignis</i> [68]

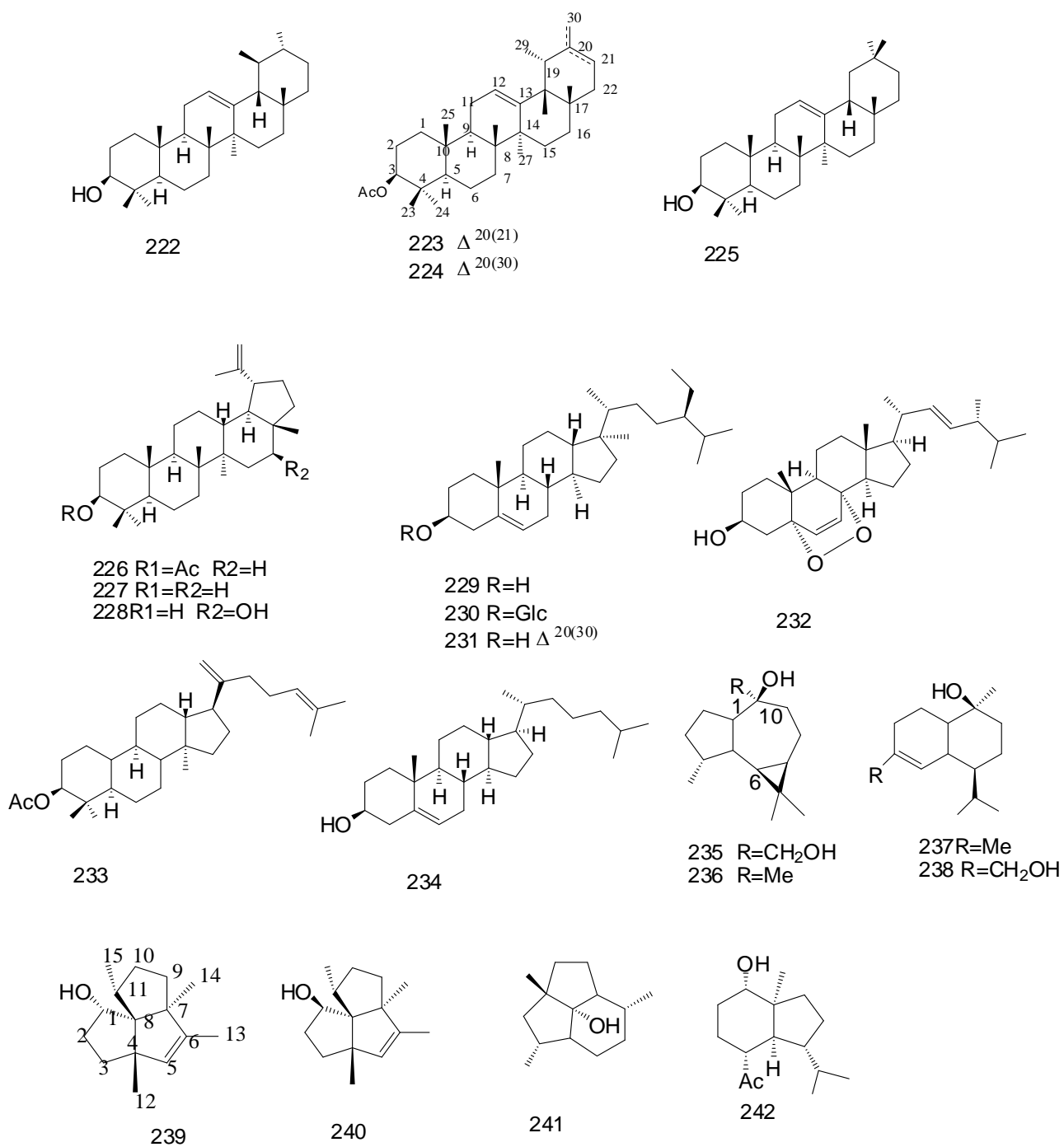


Figure 10: Triterpenoids, steroids and other terpenoid compounds separated from different *Pulicaria* species

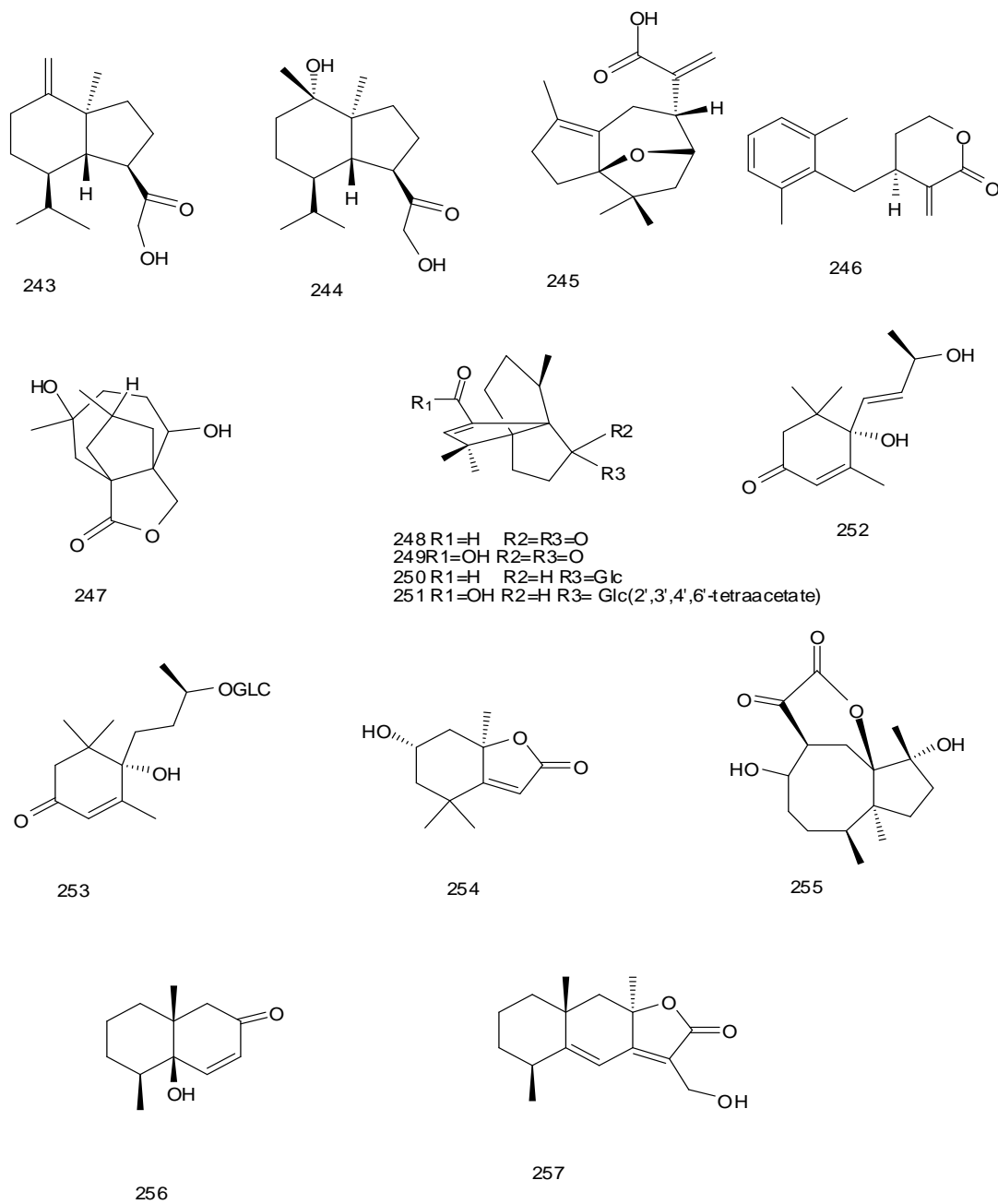


Figure 10 followed: Triterpenoids, steroids and other terpenoid compounds separated from different *Pulicaria* species

I.2.1.4. Essential oil:

Essential oils have also been isolated from many species that show several biological activities as essential ingredients in the *Pulicaria* species.[66, 69-73]

I.3. *Pulicaria* Biological Screening:

I.3.1. Anti-microbial activities:

The extracts of the aerial parts of *P. dysenterica*: aqueous, methanolic, and chloroformic were tested for their anti-bacterial activities against six pathogens (*Shigella dysenteriae*, *Salmonella typhi*, *Escherichia coli*, *Vibrio cholerae*, *Staphylococcus aureus*, and *Bacillus cereus*) using the disk-diffusion assay technique. These tests have shown that the methanolic extract is the most effective against three tested bacteria (*S. aureus*, *B. cereus*, and *V. cholera*). In contrast, all extracts were active against only the bacterium *V. cholera*. [74] The Methanolic extract of *Pulicaria crispa* has tested for their anti-bacterial against *Staphylococcus aureus* (ATCC 29213), *Staphylococcus aureus* (clinical isolate), *Bacillus subtilis* (ATCC 10400) as Gram-positive bacteria and *Escherichia coli* (ATCC 10536), *Klebsiella pneumonia* (ATCC 13882), *Proteus vulgaris* (clinical isolate) as Gram-negative bacteria. *Aspergillus niger* (ATCC 16404) and *Candida albicans* (NCYC 1363) were used for the anti-fungal study. The anti-bacterial activity showed that the Methanolic extract was effective on *K.pneumoniae* (28 mm), *B. subtilis*(22 mm), and *E.coli*(21 mm), which are comparatively less, potent than Ampicillin. No considerable action on the three strains, *Staphylococcus aureus* (ATCC 29213), *Staphylococcus aureus* (clinical isolate), and *Proteus Vulgaris* (clinical isolate), was seen. For the anti-fungal activity, the methanolic extract has comparatively less inhibitory effect on *Aspergillus niger* (18mm), when compared to the standard (23mm)[75].

The essential oil of *P. odora* L. has been tested against seven bacteria (*Bacillus cereus* (IPL 58605), *Streptococcus C* (IPT 2-035), *Proteus Vulgaris* (CIP 58605), *Enterococcus faecalis* (CIP 103214), *Escherichia coli* (CIP 54127), *Pseudomonas aeruginosa* (CIPA 22), and *Enterococcus faecalis*) at different concentrations. The results showed that the essential oil exhibited activity with all bacteria at minimal concentrations (5 mg/disc). The potent inhibition was against *E. faecalis*, *P. Vulgaris*, *Streptococcus C*, and *B. cereus*[69]. Also, *P. stephanocarpa* methanolic extract exhibited anti-bacterial activity against *Staphylococcus aureus*(ATCC 6538), *Bacillus subtilis* (ATCC 6059), *Micrococcus flavus* (SBUG 16), *Staphylococcus epidermidis* 847, *Staphylococcus haemolyticus*535 and *Staphylococcus aureus* North German reference strain)[76]. The

ethanolic extract from *P. orientalis* showed feeble anti-bacterial activity (IC_{50} 18 mg/ml) against *Staphylococcus aureus* bacteria [77].

The anti-bacterial activities of compounds 213–220 were evaluated by the agar cup bioassay method. The compounds showed moderate activity against Gram-positive organisms, *Bacillus subtilis* (MTCC-441), *Bacillus sphaericus* (MTCC-511), and *Staphylococcus aureus* (MTCC-96). However, they were less active against *Klebsiella aerogenes* (MTCC-39) and *Chromobacterium violaceum* (MTCC-2656) and inactive against *Pseudomonas aeruginosa* [16, 64].

The anti-bacterial activity of essential oil of *P. odora*, compound 83 and compound 13 against *Staphylococcus aureus* (ATCC 34525923), *Escherichia coli* (ATCC 25922), *Pseudomonas aeruginosa* (ATCC 27853), *Salmonella typhimurium* (ATCC 43971), *Vibrio cholerae* (ATCC 14033), and *Streptococcus pyogenes* (HITM 100), as well as one fungal strain *Candida albicans* (HITM 22) by the diffusion method, showed that the essential oil of *P. odora* and compound 83 possess inhibitory activity against all bacteria and yeast tested with MIC ranging from 1 to 2 ml/ml except for *P. aeruginosa* (ATCC 27853) but compound 84 was inactive against all organisms tested [78].

Compounds 190, 193, 196, and 198 were tested for anti-microbial activities, and only strictic acid showed moderate activity against Gram-positive bacteria and the yeast *C. albicans* [57].

An anti-microbial screen of compound 141 against five microorganisms, *Staphylococcus aureus* (NCTC 6571), *Escherichia coli* (NCTC 10418), *Pseudomonas aeruginosa* (NCTC 10662), *Salmonella sp.*, and *Candida albicans* (NCTC 3153), the results showed a slight activity against *S. aureus* only (MIC 0.625 mg/ml) [34].

I.3.2. Antioxidant activity:

Previous studies reported that the anti-oxidant activity of the methanolic extract of *P. crisp* from Saudi Arabia was 79.84 % at 1000 μ g/ml using DPPH assay compared with ascorbic acid (96.51%) at the same concentration [79]. In another study, aqueous ethanolic extracts of the whole *P. crista* plant obtained from Oman exhibited IC_{50} equal to 15.2 ± 0.2 μ g/ml and inhibition value of $92.2 \pm 0.3\%$ at 50 μ g/ml concentration [80]. In another report of *P. jaubertii*, the inhibition rates in term of DPPH assay were as follow; ethyl

acetate extract (96.87%), butanol extract (63.62%), chloroform extract (33.78%) at a concentration of 50 µg/ml[81].

I.3.3. Cytotoxic Activities:

The evaluation of the cytotoxic activities against the human myeloid leukemia cell line HL-60 by the MTT for the *P. canariensis* isolated compounds (acetylation of pulicanone (96) and pulicanol (97), pulicanarals A and B (98 and 99, resp.), and pulioplopanone A (243) showed weak activity with an IC₅₀ values activities with IC₅₀ values (in mm) of 20±7, 298±22, 115±18, 264± 6, and 242±80, respectively. While pulicanone triacetate was the most potent compound, and cytotoxicity was caused by induction of apoptosis as determined by microscopy of nuclear modifications, activation of caspases, and (ADP-ribose) polymerase -1 cleavage [29]. In 2008, the isolated compound 50 from *P. crispera* was evaluated in vitro for anticancer activity in the known human bladder carcinoma cell line, EJ-138. It has shown promising behaviour in this cell line with an IC₅₀ value of 5.8±0.2 mm. Compound 141 was cytotoxic (0.2 mg/ml in 9 KB; 2 mg/ml in 9 PS) and showed borderline activity against the murine P-388 lymphocytic leukemia (T/C 123% at 75 mg/kg) [34]. Compound 144 was shown to be cytotoxic to KB cells in culture (ED₅₀ 40.4 mg/ml), and compound 141 was found to be active at almost the same level (ED₅₀ 40.33 mg/ml)[82].

I.3.4. Other Activities:

Axillary (83) possesses anti-carcinogenic activity using benzo[α]pyrene metabolism assay in cultured embryonic hamster cells, and the study revealed that axillarhjin is active at 25 mg/ml and decreased benzo[α]pyrene metabolism by an average of 61.3 percent over DMSO controls [82]. In 1997, it was reported that carvotan acetone 20 had no anti-microbial activity against *Candida albicans* B311 and *Cryptococcus neoformans* (50 ml, 1 mg/ml) compared to amphotericin B. No cytotoxicity against K562 cells, human chronic myelogenous leukemia, KB cells, human oral epidermoid carcinoma, or antiviral activity has been established [66]. In addition, anti-spasmodic activity of *P. glutinosa* has been shown[83], and *P. dysenterica* showed an anti-histaminic effect[84].

References

1. Bruneton J. Pharmacognosie et phytochimie des plantes médicinales, 3 ème édition, lavoisier. Paris; 1999.
2. Quezel P, Santa S. Nouvelle flore de l'Algérie et des regions desertiques méridionales. 1963.
3. حسين د. دراسة الأيض الفلافونيدي و التربينني لبعض أنواع نباتات ضايات الصحراء الجزائرية [دكتوراه]: جامعة منتوري قسنطينة; 2002.
4. Bonnier G. Flore complète illustrée en couleur de France, Suisse et Belgique, 4 vol. Belin; 1934. p. 188.
5. Crété P. Précis de botanique, systématique des angiospermes tome 2; 2 ième édition révisée. Faculté de Pharmacie de Paris-masson. 1965:429.
6. Guignard J. Abrégé botanique, 9 eme édition. Édition Masson, Paris. 1994;204:203-4.
7. Marie-Victorin F. Flore laurentienne. 1964.
8. Gausson H, Leroy J-F. Précis de botanique. 2ème édition ed: Masson; 1982.
9. Singh P, Sharma MC, Joshi KC, Bohlmann F. Diterpenes derived from clerodanes from *Pulicaria angustifolia*. Phytochemistry. 1985;24(1):190-2.
10. Diaz N, Ortega T, Pardo M. Pharmacognostic study of *Pulicaria paludosa* Link. An R Acad Farm. 1988;54:526-31.
11. San Feliciano A, Medarde M, Gordaliza M, Olmo Ed, Del Corral JM. *The structures of pulicaral and related sesquiterpenoids from Pulicaria paludosa*. Journal of natural products. 1988.
12. Ibraheim Z, Darwish F. Further Constituents from *Pulicaria incisa*. Bull Fac Pharm(Cairo Univ). 2002;40:167.
13. Ramadan MA. *Flavonoids from Pulicaria arabica (L.) CASS*. Bulletin of Pharmaceutical Sciences Assiut. 1998;21(2):103-8.
14. Schulte K, Rücker G, Müller F. Einige inhaltsstoffe der blütenköpfchen von *Pulicaria dysenterica*. Arch Pharm. 1968;301(2):115-9.
15. Ghouila H, Beyaoui A, Jannet HB, Hamdi B, Salah AB, Mighri Z. Lacitemzine, a novel sesquiterpene acid from the Tunisian plant *Pulicaria laciniata* (Coss. et Kral.) Thell. Tetrahedron Lett. 2008;49(40):5721-3.
16. Das B, Reddy MR, Ramu R, Ravindranath N, Harish H, Ramakrishna K, et al. Clerodane diterpenoids from *Pulicaria wightiana*. Phytochemistry. 2005;66(6):633-8.
17. Mohamed Samba, Abderrahmane Hadou, Ahmed Ismail Boumediana, Abdi Kaihil MVD, EME, Minnih MS. Etude phytochimique de *Pulicaria incisa* origine Mauritanie. Journal of the Mauritanian Chemical Society. 2018;01:31-45.
18. AM R, Hammouda F, Ismail S, Hussiney H. Constituents of plants growing in Qatar XXIII. Flavonoids of *Francoeuria crispa*. Qatar Univ Sci J. 1993.
19. Ibraheim ZZ, Salem HA. Phytochemical and pharmacological studies on *Pulicaria orientalis* Jaub & Sp. Bulletin of Pharmaceutical Sciences Assiut. 2002;25(2):189-200.
20. Mansour R, Ahmed A, Melek F, Saleh N. The flavonoids of *Pulicaria incisa*. Fitoterapia. 1990;61(2):186-7.
21. El-Negoumy SI, Mansour RM, Saleh NA. Flavonols of *Pulicaria arabica*. Phytochemistry. 1982;21(4):953-4.

22. Bishay D, Gomaa C, Assaf M. Flavonoids from *Pulicaria undulata* (L.) KOSTEL grown in egypt. Bulletin of Pharmaceutical Sciences Assiut. 1982;5(1):65-71.
23. Abdel-Mogib M, Dawidar A, Metwally M, Abou-Elzahab M. Flavonols of *Pulicaria undulata*. Pharmazie. 1989;44(11).
24. Williams CA, Harborne JB, Greenham J. Geographical variation in the surface flavonoids of *Pulicaria dysenterica*. Biochem Syst Ecol. 2000;28(7):679-87.
25. Rizk A-FM, Shams I. Flavonoids of *Francoeuria crispa*. Planta Med. 1982;45(07):146-.
26. Williams CA, Harborne JB, Greenham JR, Grayer RJ, Kite GC, Eagles J. Variations in lipophilic and vacuolar flavonoids among European *Pulicaria* species. Phytochemistry. 2003;64(1):275-83.
27. Nurmukhamedova M, Abdullaev N, Sidyakin G. Diterpenoids of *Pulicaria salviifolia*. II. Structure of salvicin. Chem Nat Compd. 1986;22(3):277-9.
28. Metwally M, Dawidar A-A, Metwally S. A new thymol derivative from *Pulicaria undulata*. Chem Pharm Bull. 1986;34(1):378-9.
29. Triana J, López M, Pérez FJ, González-Platas J, Quintana J, Estévez F, et al. Sesquiterpenoids from *Pulicaria canariensis* and Their Cytotoxic Activities. J Nat Prod. 2005;68(4):523-31.
30. Elmann A, Telerman A, Ofir R, Kashman Y. Pulichalconoid B suppresses experimental dermatitis in mice. Israel Journal of Plant Sciences. 2015;62(4):242-9.
31. Elmann A, Telerman A, Erlank H, Mordechay S, Rindner M, Ofir R, et al. Protective and antioxidant effects of a chalconoid from *Pulicaria incisa* on brain astrocytes. Oxidative medicine and cellular longevity. 2013;2013.
32. Pares JO, Oksuz S, Ulubelen A, Mabry T. 6-hydroxyflavonoids from *Pulicaria dysenterica* (Compositae). Phytochemistry. 1981;20(8):2057.
33. Ahmad V, Rasool N, Abbasi M, Rashid M, Kousar F, Zubair M, et al. Antioxidant flavonoids from *Pulicaria undulata*. Pol J Chem. 2006;80(5):745-51.
34. Al-Yahya MA, Khafagy S, Shihata A, Kozlowski JF, Antoun MD, Cassady JM. Phytochemical and biological screening of Saudi medicinal plants, Part 6. Isolation of 2 α -hydroxyalantolactone the antileukemic principle of *Francoeuria crispa*. J Nat Prod. 1984;47(6):1013-7.
35. Melek F, El-Ansari M, Hassan A, Regaila A, Ahmed A, Mabary T. Methoxylated flavonoid aglycones from *Pulicaria arabica*. Rev Latinoamer Quim. 1988;19:119.
36. Al-Hazimi H, Al-Khathlan HZ. New diterpene and flavonoids from *Pulicaria somalensis*. J King Saud Univ Sci. 1993;5:141-6.
37. Sarg T. Phytochemical investigation of *Pulicaria crispa* (Forsk.) Benth and Hook, growing in Saudi Arabia, Egypt. J Pharm Sci. 1975;16:421.
38. San Feliciano A, Medarde M, Gordaliza M, Del Olmo E, del Corral JMM. Sesquiterpenoids and phenolics of *Pulicaria paludosa*. Phytochemistry. 1989;28(10):2717-21.
39. Eshbakova K, Sagitdinova G, Malikov V, Melibaev S. Flavone sorbifolin from *Pulicaria uliginosa*. Chem Nat Compd. 1996;32(1):82-.
40. Sagitdinova G, Eshbakova K, Malikov V. Diterpenoids of *Pulicaria salviifolia*. III. The structure of salvicinin. Chem Nat Compd. 1994;30(2):226-8.
41. Hafez S, Sarg T, El-Domiatty A, Ahmed F. Caryophyllene derivatives from *Pulicaria arabica*. Phytochemistry. 1987;26:3356.

42. Zdero C, Bohlmann F, Rizk A. Sesquiterpene lactones from *Pulicaria sicula*. *Phytochemistry*. 1988;27(4):1206-8.
43. Marco JA, Sanz JF, Albiach R. Caryophyllene derivatives from *Pulicaria dysenterica*. *Phytochemistry*. 1992;31(7):2409-13.
44. Bohlmann F, Zdero C. Caryophyllene derivatives and a hydroxyisocomene from *Pulicaria dysenterica*. *Phytochemistry*. 1981;20(11):2529-34.
45. Mossa JS, Al-Yahya MA, Hifnawy MS, Shehata AA, El-Feraly FS, Hufford CD, et al. Two germacrane sesquiterpenes from *Pulicaria glutinosa*. *Phytochemistry*. 1990;29(5):1595-9.
46. Bohlmann F, Knoll K-H, El-Emary NA. Neuartige sesquiterpenlactone aus *Pulicaria crispa*. *Phytochemistry*. 1979;18(7):1231-3.
47. Fraga B. Natural sesquiterpenoids. *Natural product reports*. 1992;9(6):557-80.
48. Darwish F. Terpenoids from *Pulicaria incisa*. *Alexandria Journal of Pharmaceutical Sciences*. 2001;15(1):21-4.
49. Dendougui H, Benayache S, Benayache F, Connolly JD. Sesquiterpene lactones from *Pulicaria crispa*. *Fitoterapia*. 2000;71:373-8.
50. Stavri M, Mathew K, Gordon A, Shnyder SD, Falconer RA, Gibbons S. Guaianolide sesquiterpenes from *Pulicariacrispa* (Forssk.) Oliv. *Phytochemistry*. 2008;69(9):1915-8.
51. Aberkane M, Dibi A, Haba H, Benkhaled M, Benkouider A, Mokhtari M, et al. Guaianolide and Pseudoguaianolide from *Pulicaria laciniata*. *Asian J Chem*. 2007;19(6):4954.
52. Mossa JS, Muhammad I, El-Feraly FS, Huffor CD, McPhail DR, McPhail AT. Bisabolene and guaiane sesquiterpenes from *Pulicaria glutinosa*. *Phytochemistry*. 1992;31(2):575-8.
53. Rustaiyan A, Habibi Z, Saberi M, Jakupovic J. A nor-guaianolide and a glaucolide-like eudesmanolide from *Pulicaria undulata*. *Phytochemistry*. 1991;30(7):2405-6.
54. Sadyrbekov D, Atazhanova G, Kulyyasov A, Raldugin V, Gatilov YV, Shakirov M, et al. Buddledin C from *Pulicaria prostrata* and selective synthesis of its epoxy derivative. *Chem Nat Compd*. 2006;42(1):41-5.
55. Bohlmann F, Ahmed M, Jakupovic J. Caryophyllane derivatives from *Pulicaria scabra*. *phytochemistry*. 1982;21(7):1659-61.
56. Singh P, Sharma MC, Joshi KC, Bohlman F. *Diterpenes derived from clerodanes from Pulicaria angustifolia*. *Phyrrachemurry*. 1985;24:190-2.
57. Muhammad I, El-Feraly FS, Mossa JS, Ramadan AF. Terpenoids from *Pulicaria glutinosa*. *Phytochemistry*. 1992;31(12):4245-8.
58. Eshbakova K, Saidkhodzhaev A. Hautriwaic acid from *Pulicaria salviifolia*. *Chem Nat Compd*. 2002;38(4):326-7.
59. Eshbakova K, Sagitdinova G, Levkovich M, Rasulev B, Abdullaev N, Malikov V. Diterpenoids of *Pulicaria salviifolia* IV. Structures of salvicinolide and salvicinolin. *Chem Nat Compd*. 1997;33(4):458-61.
60. Nurmukhamedova M, Kasymov SZ, Abdullaev N, Sidyakin G, Yagudaev M. Diterpenoids of *Pulicaria salviifolia*. I. Structures of salvin and salvinin. *Chem Nat Compd*. 1985;21(2):188-91.

61. Rustaiyan A, Simozar E, Ahmadi A, Grenz M, Bohlmann F. A hardwickiic acid derivative from *Pulicaria gnaphalodes*. *Phytochemistry*. 1981;20(12):2772-3.
62. Abdel-Mogib M, Jakupovic J, Dawidar A, Metwally M, Abou-Elzahab M. Sesquiterpene lactones and kaurane glycosides from *Francoeuria crispa*. *Phytochemistry*. 1990;29(8):2581-4.
63. Chiplunkar YG, Nagasampagi BA. Isolation and structure elucidation of a new isopimarane from *Pulicaria wightiana*. *J Nat Prod*. 1992;55(9):1328-9.
64. Das B, Ramu R, Venkateswarlu K, Rao YK, Reddy MR, Ramakrishna KVS, et al. New clerodane diterpenoids from the aerial parts of *Pulicaria wightiana*. *Chemistry & biodiversity*. 2006;3(2):175-9.
65. Eshbakova K, Saidkhodzhaev A. Triterpenoids and sterols from three species of *Pulicaria*. *Chem Nat Compd*. 2001;37(2):196-7.
66. Ross SA, El Sayed KA, El Sohly MA, Hamann MT, Abdel-Halim OB, Ahmed AF, et al. Phytochemical analysis of *Geigeria alata* and *Francoeuria crispa* essential oils. *Planta Med*. 1997;63(05):479-82.
67. Feliciano AS, Medarde M, Gordaliza M, Del Olmo E, Del Corral JM. *The Structures of Pulicarial and Related Sesquiterpenoids from Pulicaria paludosa*. *J Nat Prod*. 1988;51(6):1153-60.
68. Huang SZ, Li LB, Jiang SP, Chen XL, Zhu HJ. A Rarely Reported Trinorsesquiterpene-Type Structure in an Isolate from *Pulicaria insignis*. *Helv Chim Acta*. 2010;93(9):1808-11.
69. Hanbali FE, Akssira M, Ezoubeiri A, Mellouki F, Benherraf A, Blazquez AM, et al. Chemical composition and antibacterial activity of essential oil of *Pulicaria odora* L. *J Ethnopharmacol*. 2005;99(3):399-401.
70. Znini M, Cristofari G, Majidi L, Paolini J, Desjobert J, Costa J. Essential oil composition and antifungal activity of *Pulicaria mauritanica* Coss., against postharvest phytopathogenic fungi in apples. *LWT-Food Science and Technology*. 2013;54:564-9.
71. Ali NAA, Crouch RA, Al-Fatimi MA, Arnold N, Teichert A, Setzer WN, et al. Chemical composition, antimicrobial, antiradical and anticholinesterase activity of the essential oil of *Pulicaria stephanocarpa* from Soqatra. *Natural product communications*. 2012;7(1):1934578X1200700137.
72. Algabr M, Ameddah S, Menad A, Mekkiou R, Chalchat J, Benayache S, et al. Essential oil composition of *Pulicaria jaubertii* from Yemen. *International Journal of Medicinal and Aromatic Plants*. 2012;2(4):688-90.
73. Al-Hajj NQM, Wang HX, Ma C, Lou Z, Bashari M, Thabit R. Antimicrobial and antioxidant activities of the essential oils of some aromatic medicinal plants (*Pulicaria inuloides*-Asteraceae and *Ocimum forskolei*-Lamiaceae). *Tropical Journal of Pharmaceutical Research*. 2014;13(8):1287-93.
74. Nickavar B, Mojab F. Antibacterial activity of *Pulicaria dysenterica* extracts. *Fitoterapia*. 2003;74:390-3.
75. Foudah AII, Soliman GAM. Pharmacognostical, Antioxidant and Antimicrobial studies of aerial part of *Pulicaria crispa* (Family: Asteraceae). *Bull Environ, Pharmacol Life Sci*. 2015;4.
76. Mothana RA, Gruenert R, Bednarski P, Lindequist U. Evaluation of the in vitro anticancer, antimicrobial and antioxidant activities of some Yemeni plants used in folk

medicine. Die Pharmazie-An International Journal of Pharmaceutical Sciences. 2009;64(4):260-8.

77. Ali NA, Jülich W-D, Kusnick C, Lindequist U. Screening of Yemeni medicinal plants for antibacterial and cytotoxic activities. J Ethnopharmacol. 2001;74(2):173-9.

78. Ezoubeiri A, Gadhi C, Fdil N, Benharref A, Jana M, Vanhaelen M. Isolation and antimicrobial activity of two phenolic compounds from *Pulicaria odora* L. J Ethnopharmacol. 2005;99(2):287-92.

79. Foudah AI, Aftab Alam, Gamal A. Soliman , Mohammed Ayman Salkini , Elmutasim O. Ibnouf Ahmed, Yusufoglu HS. Pharmacognostical, Antioxidant and Antimicrobial studies of aerial part of *Pulicaria crispa* (Family: Asteraceae). Bulletin of Environment, Pharmacology and Life Sciences. 2015; 4(12):19-27.

80. Marwah RG, Fatope MO, Mahrooqi RA, Varma GB, Abadi HA, Al-Burtamani SKS. Antioxidant capacity of some edible and wound healing plants in Oman. Food Chem. 2007;101:465-70.

81. Algabr MN, R.Mekkiou, Ameddah S, A. Menad, O. Boumaza, Seghiri R, et al. Antioxydant activities from the aerial parts of *Pulicaria jaubertii*. Advances in Natural Applied Sciences. 2010;4(1):63-70.

82. Alo Yahya M, El-Sayed A, Mossa J, Kozlowski J, Antoun M, Ferin M, et al. Potential cancer chemopreventive and cytotoxic agents from *Pulicaria crispa*. J Nat Prod. 1988;51(3):621-4.

83. Tanira MM, ALI BH, BASHIR AK, WASFI' IA, CHANDRANATH I. Evaluation of the Relaxant Activity of some United Arab Emirates Plants on Intestinal Smooth Muscle. J Pharm Pharmacol. 1996;48:545-50.

84. Mahfouz M, Ghazal A, El-Dakhakhny M, Ghoneim M. Pharmacological studies on the active principle isolated from *Pulicaria dysenterica*. Journal of Drug Research. 1973;5(2):151-72.

*CHAPTER II
SECONDARY
METABOLITES*

II.1 Phenolic compounds generality:

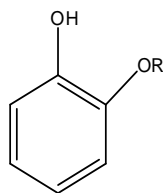
Phenolic compounds (polyphenols) are secondary metabolites of plants. They are widely present in all organs of the plant [1]. The fundamental structural element that characterizes them is the presence of at least one benzene nucleus, which is directly related to one or more hydroxyl groups, free or engaged in another chemical function (ether, methyl, ester,...) [2]. The main classes of phenolic compounds are grouped in (Table 12) [3, 4].

Table 12: Present the main classes of phenolic compounds.

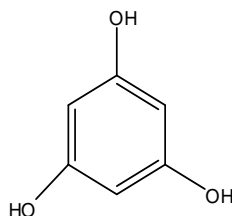
Carbon skeleton	Class	Examples
C ₆	Simple phenol Benzoquinones	Catechol
(C ₆) _n	Catechol melanins	
C ₆ -C ₁	Phenolic acid	<i>p</i> -hydroxybenzoic
C ₆ -C ₂	Acetophenone, Phenylacetic acid	
C ₆ -C ₃	Hydroxycinnamic acids Coumarins Phenylpropanes, Chromones	Caffeic and ferulic acids Scopoletin, esculetin
(C ₆ -C ₃) ₂	Lignans Neolignans	
(C ₆ -C ₃) _n	Lignins	
C ₆ -C ₄	Naphthoquinones	Juglone
C ₆ -C ₁ -C ₆	Benzophenone Xanthenes	
C ₆ -C ₂ -C ₆	Stilbens Anthraquinones	Resveratrol
C ₆ -C ₃ -C ₆	Flavonoids Isoflavonoids Neoflavonoids	Kaempferol, quercetin Cyanidin, pelargonidine Catechin
(C ₆ -C ₃ -C ₆) _{2,3}	Bi-, Triflavonoids	
(C ₆ -C ₃ -C ₆) _n	Condensed tannins	Prodelphinidin
	Hydrolyzable tannins	

II.1.2. Simple phenols:

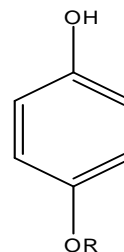
Simple phenols such as catechol, guaiacol, and other phloroglucinol form a compound with one or more linked hydroxyl groups to an aromatic nucleus. They are rather rare in nature except hydroquinone, found in several plant families, notably Ericaceae and Rosaceae, and most often in the glucoside state of diphenol (arbutoside) [2].



	R
<i>Catechol</i>	H
<i>Guaianol</i>	CH ₃



phloroglucinol



	R
<i>Hydroquinon</i>	H
<i>Arbutoside</i>	Glucose

II.1.3. Phenolic acids:

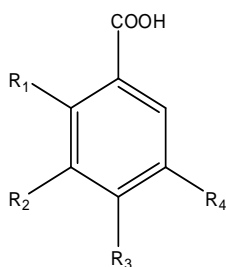
Phenolic acids are phenolic compounds having a grouping of carboxyl. These compounds include benzoic and hydroxycinnamic acids. The benzoic acids are formed from cinnamic acid and possess a C₆-C₁, while the hydroxycinnamic acids derive from p-coumaric acid, itself formed from cinnamic acid.

II.1.4. Phenolic acids Classification:

Two classes belong to this category. The derivatives of the acid benzoic acid and cinnamic acid derivatives.

II.1.5. Phenolic acid derived from benzoic acid:

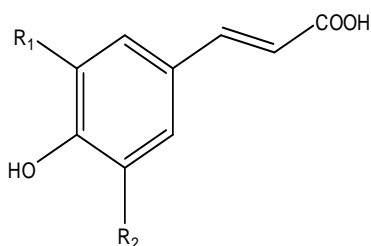
Phenolic acids C₆-C₁, hydroxylated benzoic acid derivatives, are very common in both free form and combined in the ester or heteroside state [5]. These compounds are derived from the degradation of the side chain of cinnamic compounds.



	R1	R2	R3	R4
<i>p</i> -hydroxy benzoic acid	H	H	OH	H
protocatechic acid	H	OH	OH	H
vanillic acid	H	OH	OH	OCH ₃
gallic acid	H	OH	OH	OH
syringic acid	H	OCH ₃	OH	OCH ₃
salicylic acid	OH	H	H	H
gentisic acid	OH	H	H	OH

II.1.6. Phenolic acids derived from cinnamic acid:

The hydroxycinnamic acids are mainly composed of *p*-coumaric acids, caffeic, ferulic, and sinapic [1]. They are found in the free or combined state (esters, amide, glucosides). They frequently acylate the most diverse metabolites [2].



	R1	R2
<i>p</i> -coumaric acid	H	H
caffeic acid	H	OH
ferulic acid	H	OCH ₃
Sinapic acid	OCH ₃	OCH ₃

II.1.7. Biogenesis of simple phenols and phenolic acids:

The phenolic compounds come from two main pathways of aromagenesis, the pathway of shikimic acid and acetate. The most common route is through shikimate, which plays a critical role in controlling the metabolism of the phenylpropanoid pathway [6].

The compounds of the C₆-C₁ type (benzoic acid derivatives) come from the degradation of the side chain of the corresponding cinnamic acids (certain compounds of type C₆-C₂ come from cinnamates). Decarboxylation of benzoic acids allows for obtaining simple phenolic compounds [2]. All the phenolic phytochemicals are derived from a common biosynthetic pathway, incorporating precursors from both the shikimate and/or the acetate-malonate pathways. The synthesis of phenolic phytochemicals first involves the commitment of glucose to the pentose phosphate pathway (PPP), which generates reducing equivalents required for anabolic reactions in the cell, such as phenolic synthesis. PPP generates erythrose-4-phosphate, which is channelled to the shikimate pathway to produce phenylalanine, which is further metabolized in the phenylpropanoid pathway to produce phenolic phytochemicals in plants [7, 8].

Phenylpropanoids are derived from the shikimate biosynthetic pathway. This last one is the precursor of the three aromatic amino acids that are formed in plastids: phenylalanine, tyrosine, and tryptophan. The enzyme phenylalanine ammonia-lyase (PAL) catalyzes the conversion reaction of phenylalanine into cinnamate in the cytosol. Cinnamate is then converted to p-coumarate by a catalyzed hydroxylation reaction by cinnamate 4-hydroxylase (C4H). P-coumarate can also be formed from tyrosine by the action of a tyrosine ammonia-lyase (TAL) in Monocotyledons. A coenzyme A is added by p-coumarate-CoA ligase (4CL) to form p-coumaroyl-CoA, a precursor compound for lignin and flavonoid biosynthetic pathways. The three molecules are phenylalanine, cinnamate, and p-coumarate, are the precursors of C₆, C₆-C₁, C₆-C₂, C₆-C₃, C₆-C₄, C₆-C₁-C₆, C₆-C₂-C₃. [9]. It should be noted that methyl salicylate, a volatile salicylate derivative, could be obtained from the isochorismate [10] precursor of phenylalanine.

The formation of phenylpropenes begins with reducing the carboxyl group of p-coumarate to alcohol. An acyltransferase then adds an acetate group which is reduced by a

phenylpropene synthase. In petunia, coniferyl alcohol acyltransferase (CFAT) catalyzes the formation of coniferyl acetate, which is the precursor of isoeugenol and eugenol formed by isoeugenol and eugenol synthase (IGS and EGS), respectively. [11]

The carboxyl group of cinnamate is reduced in the same way as phenylpropenes to form benzenoids. The prenyl group undergoes β -oxidation before oxidative decarboxylation. These compounds can then be modified by hydroxylases, methyltransferases, acetyltransferases, and ligases. For example, the benzoate/salicylate carboxyl methyltransferase (BSMT) petunia is responsible for the formation of methyl benzoate in flowers[12]

A benzoyltransferase carries out the condensation of 2 benzenoids or one benzenoid and 1phenylethanol to form molecules with two benzene rings. In petunia, the benzyl alcohol/phenyl ethanol benzoyltransferase (BPBT) is responsible for creating phenyl ethyl and benzyl benzoate. Phenyl ethanol would come to the reduction of the aldehyde group of phenylacetaldehyde, itself formed by a phenylacetaldehyde synthase (PAAS) from phenylalanine[13].In (Figure11) will abbreviate the biosynthesize of different phenolic compounds[14]

This diagram gathers the reactions and the enzymes discovered from flowers of different model plants for the study of volatile floral compounds (petunia, brewer's clarkie) according to the review by Pichersky and Dudareva (2007)[14]. The multiple arrows in solid lines represent numerous stages. Single arrows in solid lines represent the characterized reactions. The dashed arrows represent the possible steps for which the enzymes have not been characterized.4CL: p-coumarate-CoA ligase; BA2H: benzoate 2-hydroxylase; BPBT: benzoyl-CoA: benzyl alcohol/phenyl ethanol benzoyltransferase; BSMT: benzoate/salicylate carboxyl methyltransferase; C3'H: coumaroyl-shikimate / quinate 3'-hydroxylase; C4H: cinnamate 4-hydroxylase; CA5H: con-formaldehyde 5-hydroxylase (F5H: ferulate 5-hydroxylase); CFAT: coniferyl alcohol transferase; EGS: eugenol synthase; IGS: isoeugenol synthase; PAAS: phenylacetaldehyde synthase; PAL: phenylalanine ammonia-lyase; TAL: tyrosine ammonia-lyase.

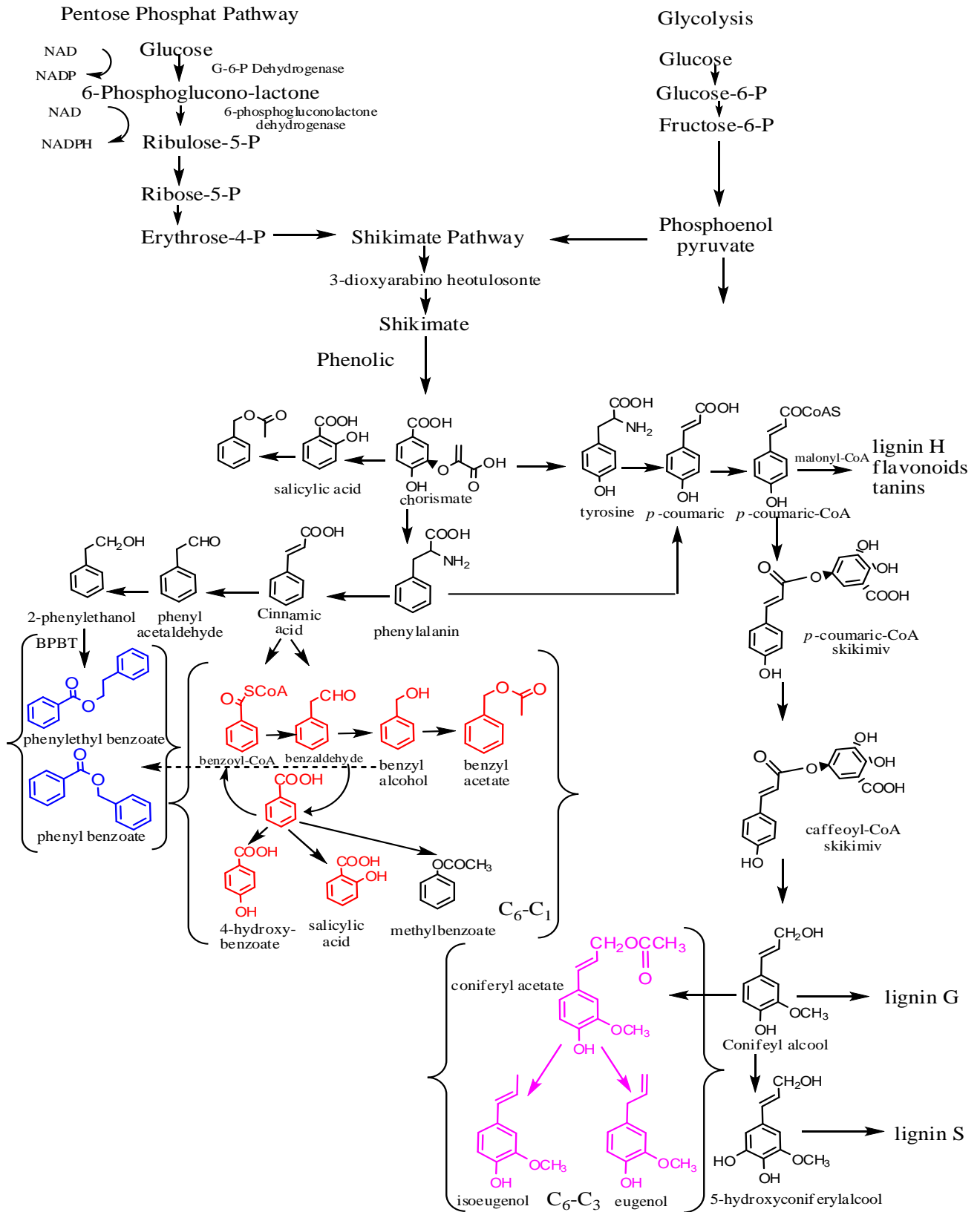
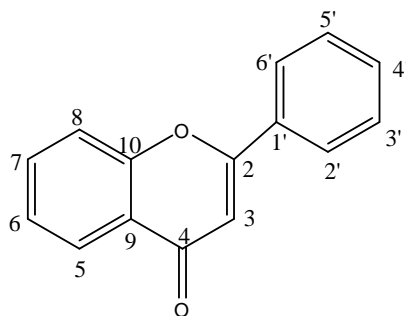


Figure 11: Biogenesis of simple phenols and phenolic acids.

II.2. Flavonoids:

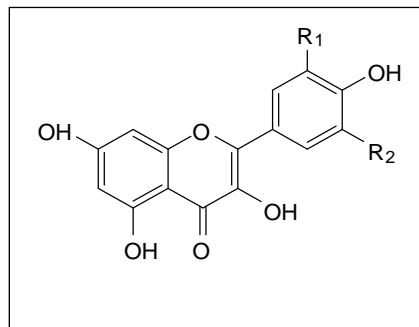
Flavonoids (flavus, yellow in Latin) represent a class of compounds polyphenolics widespread in the plant kingdom, of which several thousand compounds have already been identified. They are present in fruits, seeds, bark, roots, and flowers. They contribute to the different shades of blue, red, and yellow with flowers, leaves, and fruits. The structure of flavonoids is organized around a 1,3-diphenylpropanoid skeleton C₆-C₃-C₆, wherein two aromatic rings, C₆ (named A and B), are connected via a propanoid link C₃. This one is often engaged in an ether link with one of the aromatic rings C₆, leading to a heterocycle named C. According to the relative position of the two aromatic rings C₆ on the propanoid chain, three families of natural isomers have been defined: flavonoids, isoflavonoids, and neoflavonoids^[2].

Other naturally occurring compounds with a C₆-C₃-C₆ structure are considered minor flavonoids. These are the different structures of chalcones and aurones^[15]



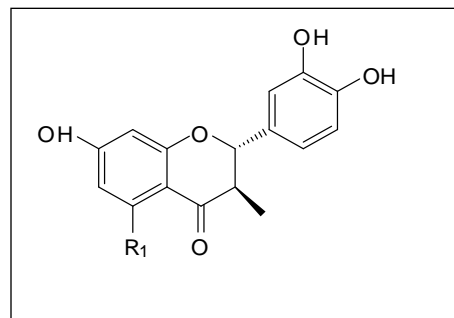
II.2.1. Flavonoids Classification:

In flavonoids, the categories are distinguished according to the degrees of oxidation and saturation of the C cycle. In contrast, within each category, the compounds are differentiated according to the substituents present on the rings A and B. Flavonoids are often hydroxylated in positions 3, 5, 7, 3', 4' and/or 5'. Frequently, one or more of these hydroxyl groups are methylated, acetylated, prenylated or sulfated. In plants, flavonoids are often present as O- or C-glycosides. The O-glycosides have sugar substituents bound to a hydroxyl group of the aglycone, usually located at position 3 or 7, whereas the C-glycosides have sugar groups bound to a carbon of the aglycone, usually 6-C or 8-C. [15]. Below main classes of flavonoids with examples.



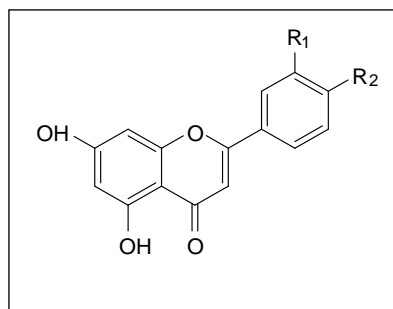
Flavonols

	R ₁	R ₂
kaempferol	H	H
Mirecytin	OH	OH



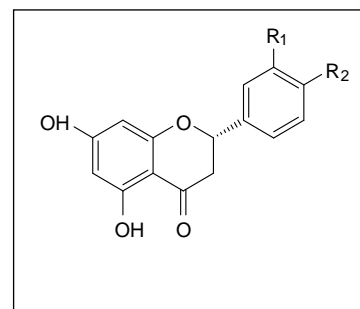
Dihydroflavonols

	R ₁
Taxifolin	OH
Fusetin	H



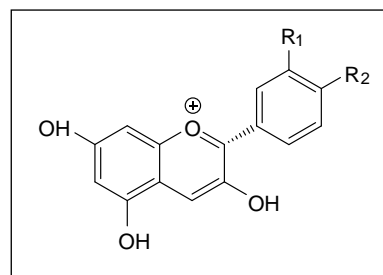
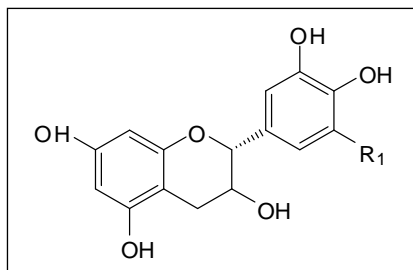
Flavons

	R ₁	R ₂
Apigenin	H	OH
Chrysin	H	H



Flavanones

	R ₁	R ₂
Hesperetin	OH	OMe
Naringenin	H	OH

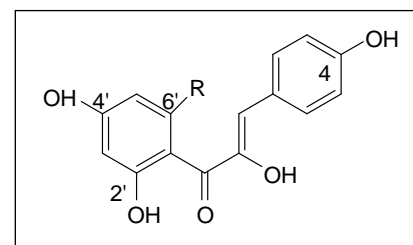
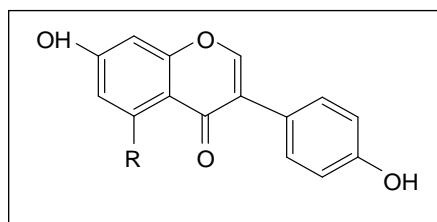


Flavanols

	R ₁
Catechin	H
Gallocatechin	OH

Anthocyanes

	R ₁	R ₂
Cyanidin	OH	OMe
Delphinidine	H	OH

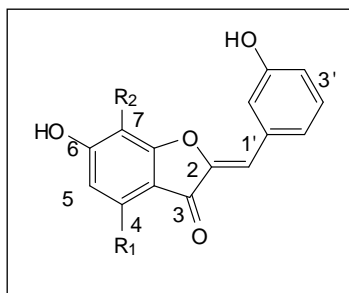


Isoflavones

	R ₁
Daidzein	H
Genistein	OH

Chalcons

	R ₁
Davidigenin	H
Asebogenin	OH



Aurones

	R ₁	R ₂
Leptosidine	OH	OMe
Maritimétine	OMe	OH

II.2.2. Flavonoids biosynthesis:

The biosynthesis of flavonoids begins with the formation of 3,5,7-trioxyacetate through several steps of acetyl-S-CoA and malonyl-S-CoA. The reaction between this precursor and p-hydroxycinnamyl-S-CoA makes it possible to form a chalcone (Figure 12). In the presence of an isomerase, the latter is in equilibrium with a (2S)-flavanone. This chalcone is also the forerunner of all classes flavonoids [2].

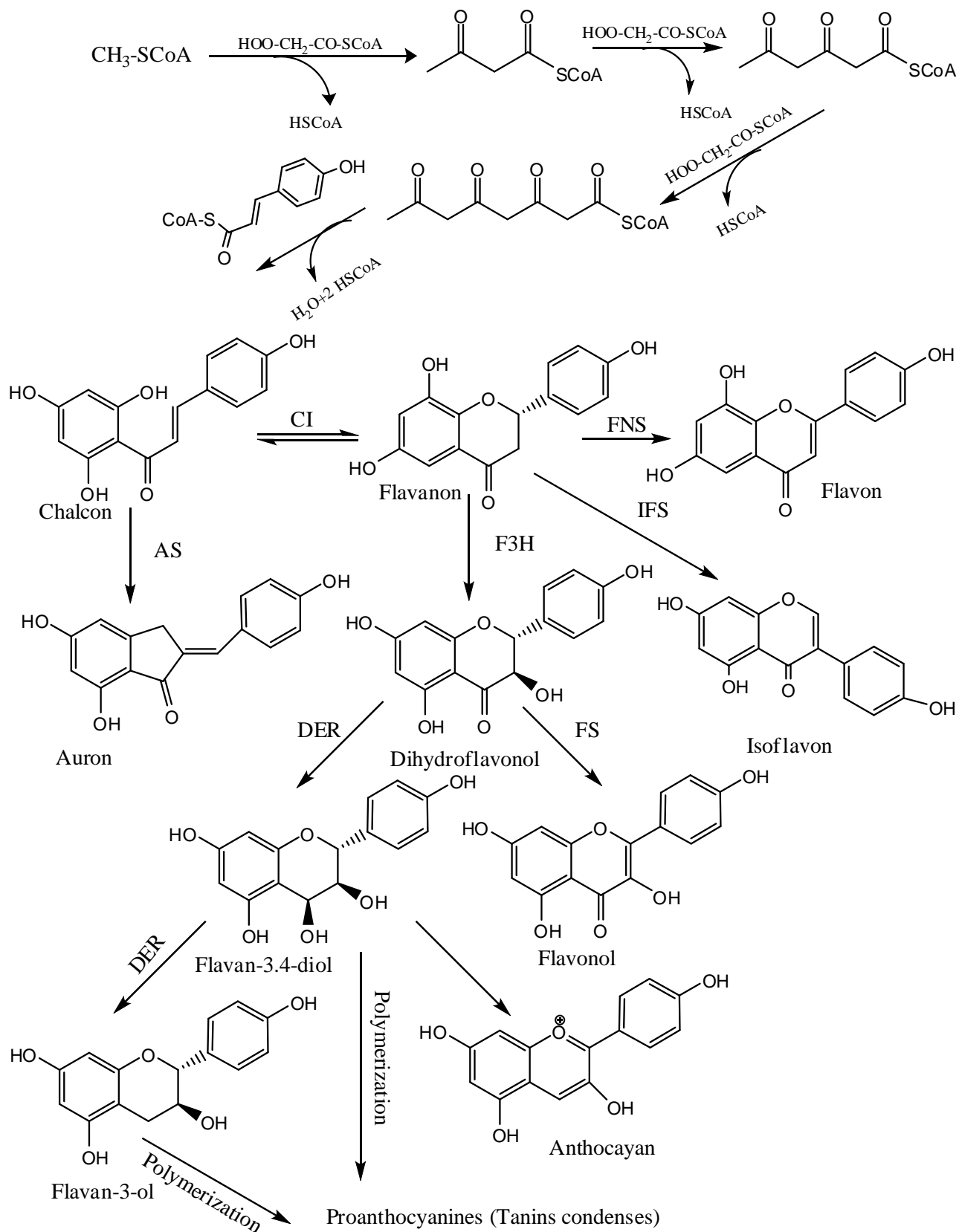


Figure 12: Flavonoids biosynthesis.

II.3. Terpenoids:

Terpenes are the most numerous and structurally diverse plant natural products[16],the isoprene unit, which can build upon itself in various ways, is a five-carbon molecule. The single isoprene unit presents a basic class of terpenes. The hemiterpenes are classified into the following categories according to the number of condensing units: hemiterpenoid (C₅), monoterpenoids (C₁₀), sesquiterpenoid (C₁₅), diterpenoid (C₂₀), triterpenoid (C₃₀), triterpenoid (C₄₀) or polyterpenoids (number of carbons greater than C₄₀).

Table 13: Present the main classes of terpenoid compounds.

<i>Carbon skeleton</i>	Class	Examples
<i>C₅</i>	Hemiterpenes	Prenol,3-methylbut-3-en-2-ol
<i>C₁₀</i>	Monoterpenoids	Limonene,α-pinene
<i>C₁₅</i>	Sesquiterpenoid	α-bisabolol
<i>C₂₀</i>	Diterpenoid	Abietic acid
<i>C₃₀</i>	Triterpenoid	Lanosterol
<i>(C₄₀)_n</i>	Polyterpenoids	β-carotene

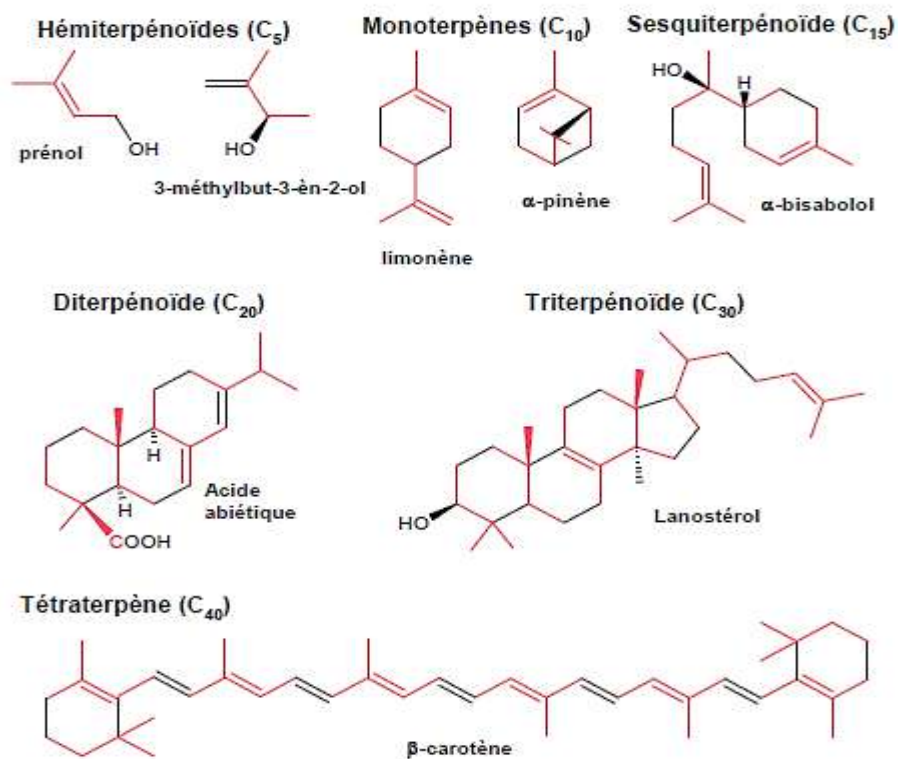


Figure 13: Present examples of terpenoid compounds.

II.3.2. Biosynthesis of the terpenoids, the voice of the mevalonate:

The biosynthesis of terpenoid compounds is very complex and multi-branched (Figure 14). However, it can be divided into five major processes. Acetyl coenzyme A is first converted to isopentenyl diphosphate (IPP). The action of various isoprenyl diphosphate synthases then generates, from the IPP, intermediates higher-order isoprenics, which contain 10, 15, or 20 carbon atoms and which are geranyl diphosphate (GPP), farnesyl diphosphate (FPP), and geranylgeranyldiphosphate (GGPP), respectively. There is the formation of C₃₀ and C₄₀ compounds from these intermediaries, which represent the precursors of sterols and carotenoids. These precursors may also undergo cyclization and constitute the basic skeleton of various terpenoid families or be used in alkylation reactions to provide the prenyl chain of non-terpenoid compounds. At present, several stages in the route of synthesis of isoprenoids are not still elucidated in plants. We present a summary of the biosynthesis process-based, in particular, on the work carried out in the mammals and Yeast [17].

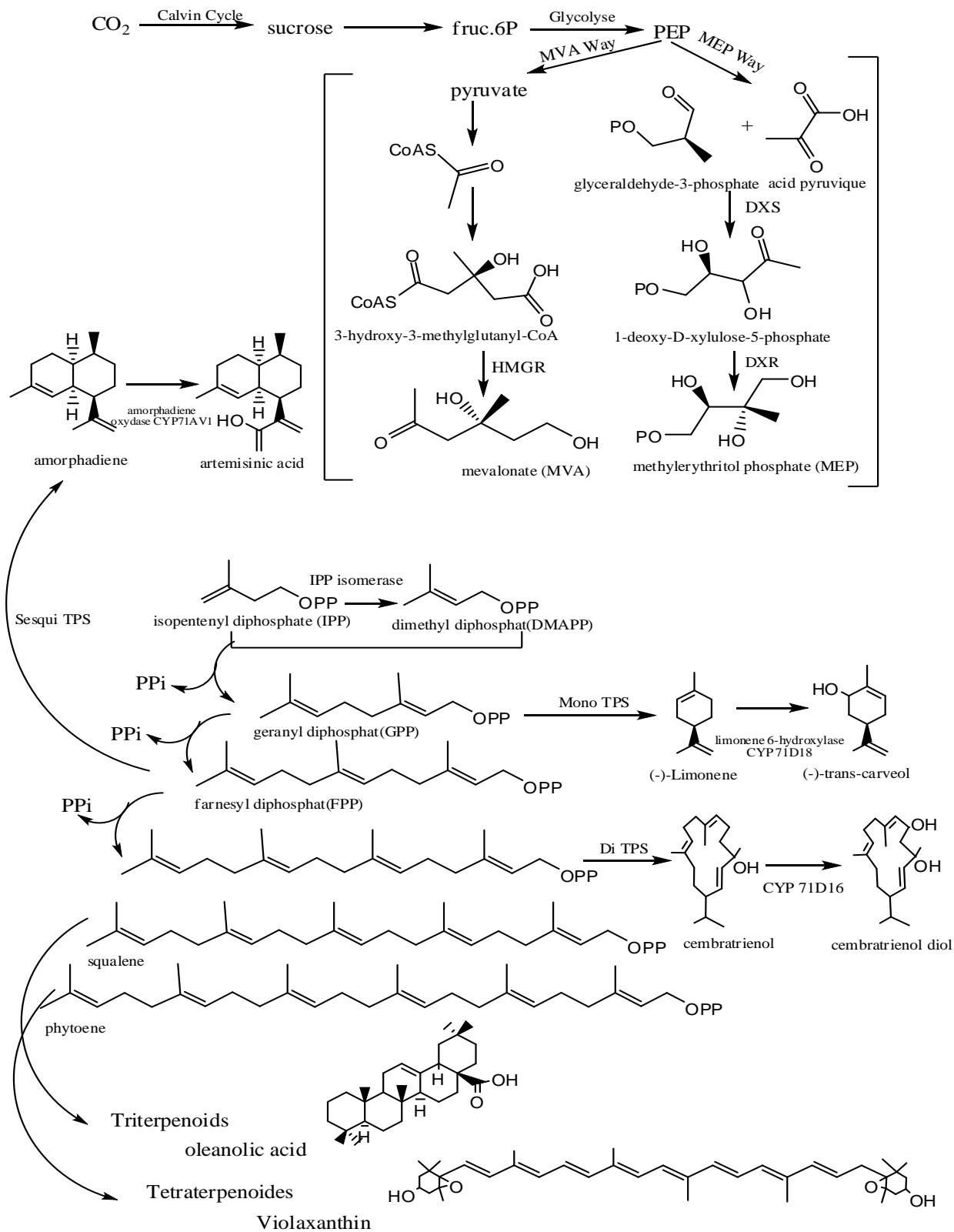


Figure 14: Biosynthesis of the terpenoids

The discovery of precursors of IPP was initiated by tracing experiments isotopic. The incorporation of sodium acetate in mice and rats allowed the formation of deuterated cholesterol [18]. In plants, IPP and its isomer allyl, dimethylallyl diphosphate (DMAPP), are generated from the pathway metabolism of mevalonate in the cytosol (MVA) or phosphate metabolic pathway of methylerythritol in the plastid (MEP).

At first, the DMAPP is condensed in "head-to-tail" with 1, 2, or 3 PPI units by prenyl transferases to form, respectively: the diphosphate of geranyl (GPP), the precursor of monoterpenoids (C10), farnesyl diphosphate (FPP), the precursor of sesquiterpenoid (C15), or geranylgeranyl diphosphate (GGPP), the precursor of diterpenoids (C20).

It is historically accepted that cytosolic PPI from the MVA pathway is the precursor of FPP and sesquiterpenoids. In contrast, the metabolic pathway of MEP provides PPI to form GPP and GGPP precursors of monoterpenoids and diterpenoids in the plastid. However, several studies have demonstrated the existence of PPI or DMADP exchanges between the two metabolic MVA and MEP, thus making it difficult to identify the origin of the biosynthesis of mono-, sesqui- and diterpenoids[19, 20] Squalene, precursors of triterpenoids (C30) and phytoene, tetraterpenoid precursors (C40) are obtained by condensation of 2 FPP and 2 GGPP, respectively.

References

1. Beta T, Nam S, Dexter JE, Sapirstein HD. Phenolic content and antioxidant activity of pearled wheat and roller-milled fractions. *Cereal Chem.* 2005;82(4):390-3.
2. Bruneton J. *Pharmacognosie: phytochimie plantes médicinales*. 5 editing, 2015.
3. Lattanzio V. Phenolic Compounds: Introduction. *Natural Products* 2013. p. 1543-80.
4. Bruneton J. *Pharmacognosie et phytochimie des plantes médicinales*, 3 editing, lavoisier. Paris; 1999.
5. Ribéreau-Gayon P. *Les Composés phénoliques des végétaux: par Pascal Ribéreau-Gayon: Dunod; 1968.*
6. Yao K, De Luca V, Brisson N. Creation of a metabolic sink for tryptophan alters the phenylpropanoid pathway and the susceptibility of potato to *Phytophthora infestans*. *The Plant Cell.* 1995;7(11):1787-99.
7. D. A. VATTEM 1 R RaKS. Cranberry phenolics-mediated elicitation of antioxidant enzyme response in fava bean. *J Food Biochem.* 2004(2225–2238):40-69.
8. Lin D, Hu L, You H, Sarkar D, Xing B, Shetty K. Initial screening studies on potential of high phenolic-linked plant clonal systems for nitrate removal in cold latitudes. *Journal of Soils and Sediments.* 2010;10(5):923-32.
9. Gavira C. *Production de terpènes fonctionnalisés par les cytochromes P450 de plantes recombinants: Université de Strasbourg; 2013.*
10. Mary C. Wildermuth , Julia Dewdney , Wu G, Ausubel FM. Isochorismate synthase is required to synthesize salicylic acid for plant defence. *letters to nature.* 2001;414:562-71.
11. Dexter R, Qualley A, Kish CM, Ma CJ, Koeduka T, Nagegowda DA, et al. Characterization of a petunia acetyltransferase involved in the biosynthesis of the floral volatile isoeugenol. *Plant J.* 2007;49(2):265-75.
12. Negre F, Kish CM, Boatright J, Underwood B, Shibuya K, Wagner C, et al. Regulation of methylbenzoate emission after pollination in snapdragon and petunia flowers. *Plant Cell.* 2003;15(12):2992-3006.
13. Boatright J, Negre F, Chen X, Kish CM, Wood B, Peel G, et al. Understanding in vivo benzenoid metabolism in petunia petal tissue. *Plant Physiol.* 2004;135(4):1993-2011.
14. Pichersky E, Dudareva N. Scent engineering: toward the goal of controlling how flowers smell. *Trends Biotechnol.* 2007;25(3):105-10.
15. Marais JP, Deavours B, Dixon RA, Ferreira D. The stereochemistry of flavonoids. *The science of flavonoids: Springer; 2006.* p. 1-46.
16. Croteau R, Kutchan TM, Lewis NG. Natural products (secondary metabolites). *Biochemistry and molecular biology of plants.* 2000;24:1250-319.
17. Kribii R, Soustre I, Karst F. Biosynthèse des isoprénoides. *Acta Botanica Gallica.* 1999;146(1):5-24.
18. Konrad Bloch RD. On the utilization acitec acid for cholesterol formation *J Biol Chem.* 1942(145):625-36.
19. Natalia Dudareva SA, Irina Orlova, Nathalie Gatto, Michael Reichelt, David Rhodes, Wilhelm Boland, and Jonathan Gershenzon. The nonmevalonate pathway supports both monoterpene and sesquiterpene formation in snapdragon flowers. *Proc Natl Acad Sci U S A.* 2005;102:933–8.

References

20. Oliver Laule AFr, Hur-Song Chang , Tong Zhu , Xun Wang , Peter B. Heifetz , Wilhelm Grisseem , et al. Crosstalk between cytosolic and plastidial pathways of isoprenoid biosynthesis in *Arabidopsis thaliana*. *Proc Natl Acad Sci U S A*. 2003;100:6866–71.

CHAPTER III
PHYTOCHEMICAL
INVESTIGATION

III.1. Materiels

III.1.1. Plant material

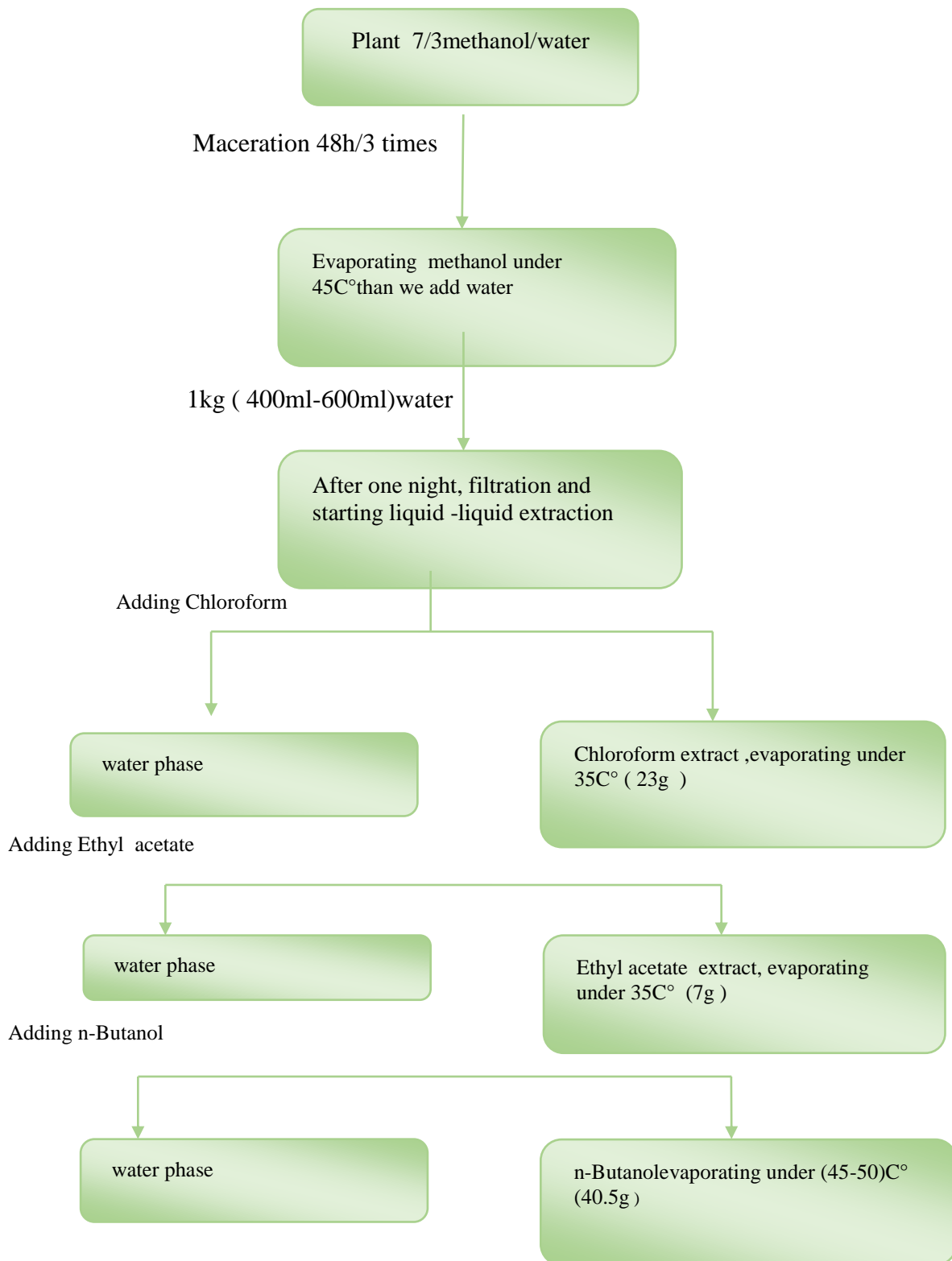
The aerial parts of *P. laciniata* were collected in April 2016 from Zelfana Ghardaia, Algeria. The plants were identified and authenticated (201604zel/pullac) by Dr. Iddoude, Faculty of Science of Nature and Life, Department of Biological Sciences, Kasdi Merbah University, Ouargla, Algeria. The fresh aerial parts were cut into small pieces and air-dried at room temperature. The final weight was 3kg.



Figure 15: *Pulicaria laciniata*(Cross. and kral.) 2016

III.1.2. Sample preparation

The dried and powdered plant was macerated with petroleum ether for 24 hours. After filtration, the plant was left to dry at room temperature. Then the plant was macerated again with a mixture of ethanol/water (70/30, v/v) for 48 h at room temperature three times, in each time, the solvent was renewed. After filtration and the concentration under pressure, the methanoic extract was diluted with distilled water at 400-600 ml per 1kg of dry matter. The solution was left to rest overnight and then filtered. The filtrate was extracted successively (liquid-liquid extraction) by solvents with increasing polarity, such as CHCl_3 , ethyl acetate, and n-butanol; each extraction was repeated three times except with ethylacetate. The extraction protocol is summarized in (Figure 16).

**Figure 16:** Protocal extraction

III.2. Methods

III.2.1. Phytochemical fingerprint

The phytochemical fingerprint profiles of the different extracts were performed by vanillinsolution [1], methanolic KOH solution (5% m/v), and Lieberman-Bürchard reagent [2].

III.2.2. Screening of Phytochemicals:

The phytochemical fingerprint profiles were followed using several phytochemical analyses described by [3].

-Phenols Test: A mixture of a small amount of the extract was placed in a test tube with 1 ml of water and one to two drops of Iron (III) chloride. Blue, green, red, or purple color formation indicates the presence of phenols.

- Tannin Test: Five ml of each extract was placed in a test tube, and 2 ml of iron (III) chloride (5% w/v) solution was added. A greenish-black coloration means the presence of tannins existence

- Flavonoids Test: The extracts were mixed with five drops of concentrated hydrochloric acid. Immediate production of red color indicates the presence of flavonoids.

- Glycosides Test: An amount of extract was mixed with 1 ml of water and a few drops of aqueous sodium hydroxide. Yellow coloration indicates the presence of glycosides.

- Alkaloids Test: 1 ml of the extracts was added in a test tube with 0.2 ml of diluted hydrochloric acid. After a few seconds, 1 ml of dragendorff's reagent was mixed. The appearance of white precipitation indicated the presence of alkaloids.

-Terpenoids Test: A mixture of 0.5 ml of the extracts with 2 ml of CHCl_3 and 3 ml of concentrated sulphuric acid giving the brown-reddish interface coloration, indicates the presence of terpenoids.

III.2.3. Quantification of phenolic classes :

III.2.3.1. Total phenol quantification :

The total phenolic content (TPC) was performed with a minor modification using the

Folin-Ciocalteu reagent [5]. Briefly, 50 µl of 10 times diluted Folin-Ciocalteu, and 200 µl of sodium carbonate (20% w/v) were mixed. After 30 min of incubation in the dark at room temperature, 10 µl of each diluted extract was added to a 96-well-microplate. The absorbance was measured at 760 nm. Results were expressed as mg Gallic Acid equivalent (GAE)/g of extract.

III.2.3.2. Flavonoid quantification:

Flavonoid quantification (FQ) was determined [5] with a minor modification. In brief, 150 µl of aluminium (III) chloride (2% w/v) was added to 150 µl of each diluted extract in 96-well-microplates. The absorbance was measured at 430 nm after 10 min of incubation. Results were expressed as mg Quercetin equivalent (QE)/g of extract.

III.2.3.3. Tannin quantification:

Tannin quantification (TQ) was evaluated [4]. 5 µL of diluted samples, 300 µl of vanillin (4% w/v) methanolic solution, and 150 µl of concentrated HCl were mixed, and the mixture was allowed to stand for 15 min. Then, the absorbance was measured at 500 nm. Results were expressed as Catechine equivalent (CE)/g of extract.

III.3. Result:

III.3.1. Extraction yield:

Dried aerial parts of *P. laciniata* were extracted by maceration technique using solvents with increasing polarity, such as petroleum ether, CHCl₃, ethyl acetate, and n-butanol. The yield of dried extracts showed the extraction capacity of each solvent. The BuOH extract exhibited the highest yield (40.5 g), followed by the CHCl₃ extract (23.5 g) and EtOAc extract (5.5 g). In terms of the yield percentage and solvent polarity, we suggest that using each solvent with different polarity resulted in an additional extract yield due to the nature and quantity of secondary metabolites dissolved in the solvents. n-butanol extracts exhibited the highest yield, which can be attributed to the solubility of polar carbohydrates and secondary metabolites glycosides.

III.3.2. Phytochemical fingerprint:

The results of the phytochemical screening by thin-layer chromatography (TLC) of the extracts are indicated in Orange, yellow, blue, green, and purple... spots were observed under UV 254nm and 365 nm on the chromatogram. Those spots corresponded to several classes of secondary metabolites. To specify the nature of these compounds, the chromatograms were developed in different solvent systems until we got a good separation of the spots. The chosen ones were:

CHCl₃ extract; Hexane/EtOAc 1/0.1 (v/v)

EtOAc extract; CHCl₃/EtOAc / MeOH 2/0.5/0.250 (v/v/v)

n-BuOH extracts; CHCl₃/MeOH /H₂O 40/9/1 (v/v/v)

After that, the TLC plates were revealed with specific reagents such as Libermann-Bürchard, potassium hydroxide, and vanillin solution. The chromatograms were used to purify chemical compounds to establish phytochemical sample fingerprints. (Figure 17) showed that the structural diversity of compounds reacted on the chromatogram indicated the existence of various secondary metabolites found in different extracts. Sterols generally fluoresce in blue, yellow, and green under UV/366 nm, while terpenes were in blue, yellow, green, and purple. If the spots have an invisible orange-yellow fluorescence after spraying Libermann-Bürchard reagent on the chromatogram, that's indicated the presence of lupine-type triterpenes. If the spots are colored red, oleanane- and ursane-type triterpenes exist. (Brou Kouassi Guy, 2010) [2]. Most coumarins are fluorescent under UV at 366 nm in blue, purple, pink, green, yellow, and purple. Some coumarins are colored with yellow invisibly due to their structure based on daphnetin, and their color intensifies after treatment with a methanolic solution of KOH (5%, m/v) [2]. Our extract contains lupane-type triterpenes and coumarins, depending on this previous research. Also, other active compounds react with the vanillin solution, which could be sterols, according to (Kotze, M.2000)[1]. More analyses are needed to identify the other active substances that need to be determined.

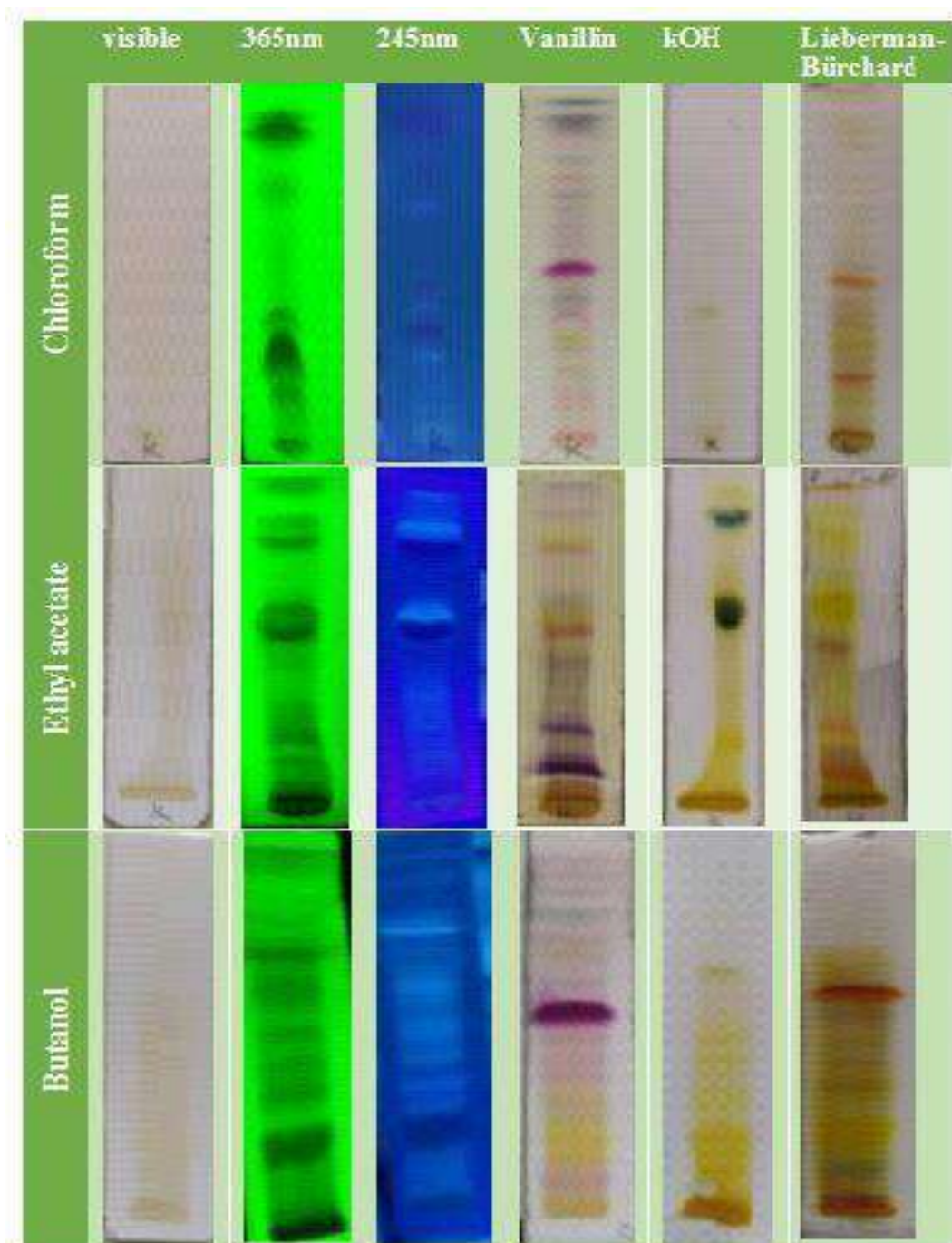


Figure 17: Phytochemical fingerprint Chromatograms. The chromatograms were developed in the different solvents.

III.3.3. Phytochemicals screening.

The phytochemical screening carried out on the different extracts of *P. laciniata* makes it possible to highlight the presence of some chemical groups represented in Table 14.

Table 14: Phytochemicals screening of *P. laciniata* extracts.

	n-BuOHextract	EtOAcextract	CHCl ₃ extract
Phenols	+	+	+
Flavonoids	++	++	+
Glycosides	++	+	-
Alkaloids	+	++	++
Tannins	+	+	+
Terpenoids	-	+	+++
(+) = positive, (-) = negative			

III.3.4. Quantification of phenolic classes:

The total phenolic, flavonoid, and tannin content of different extracts are listed in Table 15. The results showed that BuOH and EtOAc extracts exhibited the highest phenolics and flavonoids. In contrast, CHCl₃ extract presented a tiny amount of phenolics and flavonoids. On the other hand, CHCl₃ extract showed the most elevated total tannins (8.44 ± 0.79 mg C.T./g), EtOAc extract, and BuOH extract (5.24 ± 0.68, 4.240 ± 0.583 TCC mg C.T./g), respectively. This difference is due to the increased polarity of each solvent and the solvent's capacity to entrain different secondary metabolites.

Table 15: Different extracts' total phenolic, flavonoid, and tannin content.

Extract	n-BuOH	EtOAc	CHCl ₃
TFCmgQE/g	437.66 ± 1.82	497.92 ± 2.41	43.3 ± 1.83
TPCmgGAE/g	231.67 ± 20.05	221.59 ± 12.91	178.80 ± 17.53
TTCmgCE/g	5.240 ± 0.583	5.246 ± 0.685	8.44 ± 0.790
Results are expressed in terms of SD (n = 3)			

References

Reference

1. Kotze M, Eloff J, Houghton P. Extraction of antibacterial compounds from *Combretum microphyllum* (Combretaceae). *South African journal of botany*. 2002;68:62-7.
2. Brou Kouassi Guy, Mamyrbekova-Bekro Janat Akhanovna, Dogbo Dénézon Odette, Gogbeu Seu Jonathan, Yves-Alain B. On the Qualitative Phytochemical Composition of Crude Hydromethanolic extracts of the Leaves of 6 Varieties of *Manihot Esculenta* Crantz of Côte d'Ivoire. *European Journal of Scientific Research*. 2010;Vol.45 No.2 200-11.
3. Boulenouar N, Marouf A, Cheriti A. Antifungal activity and phytochemical screening of extracts from *Phoenix dactylifera* L. cultivars. *Natural product research*. 2011;25:1999-2002.
4. Medini F, Fellah H, Ksouri R, Abdelly C. Total phenolic, flavonoid and tannin contents and antioxidant and antimicrobial activities of organic extracts of shoots of the plant *Limonium delicatulum*. *Journal of Taibah University for science*. 2014;8:216-24.

CHAPTER IV
SEPARATION AND
PURIFICATION

IV.1. Fractionation of Ethyl acetate extract:

The various extracts obtained, CHCl_3 extract (23 g), EtOAc (5.5g), and n-BuOH (40.5 g) were analyzed by TLC in elution systems compatible with the nature of the extract to assess their richness in metabolites secondary globally. The results of the chromatographic tests prompted us to explore the EtOAc extract chemically.

The ethyl acetate extract weighed 5.5 grams and was first put through a Sephadex LH-20 column chromatography and eluted with methanol.

Table 16: The obtained results of Separation chromatography on the Sephadex LH-20 column of the EtOAc extract.

N.Fractions	Important notes
1	No trace of compounds
2	
3	A mixture of compounds named fraction A was treated
4	
5	
6	A mixture of compounds named B fraction was not treated due to its small quantity
7	
8	
9	A mixture of compounds named fraction C was treated
10	
11	
12	A mixture of compounds named fraction D was treated
13	
14	
15	
16	
17	A mixture of compounds named fraction E was treated
18	
19	Fraction F Easy separation mixture
20	
21	A mixture of minimal amounts
22	
23	
24	
25	
26	

This separation made it possible to collect 26 fractions; those fractions were evaluated in a variety of systems, after which it was compiled and evaluated once more to generate the five primary fractions A, B, C, D, and E, which are shown in the following table and (Figures 18 and 19).

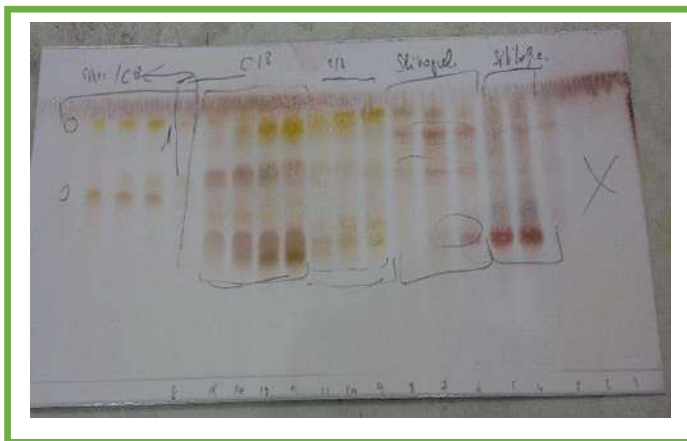


Figure 18: TLC of the first column fractions after collection of similar ones after the revelation

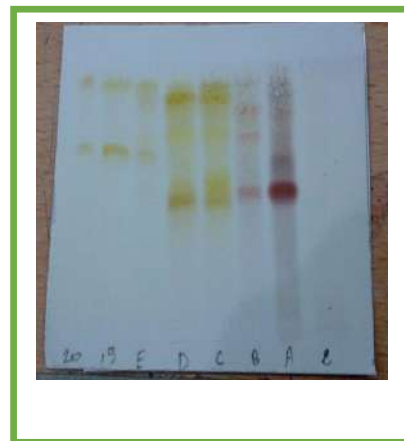


Figure 19: TLC of the second collection of the LH-20 column after the revelation with acidic solution

IV.2. Fractionation of fraction A:

The fractions 3, 4, and 5 were combined to create fraction A, which was then fractionated using a C18 column eluted by water and methanol in various proportions, beginning with 9/1, 8/2, 7/3, and 1/1 until it was entirely composed of methanol

This separation produced more than thirty fractions, all the fractions tested on TLC where similar ones were collected to get 12 fractions. the vast majority of them were complicated and did not support a further separation of the substance. Because of this, the primary emphasis was placed on isolating the compounds that could be seen clearly and easily on fractions F-7 and F-8, as represented on the (Figure20).

Table 17: The obtained results of Separation chromatography on C18 Silica Gel column of fraction A

H ₂ O/MeOH	Before collection	After collection
90/10	1-3	F-1
90/10	4-6	F-2
85/15	7-9	F-3
85/15	10-12	F-4
80/20	13-15	F-5
75/25	16-18	F-6
75/25	19-24	F-7
70/30	25-30	F-8
70/30	31-33	F-9
70/30	34-35	F-10
65/35	36-37	F-11
50/50 until MeOH	38 -45	F-12

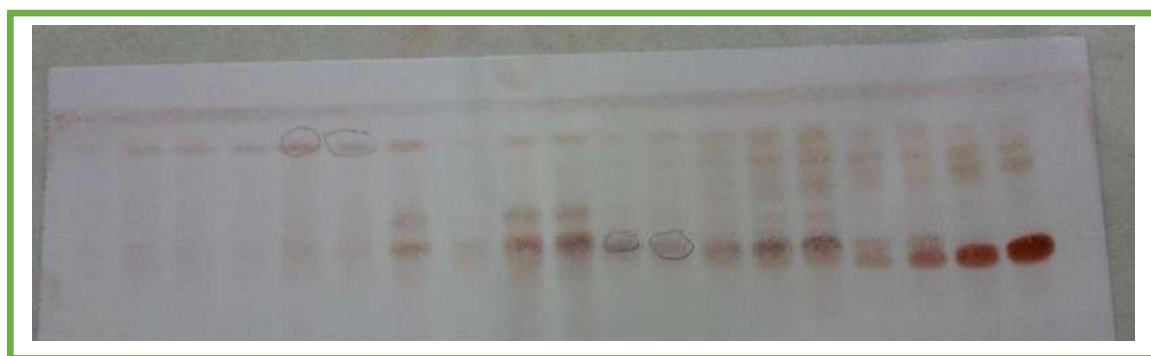


Figure 20: TLC of the fraction A separation using C-18 after revelation.

The fraction F-7 and F-8 was collected, then fractioned with silica gel using (CHCl₃/MeOH) eluted in various ratios beginning with 99/1 until methanol became their only solvent. This separation produced more than 60 fractions. All fractions were put through a series of tests (Figure 21).

The fractions 29–42 were recollected and put through one more purification step on a column containing Sephadex LH 20 eluted by Toluene/MeOH starting with 6/1, 5/2, 4/3, 1/1, then 100% methanol. This step was the last in the purification process. The pure compound K1 (35mg) appeared as white needles.

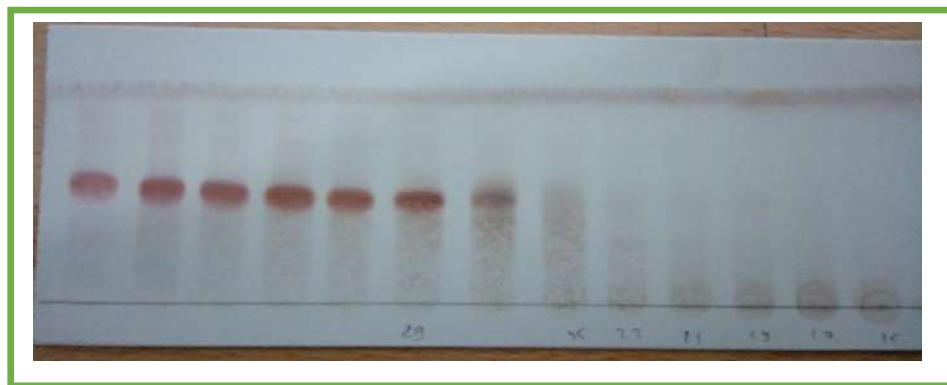


Figure 21: TLC of fraction during purification of compound K1

Table 18: The obtained results of Separation chromatography on Silica gel column of F-7 and F-8 sub-fraction

F-7 and F-8 sub-fraction / Silica gel column			F-8 fraction / LH-20 column		
CHCl ₃ /MeOH	Before collection	After collection		Before collection	After collection
CHCl ₃	1-2	F-1		1-13	tiny amount
99/1	2-3	F-2		14-29	tiny amount
97/3	4-6	F-3		30-39	tiny amount
95/5	7-9			40-45	tiny amount
90/10	10-12	F-5		(46-60) : K1 in pure state crystallized as white needles	
85/15	13-16	F-6			
80/20	17-28	F-7			
70/30	29-42	F-8	F-8		

IV.3. Fractionation of fraction F:

The fraction F from the first column, which contained one primary compound with impure once, was separated by a silica gel column eluted by $\text{CHCl}_3/\text{MeOH}$ with several proportions, including 9/1, 8/2, 7/3, and 3/2. Then it was purified using Sephadex LH-20 eluted with $\text{CHCl}_3/\text{MeOH}$ (2/1). Finally, the compound K2 (9mg) is pure as yellow needles.

IV.4. Fractionation of fraction C and D:

The fractions C and D from the first column were combined because of the remarkable similarity between them, so they were run through a C18 Silica Gel column chromatography and eventually eluted using many different water/methanol ratios, such as 8/2, 7/3, 6.5/3.5, 6/4, 5/5, and 100% methanolreaching more than 100 fraction

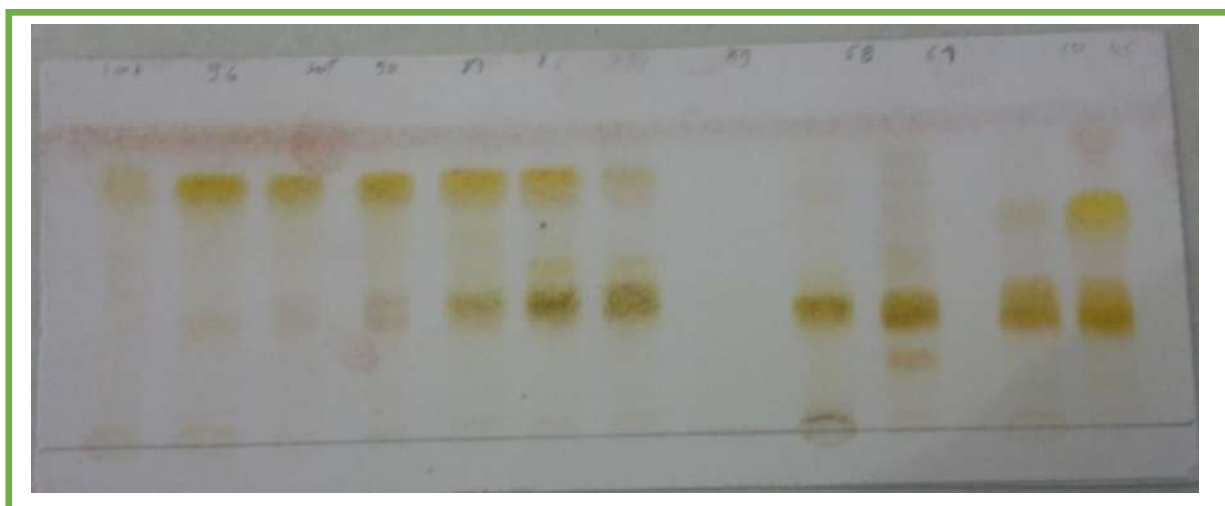


Figure 22: TLC of the fraction C+D separation using C-18 after revelation with an acid solution

Table 19: The obtained results of Separation chromatography on C18 Silica Gel column of fractions C and D.

F-C and F-D / C18 column		
H₂O/MeOH	Before collection	After collection
95/5	1-3	F-1
90/10	4-6	F-2
85/15	6-14	F-3
85/15	15-20	F-4
85/15	21-22	
85/15	21-25	F-5
80/20	26-30	F-6
80/20	31-34	F-7
80/20	35-38	
75/25	39-40	F-8
75/25	41-50	F-9
75/25	51-61	F-10
70/30	62-71	F-11
70/30	72-835	F-12
70/30	81-89	F-13
68/32	90-98	F-14
50/50 until MeOH	98-105	F-15

After analyzing the entire fraction using several TLC, a decision was reached on combining fractions as 15 fractions. The following fractions, F-4, F-7, F-11, and F-14, were fractionated and re-evaluated by TLC. It was decided to separate a second time.

III.4.1. Fractionation of sub-fraction F-11 from the separation of fractions C and D:

After obtaining the F-11 subfraction, it was subjected to a second round of separation using a silica gel column, this time with $\text{CHCl}_3/\text{MeOH}$ serving as the elution solvent. The polarity was raised gradually from its initial state of 100% CHCl_3 up to its final state of 100% MeOH. This separation produced more than sixty different fractions, and TLC was used to evaluate each. The similar ones were merged to create seven subfractions, which were later re-evaluated using TLC. It was discovered that fraction four had one main product, which was refined by passing it over a Sephadex LH-20 column while eluting it with toluene and methanol (6/1). These separation steps give K3 in the form of pure yellow needles. All steps of purification are summarized in Table 20.


Table 20: The obtained results of Separation chromatography on Silica gel and Sephadex LH-20 column of sub-fraction 11

F-11 sub-fraction / Silica gel column			F-4 fraction / LH-20 column		
$\text{CHCl}_3/\text{MeOH}$	Before collection	After collection	F-4	Before collection	After collection
CHCl_3	1-5	F-1		1-13	tiny amount
99/1	6-15	F-2		14-29	complicated
97/3	16-25	F-3		30-39	complicated
95/5	26-37	F-4		40-50	tiny amount
90/10	38-48	F-5		(51-67) : K3 in pure state crystallized as yellow needles	
85/15	49-55	F-6			
80/20	56-60	F-7			

III.4.2. Fractionation of sub-fraction F-14 from the separation of fractions C and D:

The resultant subfraction F-14 was subjected to a second separation on a silica gel column using $\text{CHCl}_3/\text{MeOH}$ as the elution solvent. The polarity was increased from 100% CHCl_3 to 100% MeOH over time. TLC examined all of the more than 70 fractions that were obtained after this separation. The TLC analysis was repeated with six subfractions obtained by combining similar ones. It was found that the fourth fraction included one main product, which was purified by passing it through Sephadex LH-20 eluted with Toluene/MeOH (6/1). It resulted in the formation of K3 in the form of pure yellow needles. All steps of purification are summarized in table 21.

Table 21: The obtained results of Separation chromatography on Silica gel and Sephadex LH-20 column of sub-fraction 14

F-14 sub-fraction / Silica gel column			F-4 fraction / LH-20 column		
$\text{CHCl}_3/\text{MeOH}$	Before collection	After collection		Before collection	After collection
CHCl_3	1-5	F-1		1-7	tiny amount
99/1-97/3	6-25	F-2		8-29	tiny amount
95/5 -90/10	26-40	F-3		30-39	tiny amount
85/15	40-50	F-4		45-51	tiny amount
80/20	51-63	F-5		(52-68) : K4 in pure state crystallized as yellow needles	
85/25	64-70	F-6			

III.4.3. Fractionation of sub-fraction F-7 from the separation of fractions C and D.

The F-7 subfraction was separated again using a silica gel column with $\text{CHCl}_3/\text{MeOH}$ as the elution solvent. The polarity increased from 100% CHCl_3 to 100% MeOH. TLC evaluated over seventy fractions from this separation. Ten identical subfractions were created

and re-evaluated using TLC. Fraction 8 had one major product, which was refined on a Sephadex LH-20 column using toluene and methanol (6/1). K3 was pure yellow needles after separation. Table 22 lists all purification stages.

Table 22: The obtained results of Separation chromatography on Silica gel and Sephadex LH-20 column of sub-fraction 7.

F-7 sub-fraction / Silica gel column			F-8 fraction / LH-20 column		
CHCl ₃ /MeOH	Before collection	After collection		Before collection	After collection
CHCl ₃	1-2	F-1		1-3	tiny amount
99/1	3-5	F-2		4-6	tiny amount
97/3	6-10	F-3		7-10	complicated
95/5	11-15	F-4		11-16	complicated
90/10	16-21	F-5		17-21	complicated
85/15	22-30	F-6		22-27	complicated
80/20	31-40	F-7		28-31	tiny amount
75/25	41-50	F-8	F-8	32-35	tiny amount
75/25	51-65	F-9		(36-48) : K5 in pure state crystallized as yellow needles	
70/30	64-70	F-10			

III.4.4. Fractionation of sub-fraction F-4 from the separation of fractions C and D.

A silica gel column was used to separate the F-7 subfraction once more, with CHCl₃/MeOH serving as the elution solvent. Going from 100% CHCl₃ to 100% MeOH enhanced the polarity. TLC examined almost 65 fractions from this separation. TLC was used to re-evaluate nine subfractions that were generated. One notable product from fraction seven

was refined using toluene and methanol on a Sephadex LH-20 column (6/1). After separation, K6 was made entirely of yellow needles. All purification steps are listed in Table 23.

Table 23: The obtained results of Separation chromatography on Silica gel and Sephadex LH-20 column of sub-fraction 4.

F-4 sub-fraction / Silica gel column			F-7 fraction / LH-20 column		
CHCl ₃ /MeOH	Before collection	After collection		Before collection	After collection
CHCl ₃	1-2	F-1		1-3	tiny amount
99/1-90/10	3-10	F-2		4-5	tiny amount
	11-18	F-3		6-9	tiny amount
85/15-80/20	19-27	F-4		10-15	tiny amount
75/25	16-21	F-5		16-22	complicated
	22-30	F-6		23-30	complicated
70/30	31-40	F-7	F-7	31-48	tiny amount
65/35	41-50	F-8		(49-60) : K6 in pure state crystallized as yellow needles	
60/40	51-65	F-9			

III.5. Gc-MS analyses of the Chloroform extract:

The chloroform extract was further analyzed by Shimadzu Gas Chromatography-Mass Spectrometry Apparatus (GC-MS -TQ8040 NX]. 1 µl of the chloroform extract was injected in a DB-5 fused silica column (30 m length × 0.25 mm diameter, 0.25 µm film thickness). The injector was set at 200C° and the detector at 250C°. The stepped temperature program was as follows: held at 60C° for 3min, then, from 60 to 246 C° at the rate of 10C/min, held for 10 min. The total run time was of 80min. The GC-MS interface temperature was 11 at 24 C°. The injection volume was one. The solvent delay was 2 min and injected in a split ratio of 1:10. The MS scan range was from 35 –6,000 Da. Compound identification was obtained by

comparing the retention times with those of authentic compounds and the spectral data obtained from the library data of the corresponding compounds.

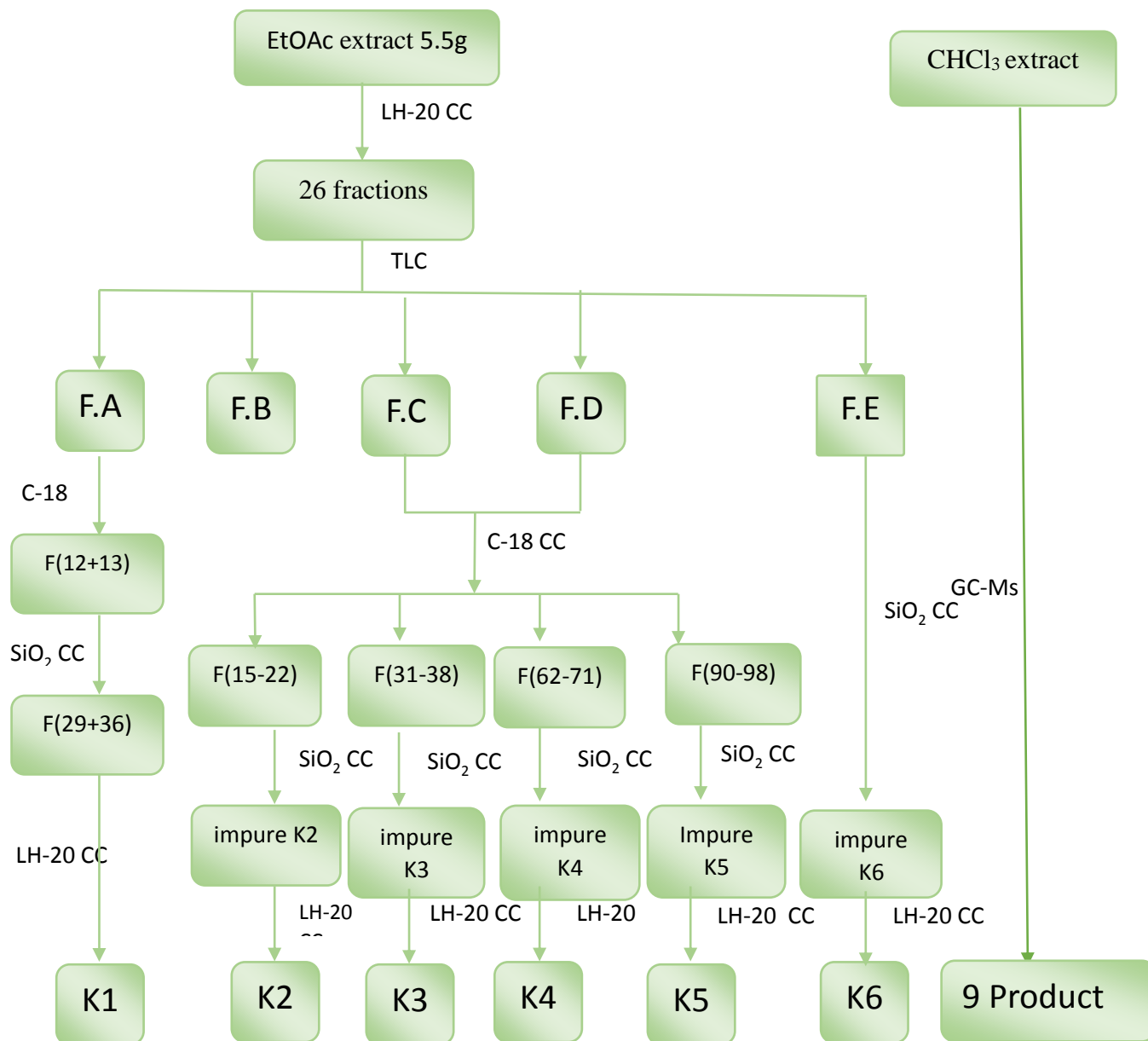


Figure 23: Phytochemical study of the Ethyl acetate and Chloroform extracts.

CHAPTER V
STRUCTURE
ELUCIDATION

V.1. Structure elucidation of compound K1:

This compound is in the form of brilliant white needles. Simultaneous examination of the spectra: ^{13}C NMR (spectrum-24), DEPT-135 (spectrum 25) ^1H NMR s (spectrum-26, 27 and 28), and HSQC (spectrum-29) show the presence of twenty-one carbon atoms shows a typical profile of a glycosylated sesquiterpene that distributed as follows:

- Three CH_3 groups at $\delta_{\text{c}}=13.71$; 23.79 and 28.13ppm;
- Two non-oxygenated CH_2 groups sp^3 hybridized at 24.96 ppm and 27.67 ppm;
- One oxygenated CH_2 group sp^3 hybridized at 64.71 (sugar)
- 11CH including four ethylenic groups at $\delta_{\text{c}}=133.3$; 136.8; 138.0; 148.2 ppm, two CH sp^3 hybridized that resonates at 87.73 and 90.07 ppm, and five oxygenated CH groups sp^3 hybridized at 101.89 ppm as an anomeric proton, 72.54, 75.90, 77.43 and 78.41 (sugar).
- Four quaternary carbons, including:
 - A carbonyl characteristic of a γ -lactone at $\delta_{\text{c}} = 172.78$ ppm;
 - A sp^3 hybridized C_q at $\delta_{\text{c}} = 42.71$ ppm;
 - Two sp^2 hybridized C_q at $\delta_{\text{c}} = 136.60$ and 142.37 ppm.

A return to the heteronuclear spectrum (^1H - ^{13}C): HSQC at a short distance makes it possible to distinguish the chemical shifts of carbons from the respective shifts of their protons established in Table 24.

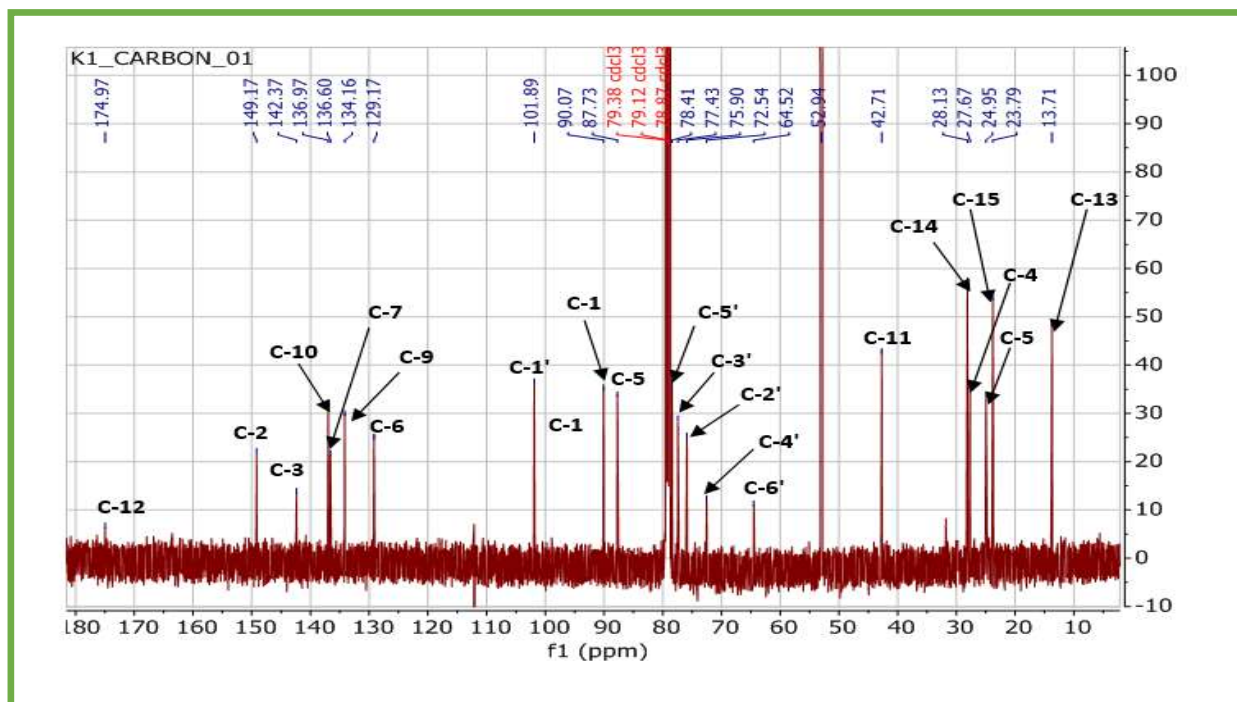


Figure 24 Spectrum :RMN ^{13}C (125MHz,CDCL $_3$) of compound K1

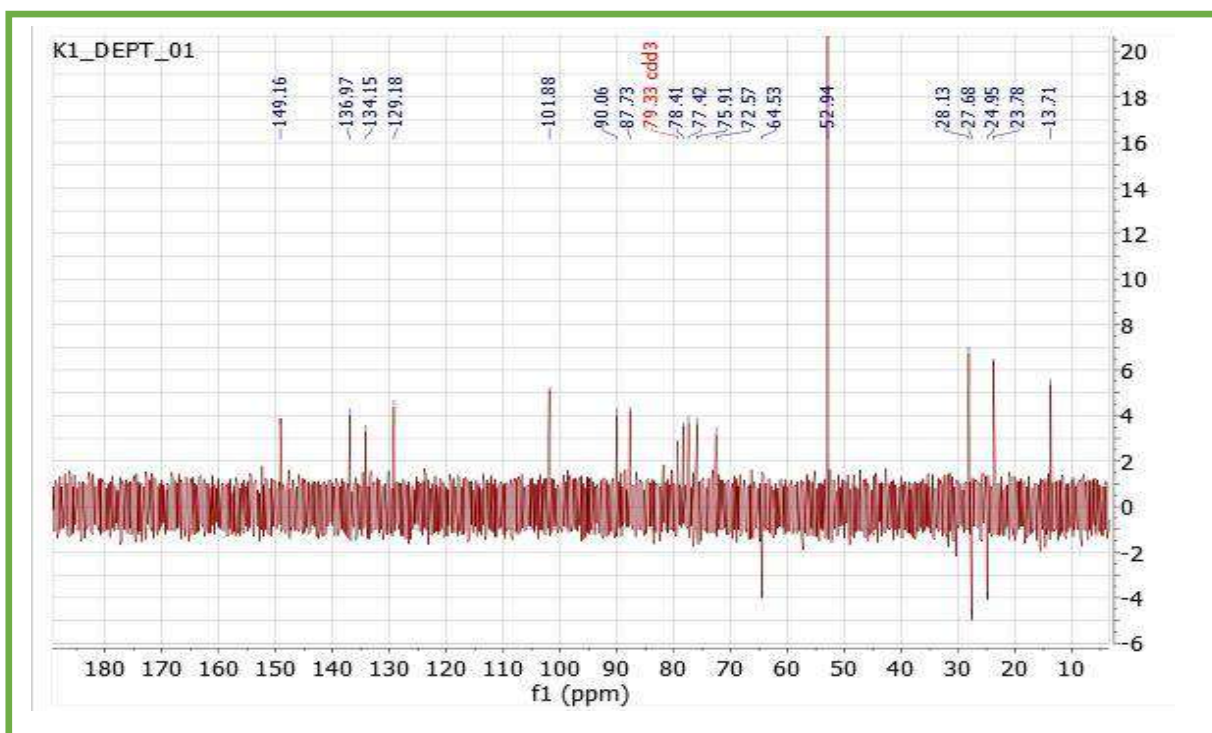


Figure 25: Spectrum RMN DEPT -135 (500 MHz,CDCL $_3$) of compound K1

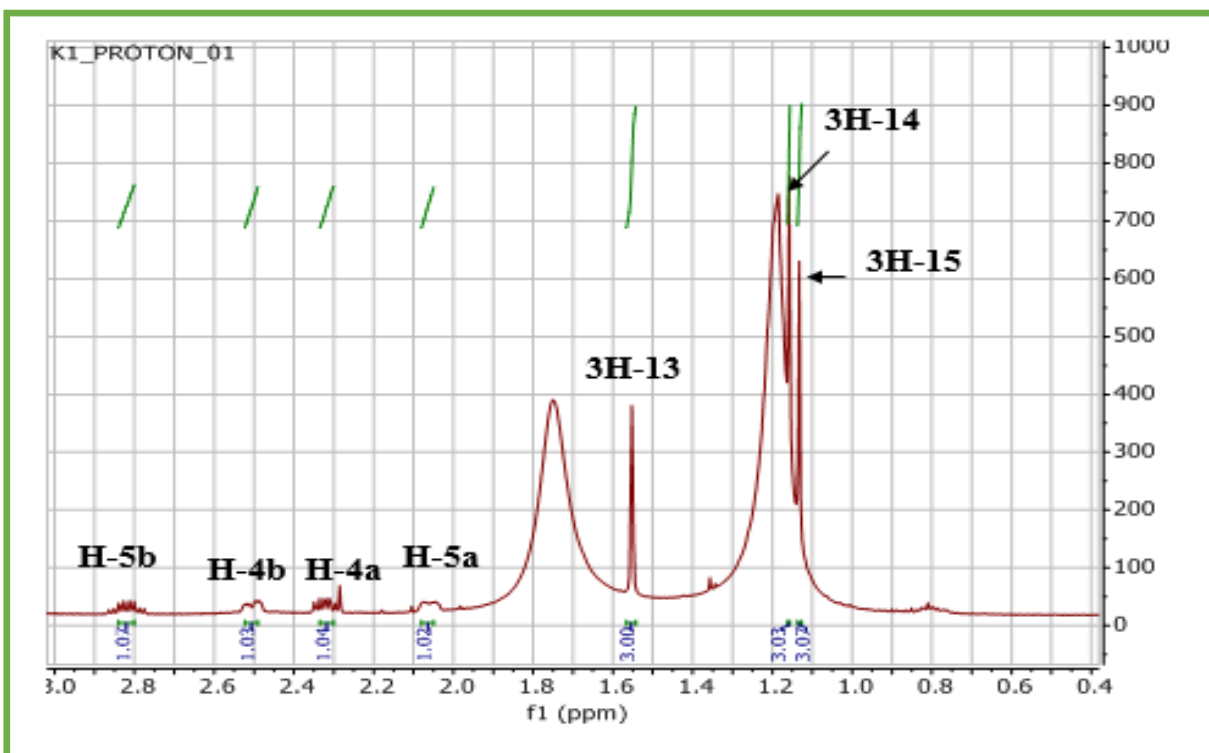


Figure 26: Spreadspectrum of RMN 1H(125 MHz,CDCl₃) of compound K1

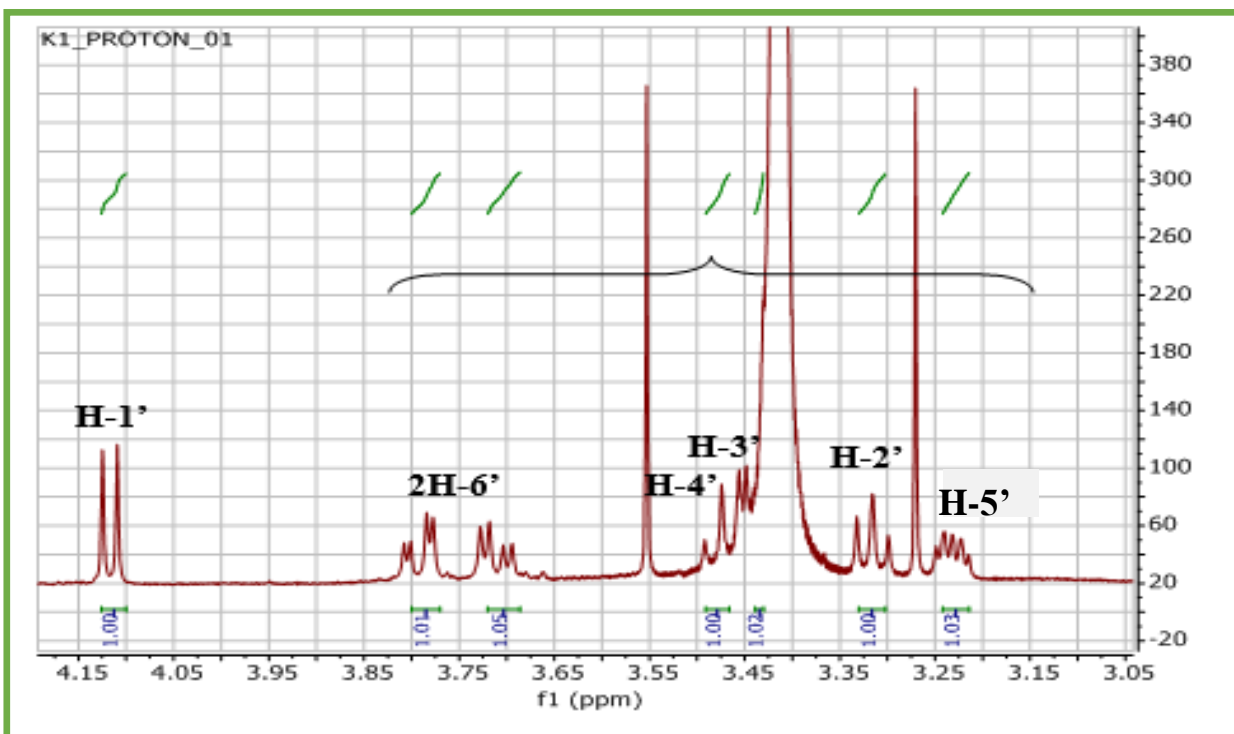


Figure 27: SpreadSpectrum RMN 1H(500 MHz,CDCl₃) of compound K1

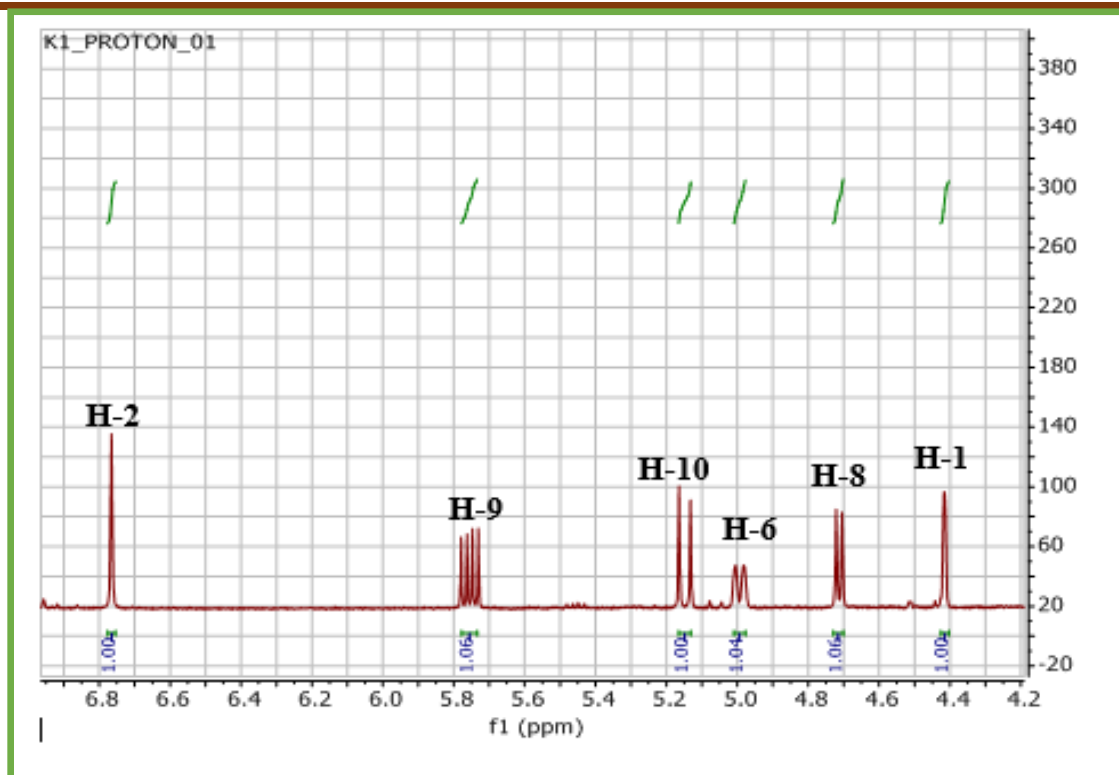


figure 28: Spread spectrum RMN ^1H (500 MHz, CDCl_3) of compound K1

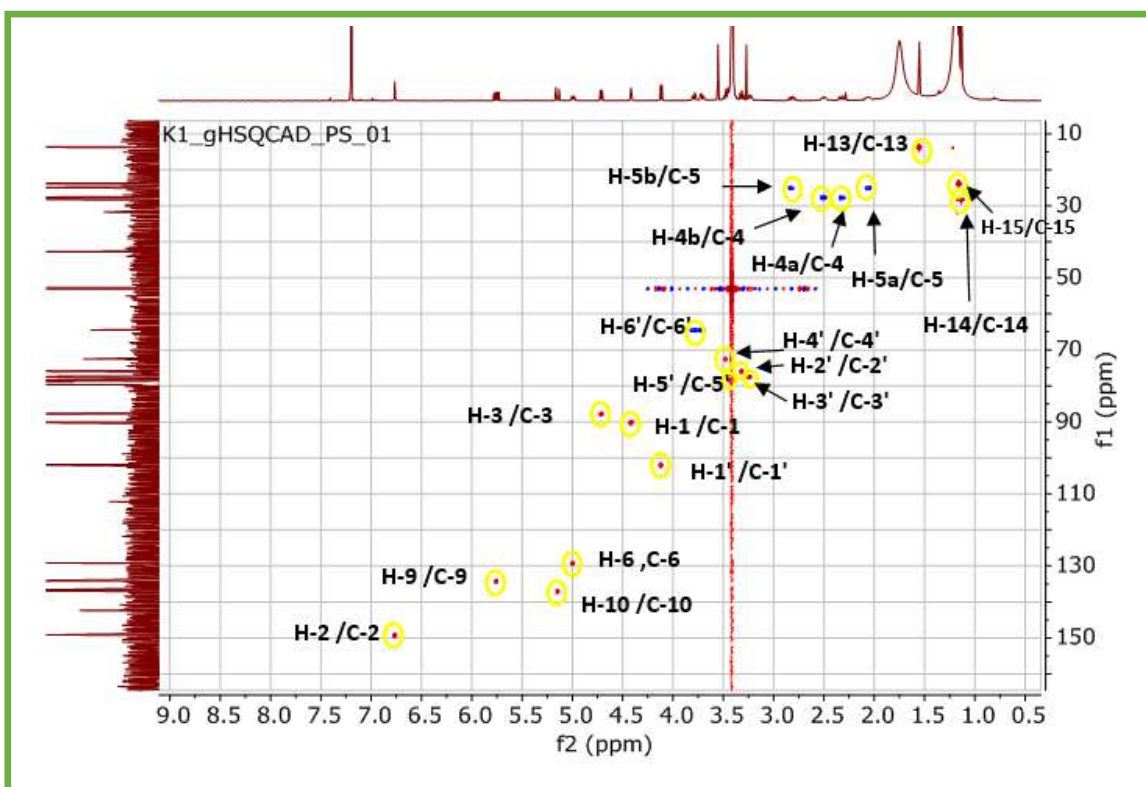


Figure 29: Spectrum of HSQC (500 MHz, CDCl_3) of compound K1

As for the presence of the γ -lactonic ring in this compound, it is confirmed by the presence on the spectrum HMBC (Figure30) of a correlation spot between the C-12 carbon of the carbonyl at δ_c 172.78 ppm and the proton H-1 of the oxygenated methine group at δ_H 4.42 ppm (δ_c 90.07 ppm).

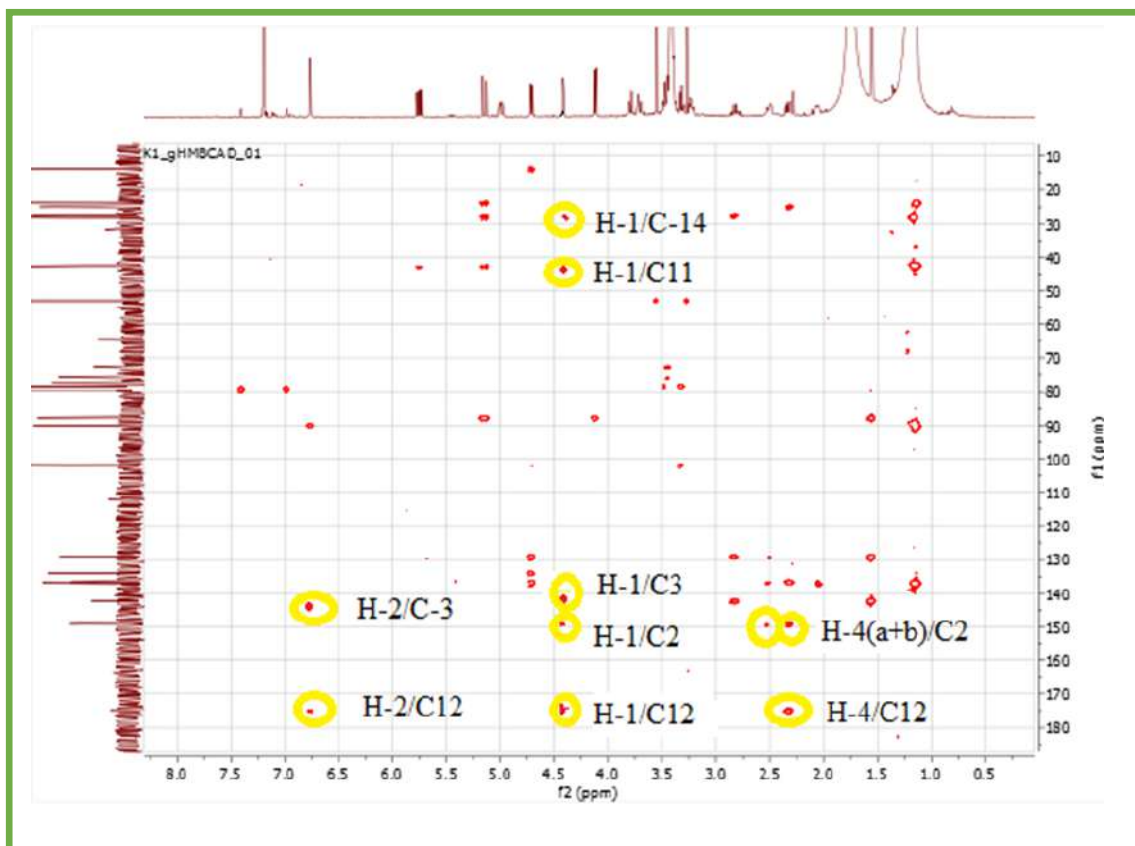


Figure 30: Spectrum of HMBC (500 MHz, CDCL₃) of compound K1

Extensive analysis was performed simultaneously on the homonuclear Cosy spectrum and hetero-nuclear HMBC to reconstruct this molecule and confirm the assignment of all of these atoms (protons and carbons).

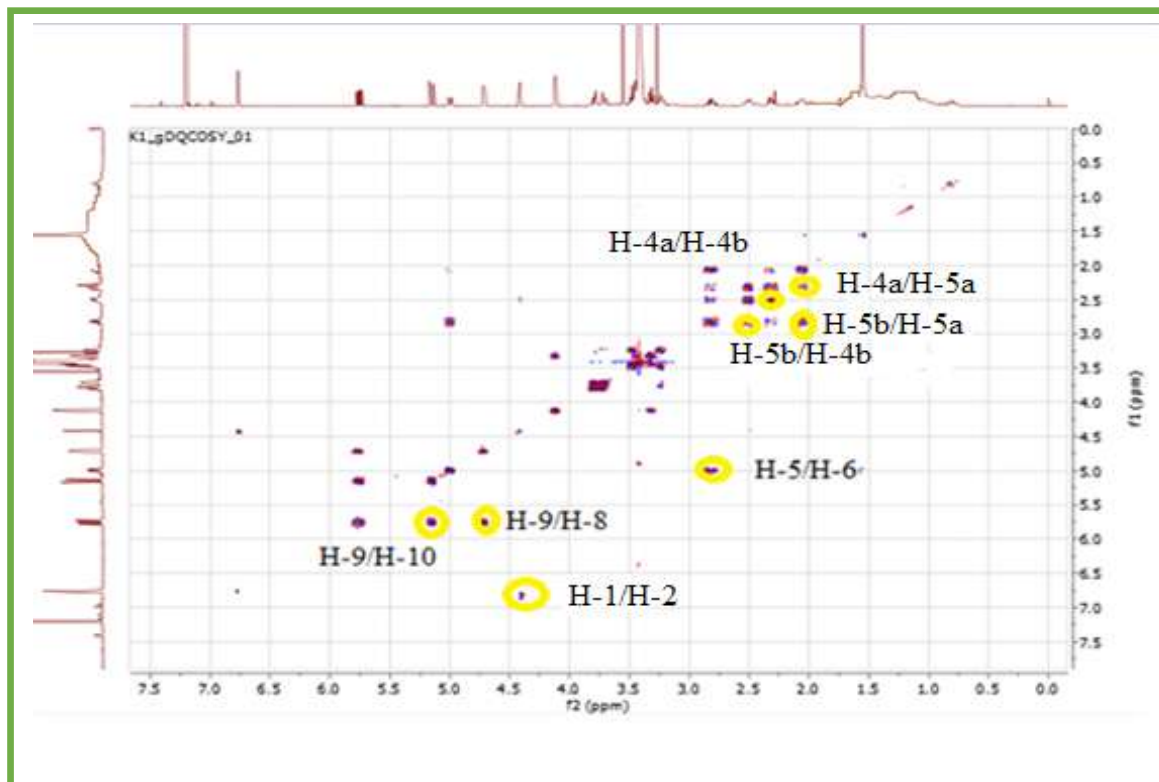


Figure 31: Spectrum of COSY (500 MHz, CDCl₃) of compound K1

The Cosy spectrum (Figure 31) shows a correlation between the proton H-1 of the oxygenated methine group and the H-2 proton of the ethylenic CH group at δ_H 6.77 ppm (δ_C 149.17 ppm). This ethylenic proton also shows two correlation spots on the HMBC spectrum, one with the carbonyl's C-12 carbon, which resonates at $\delta_C = 172.78$ ppm, and the second with the C-4 carbon of the methylene group, which moves at $\delta_C = 27.67$ ppm.

These notes undoubtedly indicate that the double bond carrying this ethylenic proton is delimited by an ethylenic quaternary carbon, in this case, C-3 (δ_C 142.37 ppm), which shows a strong correlation with this same ethylenic proton, and that this ethylenic quaternary carbon

is linked to the CH₂ group (δ_{Ha} 2.33; δ_{Hb} 2.49 ppm) on the one hand and to the carbonyl group (δ_{c} = 172.78) ppm on the other hand.

A return on the spectrum (Cosy) indicates the presence of a second methylene group whose two magnetically non-equivalent protons that resonate as two multiplets each at (δ_{H} 2.06 and 2.82 ppm) show two correlation spots: one with the protons of the anterior group CH₂ and the second with the proton H-6 of another ethylenic CH group, resonant as a doublet of doublets at δ_{H} 4.99 ppm ($J=12.1$; 6.4 Hz). At this stage of our analysis, we can propose the following entity-1:

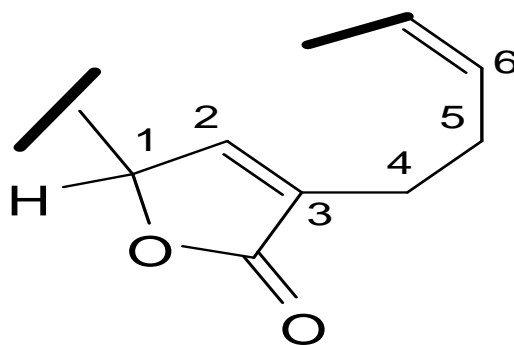


Figure 32: semi-structure

Moreover, a return to the HMBC spectrum shows a correlation spot between the proton H-1 of the CH group of the lactone closure, with a quaternary carbon at δ_{c} 42.71 ppm, in this case, C-11. The latter clearly correlates with the protons of two methyl groups which resonate in the form of two singlets each at δ_{H} 1.13 ppm (δ_{C} 28.13 ppm) and δ_{H} 1.16 ppm (δ_{C} 23.79 ppm), which places these two methyl groups on this carbon, C-11, in position vicinal to carbon C-1 of the lactone closure.

The quaternary carbon (C-11) also shows two spots of correlations with the two protons of the two ethylenic groups CH ($\delta_{\text{C-9}}$ 134.16, $\delta_{\text{C-10}}$ 136.97) which resonate, respectively, in the form of a doublet each at $\delta_{\text{H-9}}$ 5.75 ppm ($J = 15.9$ Hz) and $\delta_{\text{H-10}}$ 5.15 ppm ($J = 15.9$ Hz) and which correlate with each other in the Cosy spectrum; this places the double bond in the vicinal position of this quaternary carbon the C-11.

. The ^{13}C and ^1H data of compound **K1** are shown in (Table 20). The analysis of ^1H , ^{13}C , and DEPT-135 NMR spectra of (**K1**) revealed the presence of sesquiterpene lactone of the humulene skeleton in the glycoside form. Both HMQC and HMBC spectra confirmed the protons' connectivities. Comparing the NMR data with the reported one revealed the structure of asteriscunolide D [1], except for the absence of a carbonyl signal at C-8, which was replaced by an oxygenated methine at δC 87.73, attached for a sugar moiety.

The osidic unit was identified by Cosy H-H analysis (Figure 29), which clearly shows the presence of a seven-proton spin system of a hexose. Indeed, starting from H-1'' anomeric proton signal existing at 4.12 ppm (1H, d, $J = 7.7$ Hz) cited above, we connect through their correlation spots, the protons H-2' (3.31 ppm, d, $J = 8.36$ Hz), H-3 (3.45 ppm, d, $J = 3.78$ Hz), H-4' (3.47 ppm, d, $J = 8.96$ Hz), H-5' (3.23 dd (4.12, 8.81)) and finally the 2H-6'' protons (3.79 dd (3.40, 11.90) Hz, H-6'a; 3.71 dd (4.68, 11.92) Hz, H-6''b). The large values of coupling constants make it possible to identify glucose of β configuration ($J_{1''-2''} = 7.7$ Hz).

The α -orientation of the hydroxy group at C-8 was deduced from the chemical shift and coupling constant value of H-8[2]. Based on the NMR data and comparison with the literature, the sugar moiety was concluded to be β -D-glucose[3]. The correlations of H-1' (δH 4.12) with C-8 (δC 87.73) and H-8 (δH 4.71) with the anomeric carbon (δC 101.89) in the HMBC spectrum revealed the sugar connection at C-8.

In conclusion, The analysis of 1D and 2D NMR spectra of (**K1**) revealed the presence of sesquiterpene lactone in the humulene skeleton in the glycoside form. Both HSQC and HMBC spectra confirmed the protons' connectivities, and the humulanolide structure was established. Comparing the NMR data with the reported one revealed the structure of asteriscunolide D [1], except for the absence of a carbonyl signal at C-8, which was replaced by an oxygenated methine at δC 87.73, attached for a sugar moiety. The structure of **K1** was established to be (-)-(2Z,6E,9E)8 α -hydroxy-2,6,9-humulatrien-1(12)-olide (Humulene-glucoside).

Table 24: Chemical shift values of 1D and 2D NMR of compound K1.

Position	δC (ppm), (DEPT)	δH (ppm), mult., J (Hz)	Correlation HMBC
1	90.07(CH)	4.42d(1.3)	C-1/H-2
2	149.17(CH)	6.77s	C-2/H-1; H-4
3	142.37	/	C-3/H-4
4	27.67(CH ₂)	2.33 m	
		2.49 dd (4.72,14.78)	
5	24.96(CH ₂)	2.06 d (14.8)	
5		2.82 m	
6	129.17(CH)	4.99d(12.1)	C-6/H ₃ -13;H-4b; H-5b; H-8
7	136.60	/	2.49,4.42
8	87.73(CH)	4.71d(8.2)	C-8/ H ₃ -13; H-1'
9	134.16(CH)	5.75dd(8.2, 15.9)	C-9/H-8
10	136.97(CH)	5.15 d(15.9)	C-10/H ₃ -15 ;H-8
11	42.71	/	C-11/H-1 ;H-10 ;H-9
12	172.78	/	C12/H-1 ;H-2 ;H-4
13	13.71(CH ₃)	1.55 s	C-13/H-8
14	28.13(CH ₃)	1.13 s	C-14/H-10 ;H ₃ -15
15	23.79(CH ₃)	1.16 s	C-15/H-10 ;H ₃ -14
1'	101.89(CH)	4.12d (7.7)	C1'/H-8 ;
2'	75.90(CH)	3.31 d (8.36)	C2'/H-4'
3'	77.43(CH)	3.45 d (3.78)	
4'	72.54(CH)	3.47 d (8.96)	
5'	78.41(CH)	3.23 dd (4.12, 8.81)	
6'	64.71(CH ₂)	3.79 dd (3.40 ,11.90) H _a	
		3.71 dd (4.68 ,11.92)H _b	

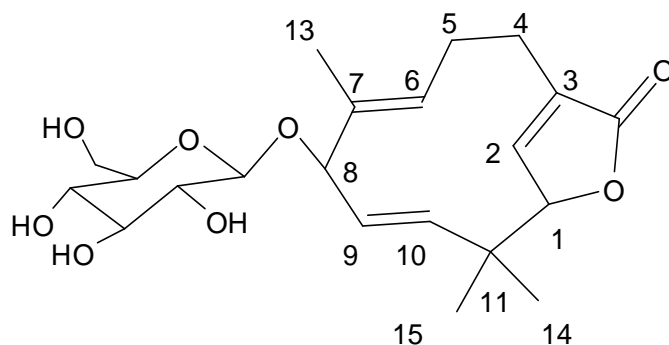


Figure 33: Chemical structure of K1
Humulene-glucoside

V.2. Structure elucidation of compound K 2:

This compound is in the form of soluble yellow needles in methanol. The ^{13}C NMR spectrum (Figure 35) shows the presence of many signals. Signals resonating between 95 and 180 ppm are characteristic of the aromatic carbons of the flavonoid. Also, a carbon of the methoxyl group was detected at 49.07 ppm, and one carbonyl at $\delta\text{C}176.28$ corresponds to the C-4 carbon of a flavonoid.

After this first analysis, the identification of the flavonoid is initiated by analysis of the ^1H NMR spectrum (Figure 33) which exhibits signals resonating at δH 7.74 (1H, d, $J = 2.3$ Hz), δH 6.95 (1H, d, $J = 8.4$ Hz) and δH 7.60 (1H, dd, $J = 8.4; 2.3$ Hz), characteristics of the H-2', H-5' and H-6' protons of the di-substituted B ring of the flavonoid. The two resonant doublets at δH 6.25 and δH 6.47 of 1H integration, each with the same coupling constant value (2.1 Hz), are attributable to the H-6 and H-8 protons of the A cycle.

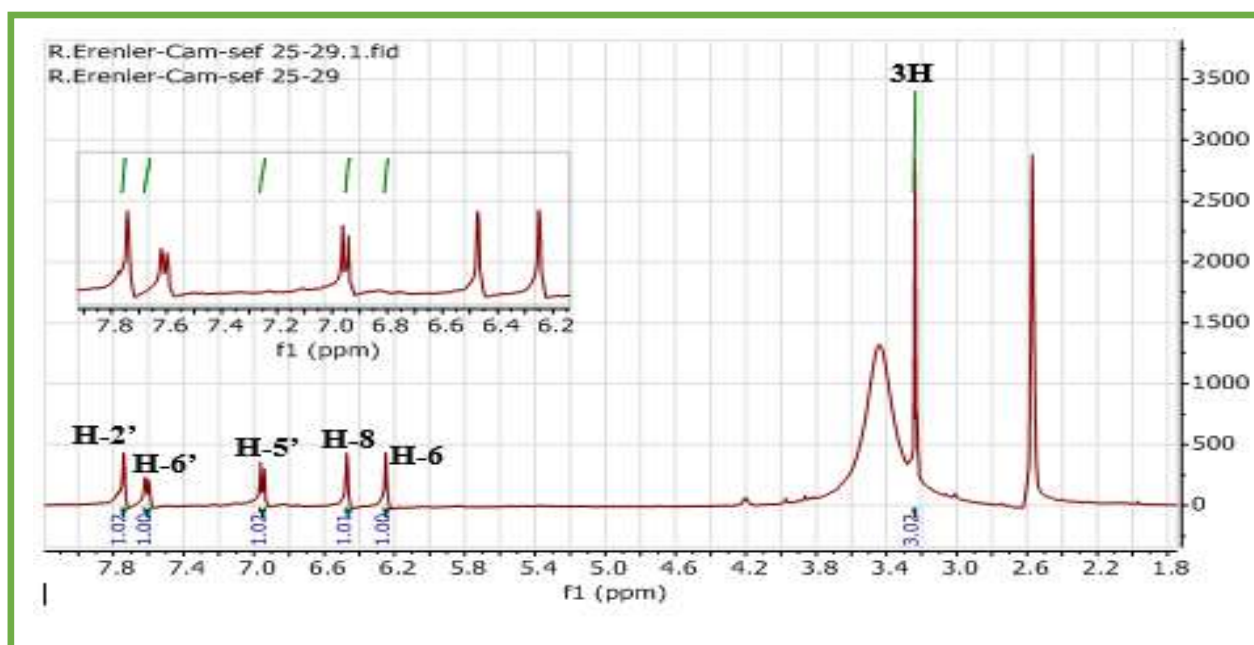


Figure 34 Spectrum RMN ^1H (500 MHz, CD_3OD) of compound K2

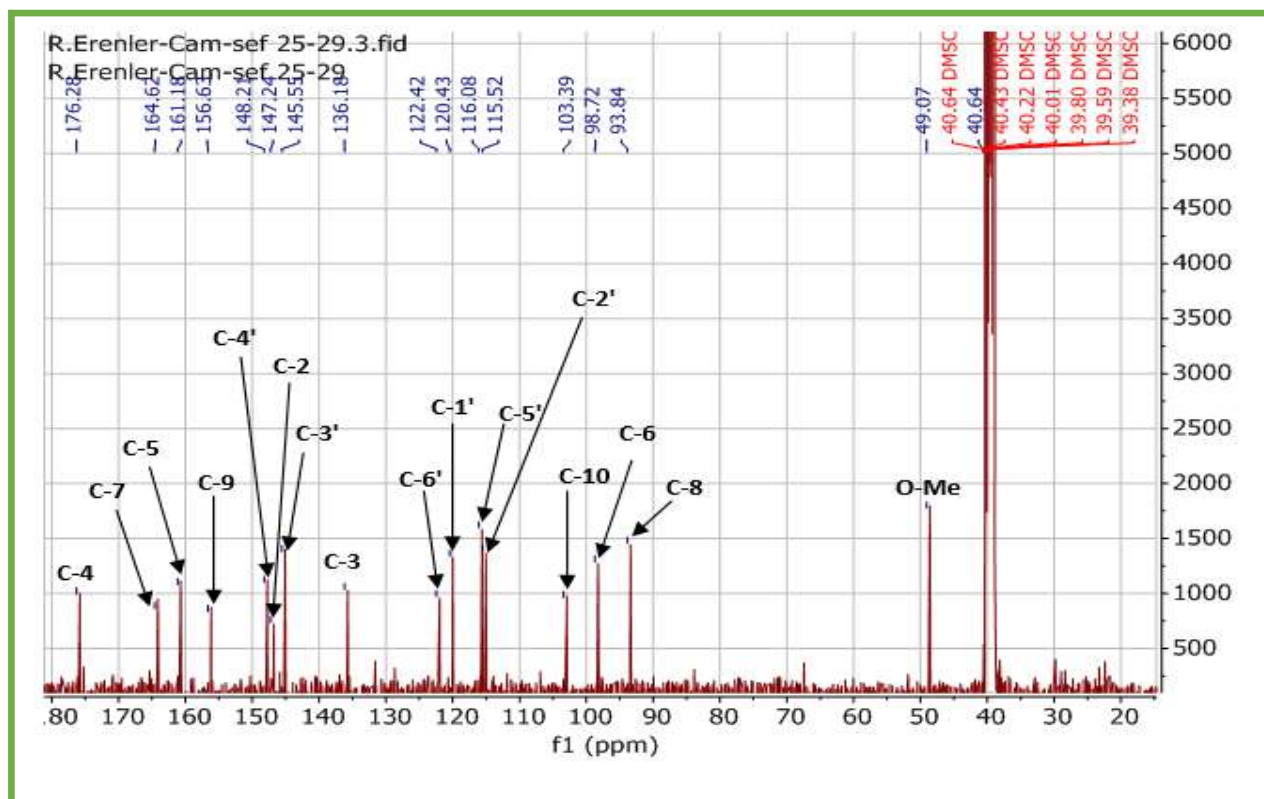


Figure 35: Spectrum RMN ^{13}C (125 MHz, CD_3OD) of compound K2

This was confirmed by the analysis of the couplings observed on the Cosy H-H spectrum (Figure 36), where the couplings between the protons are observed:

- H-6/H-8 with constant coupling value $J = 2.1$ Hz corresponds to a meta coupling in the A cycle.
- H-2'/H-6' with constant coupling value $J = 2.3$ Hz corresponds to a meta coupling in the B cycle
- H-5'/H-6' with constant coupling value ($J=8.4$ Hz) corresponds an ortho coupling in the B cycle.

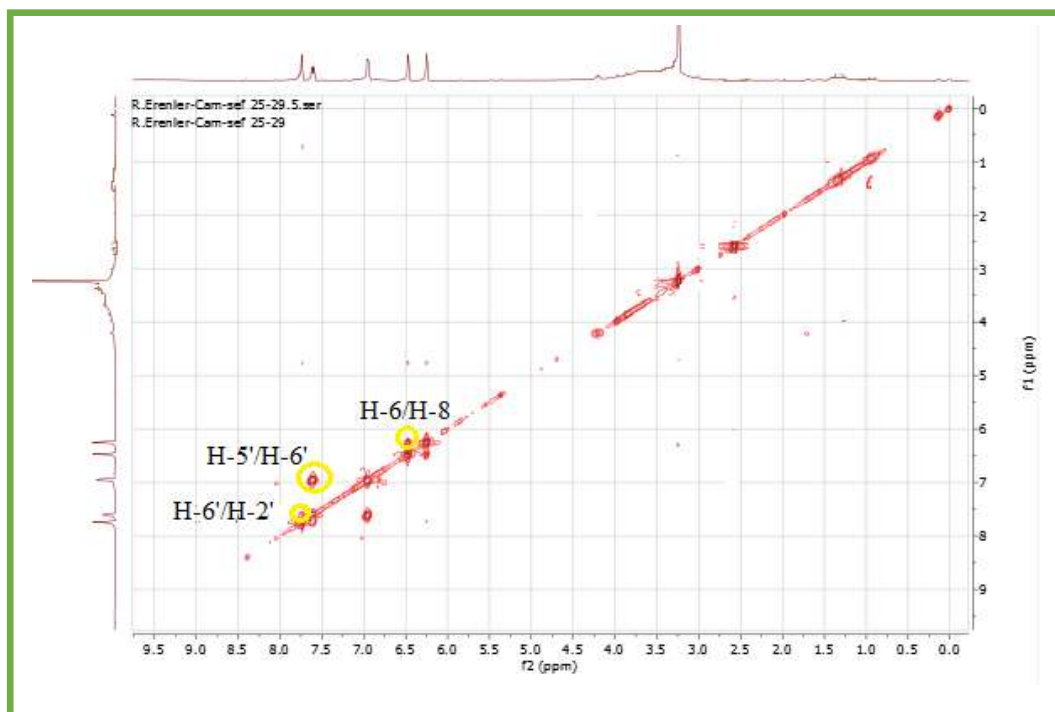


Figure 36: Spectrum Cosy (500 MHz, CD₃OD) of compound K2.

From the protons mentioned above, the HSQC experiment (Figure 36) makes it possible to identify the carbons C-2' (δC 115.52), C-5' (δC 116.08), C-6' (δC 121.43), C-6 (δC 98.72) and C-8 (δC 93.84).

The HMBC experiment (Figure 38) clearly shows a correlation between the H-2'/H-6' protons of the B ring and a resonant quaternary carbon at δC 147.24, corresponding to the C-2

carbon of the flavonoid. This chemical shift value favors a flavonol substituted in position 3. The carbon signal observed at δC 136.28 is attributable to carbon C-3.

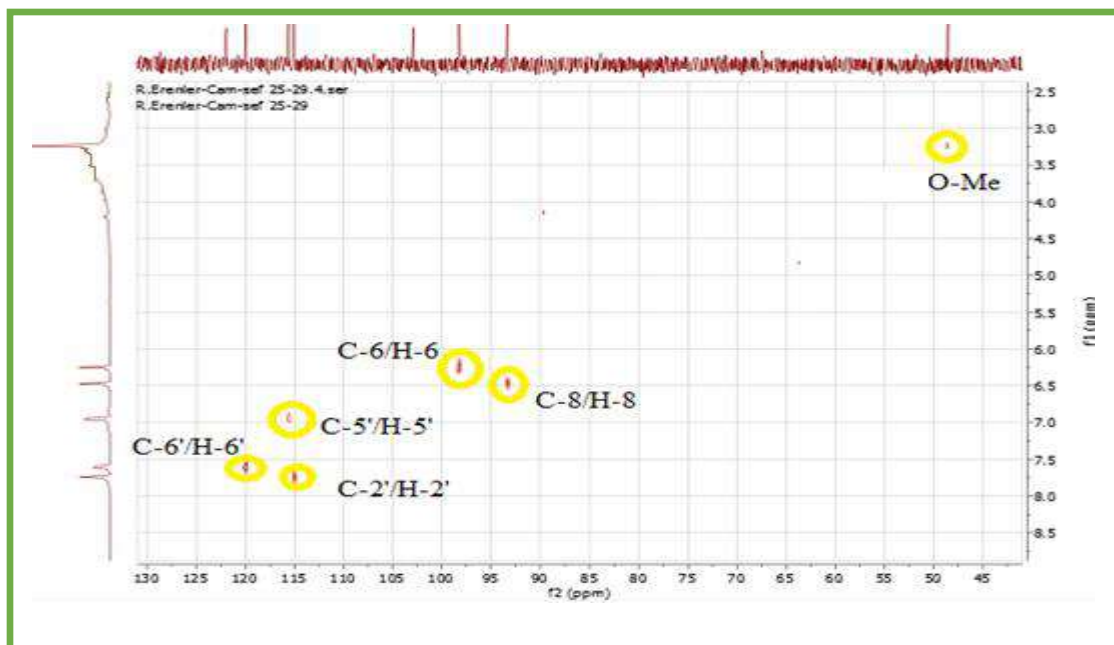


Figure 37: Spectrum of HSQC (500 MHz, CD_3OD) of compound K2

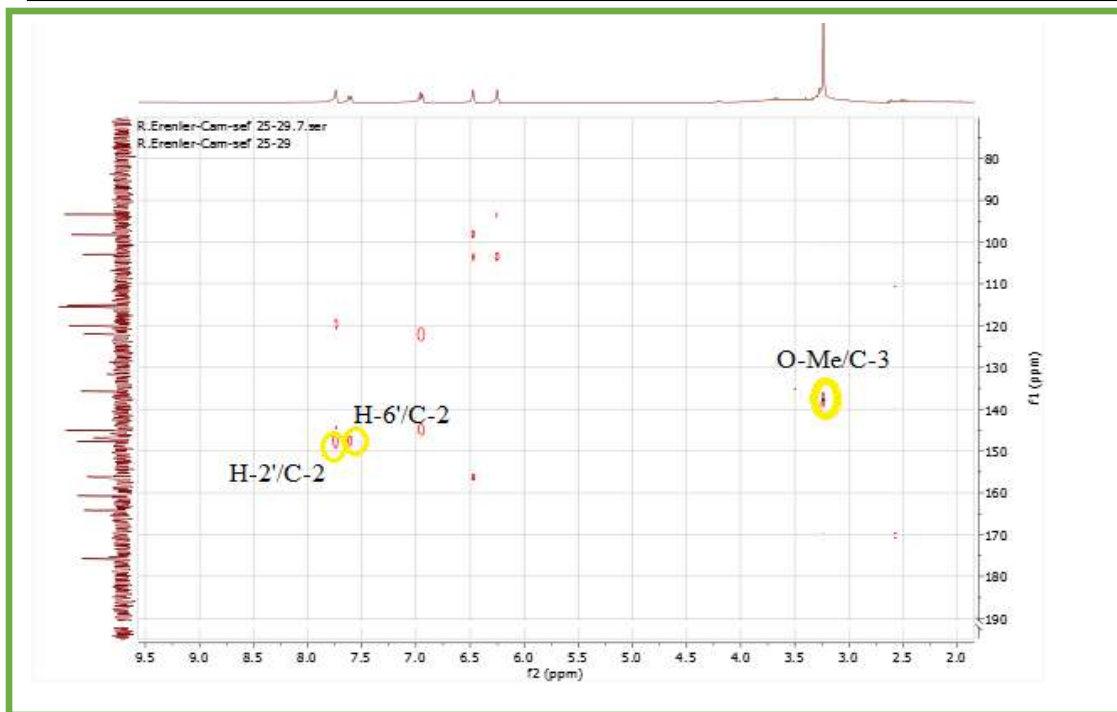


Figure 38: Spectrum of HMBC (500 MHz, CD_3OD) of compound K2

All these spectral data, as well as the value of the chemical shifts of carbons compared with those of the literature, suggest that genin is a flavonol called Quercetin, substituted in 3 [4] by a methoxyl group which was confirmed by HMBC experiment (Figure 38) which clearly shows a long-distance heteronuclear coupling between the protons (3H, s, δ H 3.17) and carbon C-3 (δ C 136.28).

Table 25: Chemical shift values of 1D and 2D NMR of compound K2

Position	C(δ) ppm	H(δ) (ppm, m, J en Hz)	Cosy
2	147.24		
3	136.28		
4	176.28		
5	161.18		
6	98.72	6.25(d)J=2.1	H-6/H-7
7	164.62		
8	93.84	6.47(d)J=2.1	H-6/H-7
9	156.64		
10	103.39		
O-Me	49.07	3.17(s) 3H	
1'	120.43		
2'	115.52	7.74(d)J=2.3	H-2'/H6'
3'	145.55		
4'	148.21		
5'	116.08	6.95(d)J=8.4	H-5'/H-6'
6'	121.43	7.61(dd)J=2.3, 8.4	H6'/H2'/H5'

Analysis of the HMBC spectrum (Figure 38) also makes it possible to visualize long-distance couplings between:

- H-2'/H-6' protons and an oxygenated C-4' quaternary carbon (δ C 148.21).
- The proton H-5' and two quaternary carbons C-3' (δ C 145.55) and C-1' (δ C 120.43).

- The H-6/ H-8 protons of cycle A and the quaternary carbons C-10 (δC 103.39) and C-7 (δC 164.62).
- The proton H-6 and the oxygenated carbon C-5 (δC 161.18).
- The H-8 proton and a resonant quaternary carbon at δC 156.64 can only be the carbon C-9.

Also, the reported data [4] shows a good agreement with the proposed structure: Quercetin -3-methylether, which separated before from *P.crisp*[5]*P.orientalis*[6]*P.incisa*[7, 8]*P.arabica*[9].

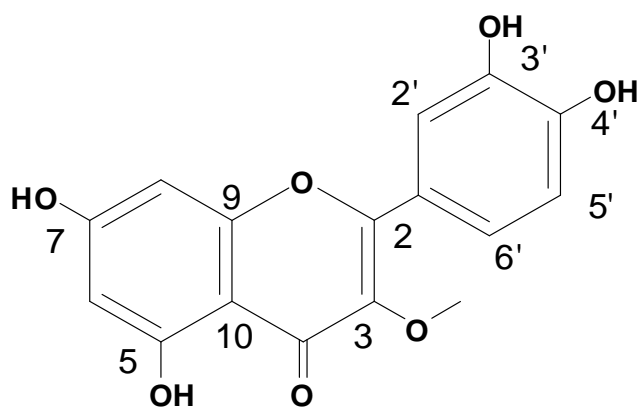


Figure 39: Chemical structure of compound K2.
Quercetin -3-methylether

V.3. Structure elucidation of K3:

Examination of the ^1H NMR spectrum (500 MHz) recorded in CD_3OD shows the signals characteristics of a flavonoid and, in comparison with the spectrum of the compound K2, noted that there is an agreement between the spectrum, except for the presence of two methoxyl with:

- A ^1H integration doublet at δH 7.65 ppm ($J = 2.1$ Hz, meta coupling) attributable to H-2'.
- A doublet of ^1H integration doublet ($J = 8.4$ and 2.1 Hz, ortho and meta coupling) at δH 7.56 ppm attributed to the proton H-6'.
- A ^1H integration doublet at δH 6.91 ppm ($J = 8.3$ Hz, ortho coupling) attributable to H-5'.

- A 1H integration singlet at δ H 6.74ppm is attributable to H-8 due to the value of its chemical shift, which means that the A cycle is Tri-substituted.
- Two 3H integration singlets each at δ H 3.71 ppm and δ H 3.90 ppm).

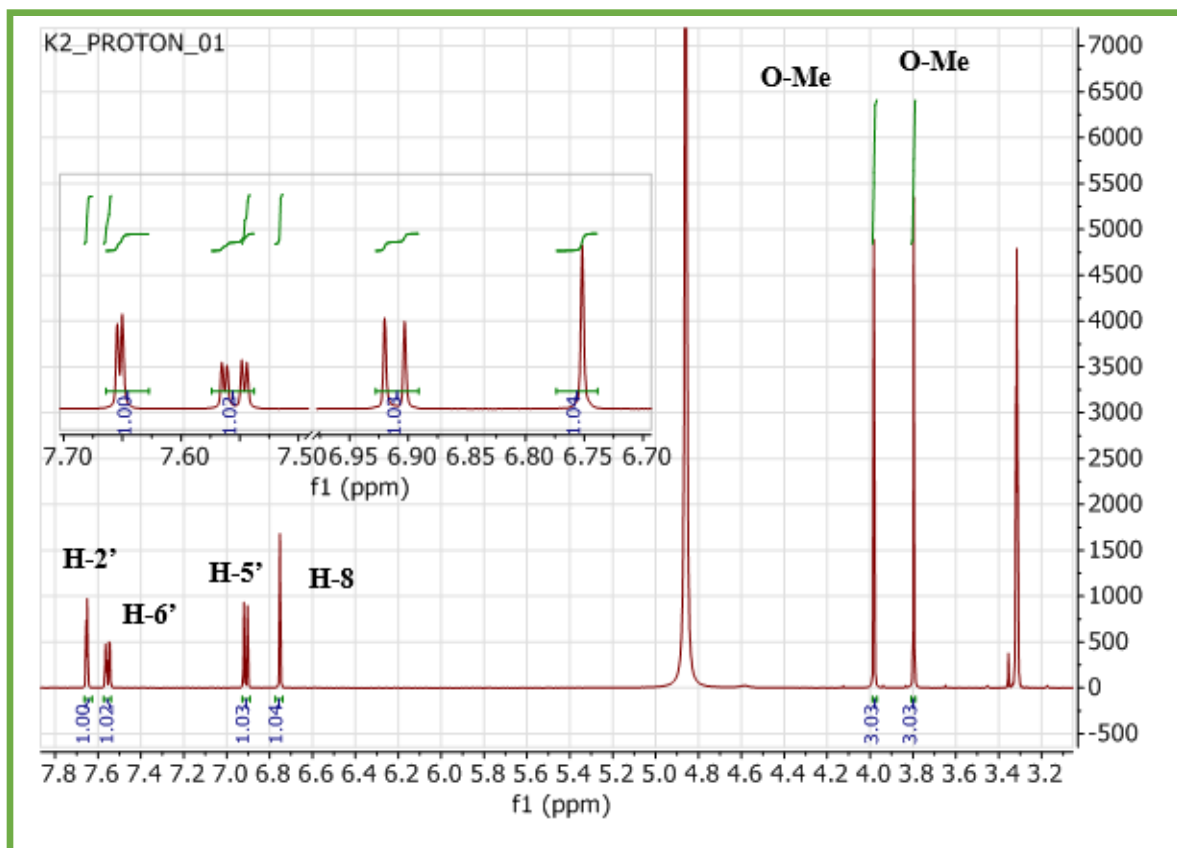


Figure 40: Spectrum RMN 1H(500 MHz,CD₃OD) of compound K3

From the examination of the HSQC correlations (Figure42), we confirm the attribution of the signal to δ H6.74 ppm to proton H-8 due to its correlation with carbon at δ C = 90 ppm. The 1H integration signals (H-5', H-6' and H-2') at δ H 6.91; 7.56 and 7.65 ppm correlate with C-5', C-6' and C-2' carbons, respectively, at δ C 115.00; 115.16 and 120.90 ppm.

The methoxy groups at δ_H 3.80 ppm and at $\delta_H = 3.98$ ppm correlate with the carbons C-3: δ_C 59.09 ppm and to C-7: δ_C 55.54 ppm. The precise location of these two groups on the flavonic skeleton is given by the HMBC(Figure44) correlations.

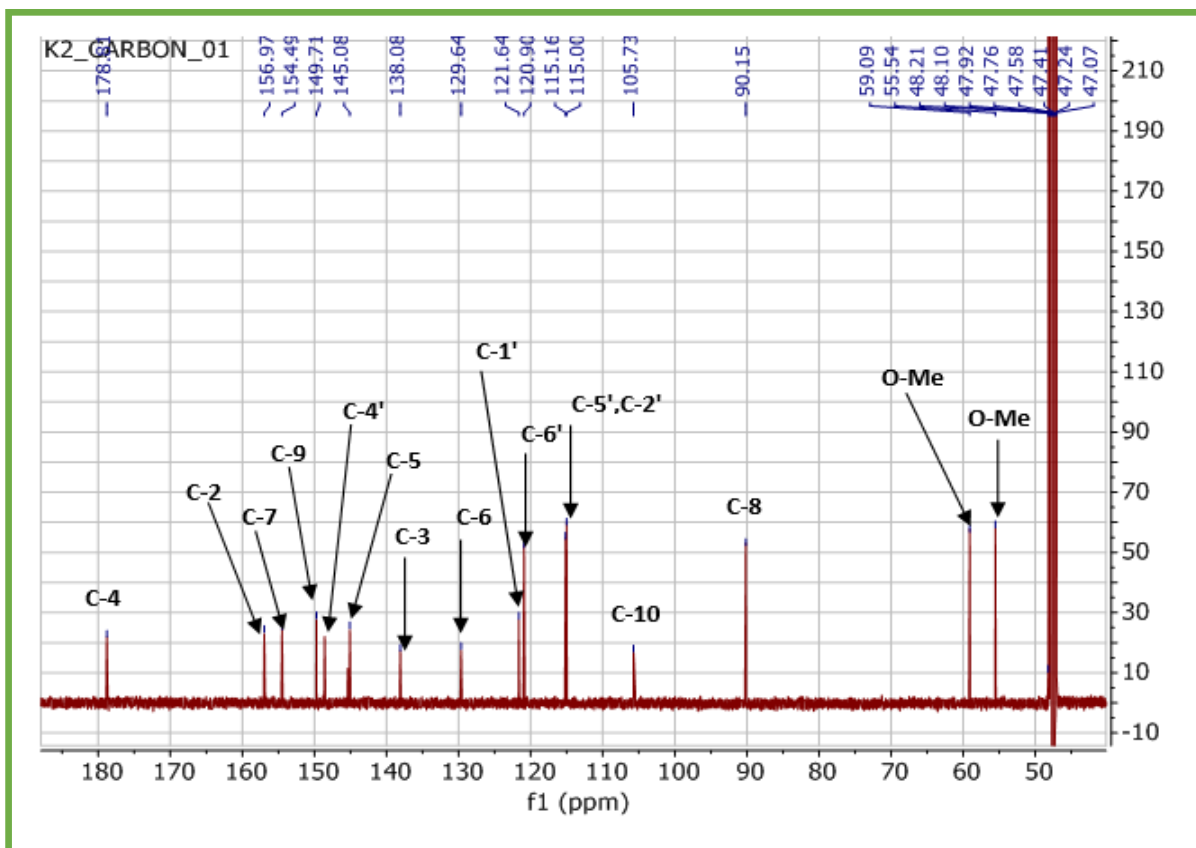


Figure 41: Spectrum RMN ^{13}C (125MHz, CD_3OD) of compound K3

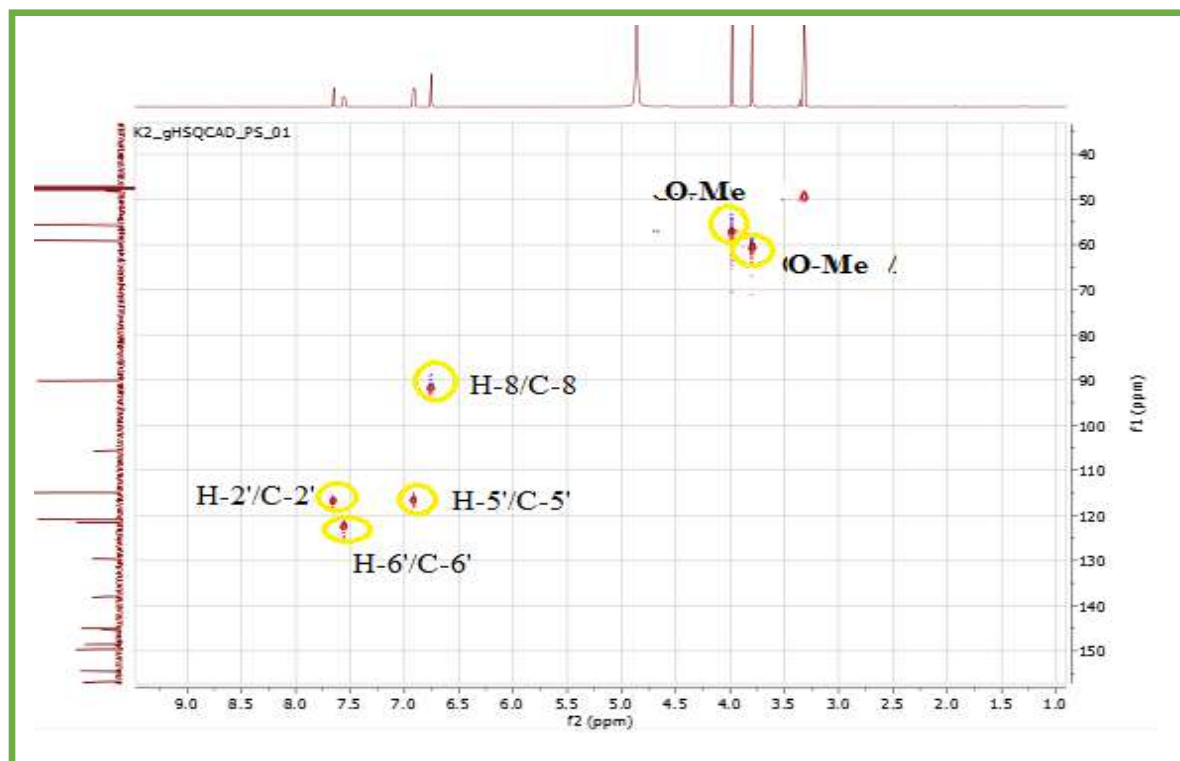


Figure 42: Spectrum of HSQC (500 MHz, CD₃OD) of compound K3

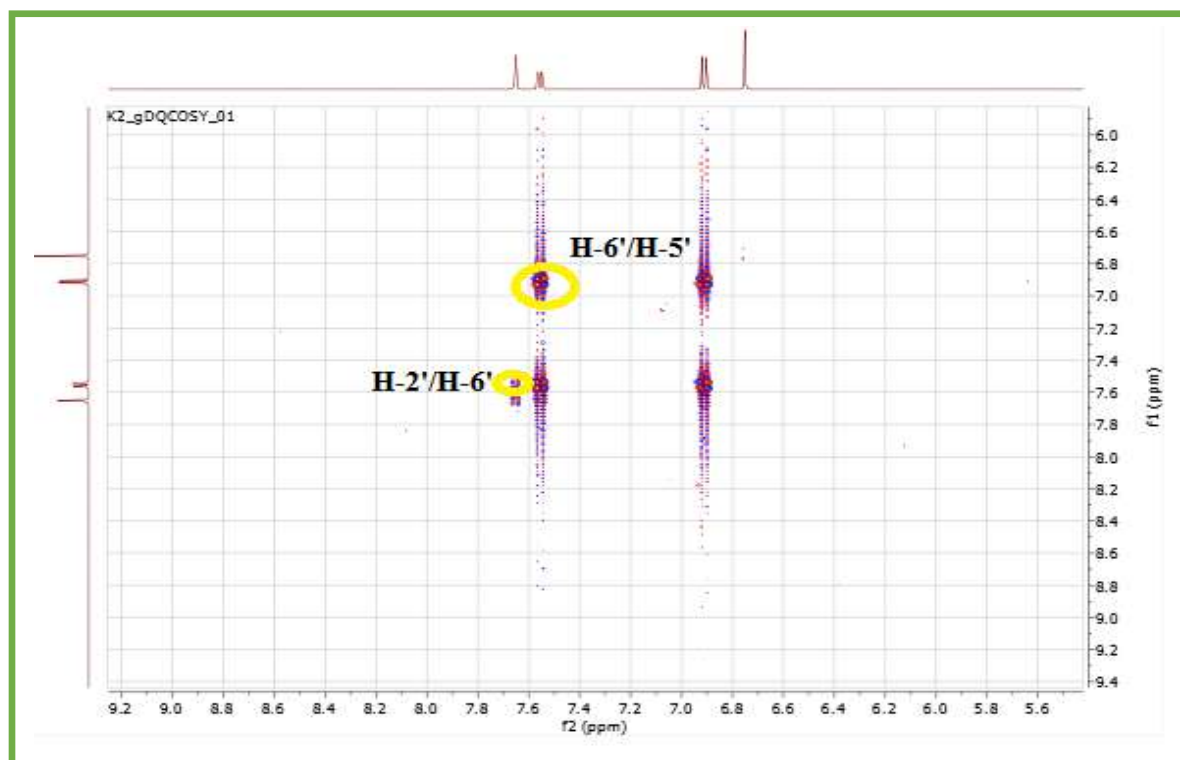


Figure 43: Spectrum of Cosy (500 MHz, CD₃OD) of compound K3

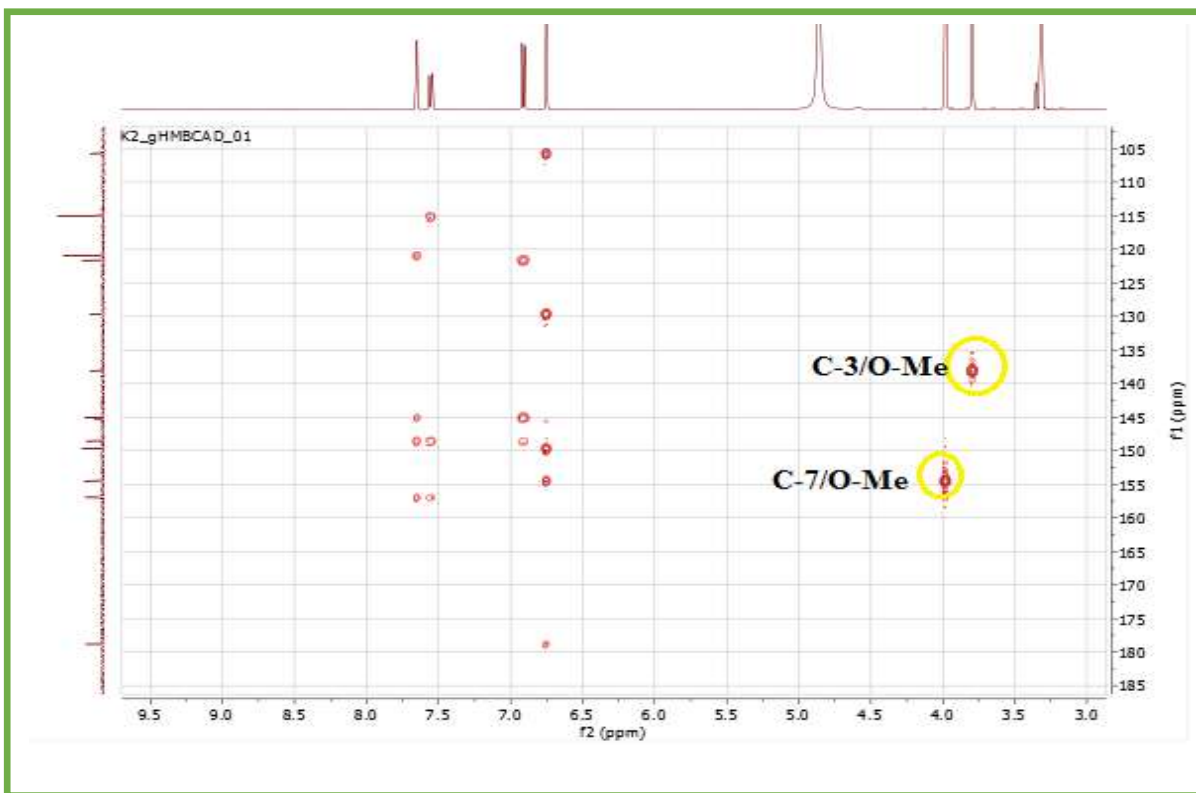


Figure 44: Spectrum of HMBC (500 MHz, CD₃OD) of compound K3

Table 26: Chemical shift values of 1D and 2D NMR of compound K3

Position	C(δ) ppm	HSQC H(δ) (ppm, m, J en Hz)	HMBC
2	156.97		
3	138.08		
4	178.81		
5	145.08,		
6	129.64		
7	154.49		
8	90.15	6.74(s)	C10-C6-C5-C7
9	149.71		
10	105.73		
1'	121.64,		
2'	115.16	7.65(d) $j=2.1$	C2-C4'
3'	145.39		
4'	148.57		
5'	115.00	6.91(d) $j=8.3$	C1'
6'	120.90	7.56(dd) $j=2.1, 8.4$	C2-C4'-C5'
11	59.09,	3.80 s 3H	C3
12	55.54.	3.98 s 3H	C7

From all data and the references [12], this compound was determined as Quercetagenin 3,7-dimethyl ether, and this compound was separated from *P.arabica* [9]*P.dysenterica* [10]

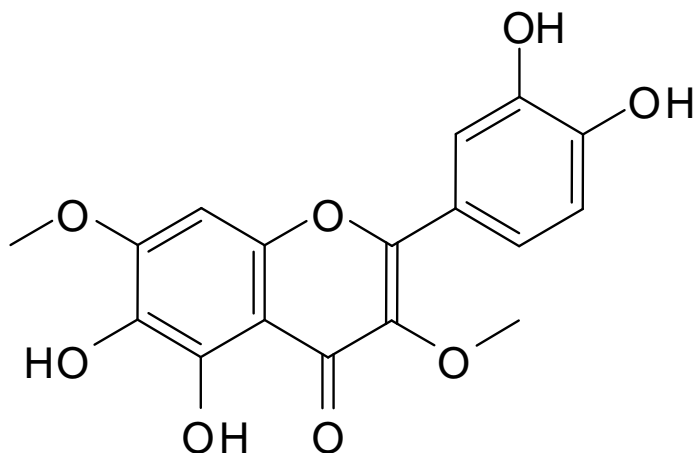


Figure 45: Chemical structure of compound K3

Quercetagenin 3,7-dimethyl ether.

V.4. Structure elucidation of K4:

Examination of the ^1H NMR spectrum (400 MHz) recorded in CD_3OD of compound K4 shows two methoxyl groups and aromatic protons.

In the aromatic region, there is an AA'BB' system characteristic of a para substitution on ring B with a 2H integration doublet at δH 6.87 ppm with a coupling constant $J = 8.4$ Hz (ortho coupling) and another integrating doublet 2H to δH 7.95 ppm ($J = 8.4$ Hz; ortho coupling). These signals are attributed to the protons H-3', H-5' and H-6", H-2" respectively. The former is more shielded than the latter by grouping neighbouring C-4' hydroxyl.

A singlet was observed at δH 6.72 ppm of 1H integration, which is attributed to the proton H-3 or H-8 due to its chemical shift value.

The appearance of two signals as singlets at δH 3.75 ppm and δH 3.91 ppm of 3H integration each indicate the presence of two methoxyl groups, one of which is positioned at C-7 and the second at C-3 Figure 50.

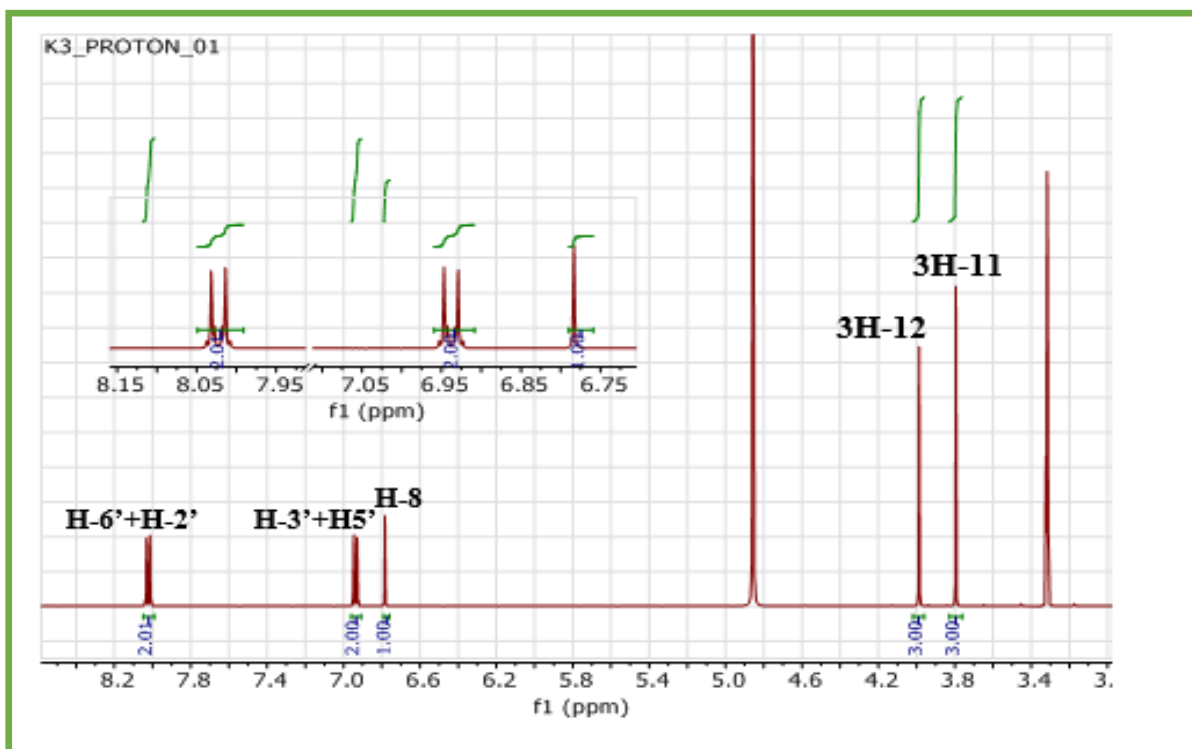


Figure 46: Spectrum RMN ^1H (500 MHz, CD_3OD) of compound K4

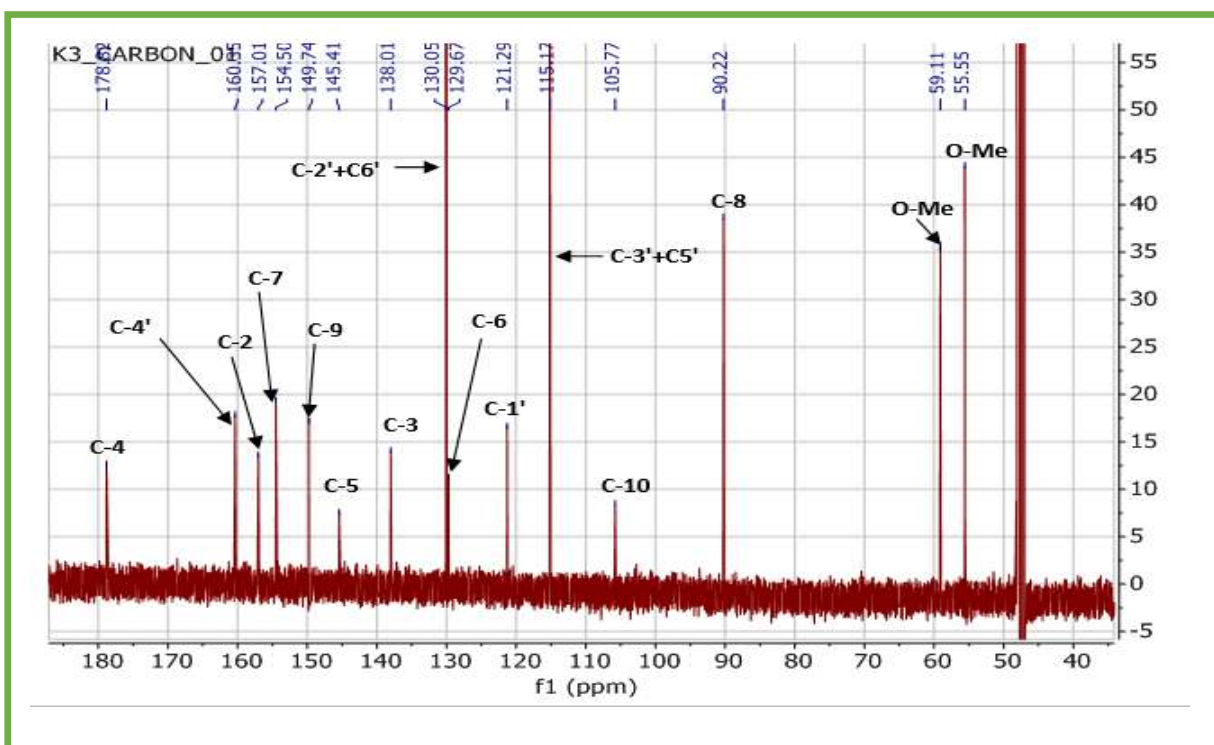


Figure 47: Spectrum RMN ^{13}C (125 MHz, CD_3OD) of compound K4.

The HSQC and HMBC correlations (Figures 51 and 50) make it possible to resolve these ambiguities. Indeed the proton at δ_H 6.72 ppm correlates with carbon at δ_C 91.5 ppm, which can only be C-8 carbon. Both methoxy groups are located in the C-7 and C-3 positions.

The other correlations are as follows:

- The 3H integration signal of the methoxyl group appears at δ_H 3.79s ppm with the carbon at δ_C 59.11 ppm.
- The 3H integration signal of the methoxyl group at δ_H 3.99 ppm with carbon at δ_C 55.33 ppm.
- The 2H integration signal (H-3', H-5') at δ_H 6.94 ppm with C-3', C-5' carbons at δ_C 115.17 ppm.
- The 2H integration signal (H-2', H-6') at δ_H 8.02 ppm with carbon C-2', C-6' at δ_C 130.05 ppm.

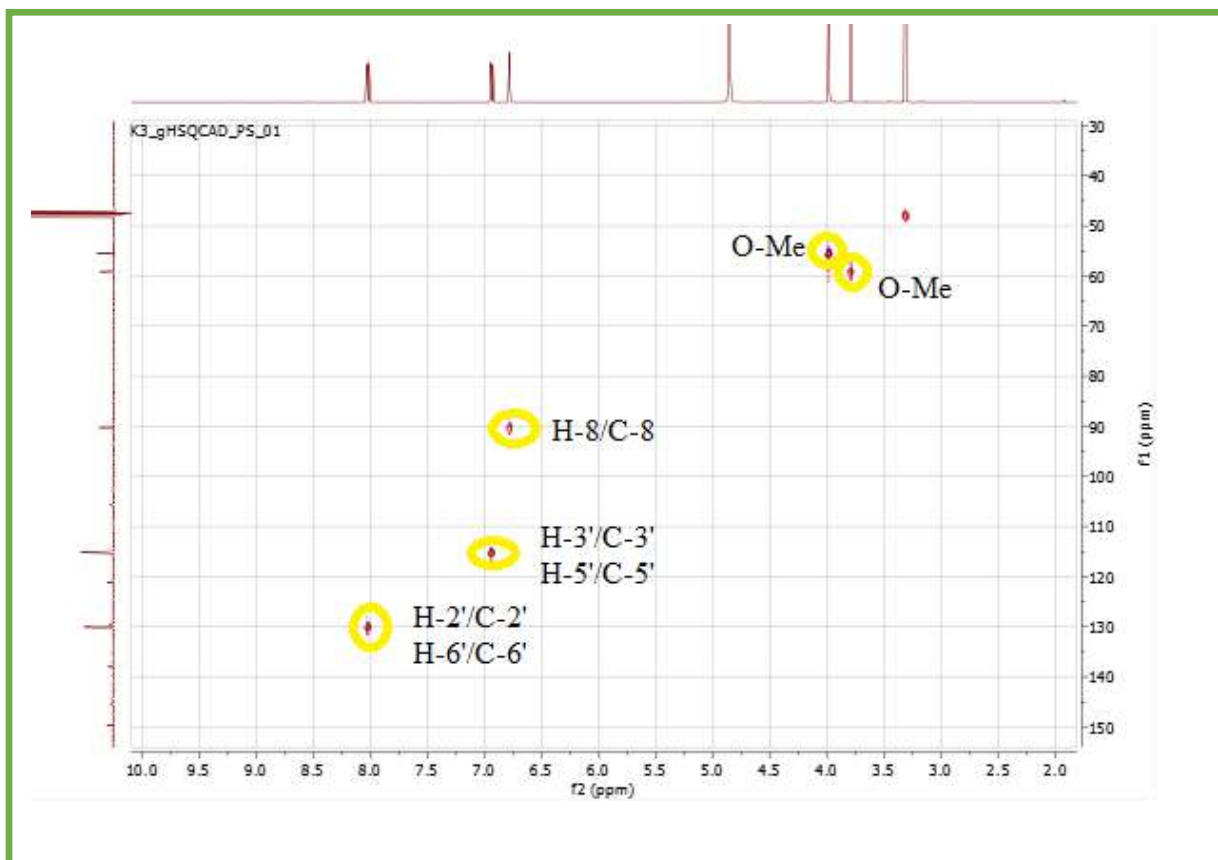


Figure 48: Spectrum of HSQC (400 MHz, CD_3OD) of compound K4

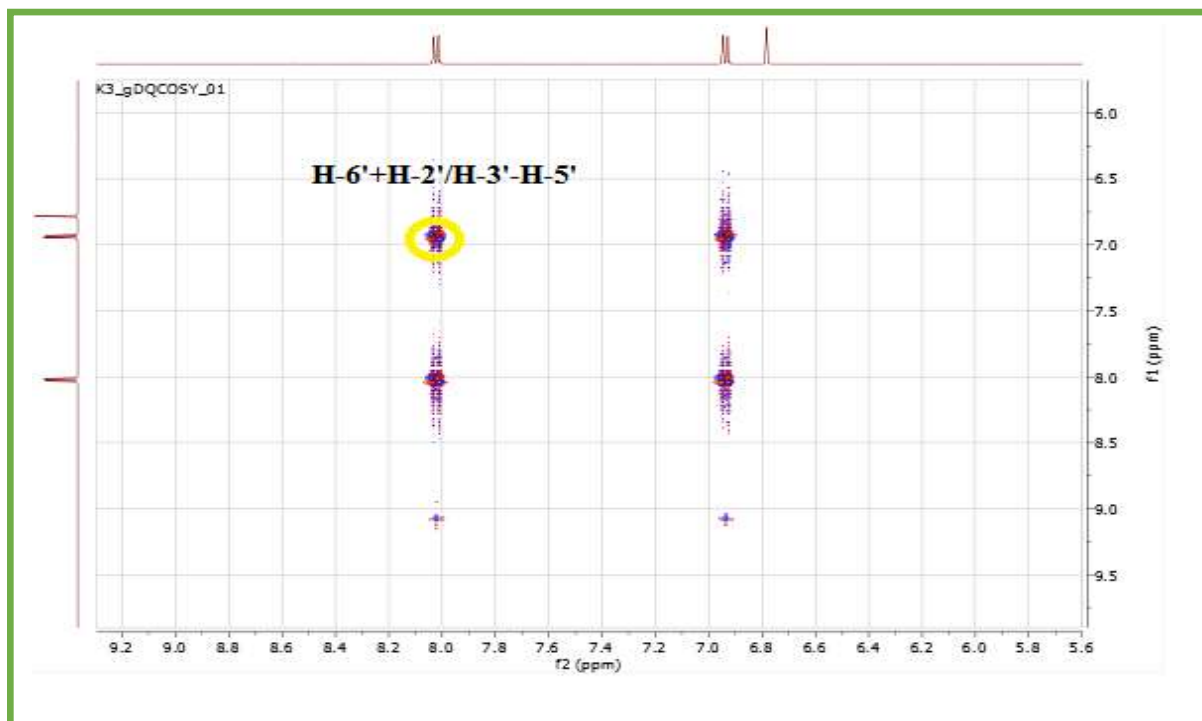


Figure 49: Spectrum of Cosy (400 MHz,CD₃OD)of compound K4.

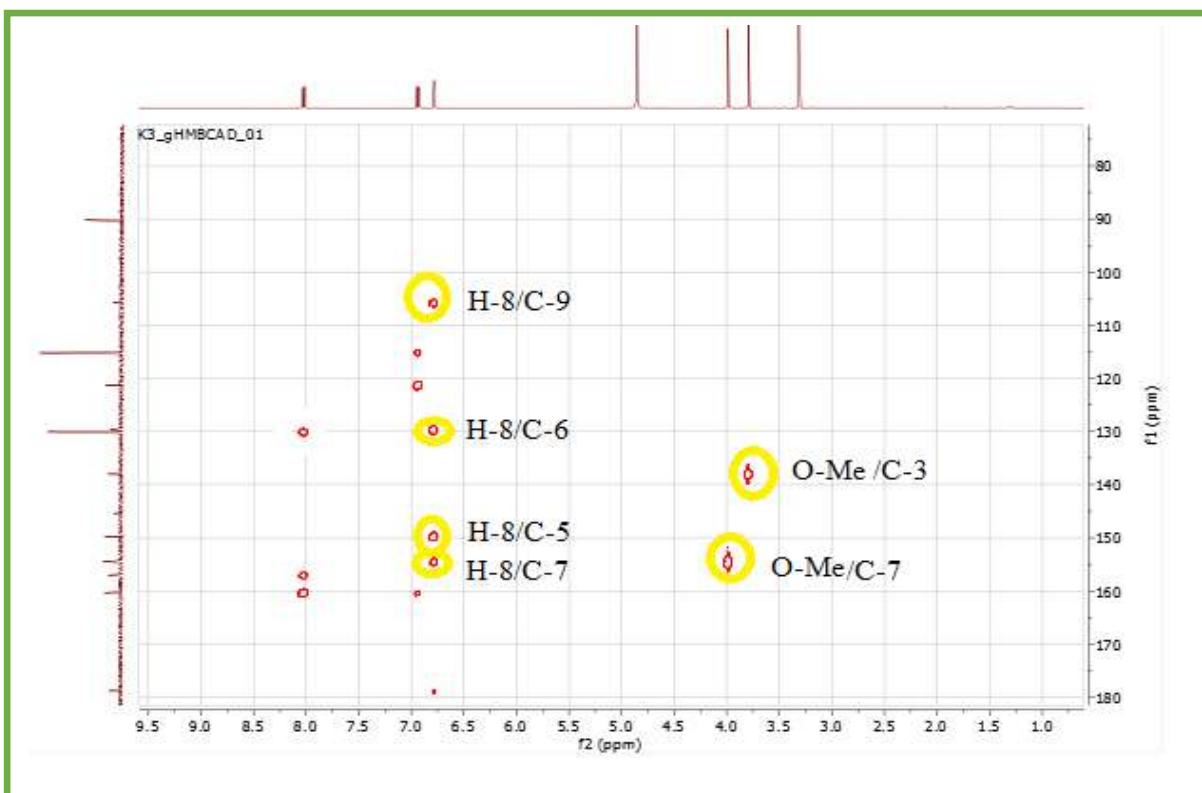


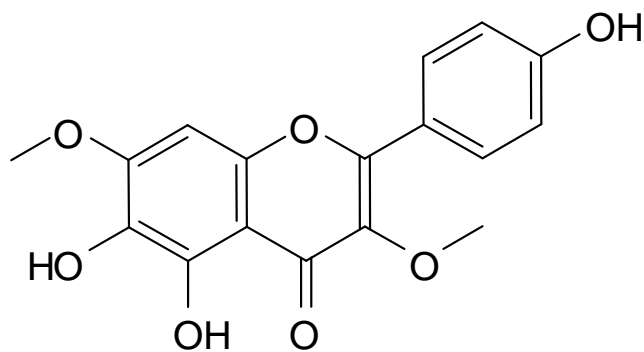
Figure 50: Spectrum of HMBC (400 MHz,CD₃OD)of compound K4.

Analysis of the HMBC spectrum shows that the two methoxy groups at $\delta\text{H} = 3.79$ ppm and at $\delta\text{H} 3.99$ ppm correlate with carbons at $\delta\text{C} 138.01$ ppm and $\delta\text{C} 154.50$ ppm, which makes it possible to locate them on the C-3 and C-7 carbons respectively. All the others correlations unambiguously confirm the structure of compound K4 as being 6-hydroxy kaempferol 3,7-dimethyl ether. The H-8 proton at $\delta\text{H} 6.78$ ppm gives an autocorrelation spot with the C-8 carbon at $\delta\text{C} 90.22$ ppm and a correlation with carbons C-10 at $\delta\text{C} 105.77$ ppm, C-9 at $\delta\text{C} 149.74$ ppm, C-5 at $\delta\text{C} 145.41$ ppm, C-4 at $\delta\text{C} 178.82$ ppm and carbon at $\delta\text{C} 129.67$ ppm which can only be the carbon C-6, this attribution confirms that this carbon is oxygenated and shielded by mesomer by the oxygen atoms carried by the C-5 and C-7 carbons. H-2', H-6' protons at $\delta\text{H} 8.02$ ppm and H-3', H-5' at $\delta\text{H} 6.94$ correlate with carbons C-3', C-5' at $\delta\text{C} 115.17$ ppm and C-2', C-6' carbons at $\delta\text{C} 130.05$ ppm respectively and with carbons at $\delta\text{C} 157.01$ ppm, $\delta\text{C} 121.29$ ppm and $\delta\text{C} 160.35$ ppm attributable to C-2, C-1', and C-4', respectively.

After completing the attributions of all carbons and comparing with the references[4], the entire structure of compound K4 confirm to be Kaempferol -6-hydroxy-3,7-dimethyl ether, which was separated before from *P.dysenterica*[10, 11]

Table 27: Chemical shift values of 1D and 2D NMR of compound K4.

Position	C(δ) ppm	H(δ) (ppm, m, J en Hz)
2	157.01	
3	138.01	
4	178.82	
5	145.41	
6	129.67	
7	154.50	
8	90.22	6.78(s) 1H
9	149.74	
10	105.77	
1'	121.29	
2'	130.05	8.02(dd)j=8.9 2H
3'	115.17	6.94(dd) j=8.9 2H
4'	160.35	
5'	115.17	6.94(dd) j=8.9 2H
6'	130.05	8.02(dd) j=8.9 2H
O-Me	59.11	3.79s 3H
O-Me	55.33	3.99 s 3H

**Figure 51:** Chemical structure of compound K4
Kaempferol -6-hydroxy-3,7-dimethyl ether

V.5. Structure elucidation of K5:

The study of the ^1H -NMR spectrum (Figure 52) in the area corresponding to the protons of the genin allowed the different signals to be assigned to the following protons: A signal in the form of a 1H integration doublet at δ 6.22 ppm with a coupling constant $J = 2.1$ Hz (a meta coupling) attributable to H-6.

Another signal in the form of a doublet and also of integration 1H at δ 6.41 ppm with the same coupling constant ($J = 2.0$ Hz; meta) coupling attributable to H8. In addition, the signal in the form of a doublet ($J = 8.4$ Hz; an ortho coupling) which appears at $\delta\text{H} = 6.87$ ppm, with an integration of 1H , is attributable to H-5', which confirms the substitution of positions 3' and 4' of cycle B.

The signal at δ 7.60 ppm, integration 1H in the form of a doublet doublet ($J = 8.4$ Hz; an ortho coupling and $J = 2.2$ Hz; a meta coupling) attributable to H-6'.

The signal at $\delta\text{H} = 7.85$ ppm, integration 1H in the form of a doublet ($J = 2.1$ Hz; a meta coupling) characterizing H-2'.

In addition, the anomeric proton resonates in the form of a doublet at $\delta\text{H} = 5.18$ ppm and the value of its coupling constant: $J = 7.7$ Hz, suggests a β osidic configuration.

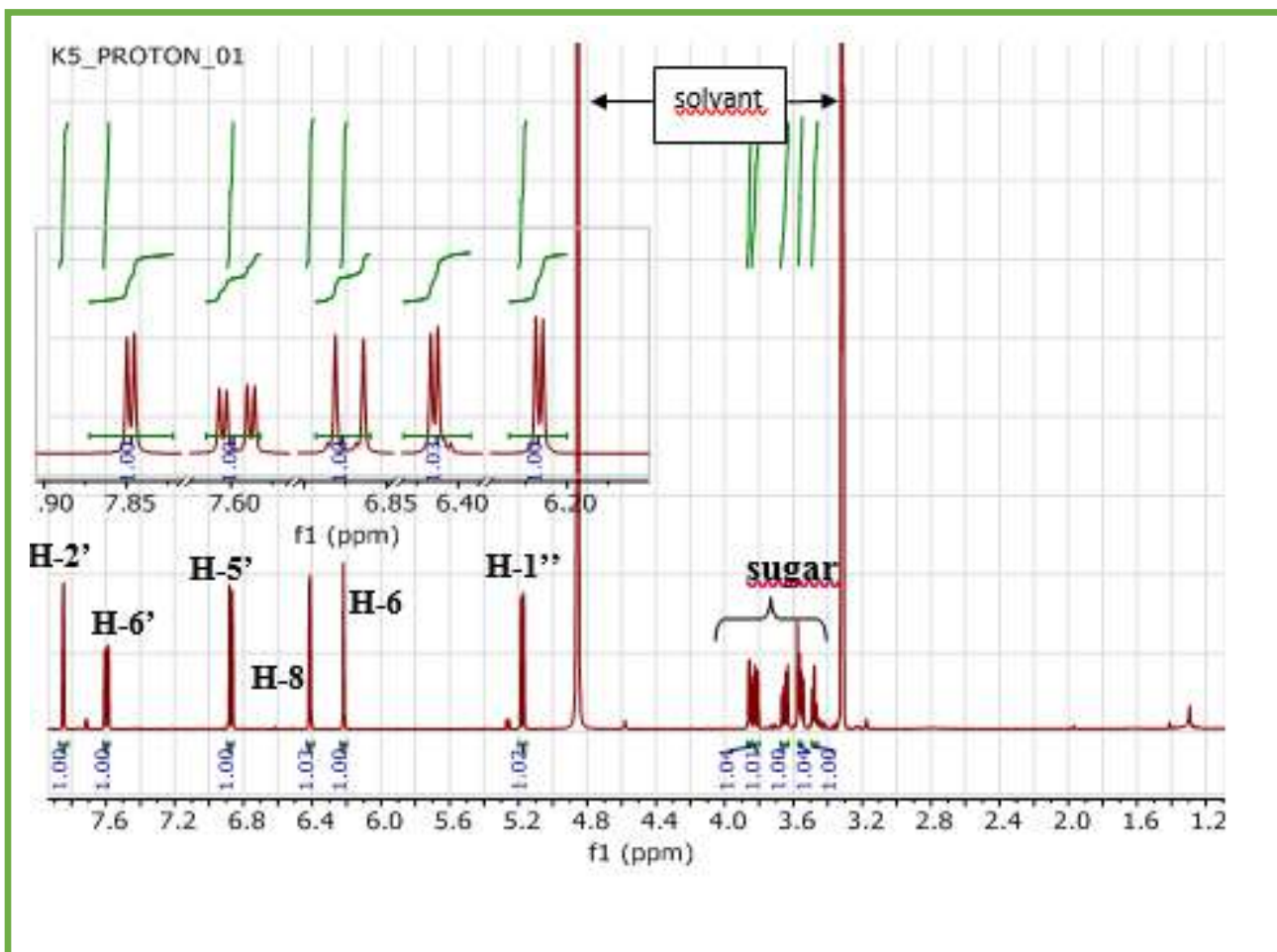


Figure 52: Spectrum RMN ¹H(500 MHz,CD₃OD) of compound K5.

The ¹³C NMR spectrum of compound K5 (Figure 53) confirms the presence of twenty-one carbon atoms and reveals the characteristic signals of a quercetin-like genine.

All the carbons of this genin are distributed as follows:

- A signal at δ_c 179.90 ppm characteristic of a carbonyl group; Nine quaternary carbons, eight of which resonate in the zone ranging from δ_c 120 ppm to 170 ppm and one at δ_c 106.12 ppm;
- Five aromatic CH; Signals characteristic of a glucopyranoside (δ_C = 78.3, 78.1, 75.7, 71.2 and 62.6 ppm) relative, respectively, to the carbon atoms: C-5", C-3", C-2", C-4" and C-6".

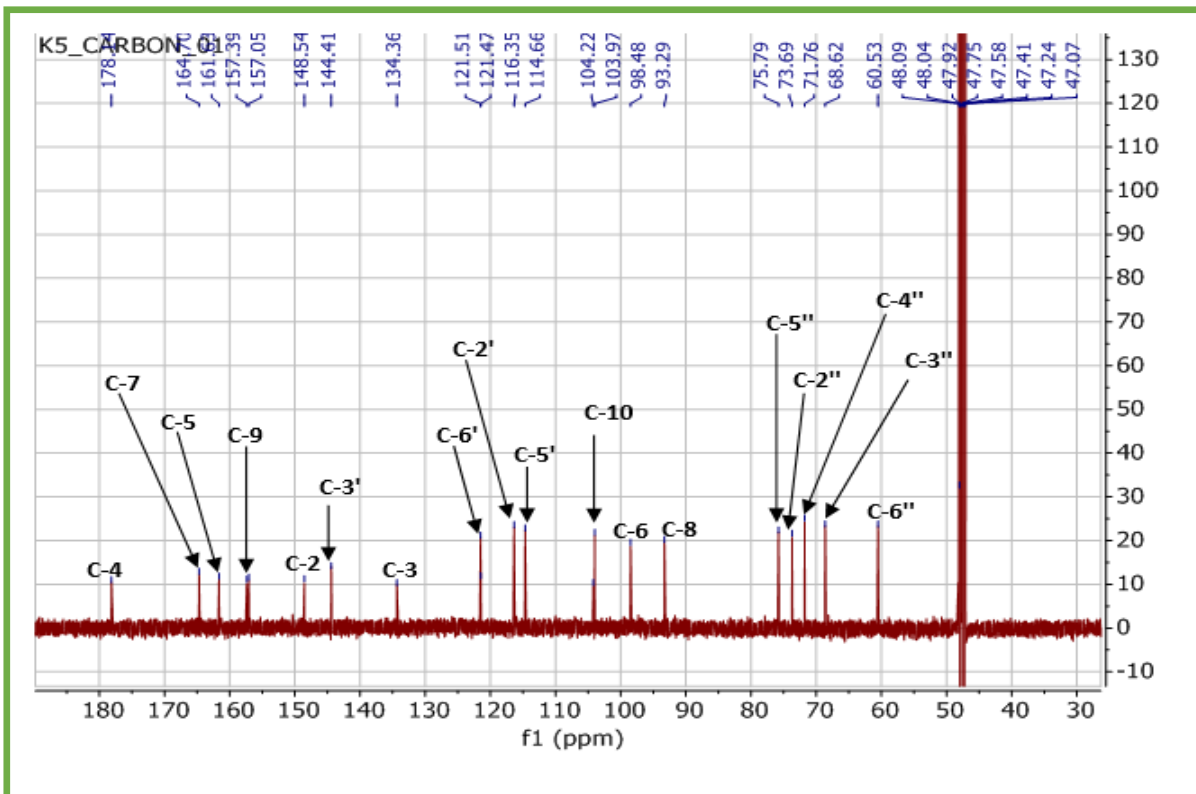


Figure 53: Spectrum RMN ^{13}C (125MHz, CD_3OD) of compound K5.

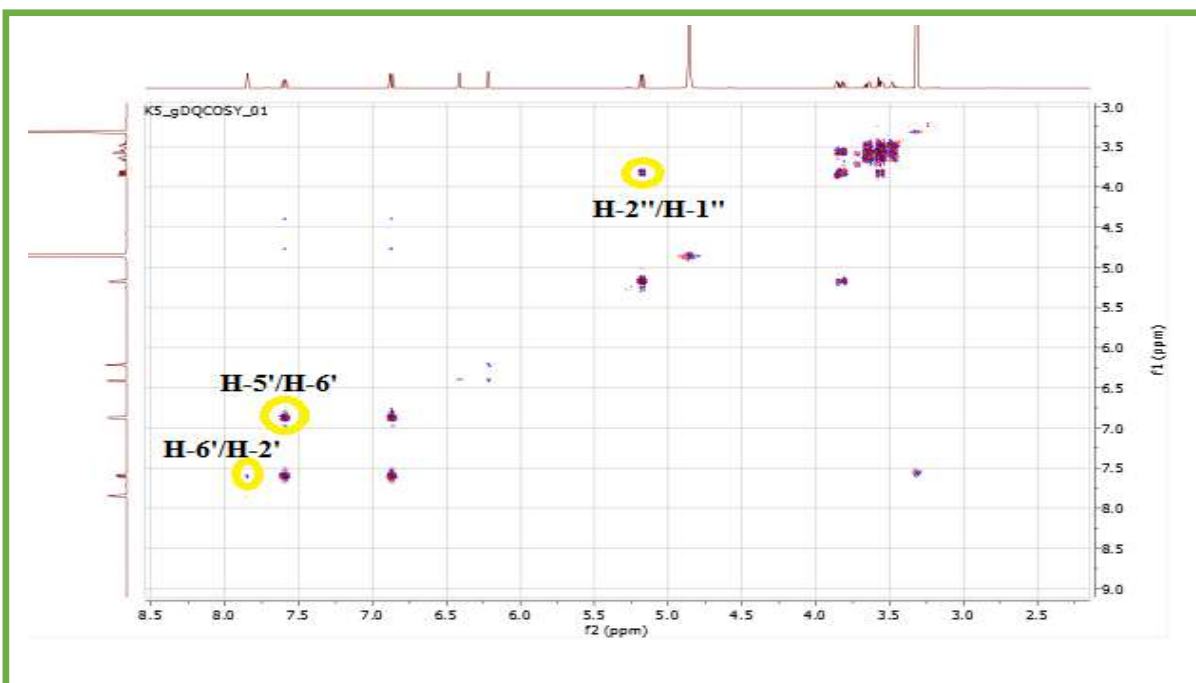


Figure 54: Spectrum of Cosy (500 MHz, CD_3OD) of compound K5.

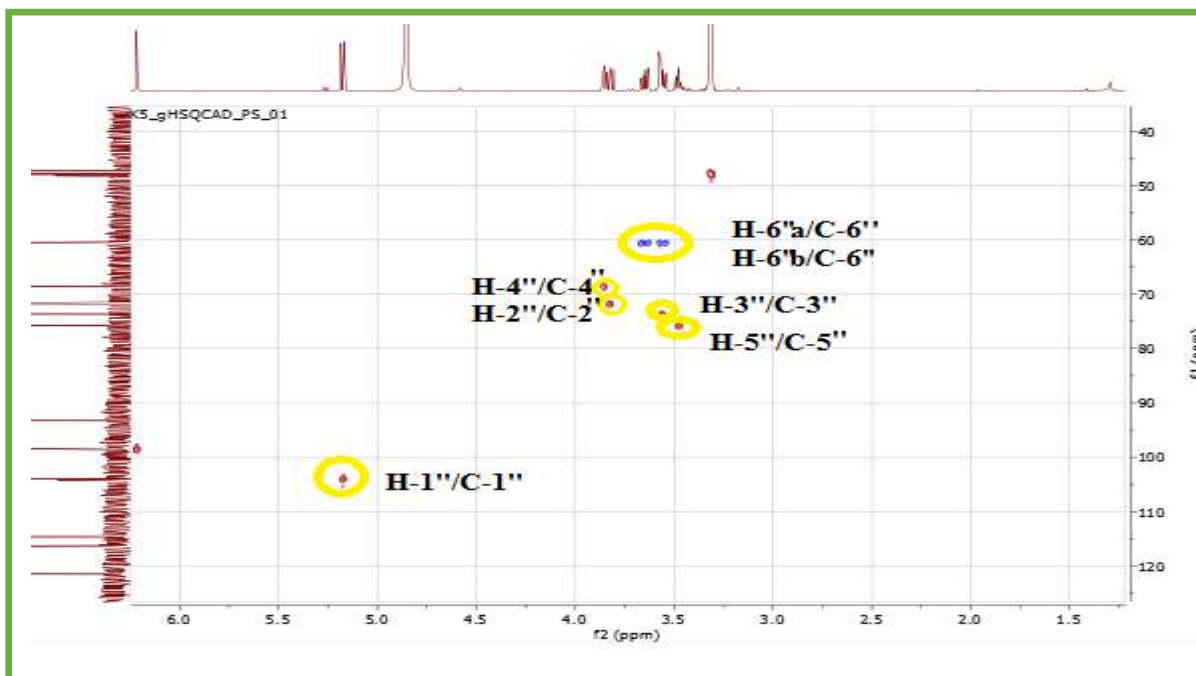


Figure 55: Spectrum of HSQC (500 MHz, CD₃OD) of compound K5

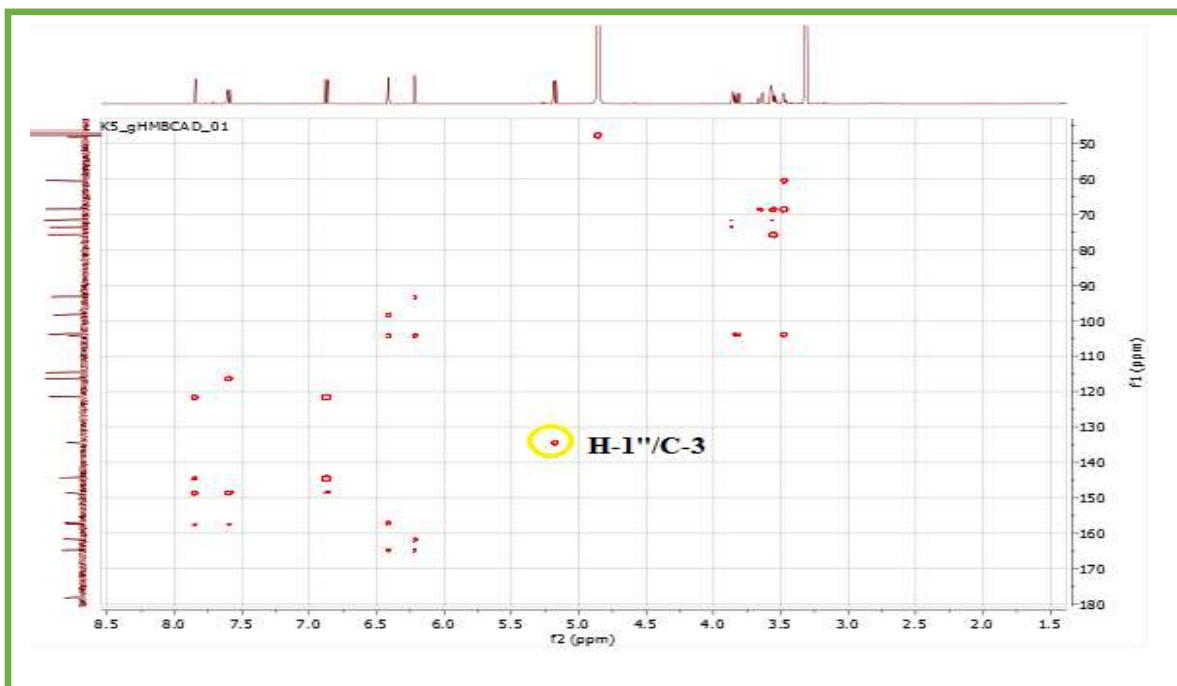


Figure 56: Spectrum of HMBC (500 MHz, CD₃OD) of compound K5.

The large values of the proton coupling constants of the sugar H5": 3.50 t (6.18 Hz); H6 ": 3.45 t (11.15 Hz); indicate an axial orientation of the protons of glucose.

The study of the HSQC spectrum (Fiquer55) also allowed us to deduce the displacements chemicals of the protons of this sugar, which clearly show spots of correlations between them in the Cosy spectrum.

Finally, the HMBC spectrum (Figure 56) shows a correlation spot between the proton, the anomeric of glucopyranose H-1 "and the C-3 carbon of the genin. In addition to the comparison with bibliographic research[7], the formula was determined to be Quercetin -3-O- β -glucoside. This compound was separated before from *P.crisp*[5] *P.orientalis* [6] *P.incisa* [8] *P.arabica* [9]

Table 28: Chemical shift values of 1D and 2D NMR of compound K5.

Position	C(δ) ppm	H(δ) (ppm, m, J en Hz)	Cosy	HMBC
2	157.39			
3	134.36			
4	178.14			
5	161.63			
6	98.48	6.22(d) $j=2.1$	H-6/H-7	C8'
7	164.70			
8	93.29	6.41(d) $j=2.0$	H-7/H-6	C6'-C10
9	157.05			
10	104.22			
1'	121.51			
2'	116.35	7.85(d) $j=2.1$	H-2'/H6'	C6'
3'	144.41			
4'	148.54			
5'	114.66	6.87d ($j=8.4$)	H-5'/H-6'	C3'
6'	121.47	7.60 dd ($j=2.2, 8.4$)	H6'/H2'/H5'	C2'-C4'
1''	103.97	5.18 d ($j=7.7$)		C3-C5''
2''	71.76	3.82 m		C4''
3''	73.69	3.65 dd ($j=6.1, 11.14$)		
4''	68.62	3.86 m		C6''
5''	75.79	3.48 td ($j=1.15, 6.18, 6.18$)		C3''
6''	60.53	3.55 m 3.57 m		

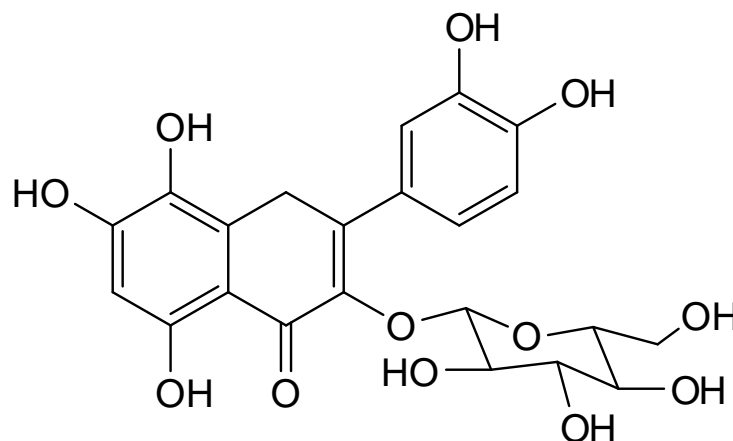


Figure 57: Chemical structure of K5
Quercetin-3-O- β -glucoside.

V.6. Structure elucidation of K6:

Examination of the ^1H NMR spectrum of compound K6 (Figure 58), recorded in CD_3OD , shows the signals characteristics of a flavonoid and, in comparison with the spectrum of the compound K2, noted that there is an agreement between the spectrum, except for the presence of sugar, distributed as follows :

- A signal at δ_{C} 177.91ppm characteristic of a carbonyl group, nine quaternary carbons, eight of them resonate in the zone ranging from δ_{C} = 120 ppm to 170 ppm and one at δ_{C} 104.11 ppm.
- Four aromatic CH; Signals (δ_{C} 76.97, 75.13, 74.62 and 72.18 ppm) relative, respectively, to the carbon atoms: C-5", C-3", C-2" and C-4" and one carbonyl group at δ_{C} 172.10ppm attributed to C-6", and a signal at δ_{C} 102.86 ppm attributed to C-1".
- A signal in the form of a ^1H integration doublet at δ_{H} = 5.96 ppm with a coupling constant $J = 1.2$ Hz (a meta coupling) attributed to H-6.

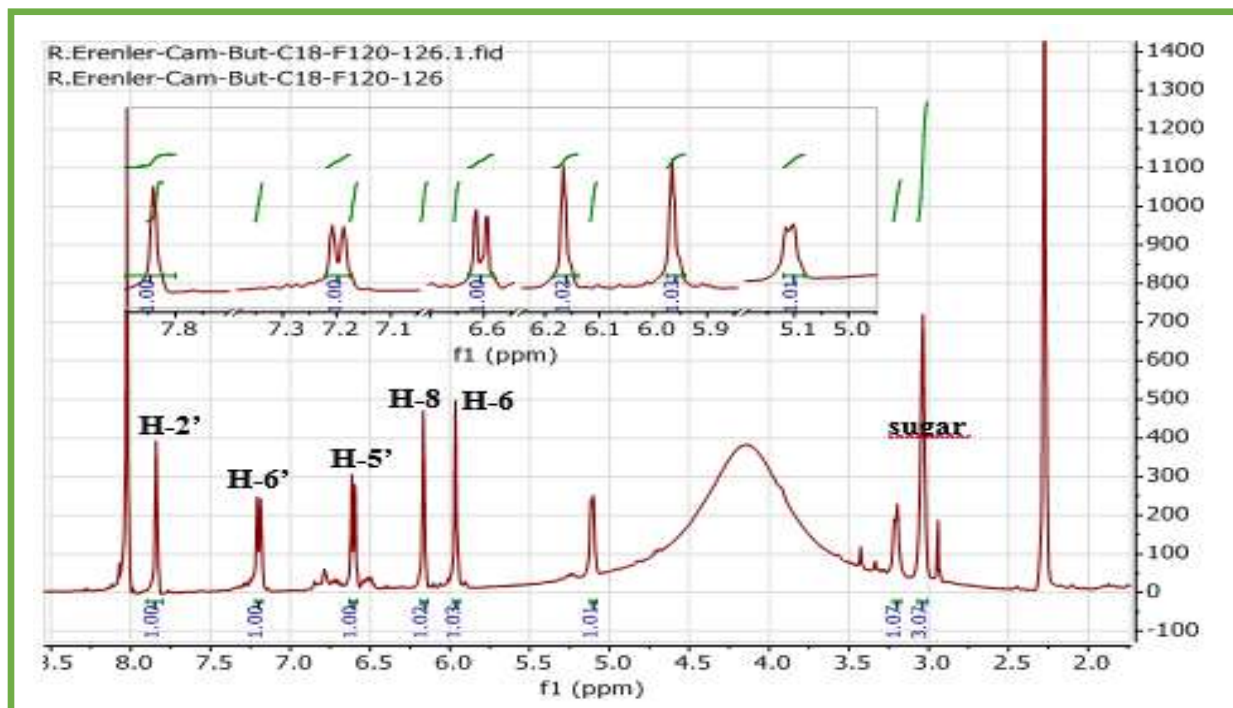


Figure 58: Spectrum RMN ^1H (400 MHz, CD_3OD) of compound K6.

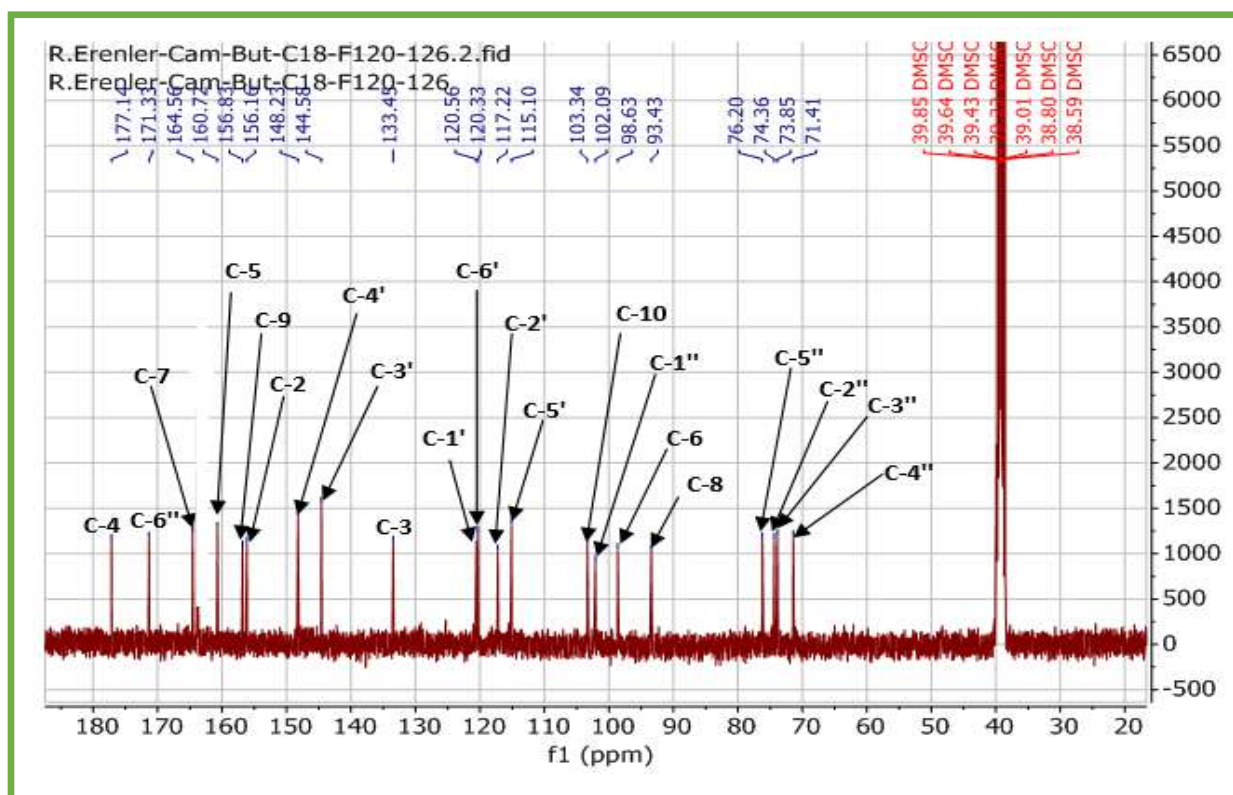


Figure 59: Spectrum RMN ^{13}C (100 MHz, CD_3OD) of compound K6.

Another signal as a doublet and integration 1H at δ H 6.18 ppm with the same coupling constant ($J = 1.1$ Hz; meta) coupling attributed to H8.

In addition, the signal in the form of a doublet ($J = 8.3$ Hz; an ortho coupling) which appears at δ 6.61ppm, with an integration of 1H, is attributable to H-5'. This confirms the substitution of positions 3' and 4' of cycle B.

The signal at δ H7.20 ppm, integration 1H in the form of a doublet doublet ($J = 8.4$ Hz; an ortho coupling and $J = 1.7$ Hz; a meta coupling) attributable to H-6'.

The signal at δ H = 7.84ppm, integration 1H in the form of a doublet ($J = 2.3$ Hz; a meta coupling) characterizing H-2'.

Furthermore, the anomeric proton resonates as a doublet at δ H 5.18 ppm, and the value of its coupling constant: $J = 7.7$ Hz, suggests a β osidic configuration.

The signal at δ H 5.12 ppm, integration 1H in the form of a doublet ($J = 5.6$ Hz) characterizing the anomeric proton of sugar.

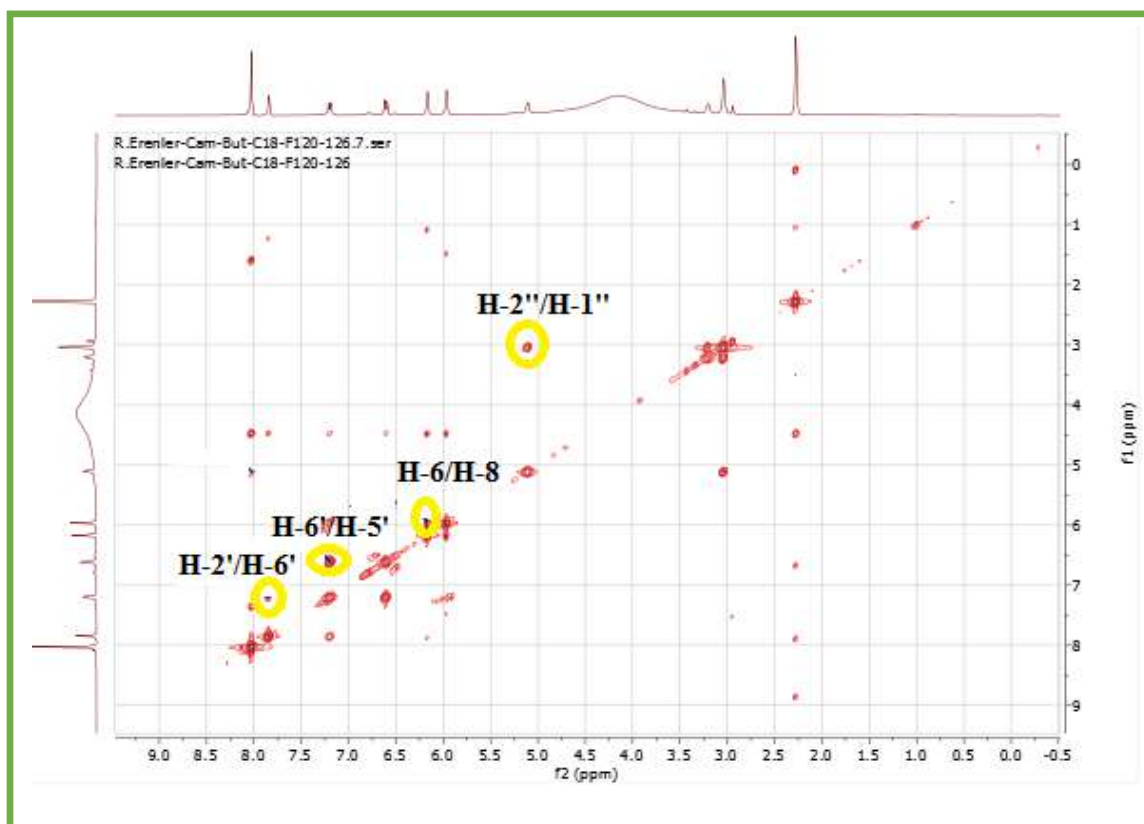


Figure 60: Spectrum of Cosy(400 MHz, CD₃OD) of compound K6.

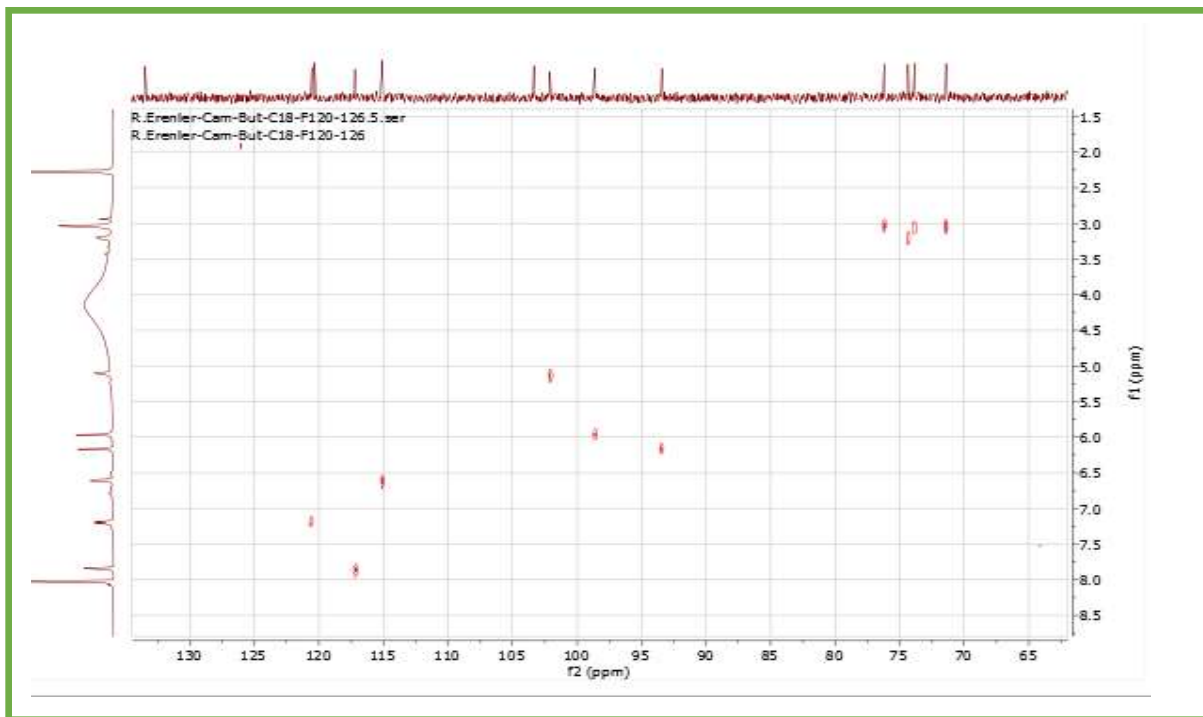


Figure 61: Spectrum of HSQC(400 MHz,CD₃OD) of compound K6.

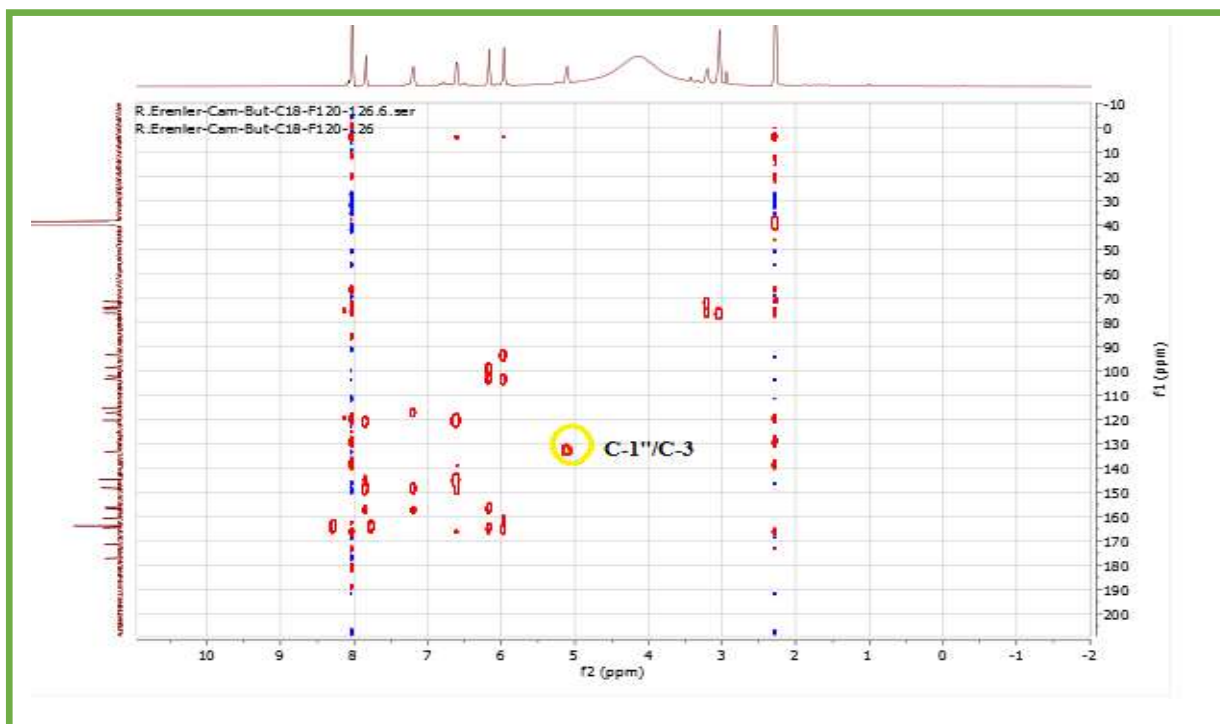


Figure 62: Spectrum of HMBC (400 MHz,CD₃OD) of compound K6.

Furthermore, an analysis of the ^{13}C NMR spectrum of compound K6 (Figure 59) indicates twenty-one distinct signals, of which fifteen are attributable to the signals of a flavonoid, broken down as follows:

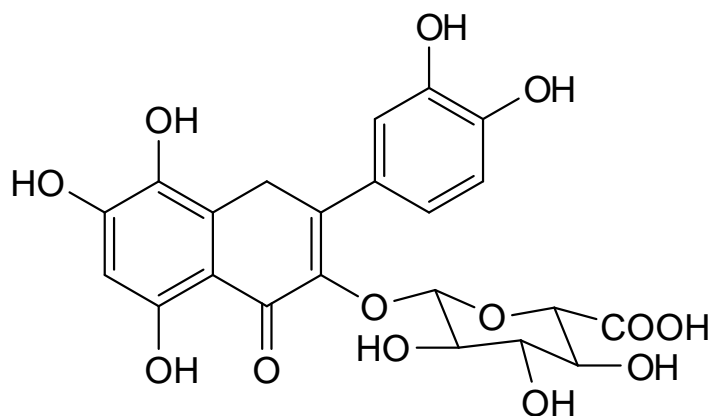
Ten quaternary carbons, including a carbonyl group at δC 177.34 ppm and five aromatic CH. Outside the sugar zone, these fifteen signals compared to those of compound k6 indicate that the genin of compound K6 is Quercetine substituted.

The attribution of the characteristic signals to the different nuclei was confirmed by an NMR analysis of the HSQC spectrum (Figure 61). From the Cosy spectrum (Figure 60), the correlations between the H-6/H-8, H-6'/H-2', H-5'/H-6', and H-1''/H-2'' clearly appear.

From in the HMBC spectrum (Figure 62) indicates without zero doubt the presence of sugre in position C-3. the formula was determined to be Quercetin -3-O- β -glucuronide. This compound was separated before from *P.arabica*[21] and *P.dysenterica*[24].

Table 29: Chemical shift values of 1D and 2D NMR of compound K6.

Position	C(δ) ppm	H(δ) (ppm, m, J en Hz)	Cosy	HMBC
2	156.93			
3	134.23			
4	177.91			
5	161.49			
6	99.40	5.96(d)j=1.2	H-6/H-7	C8'
7	165.33			
8	94.21	6.18(d)j=1.1	H-7/H-6	C6'-C10
9	157.60			
10	104.11			
1'	121.33			
2'	117.23	7.84(d)j=2.3	H-2'/H6'	C6'
3'	145.35			
4'	149.00			
5'	115.88	6.61(d)j=8.3	H-5'/H-6'	C3'
6'	121.10	7.20(dd)j=1.7, 8.4	H6'/H2'/H5'	C2'-C4'
1''	102.86	5.12(d)j=5.6		C3
2''	74.62	3.04		
3''	75.13			
4''	72.18	3.21 d j=8.4		
5''	76.97	3.04		
6''	172.10			



Figuer 63: Chemical structure of compound K6
Quercetin -3-O- β -glucuronide.

V.7. GC-MS analysis of the Chloroform extract:

The GC-MS were performed to determine nine compounds (considering compounds with an area percentage above 0.90), as shown in Table 28. According to the literature, minimal studies were carried out using GC-MS to characterize *Pulicaria* plant extracts, making this study the first report of these secondary metabolites in *P. laciniata* extracts.

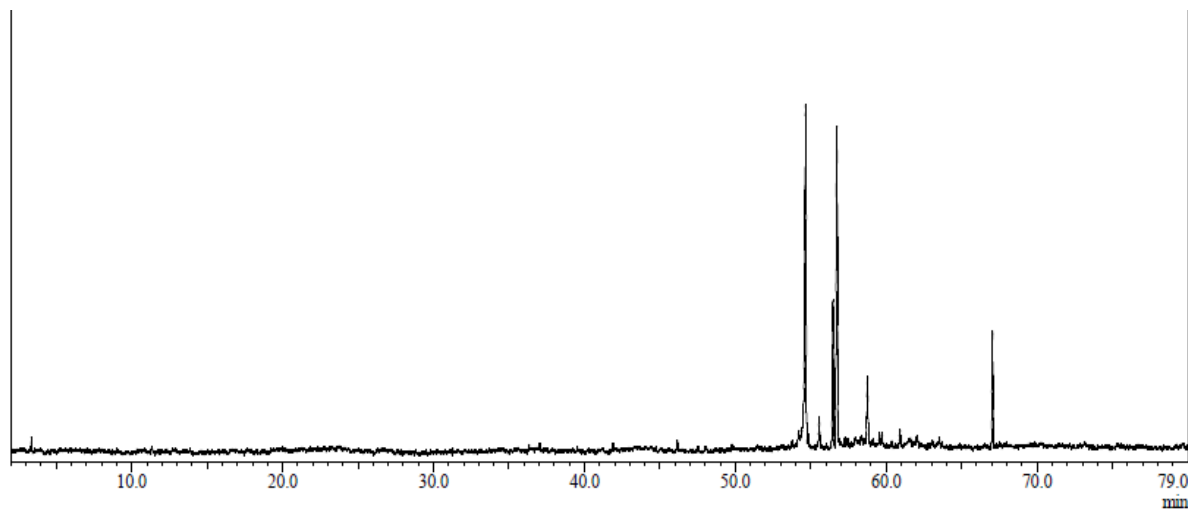


Figure 64: Gc-MS chromatogram of the CHCl_3 extract

Table 30: Represent the most abundant identified compounds from the GC-MS.

N.P	RT	Area %	Compounds	formula	MW
1	54.214	0.92	6-Methyl-2-(4-methylcyclohex-3-en-1-yl)hepta-1,5-dien-4-ol (β -Atlantol)	C ₁₅ H ₂₄ O	220.35
2	54.660	35.05	3-methyl-6-(1-methylethylidene)- 2-Cyclohexen-1-one (3-Terpinolenone)	C ₁₀ H ₁₄ O	150.22
3	55.558	2.20	3-Oxatricyclo[20.8.0.0(7,16)]triaconta-1(22),7(16),9,13,23,29-hexaene	C ₂₉ H ₄₂ O	406.9
4	56.478	12.11	3-Methyl-2-(2-methyl-2-butenyl)-furan	C ₁₀ H ₁₄ O	150.22
5	56.731	28.47	4,6,6-trimethyl-, (1S)-Bicyclo[3.1.1]hept-3-en-2-one	C ₁₀ H ₁₄ O	150.22
6	58.765	5.65	trans-Carveyl acetate	C ₁₂ H ₁₈ O ₂	194.27
7	59.722	0.93	5-(3-hydroxy-10,13-dimethyl-2,3,4,7,8,9,10,11,12,13,14,15,16,17-tetradecahydro-1H-cyclopenta[a]phenanthren-17-yl)-5-methyldihydrofuran-2(3H)-one	C ₂₄ H ₃₆ O ₃	372.5
8	60.914	1.36	2-Oxaadamantan-6-ol	C ₉ H ₁₄ O ₂	154.21
9	67.045	8.65	2,2'-methylenebis[6-(1,1-dimethylethyl)-4-methyl Phenol]	C ₂₃ H ₃₂ O ₂	340.5
N.P: Number of Peaks, RT: Retention Time, MW: Molecuair Weight					

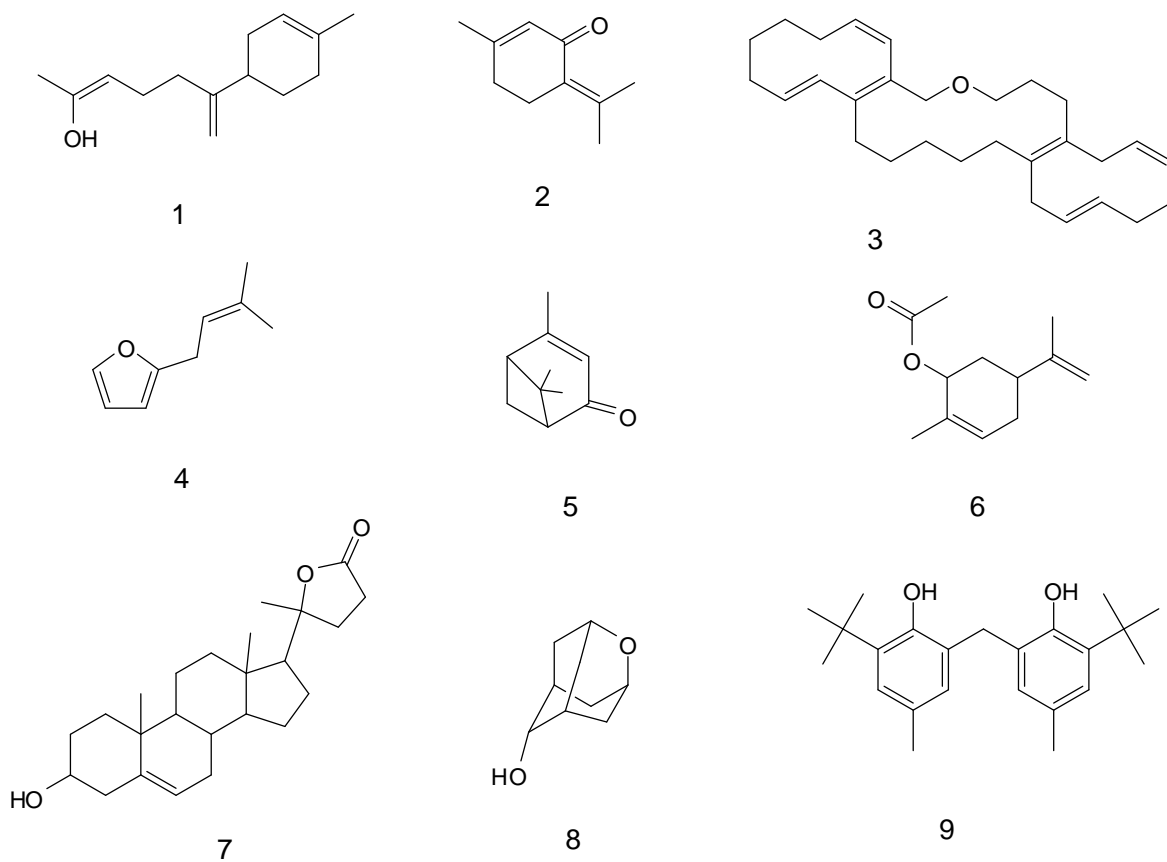


Figure 65 : The identified compounds structure from the CHCl_3 extract using GC-MS

References

References

1. San Feliciano A, Barrero A, Medarde M, del Corral JM, Aizpiri AA, Sánchez-Ferrando F. Asteriscunolides A, B, C and D, the first humulanolides; Two pairs of conformationally stable stereoisomers. *Tetrahedron*. 1984;40(5):873-8.
2. Zulfiqar F, Khan SI, Ali Z, Wang Y-H, Ross SA, Viljoen AM, et al. Norlignan glucosides from *Hypoxis hemerocallidea* and their potential in vitro anti-inflammatory activity via inhibition of iNOS and NF- κ B. *Phytochemistry*. 2020;172:112273.
3. Lin H, Ji-Kai L. The first humulene type sesquiterpene from *Lactarius hirtipes*. *Zeitschrift für Naturforschung C*. 2002;57(7-8):571-4.
4. Alvarado-Sansininea JJ, Sanchez-Sanchez L, Lopez-Munoz H, Escobar ML, Flores-Guzman F, Tavera-Hernandez R, et al. Quercetagenin and Patuletin: Antiproliferative, Necrotic and Apoptotic Activity in Tumor Cell Lines. *Molecules*. 2018;23(10).
5. AM R, Hammouda F, Ismail S, Hussiney H. Constituents of plants growing in Qatar XXIII. Flavonoids of *Francoeuria crispa*. *Qatar Univ Sci J*. 1993.
6. Ibraheim ZZ, Salem HA. Phytochemical and pharmacological studies on *Pulicaria orientalis* Jaub & Sp. *Bulletin of Pharmaceutical Sciences Assiut*. 2002;25(2):189-200.
7. Ibraheim Z, Darwish F. Further Constituents from *Pulicaria incisa*. *Bull Fac Pharm(Cairo Univ)*. 2002;40:167.
8. Mansour R, Ahmed A, Melek F, Saleh N. The flavonoids of *Pulicaria incisa*. *Fitoterapia*. 1990;61(2):186-7.
9. El-Negoumy SI, Mansour RM, Saleh NA. Flavonols of *Pulicaria arabica*. *Phytochemistry*. 1982;21(4):953-4.
10. Pares JO, Oksuz S, Ulubelen A, Mabry T. 6-hydroxyflavonoids from *Pulicaria dysenterica* (Compositae). *Phytochemistry*. 1981;20(8):2057.
11. Williams CA, Harborne JB, Greenham J. Geographical variation in the surface flavonoids of *Pulicaria dysenterica*. *Biochem Syst Ecol*. 2000;28(7):679-87.
12. Vilegas, W., Nehme, C. J., Dokkedal, A. L., Piacente, S., Rastrelli, L., & Pizza, C. 1. Quercetagenin 7-methyl ether glycosides from *Paepalanthus vellozioides* and *Paepalanthus latipes*. *Phytochemistry*. 1999; 51(3), 403-409.

CHAPTER VI
BIOLOGICAL
ACTIVITIES
EVALUATION

VI. Anti-oxidant activities:

VI.1. 2,2'-azino-bis-3-ethylbenzthiazoline-6-sulfonic acid assay (ABTS^{•+}):

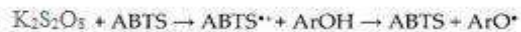
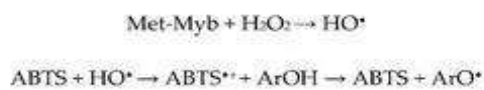
The anti-oxidant activity measurement is measured using the method known as ABTS (2,2'-azino-bis (3-ethylbenzothiazoline-6-sulphonic acid)). This method measures the ability of an anti-oxidant to react with ABTS^{•+} cation radicals produced chemically. The radical cation ABTS^{•+} has a characteristic green-blue color. It becomes colorless when proton donor substances reduce it. This method quantifies the ability of a molecule or extracts to trap radicals by measuring the absorbance of the anti-oxidant / radical reaction mixture at the spectrophotometer at 734 nm [1].

The solution of the ABTS^{•+} radical was prepared by the reaction between a solution of 7 mM ABTS^{•+} and a solution of potassium persulfate K₂S₂O₈ 2.45 mM incubated at 23 ° C for 12 to 16 hours in the dark. The ABTS^{•+} solution was diluted with ethanol (80%) until an absorbance of 0.700 ± 0.020 at 734 nm was obtained. A volume of 390 µl of this solution was mixed with 10 µl of the sample tested and prepared at different concentrations. The mixture was stirred vigorously. After standing for 6 minutes at 23 ° C., the absorbance was measured at 734 nm. As for the antiradical activity, ABTS^{•+} scavenging ability was expressed as IC₅₀ (mg/mL). The lower IC₅₀ value corresponds to higher anti-oxidant activity. The inhibition percentage of ABTS^{•+} radical was calculated using the following formula (1):

$$\text{ABTS scavenging effect \%} = ((A_0 - A_1 / A_0) * 100 \quad (1)$$

where A₀ and A₁ are the absorbances after 6 minutes of the control and the sample, respectively.

Chemical reactions:



Mechanism of reaction:

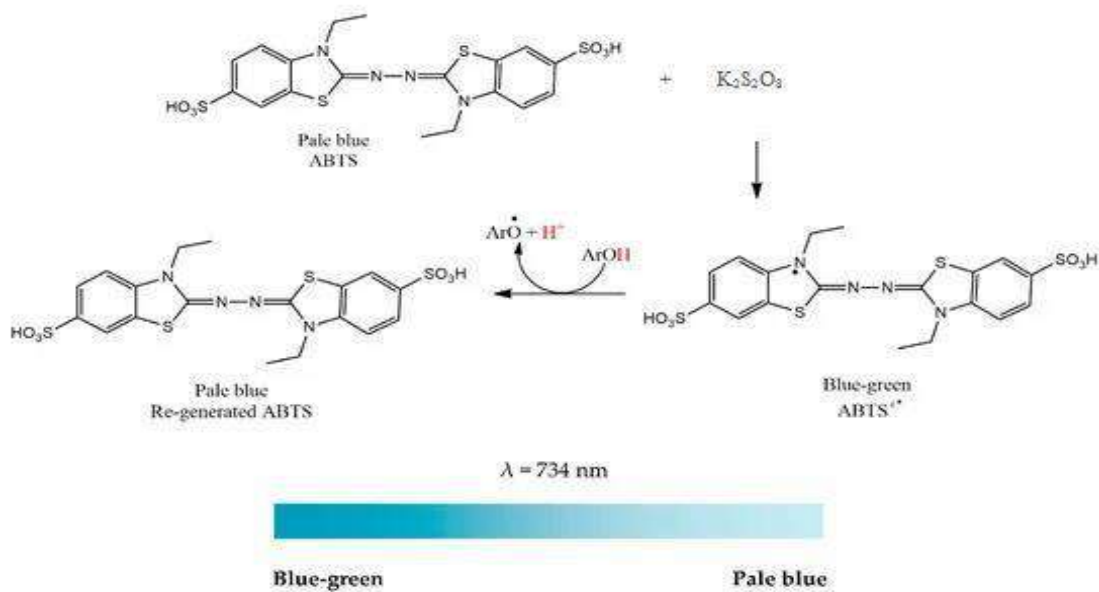


Figure 66: Formation of stable ABTS radical from ABTS with potassium persulfate [2].

VI.2. 1,1-diphenyl-2-picrylhydrazyl (DPPH•) assay:

The DPPH scavenging method is a bleaching test that measures the anti-oxidant's ability to react directly with the DPPH \cdot radical. The radical DPPH \cdot is a free organic radical rich with nitrogen, stable of a dark violet color. When reduced to its non-radical form by the anti-oxidant, it becomes yellow colorless. The DPPH assay was determined as follows: 10 μl of the diluted extracts were mixed with 390 μl of DPPH in methanol solution (0.004 mg/100 g). After standing for 30 min, the absorbance was measured at 517 nm by [3]. The inhibition of DPPH radical was calculated by the following formula (2):

$$\text{DPPH scavenging effect \%} = ((A_0 - A_1 / A_0) * 100 \quad (2)$$

Where A_0 and A_1 are the absorbances after 30 minutes of the control and the sample, respectively.

Chemical reactions:



where ArOH: phenolic AO

Mechanism of reaction:

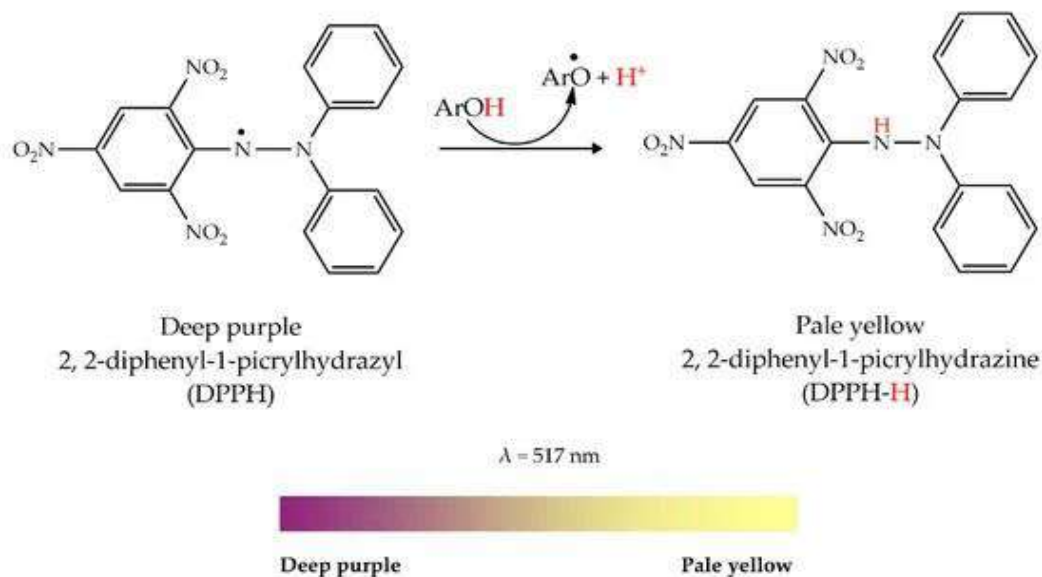
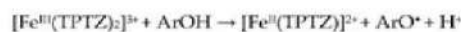


Figure 67: Reaction between DPPH• and antioxidant to form DPPH[2]

VI.3. 2,4,6-tri(2-pyridyl)-1,3,5-triazineFRAP Assay:

The FRAP assay reduces Fe^{3+} -TPTZ (2,4,6-tri(2-pyridyl)-1,3,5-triazine) to produce Fe^{2+} -TPTZ by the anti-oxidants. The binding of Fe^{2+} to the ligand creates a very intense navy blue color. FRAP reagent was prepared by mixing sodium acetate buffer (300 mM, pH 3.6) and 10 mM TPTZ solution in 40 mM HCl and 20 mM FeCl_3 . 200 μl of each extract was added to 3 ml of FRAP reagent. After incubation in the dark at 37 °C for 30 minutes, the absorbance was measured at 593 nm against the blank [4]. The results are expressed in the IC_{50} value (mg/mL), which is the effective concentration giving an absorbance of 0.5 for reducing power and was obtained from linear regression analysis. In this case, a higher absorbance indicated a higher reducing power.

Chemical reaction:



Mechanism of reaction:

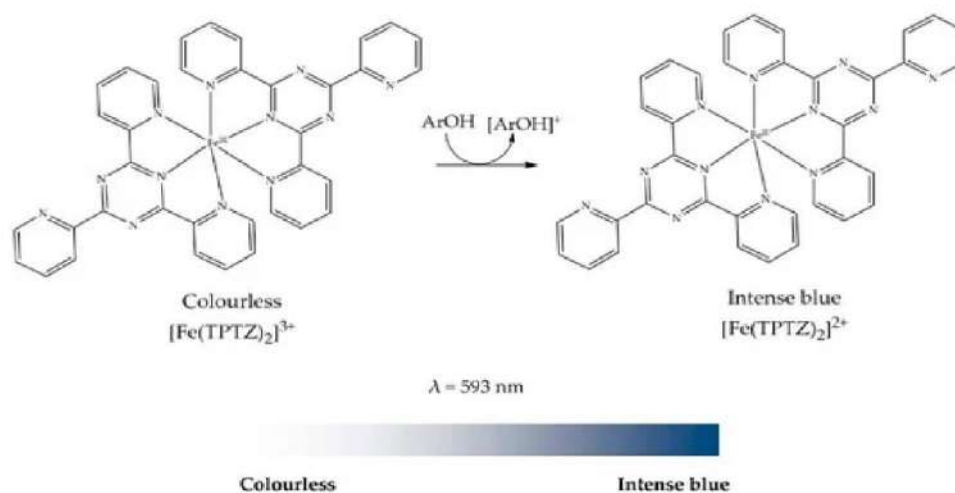


Figure 68: Formation of (TPTZ–Fe²⁺) complex from (TPTZ –Fe³⁺) complex by antioxidants

VI.4. Chelating effect on ferrous ions:

Chelation of metal ions is necessary for the functioning of processes biochemical and physiological cellular, but in some cases and when their mechanism action is not well controlled, these same ions can be the cause of peroxidation lipid, oxidative stress, or tissue injury, as an example Cu^{2+} is a stimulator peroxidation of Light density lipoproteins (LDL). The Fe^{2+} chelating activity was determined by measuring the Fe^{2+} formation of the ferrozine complex [5] with modifications.

The operation mode was as follows 2 ml of 0.1 M sodium acetate buffer pH 4.9 and 50 μL 2 mM iron (II) chloride were added to the samples (0.5 mL). After 30 min of incubation at room temperature, 0.2 mL of 5 mM ferrozine was added. After 30 min, the absorbance was measured at 562 nm. Distilled water and EDTA were used as the assay's control and standard metal chelator, respectively. The percentage prevention of complex formation of ferrozine has been estimated by the following formula (3)

$$\text{complex formation of ferrozine \%} : ((A_0 - A_1) / A_0 \times 100) \quad (3)$$

Where A_0 and A_1 were the absorbance of the control and the absorbance of the extract/EDTA absorption. The results were expressed as IC_{50}

Chemical reactions:



Mechanism of reaction:

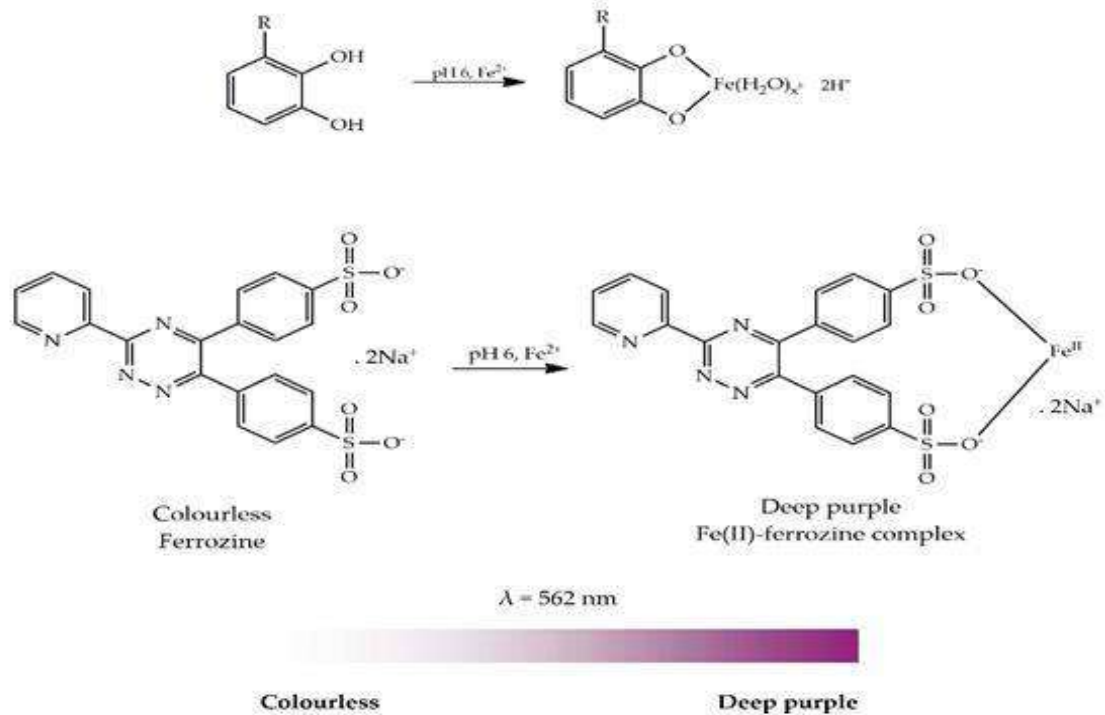


Figure 69: Metal chelating reaction mechanism.

VI.5 Anti-oxidant capacity:

The test is based on the reduction of molybdenum Mo (VI) present in the form of ions molybdate MoO₄²⁻ to molybdenum Mo (V) MoO²⁺ in the presence of the extract or an agent anti-oxidant. This reduction is materialized by forming a greenish complex (phosphate /Mo (V) at acidic pH [6]. The increase in the color of the Molybdenum (VI) complex in the presence of anti-oxidants. The method consists of introducing into a tube 200 μl of each extract into 2000 μl of a reagent composed of H₂SO₄ (0.6 M), Na₂PO₄ (28 mM), and ammonium molybdate (4 mM). The tube was closed and incubated at 95 ° C for 90 minutes. After cooling, the absorbance was measured at 695 nm. The samples and controls were

incubated under the same conditions [9]. The witness consists of 200 μ l of methanol mixed with 2000 μ l of the reagent above. The results are expressed in The IC50 value (mg/mL).

VI.6. Pyrogallol:

Pyrogallol autoxidizes rapidly in an aqueous solution and first becomes yellow-brown with a spectrum showing a shoulder between 400 and 425 nm. After several minutes, the color begins to turn green, and finally, after a few hours, a yellow color appears. The present investigation studied autoxidation during the first step(s). The rate was taken from the linear increase in absorbance at 420 nm, which is seen for several minutes after an induction period of some 10s [7].

In the Pyrogallol auto-oxidation assay (Marklund & Marklund, 1974), the inhibition rate of auto-oxidation of the pyrogallol with and without extract was determined as follows: 10 μ l of 0.01 mg/ml pyrogallol mixed with 450 μ l of phosphate buffer solution (pH 8.2) and 500 μ l of extract (0.1 mg/ml) or water at 25 °C. The mixture's absorbance was measured every 30 seconds for five minutes. The following equation was used to calculate the inhibition rate of the pyrogallol auto-oxidation effect:

$$I = (\Delta A_0 - \Delta A) / \Delta A_0 \times 100 \%$$

where I is the inhibition rate, A and A0 are the autoxidation rates of pyrogallol in the presence and absence of extract, respectively.

VI.2. Enzymatic activities:

VI.2.1. Inhibition of α -amylase:

The study of the various extracts' inhibitory activity of α -amylase (porcine pancreatic α -amylase) was carried out according to the method described by Yao X [8] with some modifications. Acarbose was used as the standard. The reaction medium was the mixture of 500 μ l of each extract at different concentrations, 500 μ l of 0.02 M potassium phosphate buffer (pH 6.9) containing 6 mM NaCl and α -amylase enzyme (0.5 mg/ml) in phosphate buffer. The mixture was incubated at 25 °C for 10 min after adding 500 μ l of starch solution (1%, w/v) in the same saline phosphate buffer. After a second incubation for 10 min at 25 °C, the reaction was stopped by adding 1 ml of reagent-colored DNS. The mixture was placed in

a boiling water bath for 10 minutes and cooled until room temperature. The absorbance was measured at 540 nm after dilution 10 times with distilled water. The following formula calculated the percentage inhibition of α -amylase:

$$I\% = ((A_b - (A_S - A_{bck}) / A_b) * 100) \quad (4)$$

Where A_S is the absorbance of the tested extract, A_b is the blank absorbance, A_{bck} is the background.

VI.2.2. Inhibition of α -glucosidase:

In vitro α -glucosidase, the inhibitory activity of the extract was evaluated with some modification. Yeast α -glucosidase (0.4 U/mL) was used as the enzyme source in 0.1 mM phosphate buffer (pH 6.8). The substrate solution of P-nitrophenyl α -D-glucopyranoside 10 mM was prepared in 0.1 M phosphate buffer (pH 6.8). The extract at different concentrations was prepared by dilution in distilled water. The diluted extract (250 μ L) was pre-incubated for 10 min with a 150 μ L enzyme source. After pre-incubation, 100 μ L of the substrate was added and further incubated for 5 min at room temperature. The reaction was stopped by adding 1 mL of 0.2 M Na_2CO_3 solution, and absorbance was measured at 405 nm on a microplate reader. The increase in absorbance on substrate addition was measured. [9]

the following formula calculated the percentage inhibition of α -glucosidase:

$$I\% = ((A_b - (A_S - A_{bck}) / A_b) * 100) \quad (4)$$

Where A_S is the absorbance of the tested extract, A_b is the blank absorbance, A_{bck} is the background.

VI.2.3. Inhibition of lipase:

Pancreatic lipase inhibitory activity was determined using *p*-nitrophenyl palmitate (*p*-NPP) as the substance, which was hydrolyzed by lipase to form *p*-nitrophenol with maximum absorption around 405 nm. Lipase (10 mg) was dissolved in 5 mL Tris buffer (50 mM, pH 8, containing 0.1% gum arabic powder and 0.2% sodium deoxycholate). The mixture was stirred for 15 minutes and centrifuged at 1,800 g for 10 minutes. The clear supernatant was used for the assay. Briefly, in a 96-well microplate, 30 μ L Tris buffer, 150 μ L enzyme, and 10 μ L of

each extract (dissolved in 50% ethanol) were mixed. The mixture was incubated at 37 °C in the microplate reader for 20 min. Then, 10 µL of 10 mM *p*-NPP pre-incubated at 37 °C was added to start the reaction. The absorbance was determined under 405 nm for 20 min with an interval of 1 min [10].

The following formula calculated the percentage of Pancreatic lipase inhibitory:

$$I\% = ((A_b - (A_s - A_{bck}) / A_b) * 100) \quad (4)$$

Where A_s is the absorbance of the tested extract, A_b is the blank absorbance, A_{bck} is the background.

VI.2.4. Anti-acetylcholineesterase

The hydrolysis of acetylthiocholine iodide (ATCI) is determined by monitoring the formation of the yellow 5-thio-2-nitrobenzoate (TNB) anion during the reaction of 6,6'-dinitro-3,3'-dithiodibenzoic acid (DNTB) with thiocholine (colorless) released by enzymatic hydrolysis of acetylthiocholine according to the following equations.

The inhibition of AChE activity was employed according to Ellman's method [11, 12] with a slight modification. 100 µl of each extract with different concentrations was mixed with 50 µl of Tris-HCl Buffer (50mM, pH=8), 125 µl DTNB (3mM), and 25 µl of AchE (0.51 U/ml) in a microwell plate. The reaction was started by adding 75 µl of acetylthiocholine iodide substrate (15 mM). The absorbance of the mixture was measured at 405 nm. The blank was carried out using methanol instead of extract, and the background reaction was carried out using Tris-HCl instead of the enzyme.

The following formula calculated the percentage inhibition of acetylcholine esterase:

$$I\% = ((A_b - (A_s - A_{bck}) / A_b) * 100) \quad (5)$$

Where A_s is the absorbance of the tested extract, A_b is the blank absorbance, and the assays are carried out in triplicate, A_{bck} is the background.

VI.5. Statistical analysis:

All the experiments were carried out at least in triplicate and presented as mean \pm standard deviation. One-way analysis of variance was used in the comparison between multiple groups. Tukey's test was applied for multiple comparisons. Differences were considered statistically significant at a level of 0.05 ($p < 0.05$). Pearson's correlation coefficient was determined to establish the relationship between all the activities (IC_{50}) and total phenolic, flavonoids, and condensed tannins using the SPSS software program (version 21.0, Chicago, IL, USA).

VI.3. Result:

VI.3.1. Anti-oxidants activity:

VI.3. 1.1. ABTS assay:

The obtained results of the ABTS evaluation of the different extracts and the purified compounds are presented in (Figures 70 and 71).

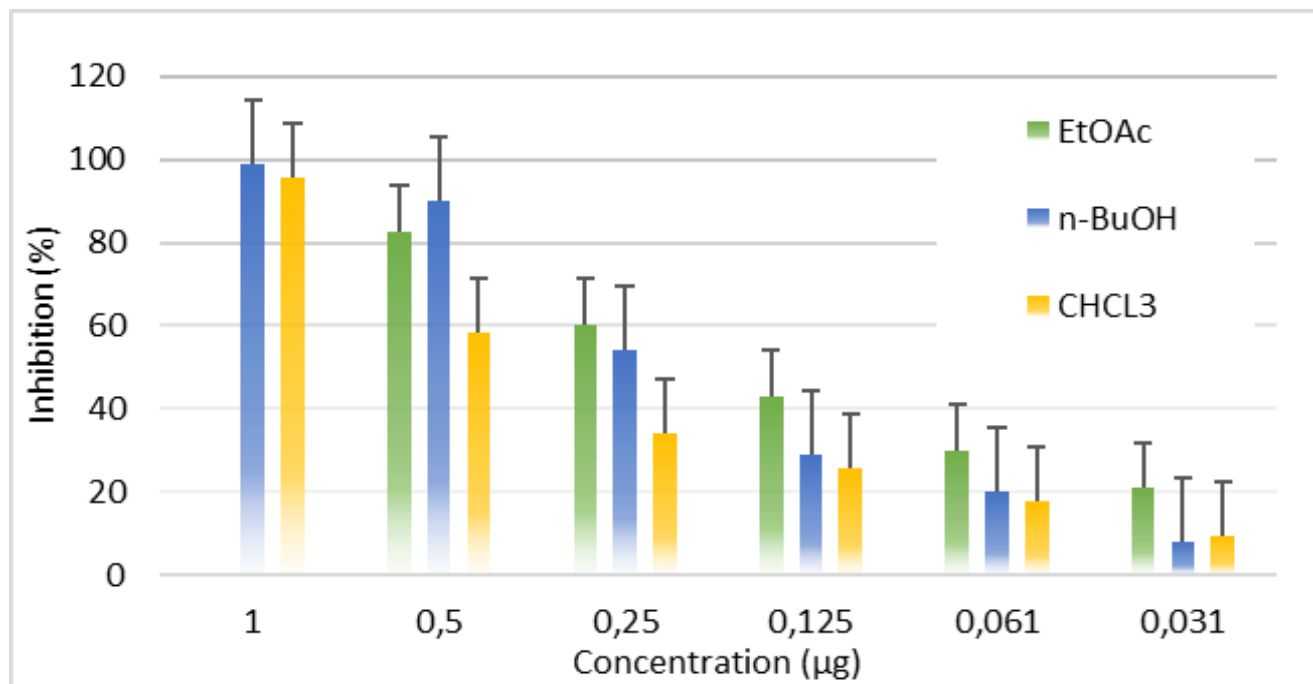


Figure 70: Inhibition rate of different extract of *P. laciniata* in ABTS assay

The n-BuOH and EtOAc e extracts give a significant anti-oxidants activity compared with the CHCl₃ extract, where the BuOH extract inhibited the ABTS cation radical with an of $6.59 \pm 0.15\%$ to $99.50 \pm 3.77\%$. For the EtOAc extract, the inhibition rate was $5.60 \pm 0.25\%$ to $98.75 \pm 3.25\%$ at the concentration range from $31.25 \mu\text{g}$ to $1000 \mu\text{g}$. In the CHCl₃ extract, the inhibition value was limited from $0.7 \pm 0.2\%$ to $10.73 \pm 1.7\%$ at the concentration of $62.5 \mu\text{g}$ to $1000 \mu\text{g}$.

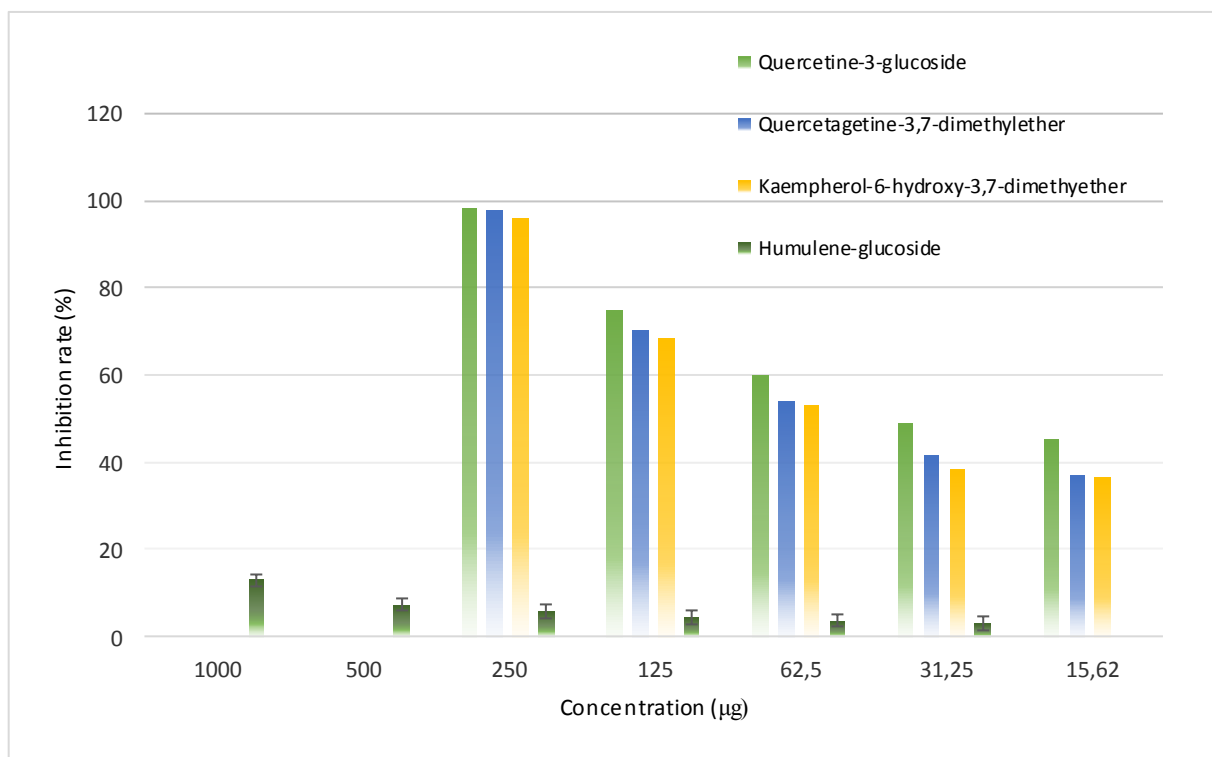


Figure71: Inhibition rate of purified compounds in ABTS assay.

As for the separated compounds, we noticed that there is similar efficacy on the anti-oxidant activity between the compounds Quercetagine -3,dimethymether and Kaempferol-6-hydroxy-3,7-dimethylether, with inhibition of $37.25 \pm 0.84\%$ to $98.03 \pm 2.65\%$ and $36.26 \pm 26\%$ to $96.03 \pm 1.99\%$ at a concentration range of $15.26 \mu\text{g}$ to $1000 \mu\text{g}$ while the compound Quercetine- 3-glucoside proved the best activity against the ABTS radical $45.34 \pm 0.95\%$ to $98.53 \pm 0.275\%$, on the other side the compound Humulene-glucoside exhibited the lowest efficacy on the ABTS scavenging with inhibition rate of $2.59 \pm 0.3\%$ to $12.90 \pm 0.78\%$ at concentration rage of $31.25 \mu\text{g}$ to $1000 \mu\text{g}$. The results show a strong correlation $p < 0.01$ between the total polyphenols $p < 0.01$ and flavonoids $p < 0.05$ with DPPH

VI.3. 1.2. DPPH assay:

The results of the antioxidant activity using the DPPH radical for the different extracts and the purified compounds were presented in (Figures 72 and 73) as inhibition rate (concentration).

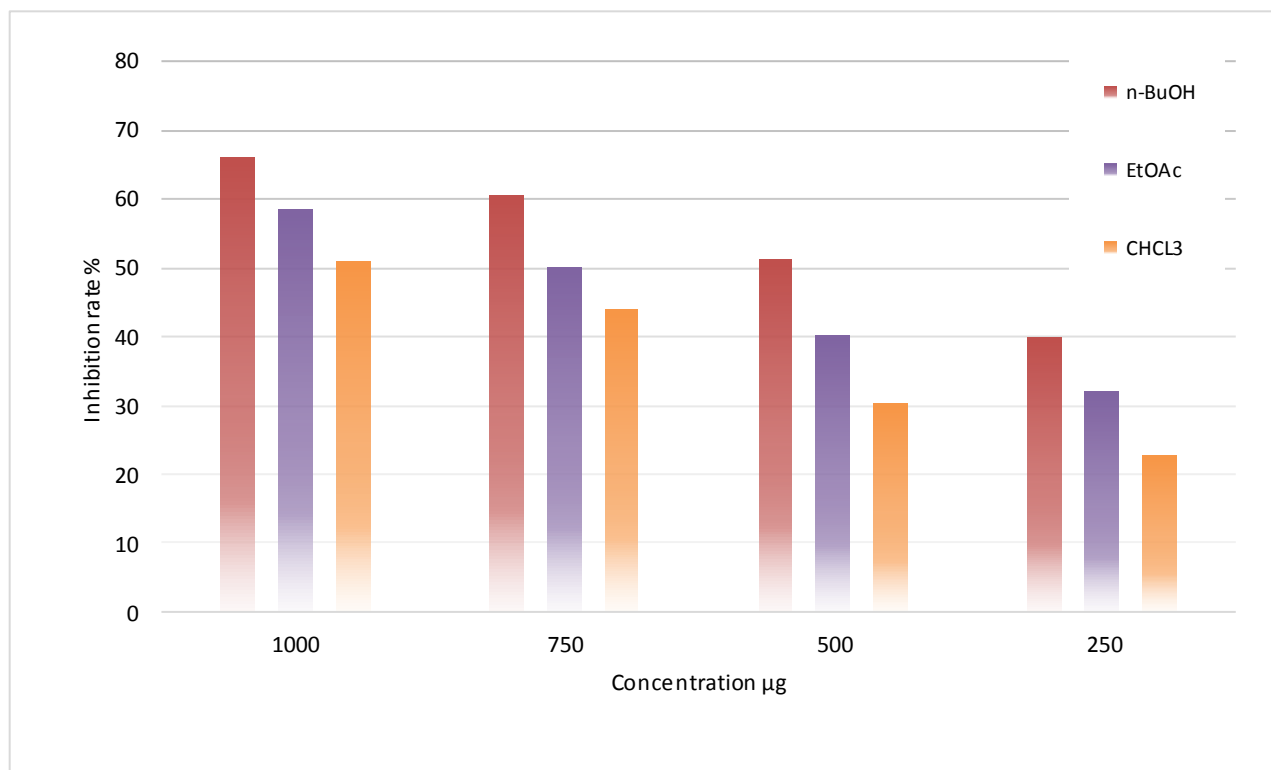


Figure72: Inhibition rate of different extract of *P. laciniata* in DPPH assay.

The inhibition rate was considerable in n-BuOH and EtOAc extracts compared with CHCl₃ extract, which was limited between 39.94 ± 0.39 % to 65.92 ± 0.21% for the BuOH extract and from 32.07 ± 0.97% to 58.49 ± 2.00 % for the EtOAc extract, while the CHCl₃ extract exhibited the lowers values which are 22.81 ± 1.37 to 50.85 ± 4.30 %, in the concentration range of 250 µg to 1000 µg. The results show a strong correlation $p < 0.01$ between the levels of total polyphenols and flavonoids with the DPPH test.

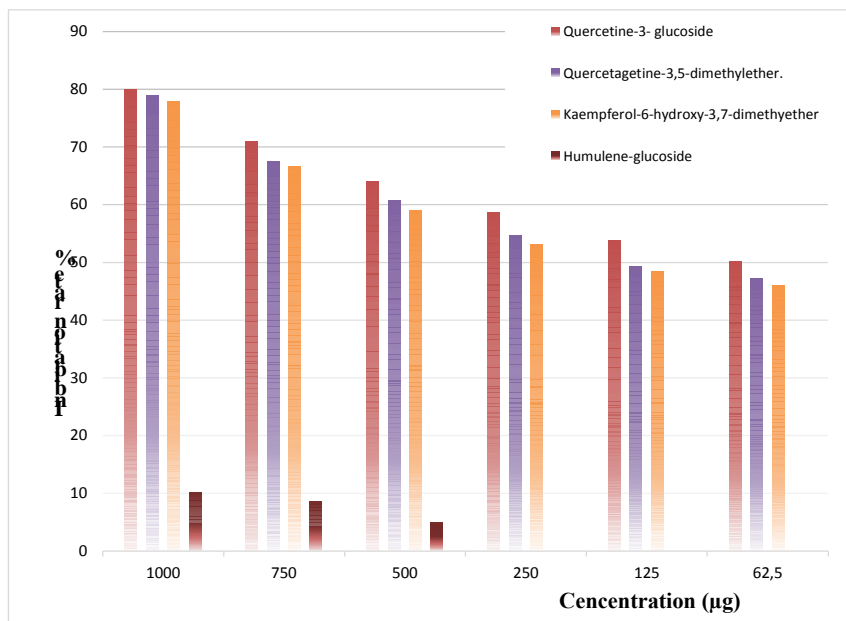


Figure73: Inhibition rate of purified compounds in DPPH assay.

While the inhibition rate in the purified compounds was as follows, the best one was Quercetine-3-glucoside, with an inhibition rate from $49.26 \pm 0.47\%$ to $80.06 \pm 1.16\%$ at the concentration range of $62.5\mu\text{g}$ to $1000\mu\text{g}$ and the low one was compound Humulene- glucoside, with inhibition rate of $10.07 \pm 0.82\%$ to $4.94 \pm 0.98\%$ at a concentration range of $500\mu\text{g}$ to $1000\mu\text{g}$ while Quercetagine -3,dimethymether and Kaempferol-6-hydroxy-3,7- dimethylether were almost similar with inhibition rate between $44.05 \pm 1.15\%$ and $78.84 \pm 1.74\%$, in the concentration range of $62.5\mu\text{g}$ to $1000\mu\text{g}$.

VI.3. 1.3. FRAP assay:

Another process of transferring electrons is reducing an oxidized anti-oxidant molecule to create the actively reduced anti-oxidant. Reducing power is an essential aspect of the estimation of the anti-oxidant activity. As shown in (Figure70) and Table 30, the n-BuOH extract ($650 \pm 0.033 \mu\text{g}$) was more important than the other extracts, followed by the EtOAc extract ($1060 \pm 0.045 \mu\text{g}$) and CHCl_3 extract. The results show a strong correlation $p < 0.01$ between the levels of total polyphenols $p < 0.01$ and flavonoids $p < 0.05$ with the FRAP test. The reducing power was expressed as IC_{50} .

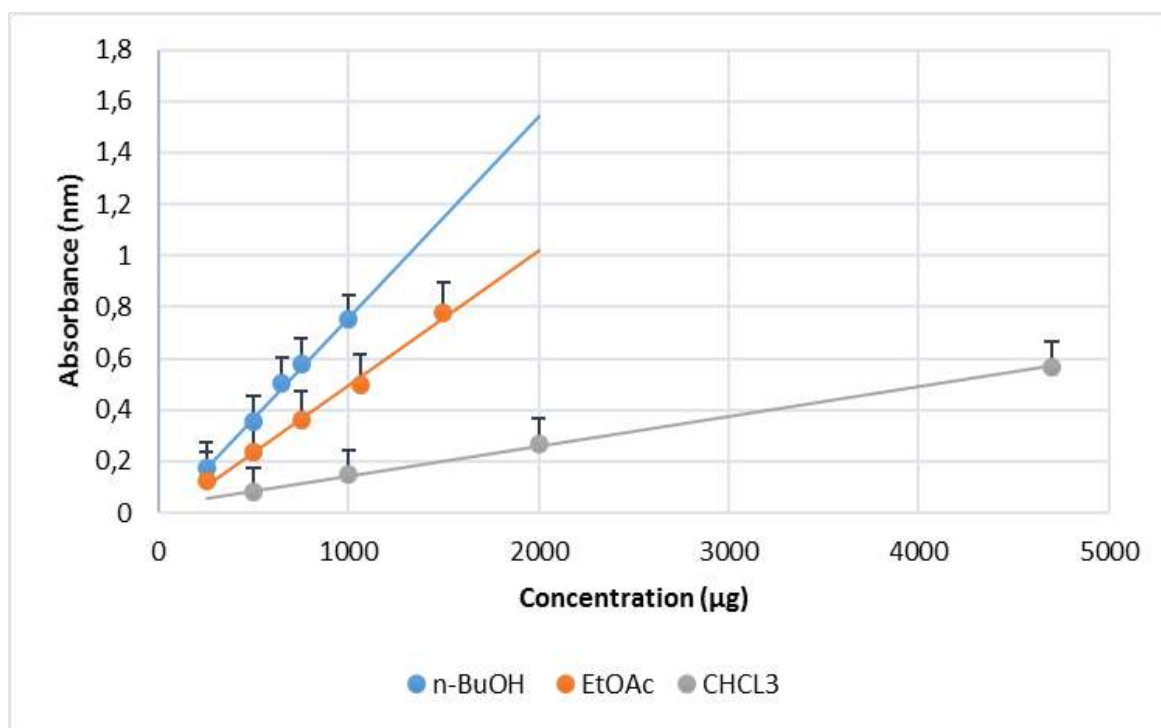


Figure74: Absorbance of different extract of *P.laciniata* in FRAP assay.

VI.3. 1.4. Chelating effect on ferrous ions:

Although iron is essential for oxygen transport, respiration, and enzyme activity, it is a reactive metal that catalyzes oxidative damage in living tissues and cells. Ferrozine can quantitatively form complexes with Fe^{+2} . In the presence of chelating agents, the complex formation is disrupted, resulting in a decrease in the blue color of the complex. Results indicate that the EtOAc extract ($1.40 \pm 0.44 \mu\text{g}$) was better than n-BuOH in this activity.

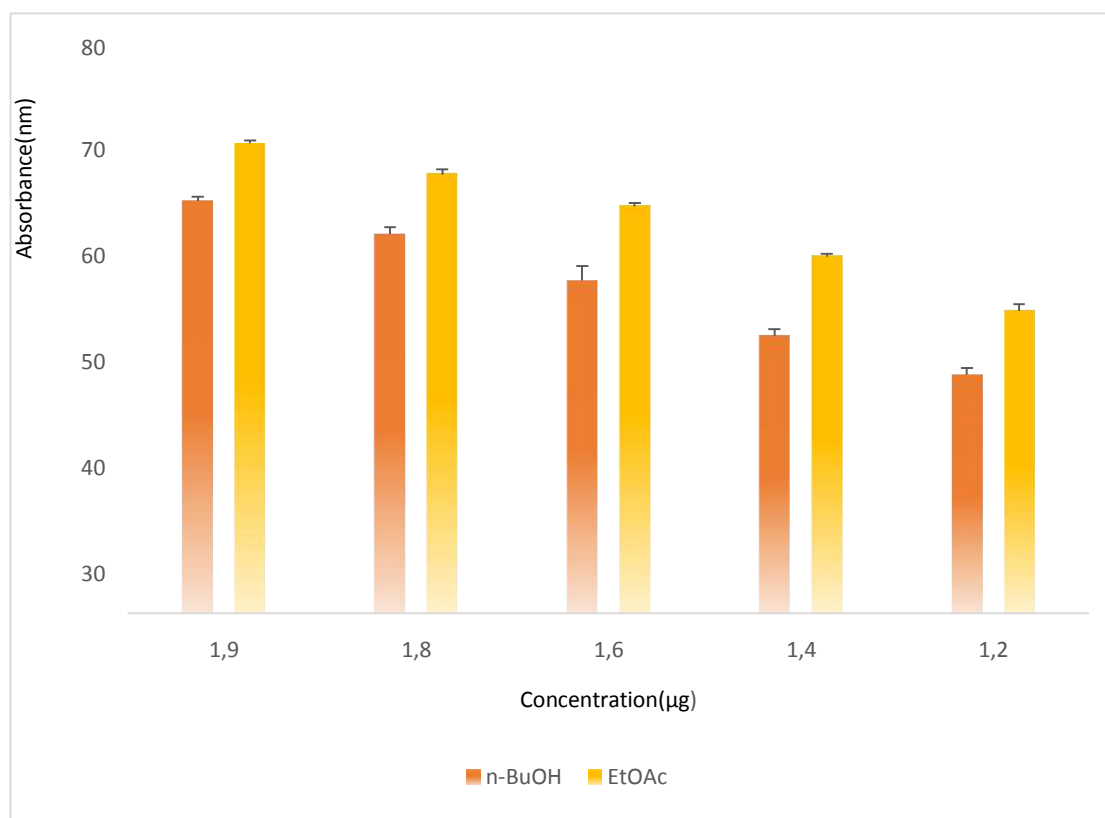


Figure75: Chelating effect on ferrous ions of *P.laciniata* different extracts.

VI.3. 1.5. Anti-oxidant capacity:

The global anti-oxidant activity of extracts was expressed as absorbance to concentration. The phosphomolybdenum method was based on the reduction of Mo (VI) to Mo (V) by the anti-oxidant compound and the formation of a green phosphate/Mo (V) complex. The antioxidant activity of all extracts was approximate in the following order, the EtOAc extract (0.48 ± 0.09 mg), BuOH extract (0.51 ± 0.02 mg), and CHCl_3 extract (0.63 ± 0.03 mg) (Table 30, Figure 76). Different extracts show a significant relationship $p < 0.05$ with TFC.

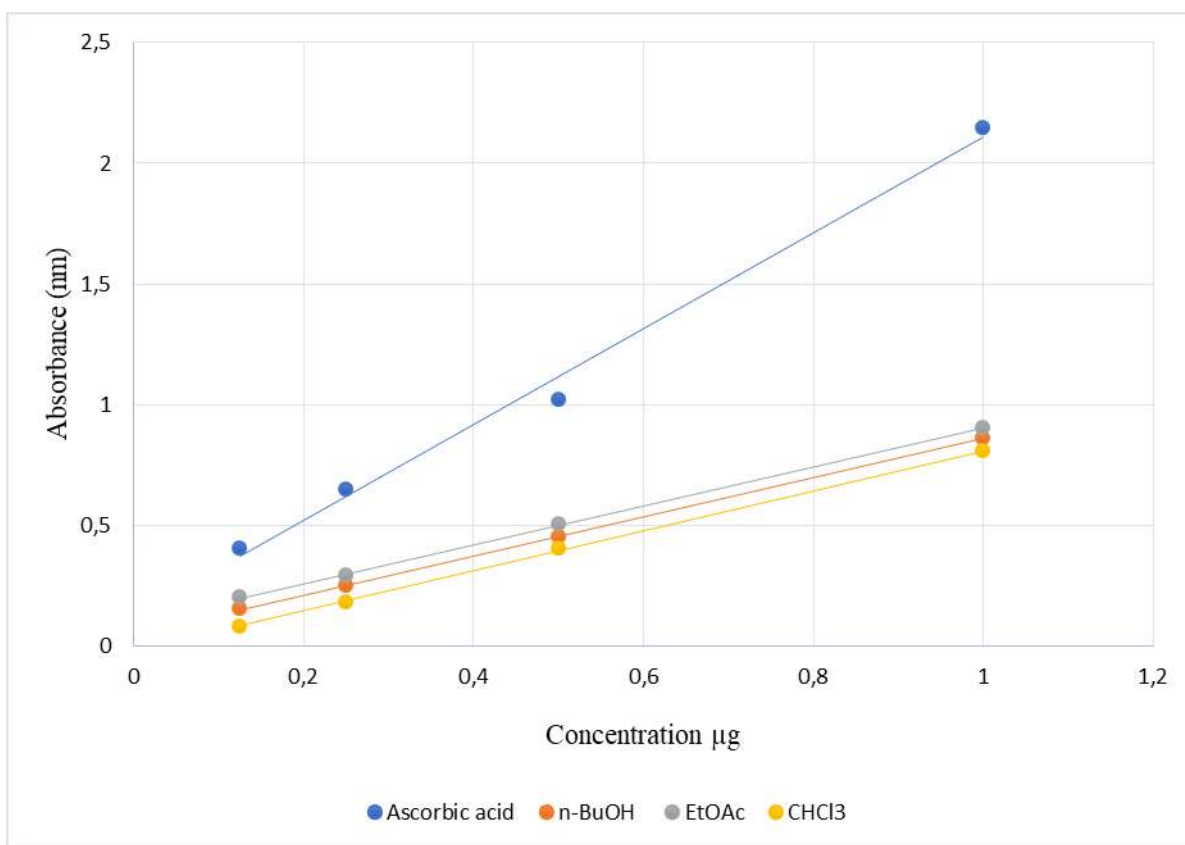


Figure76: The global antioxidant activity of *P.laciniata* different extracts.

VI.3. 1.6. Pyrogallol:

The inhibition rate of auto-oxidation of the pyrogallol with and without extract was determined. We note that all curves are on top of each other (Figure 77). The lower curve represents the least effective one, the EtOAc extract with an inhibition rate of $(5.42 \pm 0.0002 \%)$ followed by the CHCl_3 extract with an inhibition rate of $(10.02 \pm 0.0001 \%)$. At the same time, BuOH was the best inhibitor against the auto-oxidation of pyrogallol, with an inhibition rate equal to $15.44 \pm 0.0002 \%$ after five minutes. Different extracts show a significant relationship $p < 0.05$ with TPC.

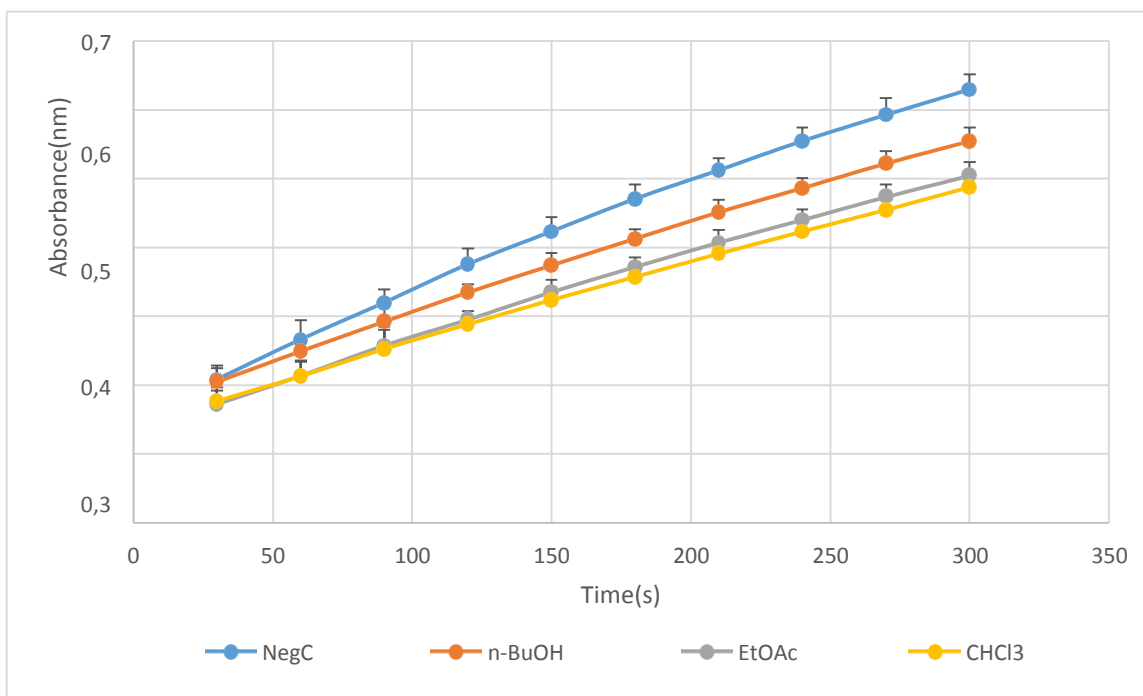


Figure 77: Pyrogallol-auto-oxidation of *P.laciniata* different extracts.

VI.3.2. Enzymatic activities:

VI.3.2.1. Inhibition of α -amylase:

This study tested n-BuOH, EtOAc, and CHCl₃ extracts of *P. laciniata* for their inhibitory activity against the α -amylase enzyme. As summarized in (Table 32), n-BuOH extract exhibited the most powerful inhibition potent activity, with an IC₅₀ of $414,8 \pm 1.77$ μ g/ml, followed by EtOAc extract with $526,58 \pm 0.017$ μ g/ml, then the CHCl₃ extract $632,92 \pm 0.028$ μ g/ml

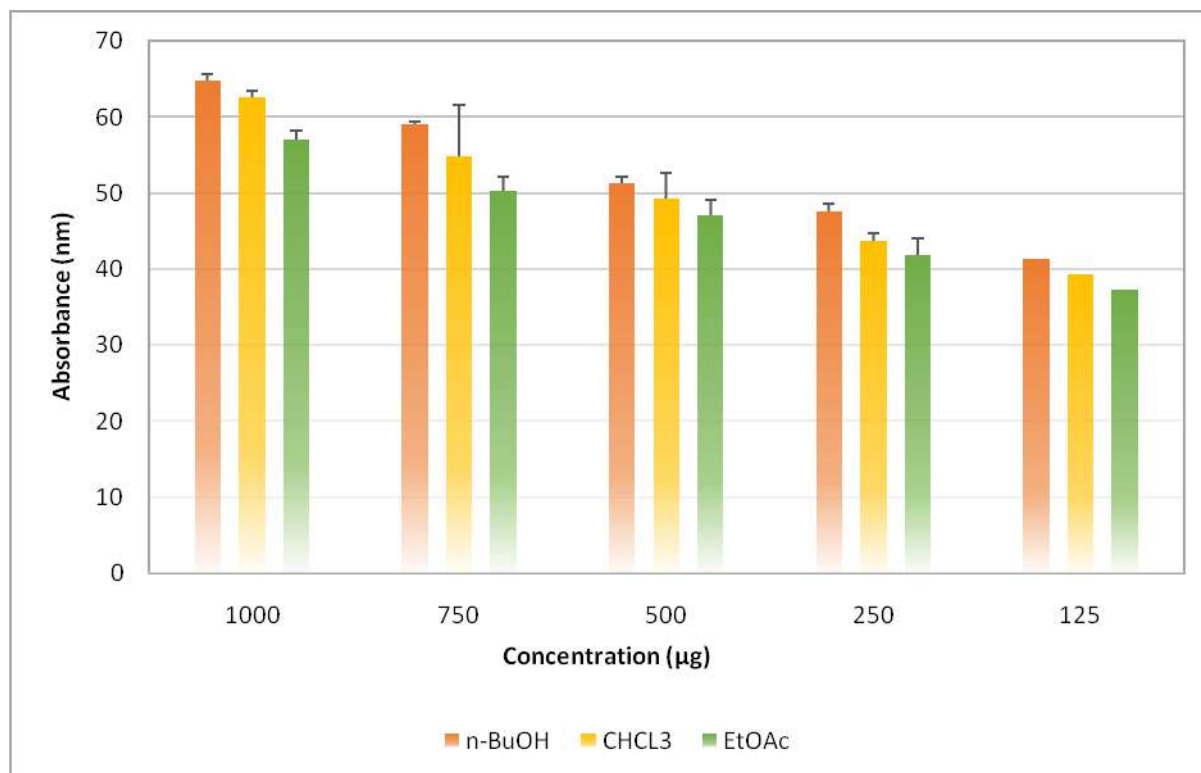


Figure 78: α -amylase inhibition rate of *P.laciniata* different extracts.

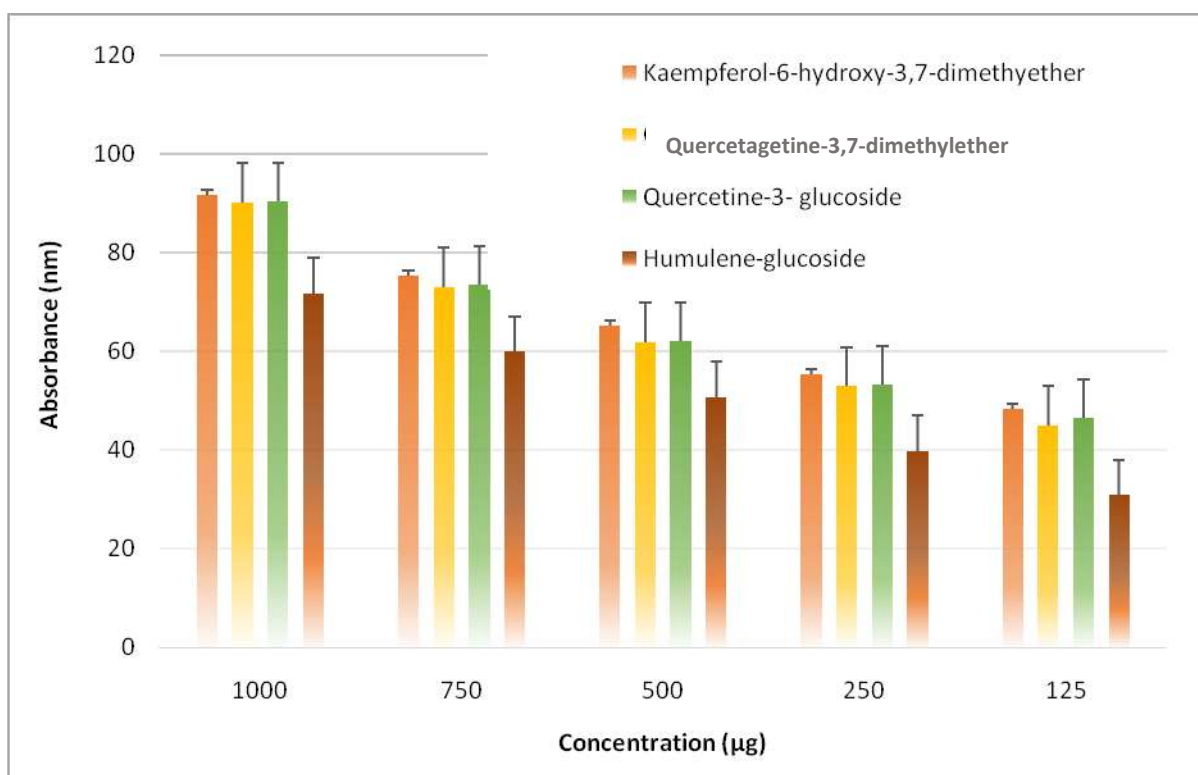


Figure 79: α -amylase inhibition rate of the purified compounds

While the inhibition rate in the purified compounds was as follows, the best one was the Kaempferol-6-hydroxy-3,7-dimethylether with an inhibition rate from $48.36 \pm 1.25\%$ to $91.716 \pm 3.02\%$ at a concentration range of $12.5\mu\text{g}$ to $1000\mu\text{g}$ and the low one was the compound 12 with inhibition rate of $30.89 \pm 1.49\%$ to $71.71 \pm 1.15\%$ at a concentration range of $12.5\mu\text{g}$ to $1000\mu\text{g}$. In comparison, Quercetagine-3,7-dimethylether and Quercetine-3-glucoside exhibited an inhibition rate as follows: 45.03 ± 1.59 to 90.23 ± 2.81 and $46.52 \pm 1.74\%$ to 90.50 ± 3.39 , respectively, in the concentration range of $12.5\mu\text{g}$ to $1000\mu\text{g}$.

VI.3.2.2. Inhibition of α -glucosidase:

The obtained results of the Inhibition of α -glucosidase assay of *P.laciniata* different extracts are presented in (Figure 80).

The CHCl_3 extract was the best inhibitor among the extract against the α -glucosides enzyme, with an inhibition rate reaching 82.16% at 50 μg followed by EtOAc extract and then BuOH extract, where at the concentration of 50 μg , the EtOAc extract inhibited 78.62%. In comparison, the n-BuOH extract inhibited 61.05% at some concentration.

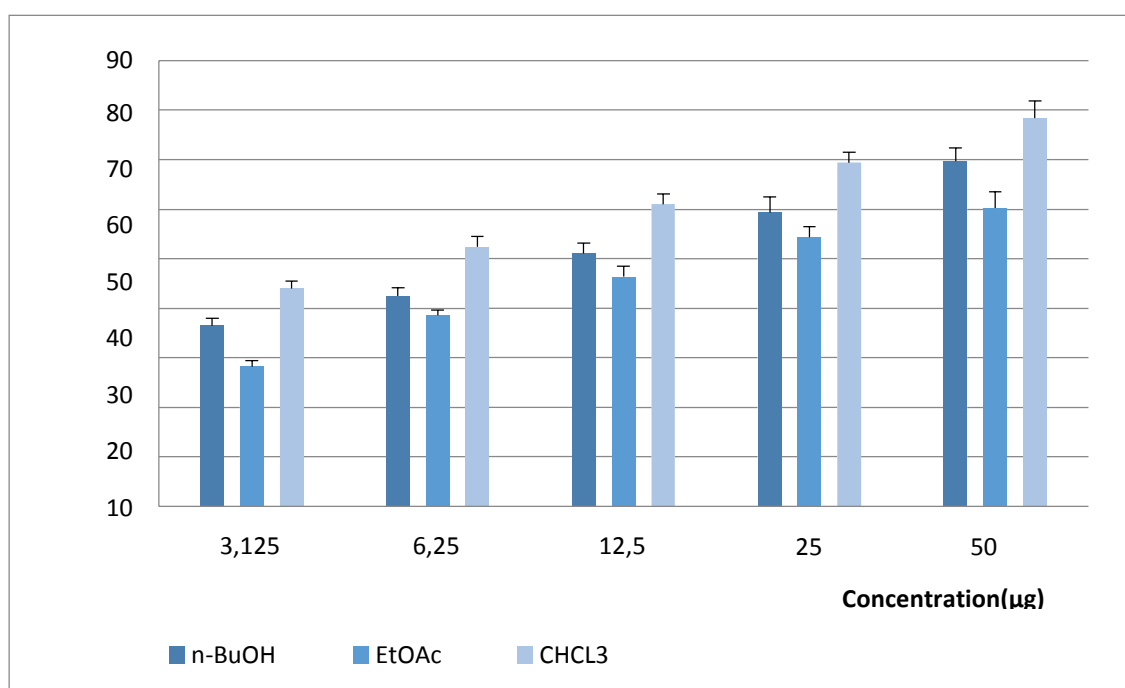


Figure 80: α -glucosidase inhibition rate of *P.laciniata* different extracts.

VI.3.2.3. Inhibition of lipase:

The inhibition rate was considerable for the CHCl_3 extract compared with the two other extracts, which were CHCl_3 extract exhibited, an inhibition rate limited between $43.99 \pm 1.48\%$ to $78.38 \pm 3.45\%$, for the BuOH extract from $36.52 \pm 1.48\%$ to $69.76 \pm 2.6\%$, while the EtOAc extract was the lowest with an inhibition rate limited between $28.29 \pm 1.12\%$ to $60.28 \pm 2.6\%$, in the concentration range of 3.125 μg to 50 μg .

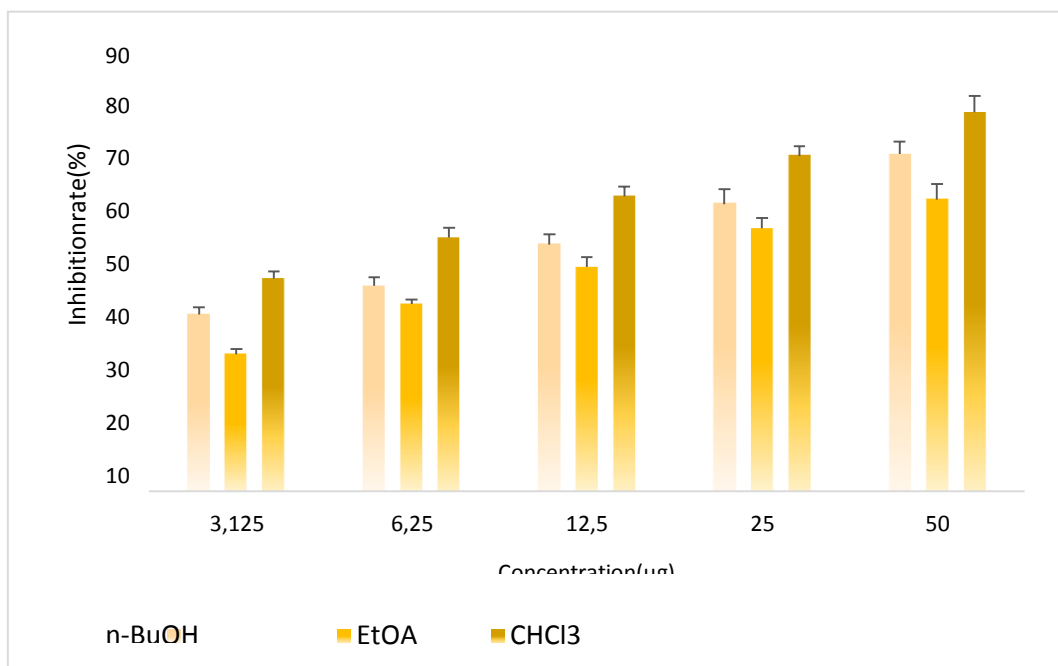


Figure 81: Lipase inhibition rate of *P. laciniata* different extracts.

VI.3.2.4. Inhibition of acetylcholinesterase (Anti-acetylcholine-esterase)

CHCl₃, ethyl acetate, and BuOH extracts of *P. laciniata* were tested against the AChE enzyme, and a considerable inhibition rate was obtained. The results were statistically significant, where the CHCl₃ extract inhibited 50% of the enzyme at 45.97 µg/ml concentration, followed by the BuOH and EtOAc extracts, respectively.

While the inhibition rate in the purified compounds was as follows, the best one was the Humulene-glucoside with an inhibition rate of 47.59 ± 0.23 % to 96.15 ± 1.15%, followed by Kaempferol-6-hydroxy-3,7-dimethylether with an inhibition value of 45.02 ± 0.25 to 91.38 ± 1.25 and the lowest one was the compound Quercetin-3,7-dimethylether with inhibition rate of 44.59 ± 0.32% to 90.68 ± 1.02% at a concentration range of 15.5 µg to 1000 µg.

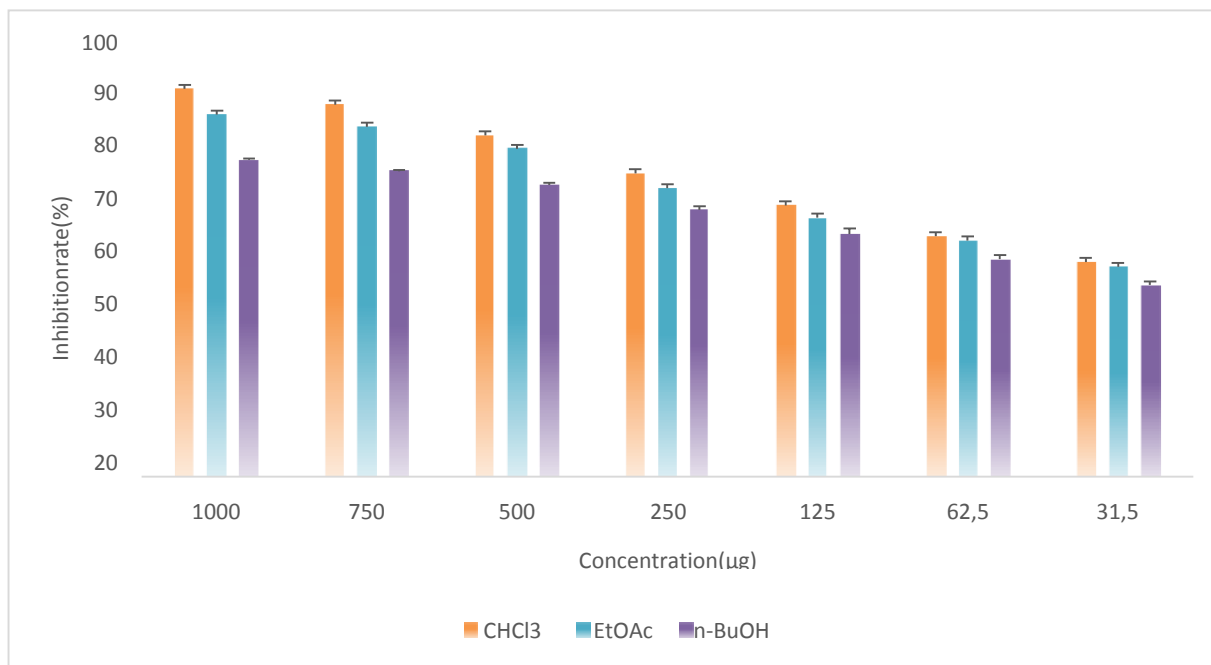


Figure 82: Acetylcholine-esterase inhibition rate of *P.laciniata* different extracts.

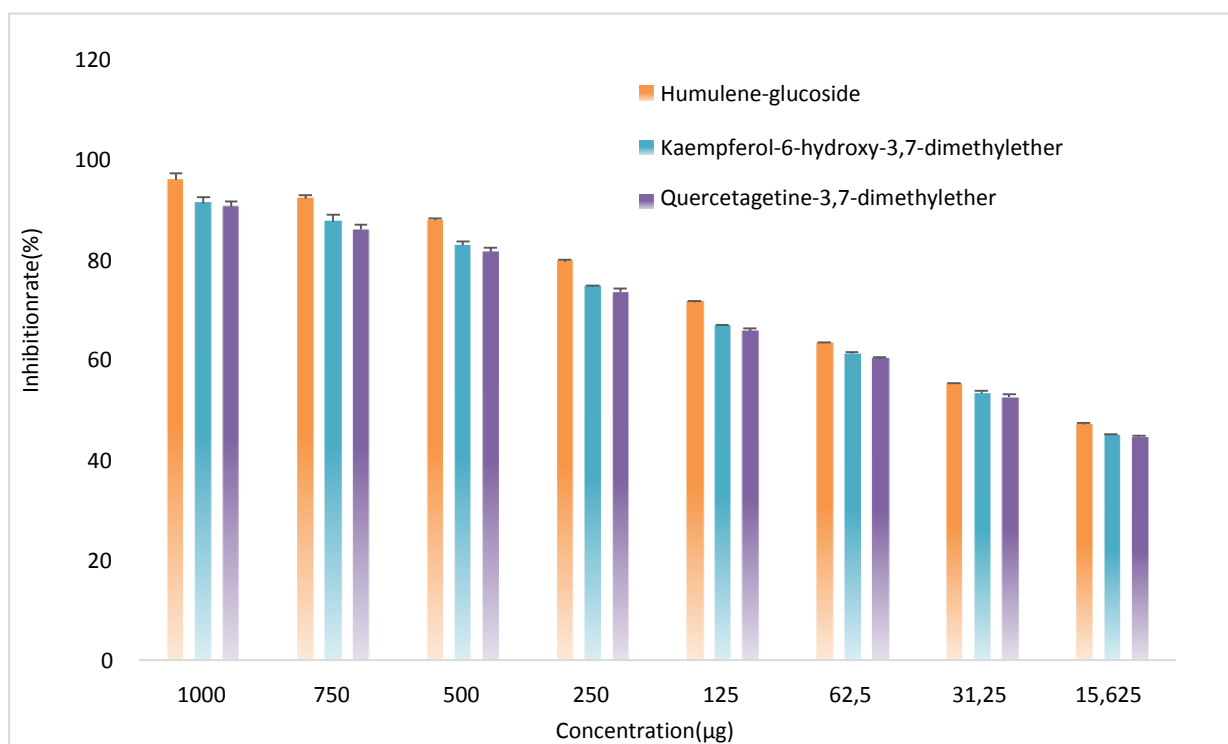


Figure83: Acetylcholine-esterase inhibition rate of the purified compounds

Table 31: Summarized results of anti-oxidant activities of *P.laciniata* different extracts.

	IC50 (µg)		A0.5 (nm)		
	DPPH+	ABTS+	Iron chelating(mg)	FRAP(mg)	Phosphor(mg)
BuOH	500.8±8,16	469.93±2,14	1,65 ± 0.81	0,65 ±0.01	0.51±0.02
EtOAc	760.7±4,08	492.74±6,17	1.40± 0.32	1.06±0.04	0.48±0.07
CHCl₃	957.94±12,43	4808,04±49,19	> 2	4.66±0.64	0.63±0.04
Ascorbic acid	90.12 ± 0.01	57.02± 0.01	/	/	0.23±0.02
BHT	/	/	/	0.23±0.03	/
EDTA	/	/	0.002±0.000	/	/

Results are expressed in terms of mean ± standard deviation (n = 3)., In statisticalanalyses by the Tukey comparison test, values with the same superscript are notsignificantly(p>0.05) different,n=3.

Table 32: Summarized results of enzymatic activities of *P.laciniata* different extracts.

	IC50 (µg)			
	α-Amylase	α-glucosidase	lipase	Anti-AchE
BuOH	414±0.34 ^{aA}	26.98±0.22 ^{aB}	10.73±0.36 ^{aC}	62,8±1,02 ^{aD}
EtOAc	742.92±0,95 ^{bA}	15.25±0.12 ^{bC}	18.33±0.80 ^{bC}	48,42±1,00 ^{bD}
CHCl₃	526.58±1.02 ^{cA}	6.23±0.07 ^{cB}	5.10±0.01 ^{cB}	40,85±1.01 ^{cC}
Acarbose	80.23±0.12 ^d	5.64±0.01 ^c	/	/
Orlistat	/	/	6.23±0.01 ^c	/
Galantamine	/	/	/	37.23 ± 0.02 ^c

Results are expressed in terms of mean ± standard deviation (n = 3)., In statisticalanalyses by the Tukey comparison test, values with the same superscript are notsignificantly(p>0.05) different,n=3.

Table 33: Summarized results of anti-oxidants and enzymatic activities of the purified compounds extracts.

	IC ₅₀ (μ g)			
	DPPH+	ABTS+	Anti-Amylase	Anti-AchE
Humulene-glucoside	4838,99 \pm 50,05	4799,39 \pm 57,14	510.7 \pm 2.60	19,68 \pm 0,89
Kaempferol-6-hydroxy-3,7-dimethylether	180.35 \pm 4,03	57.73 \pm 1,27	226.98 \pm 2.00	24,04 \pm 1,10
Quercetagine-3,7-dimethylether.	144.8 \pm 3,18	62.3 \pm 0,83	161.94 \pm 1.01	25,53 \pm 0,66
Quercetine-3- glucoside	61.23 \pm 1,25	31.84 \pm 0.16	210.99 \pm 2.16	

Results are expressed in terms of mean \pm standard deviation (n = 3)., In statistical analyses by the Tukey comparison test, values with the same superscript are not significantly (p > 0.05) different, n=3.

VI.4. Discussion:

VI.4.1 Anti-oxidant activities:

Our findings contribute to the value of some medicinal herbs from southern Algeria that have not yet been published. As a result, this study can be considered the first report on their anti-oxidant properties in polyphenol content. Notably, the biological activities and secondary metabolites estimated by the assays had a positive correlation.

The antioxidant activity was determined by DPPH, ABTS, FRAP, Phosphomolybdate, Iron chelating, and pyrogallol auto-oxidation assays. As shown in (Table 31), BuOH and EtOAc extracts exhibited a similar anti-oxidant activity compared to the CHCl₃ extract in DPPH and ABTS assays. In the DPPH radical scavenging assay, the molecules soluble in alcohols (methanol) are responsible for the scavenging activity, while in the ABTS assay, the water-soluble molecules are involved. Therefore, some molecules with radical scavenging activity may not be readily available for scavenging ABTS radicals in a methanol solution.

Furthermore, steric accessibility is an important determinant in the DPPH assay, where mostly small molecules have better access to the radical site compared to larger molecules [13]. The different constituents of each extract (hydrogen or electron donator) and these actions could explain the differences in potential observed between the two methods.

Previous studies confirm the anti-oxidant activity of *Pulicaria* species, such as *P. crispa* from Saudi Arabia, the anti-oxidant activity of its methanolic extract was 79.84 % at 1000 µg/ml using DPPH assay [14]. In another study, aqueous ethanolic extracts of the whole *P. crispa* plant obtained from Oman exhibited an IC₅₀ equal to 15.2 ± 0.2 µg/ml and an inhibition value of 92.2 ± 0.3% at 50 µg/ml concentration [15]. In another report [16] of *P. jaubertii*, the inhibition rate was 96.87% for EtOA cextract, 63.62% for butanol extract, and 33.78% for CHCl₃ extract at a concentration of 50 µg/ml in terms of DPPH assay.

Regarding the pyrogallol auto-oxidation assay, the difference in the anti-oxidant activity of the extracts is given in (Figure 77). According to the results, BuOH was the best inhibitor against auto-oxidation of pyrogallol with an inhibition rate equal to 15.44 %, followed by the CHCl₃ extract with an inhibition rate of 10.02% and EtOAc with an inhibition rate of 5.42 % after five minutes. The anti-oxidant activity of *P. laciniata* extracts could be explained through the presence of energetic secondary metabolite compounds. The specific behaviour of these extracts on the anti-oxidant activity may be explained by using the distinction of extracts related to the amount and the quality of active secondary metabolites. Various studies have cited that phenolic compounds exhibited remarkably anti-oxidant activity [17, 18].

Chelation of metal ions is necessary for the functioning of processes biochemical and physiological cellular, but in some cases and when their mechanism action is not well controlled, these same ions can be the cause of peroxidation lipid, oxidative stress, or tissue injury, as an example Cu²⁺ is a stimulator peroxidation of Light density lipoproteins (LDL)[19]. The Fe²⁺-chelating activity was determined by measuring the Fe²⁺ formation of the ferrozine complex. Although iron is essential for oxygen transport, respiration, and enzyme activity, it is a reactive metal that catalyzes oxidative damage in living tissues and cells [20]. Ferrozine can quantitatively form complexes with Fe²⁺. In the presence of chelating agents,

the complex formation is disrupted, resulting in a decrease in the blue color of the complex.

However, those extracts exhibited the following order: EDTA > ethyl extract > BuOH > CHCl₃. None of the extracts appeared to be better ion chelators than the positive control. These results suggested that our extracts are very weak ferrous chelators.

The Phosphomolybdate (PPM) is based on the reduction of molybdate Mo (VI) to molybdate Mo (V) in the presence of the extract or an anti-oxidant agent. This reduction is materialized by forming a greenish complex (phosphate /Mo (V) at acidic pH) [10]. The increase in the color of the molybdate (VI) complex in the presence of anti-oxidants. Unlike other tests, this test quantifies the anti-oxidant activity of polyphenols and other anti-oxidant compounds such as vitamins (C, E). These extracts showed exceptional values at the absorbance of 0.5 nm, where the EtOAc exhibited the highest activity with $A_{0.5} 0.48 \pm 0.09$ mg/ml, followed by the BuOH extract and CHCl₃ extract.

The Ferric Reducing Ability Power (FRAP) based on (Fe³⁺ to Fe²⁺) increased with the concentration of the extracts. This ferric reduction to ferrous ions at low pH caused the formation of a ferrous complex [21]. The present study changes the ferric ion (Yellow) into a ferric-tripyridyl triazine complex (green) during the reducing activity. In the complex mixture, the absorption change was associated with the total reducing power [22] and the highest FRAP activity, signifying richer flavonoids and phenolic compounds [23]. As shown in Table 31, the BuOH extract was the highest effective, with $A_{0.5}$ equal to 0.65 ± 0.01 mg/ml.

In our extracts, the BuOH and the EtOAc extracts showed a very approximate anti-oxidant activity in all methods compared with the CHCl₃ extract, which may be explained by containing the BuOH and the EtOAc extracts with more anti-oxidant bio active compounds. The different behaviour of these extracts on the anti-oxidant activity may be explained by the difference in composition of extracts regarding the quantity and quality of active secondary metabolites, which can be phenolic compounds known for their anti-oxidant remarkably anti-oxidant properties in *vitro* and *in vivo* [17,19].

The anti-oxidant activity of Quercetin-3,7-dimethylether and Kaempferol-6-hydroxy-7,3-dimethylether was important. It is common that flavonoids have an important anti-oxidant activity, while the Humulene-glucosid demonstrated a lower ability to inhibit oxidation compared to the other compounds, the difference of activity certainly due to the difference in the structure.

VI.4.2. Anti-diabetic:

The inhibition of carbohydrate-hydrolyzing enzymes such as pancreatic α -amylase (EC 3.2.1.1) and intestinal α -glucosidase (EC 3.2.1.20) has been found to be of huge importance in the treatment and management of diabetes mellitus [24]. Inhibitors of these enzymes have the ability to retard starch hydrolysis and hence a reduction in glucose absorption rate resulting in a delayed rise in postprandial hyperglycemia [25]. Various research has shown that flavonoids can inhibit or activate enzymes *in vitro* [26]. Also, Hargrove et al. (2011) discovered that flavonoids could inhibit intestinal α -glucosidase and pancreatic α -amylase *in vitro* [27].

α -amylase is the enzyme that starts off the digestion of starch by hydrolyzing the internal glycosidic linkages to produce oligosaccharides. Plant compounds with inhibition ability against this enzyme offer a prospective therapeutic approach for managing postprandial hyperglycemia [28].

Several studies have shown that extracts of medicinal plants and aqueous extracts can improve blood sugar levels. One possible mechanism is the inhibition of α -amylase and α -glucosidase by different metabolites [29, 30]. They can also form insoluble complexes with proteins, leading to precipitation [31]. Previous studies showed that rosmarinic, chlorogenic, caffeic, ellagic and ferulic acids were characterized by their ability to inhibit α -amylase [32, 33]. Also, flavonoids such as luteolin, myricetin, and quercetin have potent α -amylase inhibitors with different IC₅₀ values [34]. While quercetin has been previously reported to inhibit both α -glucosidase and α -amylase. Other studies confirmed that flavonoids exhibit both hypoglycemic and anti-oxidant effects in diabetic animals [35-37]

another type of secondary metabolite named terpenoids has been reported for their inhibition effect of α -glucosidase, for example, 4.4.1. (22R)-3b-hydroxy-24-methyl-lanosta-8,24(25)-dien-26,22-olide, 4.4.2. (22R)-3b-hydroxy-24-methyl-lanosta-7,9,24(25)-trien-26,22-olide [38], Jacquilenin [39], Gypsogenin -O- α -D-galactopyranosyl-(1-6)- β -D-glucopyranosyl-(1-6)-[β -D-glucopyranosyl-(1-3)]- β -D-glucopyranosyl ester, Segetalic acid and 22- α hydroxychiisanoside [40], Betulonic acid, Betulone, Spinasterol [41] those terpenoids has an inhibitory effect against α -glucosidase enzyme better than the Orlistat.

Also, CHCl₃, EtOAc and BuOH extracts of *P. laciniata* were tested for their inhibitory activity against the α -amylase and α -glucosidase enzymes. As summarized in (Table 31), the BuOH extract exhibited the most potent inhibition, with an IC₅₀ of 380.4 \pm 1.77 μ g/ml against α -amylase. In contrast, the CHCl₃ extract was the best inhibitor against α -glucosidase with an IC₅₀ equal to 5.10 \pm 0.01 μ g.

According to these results and reports, we conclude that polarity is essential in directing the extraction to a specific type of active compound with a potential inhibitor against a particular enzyme. So the diversity of molecules present in each extract is responsible for the inhibition of α -amylase and α -glucosidase, thus reducing starch degradation and decreasing glucose absorption and, consequently, the elevation of postprandial glycemia. Further more, these compounds may participate synergistically in inhibiting α -amylase and α -glucosidase. Previous studies have also reported that the *Pulicaria* genera have an anti-diabetic activity, for example, *Pulicaria dysenterica* [42].

It has been reported from docking analysis that hydroxyl groups of B-ring appear to participate in an H-bond from the positive region of the active site (A and G1 subsites [43]). At the same time, the C and A rings bind to subsites A and G. Hydrogen binding, hydrophobic bounds, and Van der Waals forces were the main interactions between the α -amylase and polyphenolic compounds. Flavonoids can link to the main domain of this enzyme by binding with five amino acid residues: Trp₅₈, Trp₅₉, Tyr₆₂, Gln₆₃ and Asp₁₉ [44].

The Quercetine-3-glucoside had a significantly ($P < 0.05$) higher inhibition ability against the α -amylase activity compared to the other compounds, followed by the Quercetagine-3,7-diethermethyl and Kaempferol-6-hydroxy-3,7-dimethymether. Where the weakest activity was demonstrated by the Humulene-glucoside, the IC₅₀ values were illustrated in (Table 24). These results agree with the hypothesized that the hydroxyl group in the chemical structure of the flavonoids could lead to the formation of hydrogen bonds with the polar groups in the allosteric site, which is close to the catalytic site. This results in a change in the enzyme's molecular configuration and its hydrophilic and hydrophobic properties, causing a decrease in enzyme activity [28].

VI.4.3. Anti-obesity:

Obesity results from the disequilibrium between energy intake and expenditure. It is believed to be associated with numerous diseases, including hyperlipidemia, hypercholesterolemia, and type 2 diabetes. Recently, newer approaches for treating obesity have involved inhibiting dietary triglyceride absorption via inhibiting pancreatic lipase, the primary source of excess calories. Phytochemicals identified from traditional medicinal plants present an exciting opportunity to develop newer therapeutics. As part of the continuing search for biologically active anti-obesity agents from natural herbal resources, various plants have been screened for their anti-lipase activity [45]

Pancreatic lipase inhibition of *P. laciniata* extracts is expressed in IC_{50} value (Table 23). The $CHCl_3$ extract exhibited the most potent inhibitory effect on lipase with an IC_{50} value of $5.10 \pm 0.01 \mu\text{g/mL}$. However, it was not more effective than Orlistat ($IC_{50} = 6.23 \pm 0.01$) $\mu\text{g/mL}$, a positive control. Orlistat has serious side effects, such as spotting, stomach pain, irregular menstrual periods, and headaches [46]. Therefore, investigating a new agent for pancreatic lipase inhibitors is still needed.

Previous results show phenolic acid compounds can inhibit pancreatic lipase activity [47-49]. For example, caffeine, chlorogenic acid, and feruloyl quinic acid [50]. Also, it has been reported that crocetin showed inhibitory activity of pancreatic lipase *in vitro* and *in vivo*. [51, 52]. Other published research noted that flavonoids, alkaloids [53, 54], and polyphenols could inhibit pancreatic lipase [55]. From those studies, we concluded that different active compounds could inhibit lipase enzymes *in vitro* and *in vivo*, which makes us conclude that different active compounds in *P. laciniata* extract, especially the $CHCl_3$, are key agents for pancreatic lipase inhibition *in vitro*. Therefore, this plant should be explored as a dietary supplement or nutraceutical food with anti-obesity properties. Our finding is the first to show that the extracts of *P. laciniata* exhibited strong anti-lipase activity.

VI.4.4. Anti-acetylcholine esterase:

Alzheimer's disease (AD) is a progressive age-related disorder characterized by the degeneration of neurological functions caused by a reduction in the level of the neurotransmitter acetylcholine with the progression of the disease, resulting in a loss of

cognitive ability [56]. Acetylcholinesterase (AChE) inhibitors have been shown the ability to increase the acetylcholine level within the synaptic region, thereby restoring deficient cholinergic neurotransmissions [57, 58]. Selective cholinesterase inhibitors, free of dose-limiting side effects, are currently unavailable and cannot always provide a sufficient modulation of the acetylcholine levels to elicit an effective therapeutic response [56]. Therefore, the search for novel AChE inhibitors with high efficacy is necessary.

CHCl₃, ethyl acetate, and BuOH extracts of *P. laciniata* were tested against the AChE enzyme, and a considerable inhibition rate was obtained. The results were statistically significant, where the CHCl₃ extract inhibited 50% of the enzyme at 40,85±1.01µg/ml concentration, followed by the BuOH and EtOAc extracts, respectively. Some AChE antagonists, such as donepezil and galantamine, are used to enhance cholinergic neurotransmission in patients with early-stage Alzheimer's disease. Sadly, these medications show insufficient activity and side effects, such as gastrointestinal problems and hepatotoxicity. Some biologically active plant substances, including terpenoids, alkaloids, flavonoids, sterols, phenolic compounds, and oils, have exhibited anti-acetylcholinesterase activities [59]. Therefore, safer AChE inhibitors must be extracted from a natural source [60, 61]. Our CHCl₃ extract has been proven to contain effective compounds against acetylcholine esterase, making it very interesting to extract AChE antagonist's compounds.

The inhibitory activity of Quercetagetine-3,7-diethermethyl and Kaempferol-6-hydroxy-7,3-dimethymether was very close with an IC₅₀ equal to (25,53±0,66 and 24,04±1,10) µ/ml, respectively. The obtained results can be explained by the similarity of the formula of both compounds, which was reported in previous works. It was mentioned that all flavanols possess a similar binding pattern with the active site of AChE [62].

The general interactions were found to be between the flavanol skeleton and enzyme active sites. Interaction of the A-ring-involved functional groups precisely between the hydroxyl group at the C-7 position and the Asp₇₄ or Tyr₇₂ residues, forming a hydrogen bond [63]. Hydroxylation of the B-ring at C-3" and C-4" may also form a hydrogen bond with the residues Ser₂₀₃ and Gly₁₂₁ and often with Gly₁₂₂.

Hight possibility of creating a covalent bounding between the C-4-keto function of C-rings of flavonoids with the residue Phe₂₉₅ was proved in multiple studies, where both compounds show high structural similarity except in the methoxy group in the 3'position in the

B-ring. Concluding that both molecules have a great capacity to decrease the AChE activity by creating bounds with the amino acids of the active sites [64].

The Humulene-glucoside was the best inhibitor against the AChE. This activity is due to its basic formula of Humulene-glucoside characterized by glucose hydroxyl groups as well as other previous reports proved that sesquiterpene lactones have the ability to inhibit the tested enzyme functionality through bonds between the hydroxyl groups as H-bond donors that bind with the amino acids of the AChE active site such as Trp₈₄, Glu₉₉, Ser₁₂₂, Tyr₁₂₁, Asp₇₂ and Ser₈₁. In addition to polar, basic and hydrophobic interactions with Ser₂₀₀, His₄₄₀, and Phe₃₃, and also by binding with Glu₁₉₉ and Tyr₁₃₀ through water molecules [65].

References

1. Re R, Pellegrini N, Proteggente A, Pannala A, Yang M, Rice-Evans C. Antioxidant activity applying an improved ABTS radical cation decolorization assay. *Free Radical Biol Med.* 1999;26:1231-7.
2. Bibi Sadeer N, Montesano D, Albrizio S, Zengin G, Mahomoodally MF. The Versatility of Antioxidant Assays in Food Science and Safety—Chemistry, Applications, Strengths, and Limitations. *Antioxidants.* 2020;9(8):709.
3. Es-Safi N-E, Kollmann A, Khelifi S, Ducrot P-H. Antioxidative effect of compounds isolated from *Globularia alypum* L. structure–activity relationship. *LWT-Food science and technology.* 2007;40:1246-52.
4. Choi JY, Desta KT, Lee SJ, Kim YH, Shin SC, Kim GS, et al. LC-MS/MS profiling of polyphenol-enriched leaf, stem and root extracts of Korean *Humulus japonicus* Siebold & Zucc and determination of their antioxidant effects. *Biomed Chromatogr.* 2018;32(5):4171.
5. Chaouche TM, Haddouchi F, Ksouri R, Atik-Bekkara F. Evaluation of antioxidant activity of hydromethanolic extracts of some medicinal species from South Algeria. *J Chin Med Assoc.* 2014;77(6):302-7.
6. Pilar Prieto, Manuel Pineda, Aguilar M. Spectrophotometric Quantitation of Antioxidant Capacity through the Formation of a Phosphomolybdenum Complex: Specific Application to the Determination of Vitamin E1. *Analytical Biochemistry.* 1999;269:337-41.
7. Stefan Marklund, Marklund G. Involvement of the Superoxide Anion Radical in the Autoxidation of Pyrogallol and a Convenient Assay for Superoxide Dismutase. *Eur J Biochem.* 1974;47:469-79.
8. Yao X, Zhu L, Chen Y, Tian J, Wang Y. In vivo and in vitro antioxidant activity and alpha-glucosidase, alpha-amylase inhibitory effects of flavonoids from *Cichorium glandulosum* seeds. *Food Chem.* 2013;139(1-4):59-66.
9. Lalegani S, Gavlighi HA, Azizi MH, Sarteshnizi RA. Inhibitory activity of phenolic-rich pistachio green hull extract-enriched pasta on key type 2 diabetes relevant enzymes and glycemic index. *Food Research International.* 2018;105:94-101.
10. Qiu X-L, Zhang Q-F. Chemical profile and pancreatic lipase inhibitory activity of *Sinobambusa tootsik* (Sieb.) Makino leaves. *Biochemistry, Biophysics And Molecular Biology.* 2019;7:e7765.
11. Ellman GL, Courtney KD, Andres Jr V, Featherstone RM. A new and rapid colorimetric determination of acetylcholinesterase activity. *Biochem Pharmacol.* 1961;7:88-95.
12. Promchai T, Saesong T, Ingkaninan K, Laphookhieo S, Pyne SG, Limtharakul T. Acetylcholinesterase inhibitory activity of chemical constituents isolated from *Milium thorelii*. *Phytochemistry Letters.* 2018;23:33-7.
13. Prior RL, Wu X, Schaich K. Standardized methods for the determination of antioxidant capacity and phenolics in foods and dietary supplements. *J Agric Food Chem.* 2005;53:4290-302.
14. Foudah AII, Soliman GAM. Pharmacognostical, Antioxidant and Antimicrobial studies of aerial part of *Pulicaria crispa* (Family: Asteraceae). *Bull Environ, Pharmacol Life Sci.* 2015;4.

15. Marwah RG, Fatope MO, Mahrooqi RA, Varma GB, Abadi HA, Al-Burtamani SKS. Antioxidant capacity of some edible and wound healing plants in Oman. *Food Chem.* 2007;101:465-70.
16. Algabr RM, S A, A M, O B, R S, S B, et al. Antioxydant activities from the aerial parts of *Pulicaria jaubertii*. *Adv Nat Appl Sci.* 2010;4:63-70.
17. Yuwang P, Sulaeva I, Hell J, Henniges U, Böhmendorfer S, Rosenau T, et al. Phenolic compounds and antioxidant properties of arabinoxylan hydrolysates from defatted rice bran. *J Sci Food Agric.* 2018;98:140-6.
18. Pang Y, Ahmed S, Xu Y, Beta T, Zhu Z, Shao Y, et al. Bound phenolic compounds and antioxidant properties of whole grain and bran of white, red and black rice. *Food Chem.* 2018;240:212-21.
19. CARTER P. Spectrophotometric determination of serum iron at the submicrogram level with a new reagent (ferrozine). *ANALYTICAL BIOCHEMISTRY* 1971;40:450-8.
20. Tiwari AK. Imbalance in antioxidant defence and human diseases: Multiple approach of natural antioxidants therapy. *CURRENT SCIENCE.* 2001;81:1179-87.
21. Benzie IF, Strain JJ. The ferric reducing ability of plasma (FRAP) as a measure of "antioxidant power": the FRAP assay. *Anal Biochem.* 1996;239(1):70-6.
22. Sudan R, Bhagat M, Gupta S, Singh J, Koul A. Iron (FeII) chelation, ferric reducing antioxidant power, and immune modulating potential of *Arisaema jacquemontii* (Himalayan Cobra Lily). *BioMed Research International.* 2014;2014.
23. Akinola AA, Ahmad S, Maziah M, Medicines A. Total anti-oxidant capacity, flavonoid, phenolic acid and polyphenol content in ten selected species of Zingiberaceae rhizomes. *African Journal of Traditional, Complementary Alternative Medicines.* 2014;11(3):7-13.
24. Asano N. Glycosidase inhibitors: update and perspectives on practical use. *Glycobiology.* 2003;13(10):93R-104R.
25. Raptis S, Dimitriadis G. Oral hypoglycemic agents: insulin secretagogues, α -glucosidase inhibitors and insulin sensitizers. *Experimental Clinical Endocrinology Diabetes.* 2001;109(Suppl 2):S265-S87.
26. Martín MÁ, Serrano ABG, Ramos S, Pulido MI, Bravo L, Goya L. Cocoa flavonoids up-regulate antioxidant enzyme activity via the ERK1/2 pathway to protect against oxidative stress-induced apoptosis in HepG2 cells. *The Journal of nutritional biochemistry.* 2010;21(3):196-205.
27. Hargrove JL, Greenspan P, Hartle DK, Dowd C. Inhibition of aromatase and α -amylase by flavonoids and proanthocyanidins from *Sorghum bicolor* bran extracts. *Journal of medicinal food.* 2011;14(7-8):799-807.
28. Oboh G, Ademosun AO, Ayeni PO, Omojokun OS, Bello F. Comparative effect of quercetin and rutin on α -amylase, α -glucosidase, and some pro-oxidant-induced lipid peroxidation in rat pancreas. *Comparative Clinical Pathology.* 2015;24(5):1103-10.
29. El-Beshbishy H, Bahashwan S. Hypoglycemic effect of basil (*Ocimum basilicum*) aqueous extract is mediated through inhibition of alpha-glucosidase and alpha-amylase activities: an in vitro study. *Toxicology and Industrial Health.* 2012;28:42-50.
30. Paloma Michelle de Sales, Paula Monteiro de Souza, Luiz Alberto Simeoni, Pérola de Oliveira Magalhães, Silveira D. α -Amylase Inhibitors: A Review of Raw Material and Isolated

- Compounds from Plant Source. *Journal of Pharmacy & Pharmaceutical Sciences*. 2012;15:141-83.
31. Makkar HPS. Protein Precipitation Methods for Quantitation of Tannins: A Review. *J Agric Food Chem*. 1989;37:1197-202.
 32. MS PPM, Shetty K. Inhibitory effects of rosmarinic acid extracts on porcine pancreatic amylase in vitro. *Asia Pacific Journal of Clinical Nutrition*. 2004;13 101-6.
 33. Narita Y, Inouye K. Kinetic analysis and mechanism on the inhibition of chlorogenic acid and its components against porcine pancreas alpha-amylase isozymes I and II. *J Agric Food Chem*. 2009;57:9218-25.
 34. Tadera K, Minami Y, Takamatsu K, Matsuoka T. Inhibition of alpha -Glucosidase and alpha -Amylase by Flavonoids. *Journal of Nutritional Science and Vitaminology*. 2006;52:149–53,.
 35. Ong KC, Khoo H-E. Biological effects of myricetin. *J General Pharmacology: The Vascular System*. 1997;29(2):121-6.
 36. Kamalakkannan N, Prince P. Rutin improves the antioxidant status in streptozotocin-induced diabetic rat tissues. *Molecular cellular biochemistry*. 2006;293(1):211-9.
 37. Wang H, Du Y-J, Song H-C. α -Glucosidase and α -amylase inhibitory activities of guava leaves. *Food Chem*. 2010;123(1):6-13.
 38. Ying YM, Zhang LY, Zhang X, Bai HB, Liang DE, Ma LF, et al. Terpenoids with alpha-glucosidase inhibitory activity from the submerged culture of *Inonotus obliquus*. *Phytochemistry*. 2014;108:171-6.
 39. Fan H, Chen J, Lv H, Ao X, Wu Y, Ren B, et al. Isolation and identification of terpenoids from chicory roots and their inhibitory activities against yeast α -glucosidase. *European Food Research and Technology*. 2016;243(6):1009-17.
 40. Shah M, Bashir S, Jaan S, Nawaz H, Nishan U, Abbasi SW, et al. Computational Analysis of Plant-Derived Terpenes as α -Glucosidase Inhibitors for the Discovery of Therapeutic Agents against Type 2 Diabetes Mellitus. *South African Journal of Botany*. 2021;143:462-73.
 41. Chukwujekwu JC, Rengasamy KR, de Kock CA, Smith PJ, Slavětínská LP, van Staden J. Alpha-glucosidase inhibitory and antiplasmodial properties of terpenoids from the leaves of *Buddleja saligna* Willd. *Journal of Enzyme Inhibition and Medicinal Chemistry* 2016;31(1):63-6.
 42. de la Luz Cadiz-Gurrea M, Zengin G, Kayacik O, Lobine D, Mahomoodally MF, Leyva-Jimenez FJ, et al. Innovative perspectives on *Pulicaria dysenterica* extracts: phyto-pharmaceutical properties, chemical characterization and multivariate analysis. *J Sci Food Agric*. 2019;99:6001-10.
 43. Qian M, Haser R, Buisson G, Duee E, Payan F. The Active Center of a Mammalian. alpha.-Amylase. Structure of the Complex of a Pancreatic. alpha.-Amylase with a Carbohydrate Inhibitor Refined to 2.2- \AA . Resolution. *Biochemistry*. 1994;33(20):6284-94.
 44. Martinez-Gonzalez AI, Díaz-Sánchez Á, De La Rosa L, Bustos-Jaimes I, Alvarez-Parrilla E. Inhibition of α -amylase by flavonoids: Structure activity relationship (SAR). *Spectrochimica Acta Part A: MolecularBiomolecular Spectroscopy*. 2019;206:437-47.
 45. Birari RB, Bhutani KK. Pancreatic lipase inhibitors from natural sources: unexplored potential. *Drug Discov Today*. 2007;12(19-20):879-89.

46. Bray GA. Medications for obesity: mechanisms and applications. *Clinics in chest medicine*. 2009;30(3):525-38.
47. Yuda N, Tanaka M, Suzuki M, Asano Y, Ochi H, Iwatsuki K. Polyphenols extracted from black tea (*Camellia sinensis*) residue by hot-compressed water and their inhibitory effect on pancreatic lipase in vitro. *Journal of Food Science*. 2012;77(12):H254-H61.
48. Uchiyama S, Taniguchi Y, Saka A, Yoshida A, Yajima H. Prevention of diet-induced obesity by dietary black tea polyphenols extract in vitro and in vivo. *Nutrition*. 2011;27(3):287-92.
49. Nakai M, Fukui Y, Asami S, Toyoda-Ono Y, Iwashita T, Shibata H, et al. Inhibitory effects of oolong tea polyphenols on pancreatic lipase in vitro. *J Agric Food Chem*. 2005;53(11):4593-8.
50. Shimoda H, Seki E, Aitani M. Inhibitory effect of green coffee bean extract on fat accumulation and body weight gain in mice. *BMC complementary alternative medicine*. 2006;6(1):1-9.
51. Lee I-A, Lee JH, Baek N-I, Kim D-H. Antihyperlipidemic effect of crocin isolated from the fructus of *Gardenia jasminoides* and its metabolite crocetin. *Biological Pharmaceutical Bulletin*. 2005;28(11):2106-10.
52. Sheng L, Qian Z, Zheng S, Xi L. Mechanism of hypolipidemic effect of crocin in rats: crocin inhibits pancreatic lipase. *Eur J Pharmacol*. 2006;543(1-3):116-22.
53. Lee EM, Lee SS, Chung BY, Cho J-Y, Lee IC, Ahn SR, et al. Pancreatic lipase inhibition by C-glycosidic flavones isolated from *Eremochloa ophiuroides*. *Molecules*. 2010;15(11):8251-9.
54. Lunagariya NA, Patel NK, Jagtap SC, Bhutani KK. Inhibitors of pancreatic lipase: state of the art and clinical perspectives. *EXCLI journal*. 2014;13:897.
55. Han LK, Sumiyoshi M, Zhang J, Liu MX, Zhang XF, Zheng YN, et al. Anti-obesity action of *Salix matsudana* leaves (Part 1). Anti-obesity action by polyphenols of *Salix matsudana* in high fat-diet treated rodent animals. *Phytotherapy Research*. 2003;17(10):1188-94.
56. Felder CC, Bymaster FP, Ward J, DeLapp N. Therapeutic opportunities for muscarinic receptors in the central nervous system. *J Med Chem*. 2000;43(23):4333-53.
57. Giacobini EJNi. Invited review cholinesterase inhibitors for Alzheimer's disease therapy: from tacrine to future applications. 1998;32(5-6):413-9.
58. Krall WJ, Sramek JJ, Cutler NR. Cholinesterase inhibitors: a therapeutic strategy for Alzheimer disease. *Annals of Pharmacotherapy*. 1999;33(4):441-50.
59. Ji Hf, ZHANG Hy. Multipotent natural agents to combat Alzheimer's disease. Functional spectrum and structural features 1. *Acta Pharmacologica Sinica*. 2008;29:143-51.
60. Murray AP, Faraoni MB, Castro MJ, Alza NP, Cavallaro V. Natural AChE inhibitors from plants and their contribution to Alzheimer's disease therapy. *Current Neuropharmacology*. 2013;11:388-413.
61. Machado LP, Carvalho LR, Young MCM, Cardoso-Lopes EM, Centeno DC, Zambotti-Villela L, et al. Evaluation of acetylcholinesterase inhibitory activity of Brazilian red macroalgae organic extracts. *Revista Brasileira de Farmacognosia*. 2015;25:657-62.
62. Remya C, Dileep K, Tintu I, Variyar E, Sadasivan C. Design of potent inhibitors of acetylcholinesterase using morin as the starting compound. *Frontiers in Life Science*. 2012;6(3-4):107-17.

63. Katalinić M, Rusak G, Barović JD, Šinko G, Jelić D, Antolović R, et al. Structural aspects of flavonoids as inhibitors of human butyrylcholinesterase. 2010;45(1):186-92.
64. Olennikov DN, Kashchenko NI, Chirikova NK, Akobirshoeva A, Zilfikarov IN, Vennos C. Isorhamnetin and Quercetin Derivatives as Anti-Acetylcholinesterase Principles of Marigold (*Calendula officinalis*) Flowers and Preparations. *Int J Mol Sci.* 2017;18(8).
65. Hegazy M-EF, Ibrahim AY, Mohamed TA, Shahat AA, El Halawany AM, Abdel-Azim NS, et al. Sesquiterpene lactones from *Cynara cornigera*: acetyl cholinesterase inhibition and in silico ligand docking. *Planta Med.* 2016;82(01/02):138-46.

CONCLUSION

Conclusion

Conclusion:

The Asteraceae plant *Pulicarialaciniata*, which had only been the subject of limited chemical analysis before this study, was extremely rich in secondary metabolites and had significant biological activity.

The extraction of the whole plant and the successive chromatographic separations made it possible to isolate six compounds consisting mainly of five flavonoids that were found to be novel in *Pulicarialaciniata*, and one humulene is new in the genus of *Pulicaria*, namely:

- ✓ Quercetine -3-O-methyl.
- ✓ Kaempferol-6-hydroxy-7,3-O-dimethymether
- ✓ Quercetagine-3,7-diethermethyl
- ✓ Quercetine -3-O-glucoside
- ✓ Quercetine -3-O-glucoronide
- ✓ Humulene - glucoside

All the compound structures were determined by one-dimensional NMR and two-dimensional sequences and compared with the literature.

The GC-MS analyze identified nine compounds from the Chloroform extract named:

- ✓ 6-Methyl-2-(4-methylcyclohex-3-en-1-yl)hepta-1,5-dien-4-ol (β -Atlantol)
- ✓ 3-methyl-6-(1-methylethylidene)- 2-Cyclohexen-1-one (3-Terpinolenone)
- ✓ 3-Oxatricyclo[20.8.0.0(7,16)]triaconta-1(22),7(16),9,13,23,29-hexaene]
- ✓ 3-Methyl-2-(2-methyl-2-butenyl)-furan
- ✓ 4,6,6-trimethyl-, (1S)- Bicyclo[3.1.1]hept-3-en-2-one
- ✓ Trans-Carveyl acetate
- ✓ 5-(3-hydroxy-10,13-dimethyl-2,3,4,7,8,9,10,11,12,13,14,15,16,17-tetradecahydro-1H-cyclopenta[a]phenanthren-17-yl)-5-methyldihydrofuran-2(3H)-one
- ✓ 2-Oxaadamantan-6-ol
- ✓ 2,2'-methylenebis[6-(1,1-di-methylethyl)-4-methyl Phenol]

Conclusion

The biological study highlighted four activities for this plant: antioxidant activity, anti-Alzheimer, anti-diabetic, and anti-obesity. The study of the antioxidant activity noted on the three CHCl₃, EtOAc, and n-BuOH extracts of *Pulicaria laciniata* using as test models: the DPPH, ABTS, metal chelating, superoxide anion, Phosphomolybdate, reducing power, showed that the n-BuOH and EtOAc extracts show significant antioxidant effect, with maximum potential for the n-BuOH extract in the most tests. In comparison, the antioxidant activities of the pure compound Quercetine-3-O glucoside were the best in DPPH and ABTS tests. The anti-Alzheimer activity was studied using acetylcholine-esterase enzyme, the CHCl₃ extract, and the Glucoside–humulene pure compound, which exhibited the best IC₅₀. The anti-diabetic activity was carried out using two enzymes, α -amylase and α -glucosidase. The results demonstrate that the n-butanol extract and the purified compound Quercetagine-3,7-diethermethyl were the best inhibitors against the α -amylase, while the chloroform extract was the best against the α -glucosidase enzyme. The anti-obesity activity was evaluated using pancreatic lipase enzyme, and the results showed that the chloroform extract exhibited the best activity.

A novelty of this study has highlighted the identification of 15 compounds that were established for the first time in the aerial part extract of *Pulicaria laciniata*. Among these compounds, one is novel to the *Pulicaria* genera. Also discovered this plant as potentially therapeutic against different diseases.

Finally, it would be interesting to research all *Pulicaria laciniata* aerial parts extracts to reach the active compounds against all the previous activities in *silico*, *in vitro*, and *in vivo*.